ANALYSE DES MECANISMES DE PENETRATION INTRAMEMBRANAIRE DE PORPHYRINES GLYCOCONJUGUEES UTILISABLES EN THERAPIE PHOTODYNAMIQUE DES CANCERS: MODELISATION DES INTERACTIONS SPECIFIQUES ET NON-SPECIFIQUES

Ali Makky

UNIVERSITÉ PARIS-SUD 11

FACULTÉ DE PHARMACIE DE CHÂTENAY-MALABRY

ECOLE DOCTORALE :

INNOVATION THÉRAPEUTIQUE : DU FONDAMENTAL A L'APPLIQUÉ

PÔLE : PHARMACOTECHNIE ET PHYSICO-CHIMIE PHARMACEUTIQUE

ANNÉE 2010 - 2011 SÉRIE DOCTORAT N° 1091

THÈSE

Présentée

À L'UNITÉ DE FORMATION ET DE RECHERCHE

FACULTE DE PHARMACIE DE CHATENAY-MALABRY

UNIVERSITÉ PARIS-SUD 11

Pour l'obtention du grade de

DOCTEUR DE L'UNIVERSITÉ PARIS-SUD 11

par

Monsieur ALI MAKKY

Titre de la thèse :

ANALYSE DES MECANISMES DE PENETRATION INTRAMEMBRANAIRE DE PORPHYRINES GLYCOCONJUGUEES UTILISABLES EN THERAPIE PHOTODYNAMIQUE DES CANCERS: MODELISATION DES INTERACTIONS SPECIFIQUES ET NON-SPECIFIQUES

Soutenue le : 26 Novembre 2010

JURY :	Pr. Agnès GIRARD-EGROT	Rapporteur
	Dr. Ralph RICHTER	Rapporteur
	Pr. Patrice PROGNON	Examinateur
	Pr. Elias FATTAL	Président
	Dr. Philippe MAILLARD	Examinateur
	Pr. Véronique ROSILIO	Directeur de thèse

"I have no special talent. I am only passionately curious."
Albert Einstein

Remerciements

Ce travail de thèse a été réalisé au sein du laboratoire de « *Physico-Chimie des Surfaces »* de l'UMR CNRS 8612 que dirige **Madame le Professeur Véronique ROSILIO**. Je tiens tout d'abord à lui exprimer toute ma reconnaissance pour m'avoir accueilli dans son laboratoire et son équipe.

Aux membres du Jury

Je remercie Madame le **Professeur Agnès GIRARD-EGROT** de l'Université de Lyon et Monsieur le **Dr. Ralph RICHTER** chef de groupe de recherche à l'unité de Biosurfaces, CIC biomaGUNE, Saint-Sébastien en Espagne, pour avoir accepté de juger ce travail de thèse en qualité de rapporteurs et pour s'être déplacés afin de participer à ce jury. Je tiens également à remercier Monsieur **Philippe MAILLARD** directeur de recherche à l'institut Curie d'Orsay, Monsieur **Elias FATTAL** professeur à la faculté de pharmacie à Châtenay-Malabry et directeur de l'UMR 8612 et monsieur le **Professeur Patrice PROGNON** pour avoir accepté de siéger le jury.

A **Madame le Professeur Véronique ROSILIO,**

Je vous suis fortement reconnaissant d'avoir bien voulu diriger et encadrer mes travaux de thèse, je vous remercie vivement pour tous vos conseils, vos renseignements, pour toutes les corrections que vous avez faites avec tant de patience, pour avoir supporté mon entêtement, pour m'avoir donné l'occasion de présenter mes travaux lors de congrès et surtout pour le temps que vous m'avez consacré tout au long de ma thèse malgré votre emploi de temps chargé. Vous étiez toujours à côté de moi pour résoudre la majorité des problèmes que j'ai rencontrés dans ma thèse et pour me donner de l'espoir pour arriver à notre but. Je ne trouverai jamais les mots pour vous dire à quel point j'ai apprécié vos qualités professionnelles et personnelles. Enfin, qu'est ce que l'on ferait sans vous ???!!!!! A ma directrice de thèse, à qui je dois tout...

Au **Dr. Jean-Philippe MICHEL,** je te remercie d'avoir assisté au bon déroulement de ma thèse, et à la correction des articles aussi pour ton aide dans les expériences de tensiométrie (Interaction Porphyrines-Modèles membranaires) et aussi de culture cellulaire. Je te remercie aussi de m'avoir appris la patience quand on rencontre les problèmes.

Je tiens également à remercier l'équipe 1 de l'UMR CNRS 8612 dans son ensemble, aussi bien les permanents : **Dr. Catherine RINGARD**, **Dr. Michel DEYME** pour leur soutien et leurs conseils tout au long de ma thèse, que les étudiantes de M2 : **Katia SOSNOWIEZ** et **Katia DAGHILDJIAN** pour les moments agréables qui ont marqué ces années de recherche. Je remercie aussi le post-doctorant **Wang YING-XIONG**.

Un grand merci au post doctorant **Dr. Anshuman AMBIKE** pour son soutien et ses conseils tout au long de ma thèse, aussi pour les moments agréables que nous avons passé ensemble pendant ces trois années de thèse.

Au **Dr. Elisabeth BRIAND**, la post doctorante avec qui j'ai partagé le bureau, je te remercie infiniment pour ta gentillesse, pour tous tes conseils sur les expériences de QCM-D et de m'avoir formé sur les bonnes utilisations. C'est grâce à toi que j'ai connu le fabuleux QCM-D qui m'a ouvert la porte pour faire beaucoup d'expériences intéressantes et qui ont aboutit à la progression significative de mes travaux de thèse.

Au **Dr. Athena KASSELOURI** du « Laboratoire de Chimie Analytique » unité EA n° 4041, je te remercie infiniment pour tes conseils sur les expériences de spectroscopie de fluorescence, pour ta disponibilité pour répondre à mes questions et de m'avoir aidée à interpréter mes résultats.

Je tiens à remercier, **Dr. Philippe MAILLARD**, directeur de recherche au CNRS au laboratoire de « Conception, synthèse et vectorisation de biomolécules » de l'UMR 176 à l'institut Curie » pour les fabuleuses molécules que vous avez synthétisées, c'est grâce à vous que j'ai pu découvrir le monde des macrocycles tétrapyrroliques qui m'ont permis d'approfondir mes connaissances dans le domaine de la PDT, je vous remercie aussi pour tous vos conseils et pour votre disponibilité pour répondre à toutes mes questions.

Un grand merci à Madame **Véronique MARSAUD** ingénieur de recherche CNRS au laboratoire de « Pharmacologie Cellulaire et Moléculaire des Anticancéreux » de m'avoir encadré dans toutes les expériences de culture cellulaire et pour tous vos conseils qui m'ont fait découvrir ce monde agréable de biologie cellulaire. Je remercie également, Mr. **Jack-Michel RENOIR** directeur de recherche, de m'avoir accueilli dans son laboratoire pour tester la phototoxicité des porphyrines en culture cellulaire.

Je tiens également à remercier le **Professeur Elias FATTAL**, directeur de l'unité UMR CNRS 8612 qui m'a soutenu tout au long de ma thèse et qui m'a aidé à obtenir l'équivalence de mon master professionnel pour pouvoir effectuer une thèse, ainsi pour tous ses conseils tout au long de ma thèse.

Un grand merci à madame le **Dr. Sylviane LESIEUR** directrice du laboratoire « Physico-Chimie des Systèmes Polyphasés » pour tous ses conseils concernant les expériences de DLS.

Aux **Dr. Sinda MOUELHI-LEPETRE** Maitre de Conférences et **Dr. DIDIER DESMAËLE** directeur de recherche au CNRS au Laboratoire de « Synthèse Organique et Pharmacochimie de Composés d'Intérêt Biologique » de l'UMR 8076 BioCIS (Biomolécules : Conception, Isolement et Synthèse) de m'avoir aidé et formé sur l'activation des phospholipides par la triazine mais aussi aux bonnes conditions expérimentales en chimie organique.

Je tiens à remercier chaleureusement tous les doctorants ayant collaboré à ce travail dont : pour la Synthèse des porphyrines: **Séverine BALLUT** de l'institut Curie Orsay.

J'adresse à l'**Association pour la Recherche sur le Cancer (ARC)** mes vifs remerciements, pour m'avoir apporté une aide financière, me permettant de mener mes travaux de thèse dans de bonnes conditions.

Un grand merci à tous les membres de **l'UMR 8612** qui ont contribué à la réalisation de ce travail. Je n'oublierais pas mes collègues à la faculté de pharmacie (Emile Jubeili, Hammadi Nciri, Mohamad Khoder, Hanadi Ibrahim…) qui m'ont encouragé et soutenu durant la préparation de mon mémoire. Je tiens à leur exprimer toute ma reconnaissance et ma profonde gratitude.

A mes amis

Je ne pouvais pas oublier mes amis (Hussein, Moustapha, Mona, Nabil, Moussa, Samer, Swido, Charbel….) je tiens à exprimer ma reconnaissance et ma profonde gratitude à vous et à tous ceux qui ont contribué de près ou de loin à la réalisation de ce travail.

A ma famille

Je tiens à dédier ce travail à mes parents, ceux à qui je dois tant pour leur amour et leur soutien continu tout le long du cursus de mes études. C'est grâce à vous que j'ai pu aller au bout de mes projets. Merci d'avoir cru à mes choix d'étude et de m'avoir donné les moyens pour accomplir ce travail dans les meilleures conditions. Que ce travail soit le témoignage sincère et affectueux de ma profonde reconnaissance pour tout ce que vous avez fait pour moi. A mes sœurs qui m'ont encouragé et soutenus dans mes moments les plus difficiles, un grand merci du fond de mon cœur.

Enfin je dédie cette thèse à **Nada,** ma fiancée. Toi qui partage ma vie, tu as supporté toutes mes colères pendant cette thèse et tu m'as aidé à résoudre pas mal de problèmes de chimie organique pendant ces trois ans et je le sais je n'ai pas toujours été facile. Mais ton soutien et ton amour m'ont permis de faire face à toutes les difficultés et les angoisses. Alors cette thèse, c'est la tienne aussi!!!…Merci…

Sommaire

Liste des abréviations

PS	Photosensibilisateurs
PDT	Photodynamic therapy ou photothérapie dynamique
QCM-D	Quartz Crystal Microbalance with Dissipation Monitoring
BAM	*Brewster* Angle Microscope
SPR	Surface Plasmon Resonance (Biacore®)
DSC	Differential Scanning Calorimetry
ITC	Isothermal titration calorimetry
DLS	Diffusion Quasi-élastique de la lumière
π	Pression de surface
ζ	Potentiel Zêta
K_{max}	Module de compressibilité maximal
ΔA^{EXC}	Excès d'aire moléculaire
ΔG^{EXC}	Excès d'énergie libre
ΔG^{IDEAL}	Energie libre d'un mélange idéal
λem	Longueur d'onde d'émission
λex	Longueur d'onde d'excitation
K_{SV}	Constante de Stern-Volmer
K_p	Partition coefficient
TPP	Tetraphenylporphyrine
α-MMP	*alpha*-Methyl-D-mannopyranoside
Con A	Concanavaline A
DMPC	Dimyristoylphosphatidylcholine
SOPC	1-stearoyl-2-oleoyl-*sn*-glycero-3-phosphatidylcholine
SOPE	1-stearoyl-2-oleoyl-*sn*-glycero-3-phosphatidylethanolamine
SOPS	1-stearoyl-2-oleoyl-*sn*-glycero-3-phosphatidylsérine
Chol	Cholestérol
MEG	Monoéthylèneglycol
DEG	Diéthylèneglycol
TEG	Triéthylèneglycol
SVF	Sérum de veau fœtal
PBS	Phosphate buffered saline
HEPES	Acide 4-(2-hydroxyéthyl)-1-pipérazine éthane sulfonique

Introduction générale

La photothérapie dynamique (PDT) constitue aujourd'hui une approche prometteuse et innovante pour le traitement de tumeurs cancéreuses de petite taille et accessibles à la lumière. [(1)] Les applications cliniques de cette thérapie sont de plus en plus nombreuses et donnent des résultats encourageants dans le traitement, notamment, de carcinomes baso-cellulaires, de petites tumeurs des voies aérodigestives supérieures accessibles par endoscopie, de tumeurs de la vessie et de tumeurs cutanées. [(2)] En raison de son efficacité thérapeutique et de ses effets secondaires mineurs par rapport à la chimiothérapie et la radiothérapie, la PDT est, pour beaucoup, considérée comme une véritable alternative thérapeutique pour le traitement de certains types de cancer comme le rétinoblastome, [(3)] une tumeur maligne intraoculaire chez l'enfant qui se manifeste avec une incidence de 1/15000 naissances. [(4)]

La PDT permet la destruction d'une tumeur par une réaction photochimique. Son principe est basé sur l'action conjuguée d'un médicament dit photosensibilisateur (PS), de lumière et d'oxygène. Le photosensibilisateur, administré par voie intraveineuse, se fixe au niveau de la tumeur. Après un délai adapté spécifiquement à la tumeur à traiter, celle-ci est irradiée par un laser dont la longueur d'onde correspond à une bande d'absorption du photosensibilisateur. La molécule excitée produit alors des espèces réactives de l'oxygène, comme l'oxygène singulet et des radicaux libres, qui entraînent une nécrose tissulaire. La plupart des photosensibilisateurs utilisés en PDT expérimentale et clinique sont des dérivés porphyriniques, constitués d'un noyau macrocyclique responsable de la réaction photochimique et de substituants périphériques qui contrôlent la pénétration et la pharmacocinétique des molécules. L'efficacité des photosensibilisateurs dépend de leur solubilité, de leur distribution préférentielle au niveau des tumeurs et de leur capacité à interagir avec la membrane cellulaire pour pénétrer dans la cellule. La sélectivité tumorale dépend essentiellement de la nature du tissu à traiter et de celle du photosensibilisateur. Plusieurs stratégies de ciblage tumoral ont été proposées parmi lesquelles la vectorisation active par des systèmes colloïdaux (nanoparticules [(5)] et liposomes [(6)], furtifs [(7)] et fonctionnalisés). Elles ne seront pas abordées dans ce mémoire. Nous nous intéresserons aux stratégies qui consistent à modifier les molécules elles-mêmes. L'une d'elles, développée par l'équipe du Dr. Philippe Maillard à l'Institut Curie (UMR CNRS 176) consiste en une glycoconjugaison de macrocycles tétrapyrroliques neutres. [(8-11)] Cette glycoconjugaison a un double intérêt : elle permet, d'une part, de modifier l'amphiphilie des macrocycles, paramètre important pour leur solubilité et leur pénétration (car les porphyrines sont très hydrophobes), et d'autre part, de cibler des récepteurs membranaires reconnaissant les sucres, surexprimés à la surface de certaines cellules cancéreuses, comme les cellules Y79 de rétinoblastome. [(8,12)]

Des études de photocytoxicité de ces dérivés glycoconjugués (en particulier les dérivés mannosylés et galactosylés) réalisées à l'institut Curie, ont montré que certains de ces composés, notamment les dérivés asymétriques présentent une pénétration intracellulaire et une phototoxicité plus élevées que les dérivés non glycoconjugués, vis-à-vis des cellules de rétinoblastome. L'équipe de Philippe Maillard s'est orientée depuis, vers la synthèse de nouvelles porphyrines avec une structure dendrimérique qui permettrait d'amplifier le caractère amphiphile de ces molécules en créant, en même temps un *cluster* de sucres. Cette nouvelle structure pourrait favoriser l'interaction spécifique de ces molécules avec les récepteurs membranaires. (Figure 1)

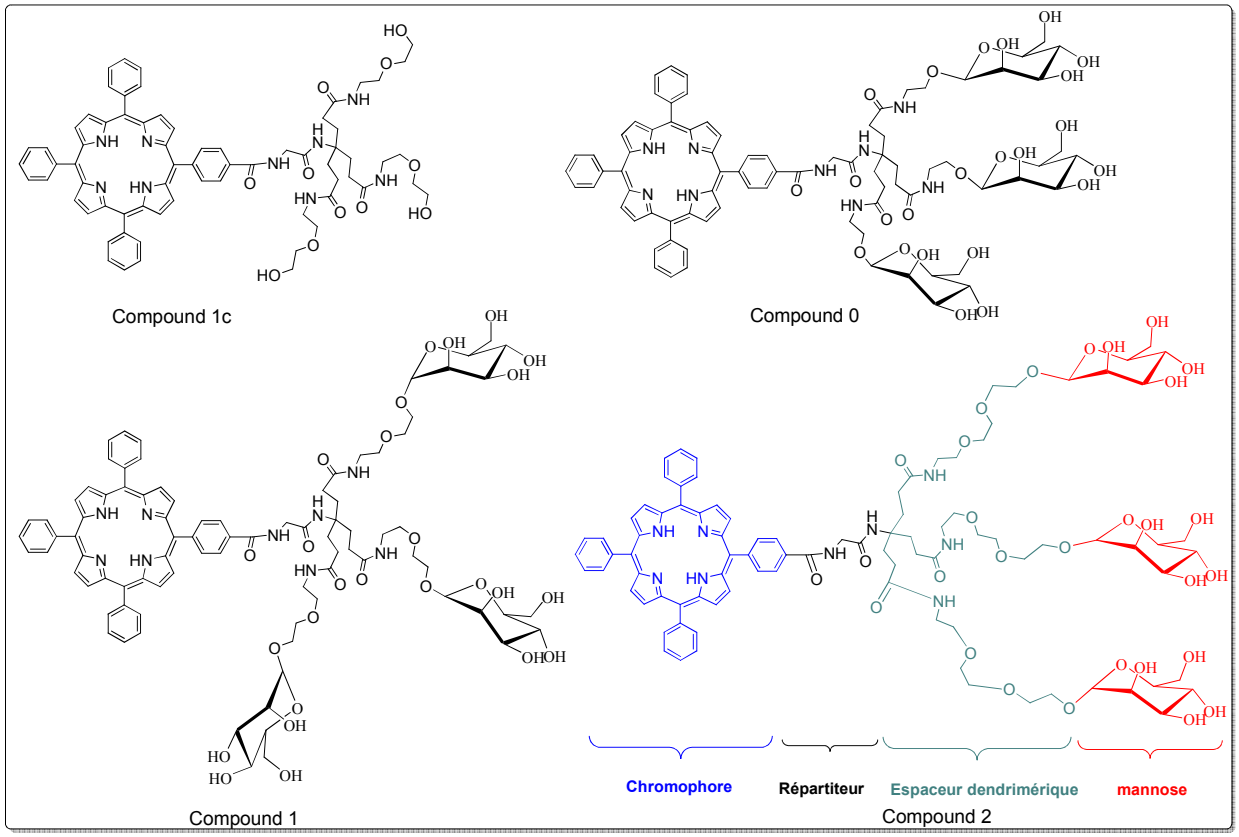

Figure 1 : Structure chimique des porphyrines dendrimériques.

L'objectif principal de cette thèse est d'identifier les caractéristiques physico-chimiques qui pourraient déterminer la pénétration intracellulaire de porphyrines dendrimériques mannosylées, destinées au ciblage de récepteurs lectiniques surexprimés à la surface des cellules du rétinoblastome.

Pour atteindre cet objectif, nous avons construit des modèles membranaires artificiels du rétinoblastome portant ou non une lectine spécifique du mannose et réalisé une série d'expériences afin d'établir une relation entre la structure de ces porphyrines et leur capacité à interagir avec la membrane cytoplasmique, d'une part, et d'être reconnu par les récepteurs

reconnaissant le mannose, d'autre part. Ce travail devait permettre d'orienter les chimistes vers la conception de nouveaux composés d'intérêt thérapeutique, ayant une sélectivité améliorée vis-à-vis des cellules tumorales.

Ce mémoire de thèse est organisé en deux parties.

La première partie, purement bibliographique (article 1), expose le contexte du sujet. Elle décrit, d'une part, la PDT et les principaux dérivés porphyriniques d'intérêt, la composition membranaire des cellules et les changements induits par le cancer et, d'autre part, les modèles biomimétiques artificiels utilisés pour l'analyse et la quantification des interactions photosensibilisateurs-membrane, avec leurs avantages et inconvénients par rapport aux cultures cellulaires.

La **deuxième partie** décrit les travaux expérimentaux. Elle est subdivisée en trois chapitres.

Le premier chapitre traite du comportement interfacial des porphyrines dendrimériques étudiées et de leur interaction non spécifique avec une matrice lipidique, présentée soit sous forme de monocouche, soit sous forme de liposome. Selon sa composition, cette matrice constitue soit leur véhicule solubilisant (article 2), soit le modèle simplifié de la membrane cellulaire du rétinoblastome (article 3).

Le deuxième chapitre est consacrée à l'étude plus particulière de l'interaction spécifique entre les porphyrines, libres ou incorporées dans des liposomes, et une lectine spécifique du mannose mimant le récepteur porté par les cellules de rétinoblastome (article 4).

Le troisième chapitre expose la construction et la caractérisation physico-chimique d'un modèle membranaire du rétinoblastome composé d'une matrice lipidique bicouche et exposant à sa surface la lectine spécifique du mannose et son interaction avec les porphyrines incorporées dans des liposomes (article 5).

Cette partie est suivie d'une **discussion générale** qui revient sur les différents points soulevés dans les trois chapitres et fait le lien avec la culture cellulaire.

Enfin, la conclusion générale dégage les principaux résultats issus de ce travail en évoquant, plus généralement, l'intérêt des modèles membranaires comme outil pour l'étude de l'interaction des substances actives avec la membrane cytoplasmique.

Références:

1. Ackroyd, R., Kelty, C., Brown, N., and Reed, M. (2001) The History of Photodetection and Photodynamic Therapy&para, *Photochemistry and Photobiology 74*, 656-669.
2. Dolmans, D. E., Fukumura, D., and Jain, R. K. (2003) Photodynamic therapy for cancer, *Nat Rev Cancer 3*, 380-387.
3. Stephan, H., Boeloeni, R., Eggert, A., Bornfeld, N., Schueler, A. (2008) Photodynamic Therapy in Retinoblastoma: Effects of Verteporfin on Retinoblastoma Cell Lines, *Invest. Ophthalmol. Vis. Sci. 49*, 3158-3163.
4. Doz, F. (2006) Rétinoblastome : aspects récents, *Arch. de Pédiatrie 13*, 1329-1337.
5. Chatterjee, D. K., Fong, L. S., and Zhang, Y. (2008) Nanoparticles in photodynamic therapy: An emerging paradigm, *Advanced Drug Delivery Reviews 60*, 1627-1637.
6. Hoebeke, M. (1995) The importance of liposomes as models and tools in the understanding of photosensitization mechanisms, *J. Photochem. and Photobiol. B. Biol. 28*, 189-196.
7. Nawalany, K., Rusin, A., Kepczynski, M., Mikhailov, A., Kramer-Marek, G., Snietura, M., Poltowicz, J., Krawczyk, Z., and Nowakowska, M. (2009) Comparison of photodynamic efficacy of tetraarylporphyrin pegylated or encapsulated in liposomes: In vitro studies, *Journal of Photochemistry and Photobiology B: Biology 97*, 8-17.
8. Laville, I., Figueiredo, T., Loock, B., Pigaglio, S., Maillard, Ph., Grierson, D.S., Carrez, D., Croisy, A., Blais, J. (2003) Synthesis, cellular internalization and photodynamic activity of glucoconjugated derivatives of tri and tetra(meta-hydroxyphenyl)chlorins, *Bioorg. & Med. Chem. 11*, 1643-1652.
9. Laville, I., Pigaglio, S., Blais, J. C., Loock, B., Maillard, Ph., Grierson, D.S., Blais, J. (2004) A study of the stability of tri(glucosyloxyphenyl)chlorin, a sensitizer for photodynamic therapy, in human colon tumoural cells: a liquid chromatography and MALDI-TOF mass spectrometry analysis, *Bioorg. & Med. Chem. 12*, 3673-3682.
10. Laville, I., Pigaglio, S., Blais, J. C., Doz, F., Loock, B., Maillard, Ph., Grierson, D.S., Blais, J. (2006) Photodynamic Efficiency of Diethylene Glycol-Linked Glycoconjugated Porphyrins in Human Retinoblastoma Cells, *J. Med. Chem. 49*, 2558-2567.
11. Maillard, P., Loock, B., Grierson, D. S., Laville, I., Blais, J., Doz, F., Desjardins, L., Carrez, D., Guerquin-Kern, J. L., Croisy, A. (2007) In vitro phototoxicity of glycoconjugated porphyrins and chlorins in colorectal adenocarcinoma (HT29) and retinoblastoma (Y79) cell lines, *Photodiag. and Photody. Ther. 4*, 261-268.

Partie bibliographique

Article 1: Interest of Biomimetic Membranes Designed for the Evaluation of Photosensitizers Interaction with a Cell Membrane

Ali Makky and Véronique Rosilio

Etude bibliographique soumise

Interest of Biomimetic Membranes Designed for the Evaluation of Photosensitizers Interaction with a Cell Membrane

Ali Makky[a,b] and Véronique Rosilio[a,b]*

[a] Univ Paris-Sud 11, UMR 8612, Laboratoire de Physico-chimie des Surfaces, IFR 141, 5 rue Jean-Baptiste Clément, F-92296 Châtenay-Malabry cedex, France; [b] CNRS, UMR 8612, F-92296 Châtenay-Malabry, France.

* Corresponding author: veronique.rosilio@u-psud.fr

Dans cette partie, nous présentons une revue bibliographique qui décrit d'abord la photothérapie dynamique, ses applications, les principaux dérivés porphyriniques d'intérêt thérapeutique, l'altération de la composition membranaire des cellules induite par le cancer. Puis, nous faisons une synthèse des travaux sur les modèles biomimétiques artificiels utilisés pour l'analyse et la quantification des interactions photosensibilisateurs-membrane, avec leurs avantages et inconvénients par rapport aux cultures cellulaires.

Introduction

Therapeutic properties of light have been known for thousands of years. However, it is only recently that light has begun to be applied repeatedly in medicine and surgery, [1] dermatology and photodynamic therapy of many cancers, [1] Photodynamic therapy (PDT) is now considered as promising for the treatment of various diseases including superficial tumours such as basal cell carcinomas of the skin or head and neck tumours, as well as those accessible by endoscopy like oesophageal and lung cancers. [2] Moreover, due to its therapeutic efficacy and its fewer side effects compared to chemotherapy and radiotherapy, PDT is considered as an alternative treatment for some rare cancer types such as retinoblastoma. [3]

PDT involves the use of a nontoxic photosensitizing agent, which accumulates preferentially in neoplasic tissues. After a certain delay, the photosensitizer is excited with light of appropriate wavelength. In this state, its interaction with molecular oxygen results in the release of reactive oxygen species (ROS), especially singlet oxygen, which oxidize intracellular targets [4] and lead to irreversible damage and consecutive cell death [5] (Figure 2). However, the selectivity of photosensitizers towards tumour cells is often insufficient for PDT efficacy. Indeed, it has been demonstrated that in most cases, the ratio of sensitizer in a tumour tissue relative to the surrounding one is about 2:1, only. [6] In addition, singlet oxygen species have a very short lifetime (< 4 μs) and their diffusion length is 0.01 to 0.02 μm during this period. [7] Therefore, photodamage is limited to the sites of PS (photosensitizer) accumulation [8] which are usually the plasma membrane, mitochondria, golgi apparatus, lysosomes, endosomes and endoplasmic reticulum. [9] Consequently, photosensitizers uptake by cancer cells and their subcellular localization are crucial for efficient photochemistry. It is noteworthy that the affinity of a photosensitizer for a cell membrane is governed by its amphiphilic character, which is dependent on the regiochemical arrangement of the hydrophobic and hydrophilic substituents in its chemical structure. [10-11] In general, amphiphilic photosensitizers show a higher photodynamic activity than hydrophobic or hydrophilic molecules. [10-12] Thus, by modifying the amphiphily of a photosensitizer it could be possible to enhance its biological distribution. Another approach for improving photosensitizers uptake by cancerous cells consists in synthesizing photosensitizers bearing a specific substrate that is recognized by receptors at the tumour cell membrane surface. [13-16] Recently, efforts have been focused on the synthesis and *in vitro* evaluation of the

phototoxicity of a broad series of PS for targeting receptors over-expressed on cancer cells surface. Maillard *et al.* [15] have described a series of glycoconjugated tetraphenyl porphyrins for targeting sugar receptors in the Y79 retinoblastoma cell line. [13-14, 16-17] Also, Swamy *et al.*[18] have synthesized estradiol-tetraphenylporphyrin conjugates to target breast cancer cells naturally over-expressing the nuclear receptor for oestrogen.

Although a large number of photosensitizers has been applied with success in various clinical situations, the mechanisms of their recognition and penetration into a cell membrane remain unclear. [19] It is known that membrane composition in proteins and lipids, [20-21] and local pH [22] may be modified in cancer. It is thus important to evaluate the penetration properties of new drugs in conditions as close as possible to the *in vivo* situation. Culture cells experiments may provide evidence of mediated transport depending on the drugs and cells, and indicate the sub-localization of drugs. [13-14] Moreover, they allow testing the photodynamic efficacy of the photosensitizers. However, they cannot give information on the primary steps of the interaction, its mechanisms (especially if there is more than one), and its kinetics. Furthermore, as in the case of retinoblastoma, cell lines may be fragile and difficult to handle, especially when they need a high concentration of foetal calf serum (FCS) (>10%) to multiply. This could strongly affect the distribution of porphyrin derivatives in cell culture media and thus, their efficiency. Moreover, these cells grow as clusters in suspension in the culture media, [23] and drugs cannot diffuse properly towards cells located in the centre of these clusters.

It is thus necessary to resort to other strategies to better understand the mechanism of interaction of new photosensitizers with a cell membrane. In the choice of the appropriate model, it should be kept in mind that a biological membrane is not only a physical boundary, but also the functional unit that senses environmental conditions and recognizes other molecules. [24] Its constituents are organized into a complex structure controlling its properties. Systems with the full biological complexity cannot be reproduced and studied in great detail, as it is difficult to control and vary single parameters. To overcome this difficulty, more simple systems, such as lipid monolayers, [25-28] liposomes [29] and planar lipid bilayers [30] have been proposed to allow a better understanding of the interaction mechanisms taking place between photosensitizers and a cell membrane.

In this review, after a brief description of porphyrins derivatives designed for photodynamic therapy of cancers, and of the alteration of membrane composition in tumour cells, we focus on the use of artificial biomimetic membrane models and analytical tools for the study and quantification of porphyrins–membrane interaction, with their advantages and drawbacks.

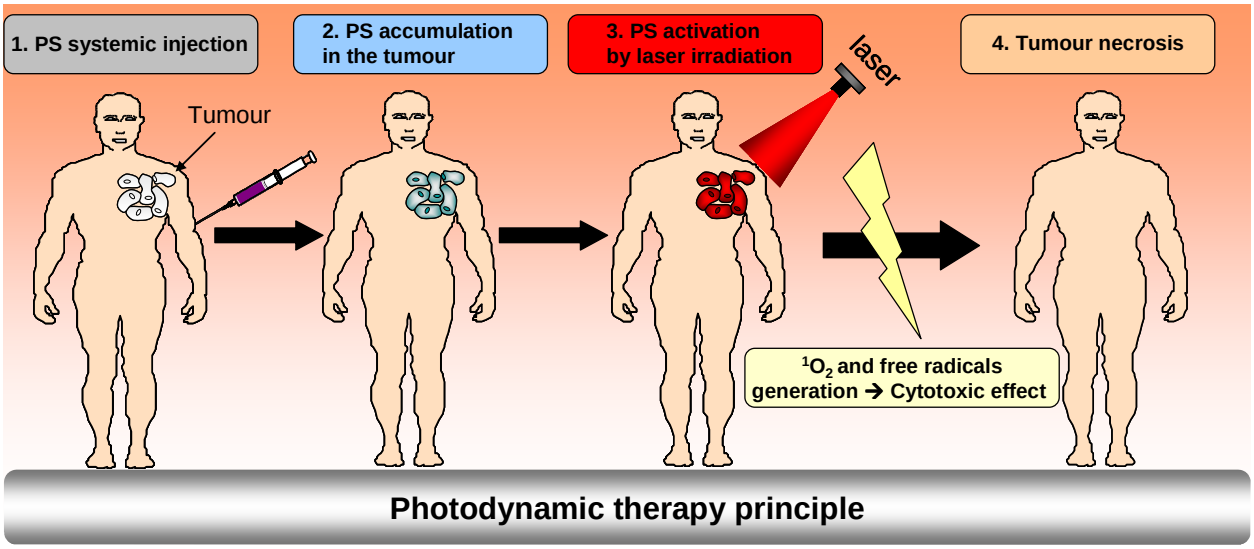

Figure 2: Principle stages of photodynamic therapy. A photosensitizer is injected intravenously (Stage I), accumulates in the tumour (Stage II) and is then activated by external illumination (Stage III). This induces cell damage and subsequent death.

Porphyrins derivatives in photodynamic therapy

The most explored class of photosensitizers in PDT today, is based upon porphyrin-like compounds with a tetrapyrrolic macrocyclic core providing the required photophysical properties. Among these photosensitizers, we find porphyrins, chlorins, bacteriocholins and phthalocyanines. [31-32] Although numerous compounds have been synthesized, modified and tested for their photophysical and physiological properties in PDT, only a few of them like Photofrin®, Visudyne® and Foscan® have been given legal approval by health agencies in a number of countries.

To this date, three generations of tetrapyrrolic photosensitizers have been proposed:

- The most popular compound of the first-generation of photosensitizers is a haematoporphyrin derivative (HpD) commercialised under the trade name Photofrin®. [33] It is a very complex mixture of approximately 60 porphyrin derivatives. Photofrin® is used for the treatment of a variety of malignancies such as oesophageal, papillary bladder, endobronchial cancers, basal and squamous cell carcinomas and Kaposi's sarcoma. However, it has many clinical limitations including poor tumour selectivity, long-lasting skin photosensitivity and weak absorbance of the red light resulting in limited tissue penetration.
- Following Photofrin®, a second generation of photosensitizers has been developed with improved characteristics. These compounds are pure, and most of them absorb red light and possess a high quantum yield of $^1O_2$. [34] In this generation, porphyrin derivatives such as *m*-THPP (meso-tetra-hydroxyphenyl-porphyrin), [33] chlorine

derivatives as *m*-THPC [31] (meso-tetra-hydroxyphenyl-chlorin also known as Foscan®), purpurins [35] and phthalocyanines [36] can be found. Although these compounds show improved pharmacokinetics properties compared to the compounds of the first generation, [37] they still present some limitations such as a poor water solubility and selectivity for tumour cells. [13-14]

- Recently, a third generation of photosensitizers has been designed for increasing their specificity. The chemical structure of these new compounds is derived from that of photosensitizers of the second generation with finely tuned properties that should allow selective delivery to tumour tissue. To achieve this goal, two main strategies have been chosen: porphyrin (i) pegylation, and (ii) linking to active substrates (saccharide, [38-40] monoclonal antibody, [41] estradiol, [18] folate [42]…). Porphyrins pegylation improves their water solubility, reduces their aggregation, [43] and lessens aggregates uptake by the reticuloendothelial system, thus increasing PS accumulation in tumours. [44] Glycoconjugation also improves porphyrin water solubility and amphiphilicity. Moreover, it can allow specific interaction of the resulting conjugates with lectinlike receptors expressed at the surface of certain malignant cells. [45-46] Many authors have demonstrated the efficiency of this strategy for improving cancerous cells targeting as well as *in vitro* phototoxicity. [13, 38-40, 47-49]

The chemical structures of some porphyrins derivatives are listed in Figure 3.

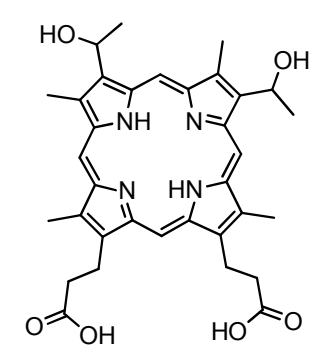

Haematoporphyrin

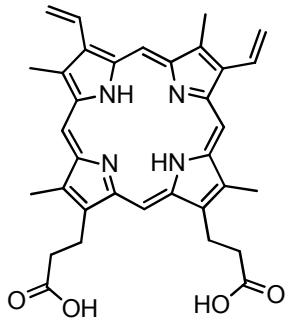

Protoporphyrin IX

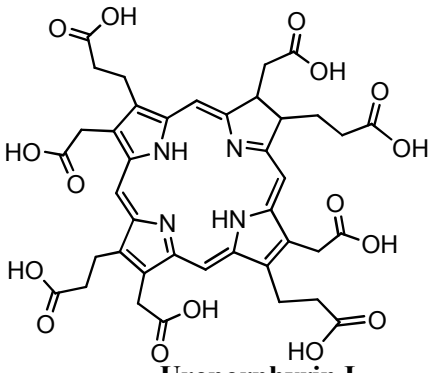

Uroporphyrin I

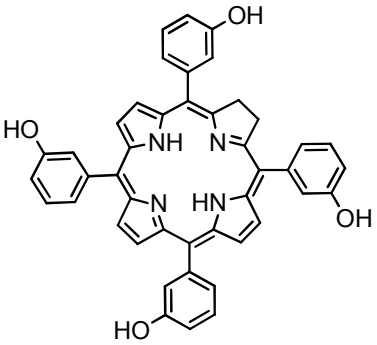

m-THPC (Foscan®)

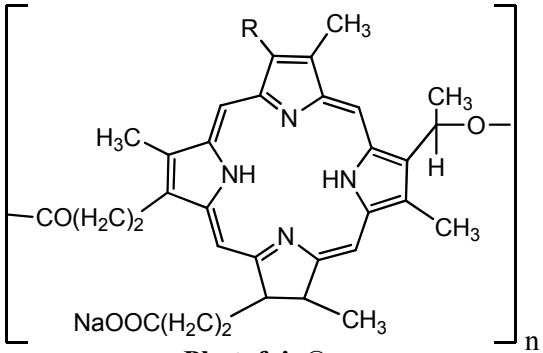

n = 0-6

R = HO—CH(CH$_3$)

or

R = —HC=CH$_2$

Photofrin®

Glycoconjugated porphyrins

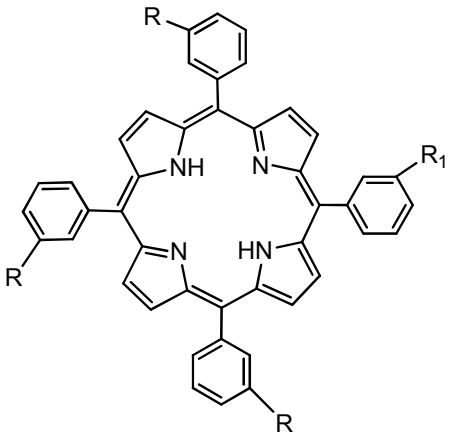

R$_1$=R=

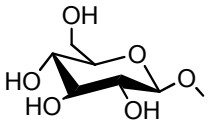

TPP(*m*-GluOH)$_4$

R$_1$=H **R=**

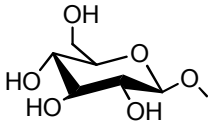

TPP(*m*-GluOH)$_3$

R$_1$=R= OH ***m*-THPP**

Pegylated porphyrins

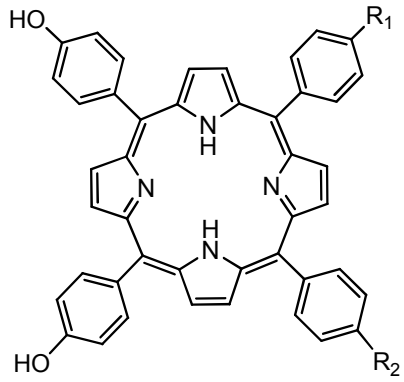

R$_1$=

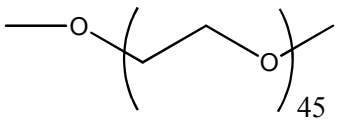

***p*-THPP-PEG-2000**

R$_2$= OH or

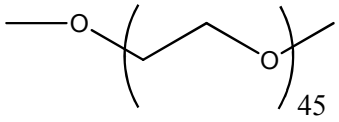

Figure 3: Examples of porphyrins derivatives whose interaction with artificial lipid membranes has been investigated.

Composition of mammalian cell membranes: Alteration in tumour cells.

Cell membranes are crucial to cell life. They define its boundaries and maintain the essential differences between cytosol and the extracellular environment. [24] They play many essential roles in a variety of cellular processes such as cell adhesion, ion channel conductance or cell signalling. They function as a selective permeability barrier, maintaining ion gradient across the membrane or controlling a drug penetration, but they also bear recognition sites for communication and interaction with other cells. [50]

Mammalian cell membranes consist of a lipid bilayer, in which proteins (receptors, transporters, or enzymes) are embedded. [51] Their lipid composition includes phospholipids, sphingolipids, glycolipids, and sterols [52] with cholesterol generally amounting to approximately 20 weight % of the total lipid content. [24] Four major phospholipids predominate - phosphatidylcholine, phosphatidylethanolamine, phosphatidylserine, sphingomyelin - and they constitute more than half the mass of lipid in most membranes. [50] They are asymmetrically distributed in the bilayer, with phosphatidylserine and phosphatidylethanolamine mainly located in the inner leaflet, [53] and phosphatidylcholine, sphingomyelin and glycolipids, in the outer one. This complex organization of lipids in cell membranes is crucial to maintain properties such as curvature and elasticity [54] as well as permeability. [55]

Numerous studies have shown that the lipid composition of cells is altered in cancer. [56-58] These alterations seem to affect the total cholesterol:phospholipid molar ratio [59] as well as the relative percentage and degree of saturation of phospholipid chains. [60] For example, Van Blitterswijk *et al.* [60] have reported a decrease in cholesterol membrane content in murine leukemic GRSL cells, with concomitant increase in lipids possessing unsaturated fatty acyl chains. These alterations have an impact on a number of important functions in plasma cell membranes. [61] However, there is no common pattern of alterations between different kinds of tumours. [20] Similar to the alteration in lipid composition of tumour cells membrane, the expression of a number of receptors located within their membranes can be also altered. Among these changes, we can mention the over-expression of LDL, [62-63] folate [64] and carbohydrate-based receptors. [45, 65] Some of cancerous cell membrane alterations are shown in Figure 4. Thus, as evoked in the previous section, the exploitation of membrane receptors as specific binding target could be a good strategy for selective delivery and accumulation of photosensitizers in cancerous cells.

1. Cholesterol content modifications

Cholesterol is a major constituent of mammalian cell membranes. It affects their physical properties, including lipid bilayer dynamics, phase behaviour, thickness, permeability and structure by modulating the packing of neighbouring phospholipid molecules. [24, 66-67] Cholesterol also plays a role in the activity of various integral proteins. It is not uniformly distributed among membranes: indeed, it can be found at concentrations around 10–30 mol% in plasma membranes, but also as high as 50 mol% in red blood cells [68] or even 70 mol% in ocular lens membranes. [69]

Any variation of cholesterol content in cell membranes alters their physical properties such as fluidity [70-71] and curvature. This has an impact on cellular functions [51] including carrier-mediated transport, endocytosis, as well as chemotherapeutic toxicity by alteration of membrane diffusion properties. [20, 72] Changes in cholesterol content can also affect drug–cell membrane interactions and thus the therapeutic efficacy of a drug. [73] Some authors have reported that cholesterol content could be significantly increased or decreased in cancer cells. For example, Liebes *et al.* observed a decrease in the cholesterol content of leukemic lymphocytes compared to normal ones, [74] whereas Calderon *et al.* who compared two prostatic cell lines with different metastatic potential, reported a higher cholesterol content in the highly metastatic one. [61] An increase in cholesterol content is suspected to play a role in multidrug resistance to chemotherapy. [20]

2. Phospholipids composition changes in tumour cell membranes

Phospholipid composition can also be altered in tumour cell membranes. Calderon *et al.* have observed a higher phosphatidylethanolamine level, and lower phosphatidylserine and phosphatidylinositol ones in highly metastatic prostatic carcinoma cells compared to less metastatic ones. [61] Merchant *et al.* [75] have also found elevated levels of phosphatidylethanolamine (+ 32%), phosphatidylinositol (+ 33%), and phosphatidylcholine plasmalogen (+ 25%), associated to a significant depression of lysophosphatidylcholine (- 44%) in malignant human breast compared to normal tissues.

3. Over-expression of cell surface receptors

The lipids are not the only components, which composition and distribution in the membrane may vary in cancer cells. Expression of cell surface receptors and proteins may also be altered. (Figure 4)

a. Over-expression of Low Density Lipoprotein (LDL) receptors

LDL is one of the five major groups of plasma lipoproteins (Chylomicrons, HDL, LDL, VLDL, IDL) that enable lipids (triglycerides, cholesterol) to be transported in the bloodstream. LDL particles are the major carriers of plasma cholesterol in humans. [76] LDL particles are recognized by a specific receptor (the apo B/E receptor), which results in rapid internalization and delivery of LDL particles to the lysosomal compartment of cells. [77] The major role of LDLs, as carriers of hydrophobic porphyrins in plasma was described by Reyfmann *et al.* [78] and Kessel *et al.* [79] Hydrophobic porphyrins are mainly carried in the blood by LDL particles and could thus be taken up by cells through the apo B/E receptor. It has been demonstrated that the expression of membrane receptors is elevated in tumour cells because of the increased need for exogenous cholesterol for membrane synthesis. [80-82] Consequently, it is thought that a porphyrin accumulation in tumours results from its delivery to cells via the LDL receptor pathway. [83-84] Candide *et al.* [85] have evaluated the selectivity of Photofrin II when complexed with LDLs on cultured fibroblasts, and they found that the presence of LDLs increased Photofrin II delivery to these cells. In another context, Schmidt-Erfurth *et al.* [86] have studied tumour accumulation and phototoxicity of Chlorin e6 (Ce6) free, complexed or covalently conjugated to LDLs, on retinoblastoma cell line culture (Y79) and fibroblast cells. They found that in both cell lines, the uptake of Ce6 covalently bound to LDL increased significantly (4 to 5 folds), compared to free Ce6 or Ce6 complexed with LDL. Moreover, these LDL conjugates were much more phototoxic. Interestingly, they demonstrated using competitive inhibition by free LDL that the accumulation of Ce6-LDL conjugates was receptor-mediated uptake. All these studies suggest an important role of LDLs in porphyrin uptake by cells, and support the hypothesis that LDLs may be responsible for selective accumulation of porphyrins in tumours. [84]

b. Over-expression of carbohydrate-based receptors in cancer cells membrane

Lectins are a family of carbohydrate-binding proteins of non-immune origin. Many lectins contain two or more sugar binding sites and can agglutinate cells and/or precipitate complex carbohydrate conjugates. They have been identified originally from plants and they have been used extensively for vertebrate cell surface characterization. Subsequently, different lectins have been isolated from various sources, such as bacteria and animals. [87-88]

The presence of lectin-like proteins in vertebrate tissue was observed 20 years ago. The first mammalian lectin was purified from liver. [89] Lectins of animal origin are often referred to as

endogenous lectins, to distinguish them from plant lectins. [87] It has been demonstrated that they are implicated in a variety of biological functions, such as the regulation of cell adhesion, immune defence, cell-matrix interaction and enzymatic activity. [90-91] They are also involved in endocytosis and intracellular traffic of glycoconjugates. [92] However, many studies have shown that the level of expression of endogenous lectins at the cell surface is significantly increased in cancer tissues [46, 93-94] and that they play key roles in the invasive capacity of cells, malignant transformation, tumour cell differentiation [95] and metastasis. [94] Thus, targeting endogenous lectins could be considered as a good strategy for enhancing drug selectivity toward cancer cells. [96-97] Following this direction, many authors have evaluated the effect of glycoconjugation on the efficiency and selectivity of photosensitizers in various cancerous cell lines. In particular, Zheng *et al.* have observed on rat thyroid cell lines, a considerable increase in the photosensitizing efficiency of purpurinimides conjugated with either galactose or lactose, compared to that of the free analogue. [48] Griegel *et al.* have investigated the expression of endogenous lectins in six human retinoblastoma cell lines, and they found that those cells exhibited a similar expression of endogenous sugar receptors with a preferential affinity for galactose and mannose residues. [65] Based on these data, Maillard *et al.* have studied the photoefficiency *in vitro* and *in vivo* of mannosylated and galactosylated tetrapyrrolic macrocycle photosensitizers for a potential PDT treatment of retinoblastoma. They have also analyzed the effect of porphyrin glycoconjugation, as well as the position of sugar moieties and length of the spacer separating the sugar from the tetrapyrrolic core, on photobiological activity. [13-14, 16, 98-99]

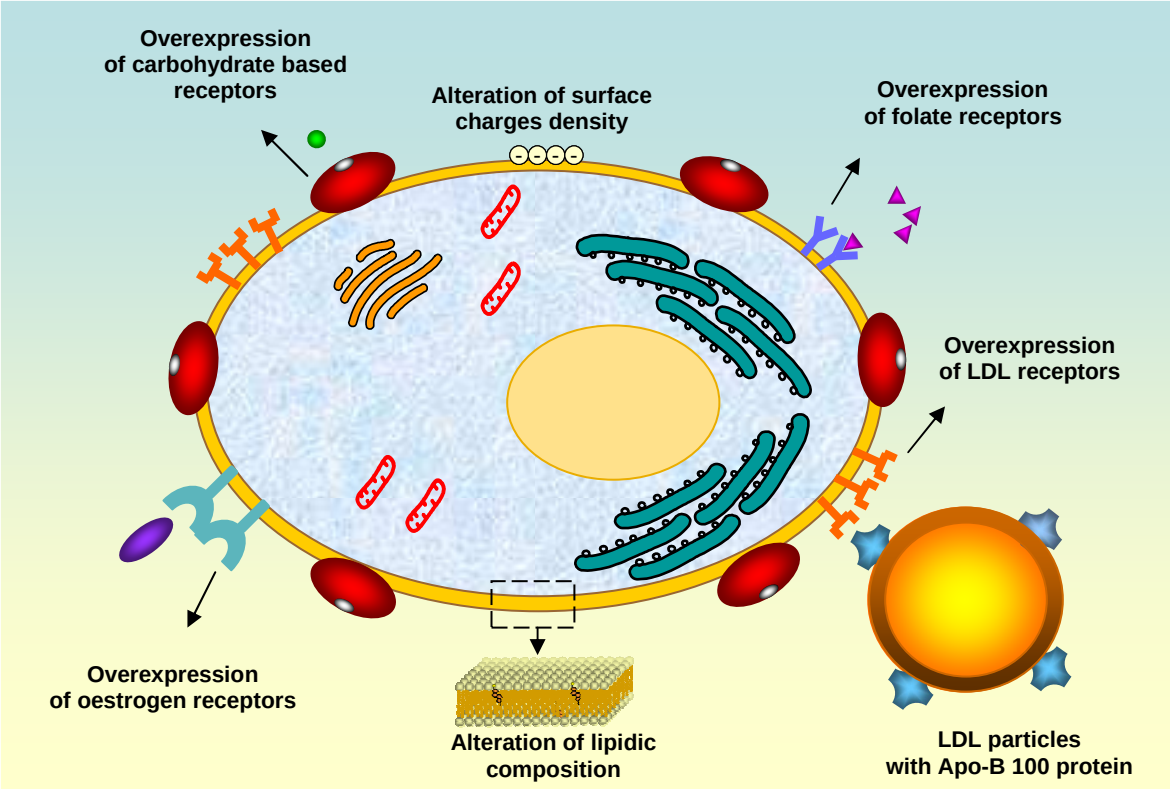

Figure 4: A schematic illustration of some alterations of cancerous cell membrane components.

Model membrane systems for studying drug-membrane interactions

Lipid membrane models are artificial lipid layers that can be classified in different types depending on their structure (monolayer or bilayer), their shape (planar or vesicular bilayers) and their mode of attachment (supported or suspended bilayers as black lipid membranes). Each membrane model has experimental advantages and disadvantages. Some of the most generally used systems for the assessment of drug interaction with a membrane are pictured in Figure 5.

1. Langmuir monolayers

A relatively simple method for studying and quantifying drug–membrane interactions is the use of planar monolayers also called Langmuir monolayers. They provide an organized interfacial structure, which is assumed to be similar to that found in biological membranes. [*100*],[*26*],[*28*] In the last decades, Langmuir monolayers have become a widespread method to characterize molecular interactions between drug candidates and a membrane. [*59, 101-107*] Although they do not reflect the complexity of biological membranes, lipid monolayers are

considered as convenient models because the nature, surface density, and packing of lipid molecules, as well as subphase composition, pH and temperature, can be finely controlled. [26, 28] Monolayers spread at the air / water interface can be analyzed by surface tension measurements, providing quantitative information on the influence of a drug on the stability, structure as well as on drug penetration kinetics. Affinity of a drug for a lipid membrane and its mixing properties to lipid components can also be assessed from the analysis of surface pressure-area isotherms. [27, 108] Moreover, considerable progress has been achieved to develop optical techniques such as fluorescence, [109-111] Brewster angle microscopy (BAM) [104, 112-115] and ellipsometric microscopy [116] to get a better insight into the organization of the amphiphilic molecules forming monolayers at the air-water interface. As to grazing incidence X-ray diffraction (GIXD), it allows determination of monolayer structure, [108] and gives information on the disorganizing effect of a drug on lipid domains. [108]

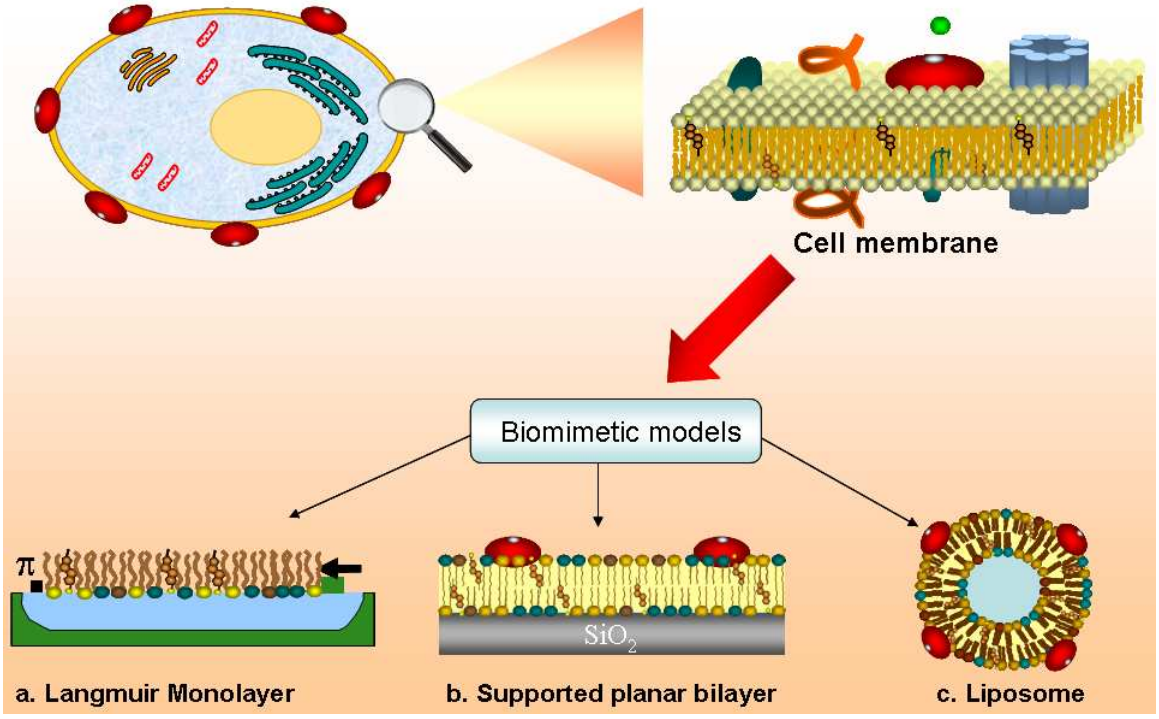

Figure 5: Schematic illustration of biomimetic models of a cell membrane.

2. Liposomes

Liposomes are vesicles in which an aqueous phase is entirely enclosed by one or several phospholipid bilayers. [117-118] According to the number of lipid layers and to vesicle size, liposomes can be classified as multilamellar vesicles (MLVs, 0.1–15 μm), [119] small unilamellar vesicles (SUVs, 25–50 nm), [120] large unilamellar vesicles (LUVs, 100 nm to 1

μm) [121] giant unilamellar vesicles (GUVs, 1.0–200 μm), and multi-vesicular vesicles (MVVs, 1.6–10.5 μm). [19, 122] Since the mid-seventies, considerable work has been devoted to use them as drug carriers. During the last decade only, many liposomal formulations have been proposed for carrying antibiotic, [123] antifungal, [124] oligonucleotide [125-126] or anticancer drugs [127] with the purpose of targeting them towards their cellular action site, thus enhancing their clinical effects, reducing their toxicity and, at the same time, protecting them from metabolism or immune responses. [128]

Long before being proposed as potential drug carriers, phospholipid vesicles were considered as a potential tool for modeling a biological cell. They allowed studying mechanical properties of lipid bilayers, [129-132] membrane adhesion and fusion, [133-135] membrane permeability to ions, [136] but also the effects of viscosity, surface charge density, cholesterol content or pH changes on the distribution of drugs in normal and cancerous tissues. [19] In addition, many works have reported on the interaction of membrane lipids with biomolecules such as DNA, [137] proteins [138] or drugs, [139] and more specifically, the evaluation of photosensitizers partitioning into vesicles. [140]

3. Planar bilayers

Following the pioneering work of Mc Connell *et al.*, [141] planar bilayers deposited on solid supports (SPBs) became very popular [142] for the study of fundamental membrane processes and biotechnological applications. [143-144] They have been proposed as biomimetic surfaces to elucidate the physical behaviour of cell membranes [145] and membrane-bound macromolecules, [146] but also for studying cell-cell recognition in the immune system [147] and cell adhesion. [148] A multitude of methods has been proposed for forming them, including Langmuir-Blodgett techniques, [149-150] and vesicles fusion on various preconditioned supports. [145, 151-154] Bilayers were also formed by adsorption of vesicles onto pre-formed phospholipids monolayers as described by Kalb *et al.* [155] Many efforts have been devoted to the improvement of SPB mimicking properties, by decoupling them from the underlying surface, thus creating an aqueous space between phospholipid headgroups and the substrate. [156-158] This may be achieved by forming the bilayer onto a *cushion* composed of a polymer or polyelectrolyte layer. [142] Such a layer may feature the cytoskeletal support found in mammalian cell membranes. [159-160] Currently, a variety of techniques including electrochemical impedance spectroscopy (EIS), fluorescence microscopy, QCM-D and atomic force microscopy (AFM), allow the analysis of SPBs properties. [145, 161]

These model membrane systems do not allow studying molecule transport since the supported bilayer is in close contact with a solid surface. Suspended bilayers seem more adequate systems for this purpose. The earliest model bilayer systems were suspended bilayers also known as "black lipid membranes". However, their persistence was very limited. Methods for forming artificially reconstituted freestanding planar lipid bilayers with increased stability have been developed. Suspended bilayers in the apertures of silicon or polymer substrates can by prepared by various techniques like spreading lipids in an organic solvent, or fusion of giant unilamellar vesicles. Typical long-term stability of these membranes may be in the order of several hours. Similar stabilities have been reported for lipid membranes formed on polycarbonate membranes with holes of 1 μm in diameter and microporous low density polyethylene or glass with hole sizes up to 500 μm. [*162-167*] These membranes allow electrophysiological studies of ion channels [*168*] and have also been proposed for pharmaceutical and sensor applications. [*152*]

Analytical Tools for the study and Quantification of Porphyrin–Membrane interactions

The development of techniques and methods for the analysis of membrane models is of great interest to medicinal chemists and pharmacologists. Indeed, the determination and quantification of the possible effects of drugs on membranes and *vice versa* can only be beneficial to the understanding of drug action. Correlating the structural properties of a studied drug with its effects on membranes with varying proteo-lipid compositions can lead to the conception of new compounds with enhanced activity. Although this concept was taken advantage of the assessment of many drugs, only a few papers dealing with the evaluation of photosensitizer-membrane interactions have been actually published from 1982 to 2010. In these studies, liposomes appeared as the preferred models. [*19*] (Figure 6 and
Table 1)

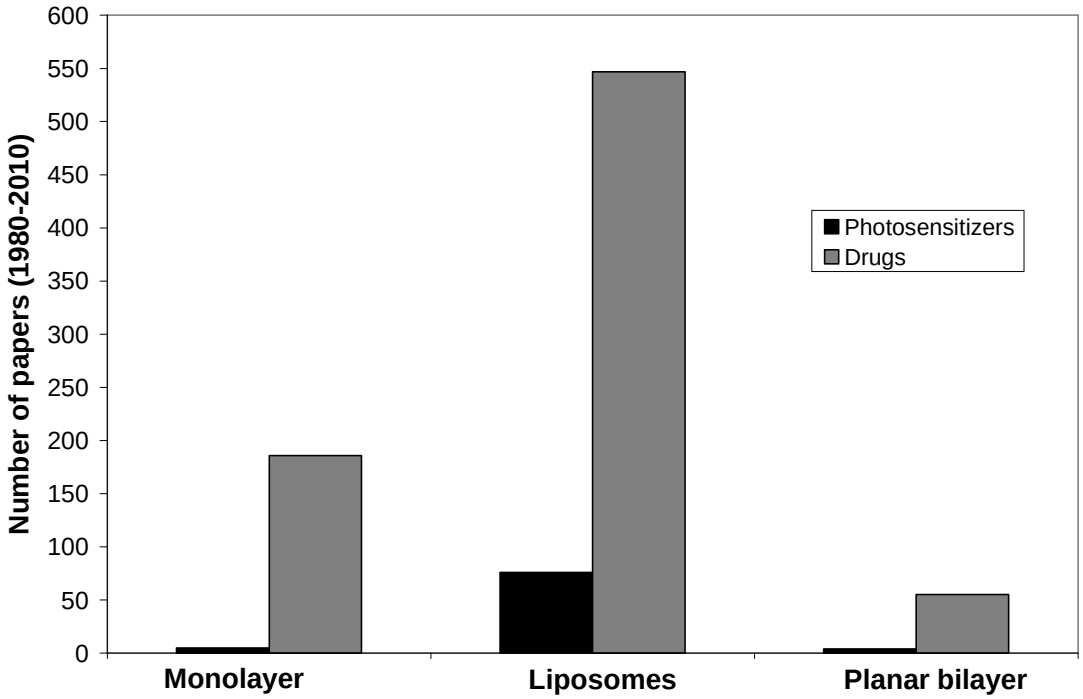

Figure 6 : The number of papers published in scientific literature from 1980 to 2010 describing experiments involving various lipid and membrane systems for the study of photosensitizers and other drugs are presented in black and grey columns, respectively. The data have been collected from *SciFinder*®.

1. Studies of Porphyrins–Membrane Interactions using phospholipid Monolayers

Many researchers have assessed the interaction of porphyrin derivatives with various phospholipids forming Langmuir monolayers by surface tension as well as by surface pressure measurements. This can be exemplified by the work of Desroches *et al.* [(103)] in which DSPC *(*distearylphosphatidylcholine) and DAPC (diarachidoylphosphatidylcholine) monolayers were used as models to evaluate the interaction of three phenylporphyrins derivatives: *m*-THPP a hydroxylated phenylporphyrin, *m*-TPP$(Glu)_3$ a triglucoconjugated phenylporphyrin and *m*-TPP$(Glu)_4$ a tetraglucoconjugated phenylporphyrin, with the cell membrane. Surface pressure measurements and grazing incidence X-ray diffraction showed that *m*-THPP and the asymmetric *m*-TPP$(Glu)_3$ which exhibited lower equilibrium surface tensions compared to *m*-TPP$(Glu)_4$, also interacted to a much larger extent with the studied phospholipids. Both porphyrin derivatives provoked a dramatic disorganization of the lipid monolayers. This effect was less significant with DAPC than with DSPC, probably due to the longer hydrophobic chains of DAPC, which could enhance phospholipid-phospholipid interactions, and limit to some extent porphyrin penetration into DAPC domains. [(103)] In a similar study, Hidalgo *et al.* [(113)] investigated the interaction of meso-tetraphenylporphyrin with DPPC and DPPG monolayers by forming mixed films of phospholipids-porphyrin with

varying porphyrin proportions (1, 2, 5, 10, 20, 50%). They used a Langmuir trough coupled with a Brewster angle microscope (BAM) for the analysis of Langmuir films, and UV-Vis spectroscopy for that of transferred layers onto solid substrates. They observed that porphyrin molecules at low surface densities and pressures provoked an expansion of DPPC and DPPG mixed monolayers, accounting for the interaction of TPP with these phospholipids. However, at high surface pressures, they observed a significant aggregation of TPP molecules into DPPC monolayers compared to DPPG ones, and suggested that the coexistence region of LE and LC phases exhibited different packing orders with segregation and accumulation of TPP at the boundaries. [*113*]

However, the models used in these two studies were far from reflecting the actual lipid composition of a tumour cell membrane. All studied phospholipids were saturated; Furthermore cholesterol was absent, although it is an essential constituent in cell membranes, which could have a crucial effect on porphyrin interaction and/or penetration. It seems thus more appropriate to build a biomimetic monolayer in which the phospholipid composition would be closer to that of a living cell, and containing cholesterol. To achieve this goal, it is necessary to select a specific cancer, as lipid composition varies from one tissue to another as previously mentioned.

2. Studies of Porphyrins–Membrane Interactions using liposomes

Liposomes have been widely used as models for the assessment of photosensitizers uptake by a cell membrane, [*19*] which was inferred from their bilayer/water partition coefficient [*169-172*] and their penetration depth in the membrane [*173-176*] deduced from fluorescence measurements and/or thermal analysis (DSC).

a. Fluorescence techniques

It is clear that fluorescence techniques have been privileged up to now for the assessment of photosensitizers interaction with a membrane, using liposomes as a model system. Indeed, photosensitizers are fluorescent molecules and their fluorescence is strongly dependent upon the nature of their environment, i.e. pH of the medium, ionic strength and polarity. For example for some porphyrins such as $TPPS_4$ (meso-tetraphenylporphine tetrasulfonate) the pH and the ionic strength determine the degree of its aggregation, which increases with acidity. [*177*] Moreover, the aggregation of photosensitizer molecules is often accompanied by spectral shifts or the appearance of new spectral bands due to the excitonic

interactions between chromophores. [178] Medium polarity also plays a crucial role on porphyrin derivatives, which are strongly aggregated in highly polar medium such as water. Conversely, in the presence of non-polar molecules such as lipids or proteins (albumin, lectin), disaggregation may occur upon formation of a non-covalent porphyrin-lipid or porphyrin-protein complex. A significant increase in fluorescence intensity follows. Thus, the determination of a photosensitizer binding constant (K_b) to membrane lipids can be assessed from the fluorescence enhancement induced by addition of increasing liposome concentrations in porphyrin solutions. [170]

As liposomes are supramolecular assemblies, and not just molecules or macromolecules (like proteins), some authors prefer to consider the membrane partition coefficient, in which water content in the liposome core is taken into account in the calculations. [169] Two experimental methods can be used to determine this coefficient. The first one consists in the centrifugation of liposome-photosensitizer mixtures to separate free aqueous drug molecules from liposome-bound ones. [19,179-180] Then, the photosensitizer concentration is determined spectrophotometrically in each separated phase. The second method, preferred by many authors, is based on the monitoring of fluorescence spectral changes upon photosensitizer titration with liposomes. [19] The gradual change in fluorescence intensity upon addition of the liposomes can be related to the gradual solubilisation of the drug within the liposomes. This yields the liposome/buffer partition coefficient (K_p) of photosensitizers.

Fluorescence spectroscopy also offers the possibility to determine the localization of the drug into the vesicles membrane. The insertion depth of a fluorophore into lipid bilayers can be assessed by two fluorescence-quenching techniques: the first one consists in injection in the aqueous phase of a heavy halogen ion like iodide or bromide, which cannot cross the lipid membrane (or only in a very limited way). Only the accessible photosensitizer molecules into the aqueous phase are quenched. This technique is considered as one of the simplest approaches to gain reliable information about the relative vertical depth of photosensitizer molecules into lipid bilayers. Another approach of fluorescence quenching called “parallax method” can be used for the same purpose. [181] This latter method is based on the use of two different membrane bound quenchers, which located at different depths in the bilayer. [181] There is complete quenching of a sensitiser if the quencher molecule is located within critical distance, whereas there is no quenching when the distance is larger. Some authors [175] have also used fluorescence emission polarization and/or anisotropy to determine the degree of rotational freedom of the fluorophore in the presence of liposomes. Thus, the liposome model allows multiple investigations of a dye-membrane interaction. (Figure 7)

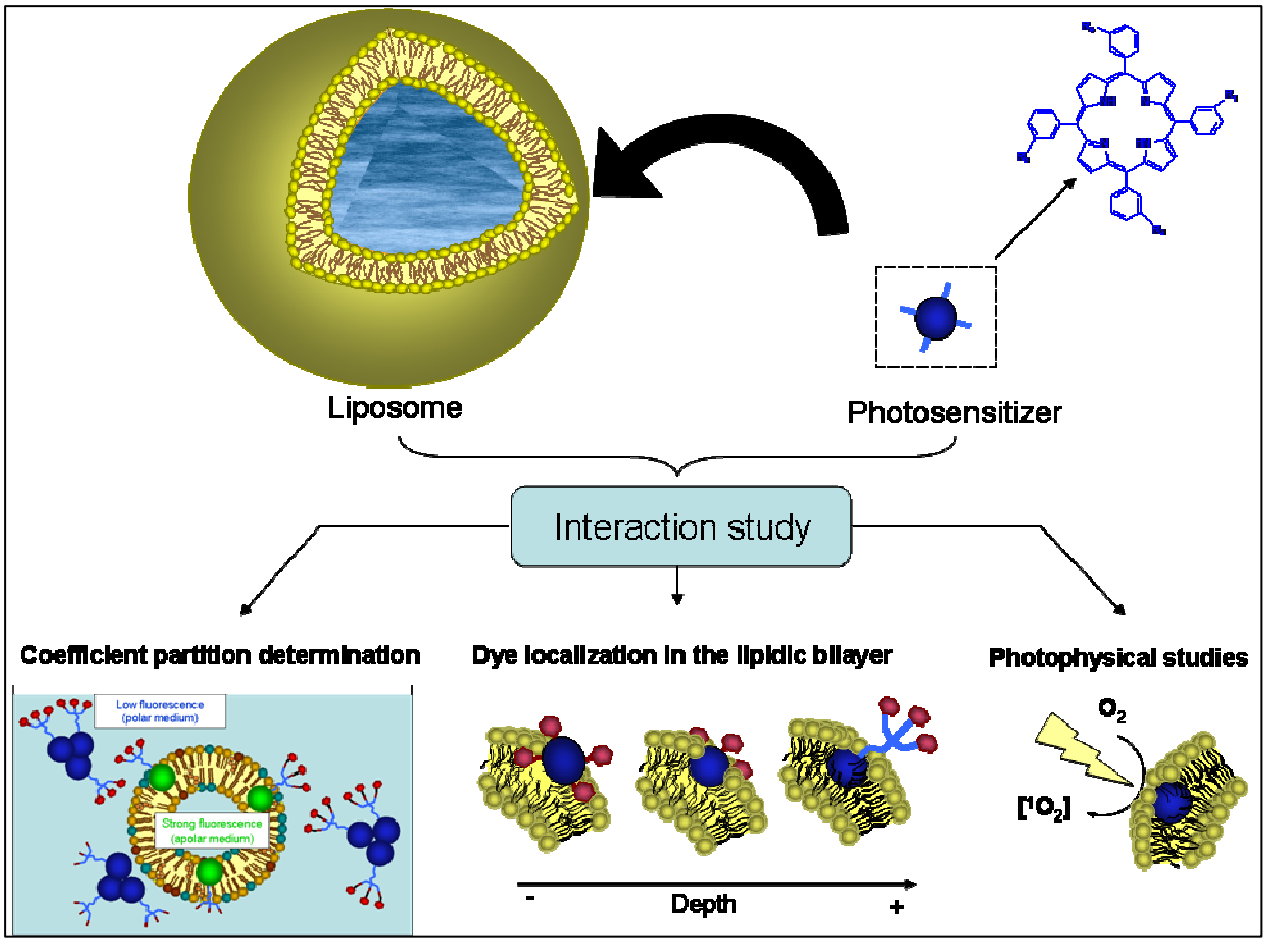

Figure 7: Interest of liposomes for the investigation of photosensitizer-membrane interaction.

Since the biodistribution of a photosensitizer as well as its penetration into cells are crucial for the efficiency of photodynamic therapy, [(14)] numerous works have been devoted to the study of the influence of parameters like lipid bilayer fluidity, phospholipids composition, cholesterol content, surface charge density, pH changes, and photosensitizer amphipathy, on the distribution properties of a photosensitizer in normal and tumour tissues. [(19)]

- Effect of amphipathy of photosensitizer molecules on their distribution into a membrane

The interaction of uroporphyrin (Up), haematoporphyrin (Hp), protoporphyrin (PP) (Figure 3) with a cell membrane has been studied by Ricchelli *et al.* [(175)] using unilamellar DPPC vesicles. They observed that the hydrophilic uroporphyrin did not significantly accumulate into liposome bilayers. They also observed that whereas protoporphyrin was located into the lipid matrix, haematoporphyrin remained into water accessible lipid regions. This was explained by the amphipathy of this compound that allowed its simultaneous interaction with phospholipid polar head groups *via* its polar acid groups, and phospholipid hydrophobic chains *via* its hydrophobic core. [(175)]

- Effect of cholesterol and lipid composition on porphyrin-liposomal membrane interaction

Membrane fluidity is considered as an essential factor influencing porphyrin binding properties to biological membranes. [175] Cholesterol is a determinant of the fluidity of eukaryotic plasma cell membranes. It also controls the fluidity of the outer mitochondrial membrane, while that of the inner one is regulated by cardiolipin, which generally enhances it. Thus, liposomes containing cholesterol or cardiolipin in their bilayers would better mimic the viscoelastic properties of a membrane than pure phospholipid ones. Literature shows that the presence of cholesterol in liposome bilayers has different effects on porphyrin association (binding constant) as well as penetration, depending on the molecular structure of the studied compound and liposome composition. For example, Ricchelli *et al*. have reported that the presence of cholesterol in DPPC vesicles could have different effects on the binding properties of haematoporphyrin (HP) and protoporphyrin (PP). They showed that whereas the presence of cholesterol (20% w/w) hindered haematoporphyin penetration and limited its distribution to the outer leaflet of the liposome bilayer, it favoured protoporphyrin distribution into the hydrophobic regions of the lipid matrix. [175] These authors attributed their results to distribution properties of cholesterol itself. Indeed, Ford *et al.* have demonstrated that below a critical concentration (15% mol), [182] cholesterol is almost equally distributed between the two leaflets of a DPPC bilayer. Above this concentration, it concentrates preferentially in the inner monolayer. Thus, a hydrophilic porphyrin such as HP, would dissolve more readily in the DPPC rich domains of the outer leaflet than in the inner one; the opposite behaviour was observed for PP (a more hydrophobic porphyrin), which was concentrated in the cholesterol-rich domains in the inner leaflet.

Using the same experimental approach, Kepczynski *et al.* [140] have determined the partition coefficient of HP and 5,10,15,20-tetrakis(4-hydroxyphenyl) porphyrin (*m*-THPP) using L-α-phosphatidylcholine (egg yolk PC) liposomes containing different cholesterol content (0-30 mol%). Contrary to their expectations, these authors found that the presence of cholesterol reduced the partitioning of both porphyrins into the liposomal bilayer in spite of the increase in hydrophobicity of the hydrocarbon region induced by the presence of cholesterol. Moreover, they have used three fluorescent molecular probes: Nile Red (a rotational probe for estimating bilayer fluidity in the polar region), 1,6-diphenyl-1,3,5-hexatriene (anisotropic probe for measuring fluidity of liposomal membrane in the acyl side-chain region) and pyrene (as hydrophobicity indicator of the hydrocarbon chain region near the polar region) to monitor membrane organization and dynamics upon increasing bilayers cholesterol content, and to understand its effect on porphyrin penetration. They have

concluded that the free volume of a bilayer rather than its hydrophobicity was a governing factor in porphyrin partitioning into lipid bilayers. [140]

Ehrenberg *et al.* [183] have compared the effect of lipid membrane composition (DMPC or DPPC) on the binding properties of Photofrin II and HP. They observed that Photofrin II was inserted less homogeneously but deeper in the bilayer than haematoporphyrin into both phospholipid bilayers. Increasing cholesterol content led to decreased association of both compounds to liposome membrane. [183] In addition, Lavi *et al.* [184] have assessed the relative depth of protoporphyrin derivatives in egg PC vesicles, and they found that addition of either cholesterol or DMPC, which are known to increase the order parameter of a lecithin bilayer and to rigidify it, moved the porphyrin deeper into the bilayer.

- Effect of liposome charge on porphyrin-membrane interactions

In another context, Voszka et *al.* [185] have investigated the effect of liposomes charge as well as that of the molecular structure of glycoconjugated tetraphenyl porphyrins (TPP) derivatives on their binding to DMPC and DMPC/DMPG (9:1 molar ratio) liposomes. With both liposome compositions, they found the highest binding constant for the asymmetrically substituted derivative, more lipophilic than the other compounds. They also observed that negatively charged liposomes enhanced the association of the symmetrically substituted hydrophilic porphyrins. [185] However, they did not give any explanation of this surprising phenomenon.

- Effect of solution electrolytes on porphyrin-membrane interactions

Minnes and coworkers [186] have studied the influence of different electrolytes on the association of haematoporphyrin to lecithin liposomes. They found that the presence of Mg^{2+} cations had a stronger effect than K^+ and Na^+ ones, and induced penetration of photosensitizer molecules from the aqueous phase into liposome bilayers by a salting-out process. They attributed their result to the chaotropic effect of ions on the structuring of water, which could in turn, have an impact on a photosensitizer solvatation in water, and affect its association to the liposome membrane. However, they did not take into account the effect of salts on lipid phase transition, [187] nor on liposome swelling and bilayer organization [188] which could strongly alter the interaction between the studied photosensitizers and the liposomal membrane.

- Effect of pH on porphyrin interactions with the lipid membrane

The acidic microenvironment, which has been observed in many tumours [22] is likely to play an important role on the selectivity of carboxylic porphyrins. [189] In addition, it has been suggested that the retention in cancer tissues of some photosensitizers such as Photofrin® is related to their increased lipophilicity at lower pH, due to the neutralization of their carboxylic groups. [190-191] Several authors have reported similar favouring effects of pH decrease on the incorporation of carboxylic derivatives (haematoporphyrin, deuteroporphyin) into DMPC vesicles, [192] DOPC vesicles [193] and vesicles containing unsaturated phospholipids with different chain lengths (14 to 22 carbons). [171]

- Other interaction studies investigated by fluorescence techniques

Added to the above described investigations, other interesting studies have been performed using liposomes as membrane models, like assessment of porphyrin distribution between lipid membranes and albumin (HSA), [194-195] or evaluation of photodamage induced by porphyrins irradiation, when they are incorporated into a lipid bilayer. [196-197]

b. Differential Scanning Calorimetry (DSC)

The use of thermal methods, especially DSC, is well established in the liposome field. Using the DSC technique, changes in phase transition properties can be measured as a function of phospholipid nature, chain length, cholesterol content, and any compound–lipid interactions. This technique is a very sensitive means for investigating alterations in bilayer packing caused by the presence of drugs. [198] For example, Cristani *et al.* [199] have shown that monoterpenes caused a decrease in DMPC liposome transition temperature, and have related this observation to the penetration of the lipophilic molecules into the ordered structure of the lipid bilayer. [199] Other researchers have used DPPC vesicles as skin model membranes and DSC, to investigate the mechanisms of enhanced skin drug delivery and the possible oxidant or antioxidant effect of certain materials. [200] Butler *et al.* have assessed by DSC the penetration of carvedilol (a β-adrenergic blocker) into DMPC/DMPG (9:1 molar ratio) liposomes. They found that this drug induced a decrease in the liposome pre-transition and transition temperatures, with unaffected enthalpy value of the main phase transition. They explained it by the penetration of carvedilol into the hydrophobic alkyl chains of the lipid bilayer. [201]

Thus, DSC can be considered as a good tool for the evaluation of drug association, as well as the level at which it takes place (i.e. phospholipid headgroups or hydrophobic chains). [100, 198] However, to our knowledge, only few researchers have used DSC to evaluate specifically photosensitizer interaction with a liposomal bilayer, and in the reported works, porphyrin molecules were already incorporated into the lipid film before hydration. For example, Voszka *et al.* [196] have prepared lamellar phases of DPPC/DOPC (7:3) incorporating two porphyrins TP(4-OGluOH)$_4$P or TPF5(4-OGalOH)$_3$P at a lipid/porphyrin molar ratio of 1000/1. [196] They found that the phase transition temperature was not influenced by the incorporation of porphyrins derivatives into the lipid bilayer; however they observed a significant increase in half-width ($T_{1/2}$) values indicating the decrease in cooperativity between carbohydrate chains. Combining these results with those of EPR spectroscopy, which gave estimations of liposome membrane fluidity, they demonstrated that the symmetrically substituted glycosylated porphyrins were localized closer to the membrane surface, whereas the asymmetrically substituted compound penetrated into deeper regions.
Furthermore, these authors have also studied the effect of symmetrically and asymmetrically glycoconjugated porphyrins incorporated into lamellar phases of DMPC or DMPC/DMPG (7/3 molar ratio) at the lipid/porphyrin molar ratio 20:1. They observed with both types of porphyrin and lipid composition, a destabilizing effect on the lipid layers. This effect was more significant for TP(4-OGluOH)$_3$ due to its stronger lipophilicity compared to the other compound. [185]

3. Studies of porphyrins–membrane interactions using supported planar lipid bilayer

a. Surface Plasmon resonance (SPR)

Surface plasmon resonance (SPR) is considered as one of the most important biochemical techniques for studying molecular interactions. This technique relies on the surface plasmon resonance phenomenon, which allows the real-time measurement of analyte binding to ligand-coated surfaces in a microfluidic system, without the application of a specific label. Indeed, this method is only dependent upon the change in adsorbed mass at the sensor surface. [202-203] The bimolecular interactions are studied at the surface of a “sensor chip”, a glass slide coated with a very thin layer of gold, where the surface plasmon resonance occurs. [203] In SPR, a polarized laser light is directed through a prism, which has a high refractive index, to the thin layer of gold that lies on the border with a medium of low refractive index. At a critical angle of incident light surface plasmons are generated at the

surface of the gold layer. Optical thickness of the formed layer is derived from the difference in refractive index between the adsorbed biomolecules and buffer. [203] Using commercial Biacore® sensor chips HPA and gold chips, it is possible to form various planar biomimetic membranes like: (i) a hybrid bilayer membrane (HBM) in which liposomes (usually SUV) injected over the surface fuse with alkanethiol molecules on the HPA chip and form a hybrid bilayer membrane, [204] or (ii) an immobilised membrane bilayer, tethered on the gold chip by thiolipids attached to the gold surface. [205] However, although these membranes have been used for many biochemical investigations, [203] no work using SPR has been reported yet on the interaction between porphyrins and membranes.

b. Quartz Crystal Microbalance-Dissipation (QCM-D)

QCM-D is a simple tool, which enables the quantification of deposited masses and characterization of their viscoelastic properties. This technique is based on measuring the resonance behaviour of a quartz crystal oscillator operating in shear mode. Due to its piezoelectric properties, the mechanical oscillation of the quartz can be excited by applying an oscillating electric field across the crystal. The resonance frequency is related to the mass of the crystal and thus, any mass added to or removed from the sensor induces a frequency shift (Δf) related to the change in adsorbed or removed mass (Δm). Simultaneously, QCM-D allows the measurement of the energy dissipation changes (ΔD) obtained from the rate of decay of the oscillation amplitude, when the driving power is turned off. ΔD values provide information on the viscoelastic properties of the adsorbed material. QCM-D has proven very valuable to study both the kinetics of SPB formation and its physical properties on a solid surface [153] and its interaction with a drug under aqueous flow. However, to our knowledge this technique has not yet been used for studying porphyrin interaction with a biomimetic membrane, probably for many reasons such as (i) the aggregation of porphyrin molecules in aqueous media which limits the number of monomers that can penetrate into the bilayer, (ii) the low molecular weight mass of porphyrins, which is below detection limits of the QCM-D apparatus, (iii) the necessity to couple QCM-D with complementary techniques such electrochemical impedance spectroscopy (EIS) for assessing bilayer resistance. [206]

c. Electrochemical measurements techniques

Among electrochemical measurements techniques, EIS (electrochemical impedance spectroscopy) and Ag-AgCl electrodes are the most used ones. In EIS, a voltage is applied

across the bilayer, and measurement of the resulting current gives information on the resistance of the membrane. A low resistance of the bilayer prior to the injection of a drug would indicate incomplete surface covering, or defects in leaflets that could affect the accuracy of the results. Following injection of a drug, the presence of even few nanometer-scale holes induced by drug-membrane interaction, would result in a dramatic decrease in bilayer resistance that could be detected by EIS or by other electrochemical measurement techniques such as Ag-AgCl electrodes.

Stozhkova *et al.* have formed a suspended planar bilayer (BLM) of L-α-phosphatidylcholine on holes 0.8 mm in diameter in a sheet of Teflon gauze to assess the membrane photodamage induced by illumination of a hematoporphyrin derivative (hematoporphyrin dimethyl ester). Using Ag-AgCl electrodes, they found that the illumination of the BLM in the presence of this photosensitizer caused an increase in conductivity ending with the rupture of the membrane. [*207*] The same results have been reported by Rokitskaya *et al.* [*208*] after irradiation of a BLM of soybean phosphatidylcholine (formed on a 0.4 mm diameter hole in a Teflon partition separating two aqueous compartments) in the presence of tri- and tetrasulfonated aluminium phtalocyanines. Moreover, they observed that the phtalocyanines did not produce any effect on the membrane conductance in the dark. Interestingly, they also reported that when Gramicidin A (an ionic channel) was incorporated into the BLM, the induced conductance by the presence of this ionic channel was almost completely blocked by irradiation of the BLM with a He-Ne laser in the presence of phthalocyanines. They related this result to a photomodification of gramicidin tryptophan residues, essential for its functioning. [*208*]

However in these studies, neither the photosensitizer binding constant nor its penetration into the bilayer was studied. They were only meant to give evidence of photosensitizer-induced photodamages in the phospholipid bilayer.

Biomimetic membrane model	Study/Determination	Techniques	References
Langmuir monolayers	PS penetration (or affinity) and mixing properties with membrane lipids	Langmuir trough (π-A) BAM, GIXD Tensiometer	(*103, 113, 209*)
Liposomes	Binding constant	Fluorescence spectrometry: (PS titration by liposomes)	(*140, 170, 183, 210-211*)
	PS penetration depth in lipid bilayers	Fluorescence spectrometry: Quenching using iodide ions or the parallax method. DSC	(*175-176, 184*) (*196*)
	Competition studies between liposomes and albumin	Fluorescence spectrometry: Measurements of fluorescence intensity	(*194-195*)
	Photophysical studies and evaluation of singlet oxygen quantum yield	Absorption or fluorescence spectroscopy 1,3-diphenylisobenzofuran (DPBF), 9,10-dimethylanthracene (DMA) probes or *p*-nitrosodimethylaniline (RNO)	(*19*)
	Membrane photodamage evaluation	Fluorescence spectroscopy: measurements of entrapped dye release after PS irradiation. DSC-EPR	(*197*) (*196*)
Planar bilayer	Interaction studies of drug with lipid membrane surface	QCM-D	----
	Suspended bilayers or supported planar bilayer on (tethered) polymers cushions: PS penetration and or membrane photodamage after dye irradiation.	EIS Ag/AgCl	--- (*207-208*)

Table 1: Some applications of biomimetic membrane models for studying photosensitizer-membrane interactions using different techniques.

Biomimetic membranes vs cells culture

Only few authors have evaluated the suitability of membrane models as a good tool to study the interaction between sensitizers and a cell plasma membrane, and they tried to find a correlation with their results and the interaction of these drugs *in vitro* with some membrane models. Using a "Stopped-flow" apparatus which allows rapid mixing (1.2 ms) of porphyrin and liposome solutions and observation of the resulting kinetic data, Bonneau *et al*. [(*212*)] have

found a correlation between the intracellular localization of two amphiphilic photosensitizers negatively charged at pH 7.4 : deuteroporphyrin (DP, bearing two carboxylic groups) and disulfonated aluminum phthalocyanine (AlPcS2a, bearing two sulfonate groups), and their association to dimyristoylphosphatidylcholine unilamellar vesicles. They found that DP crossed the lipid bilayer within seconds, whereas the transfer through the membrane was extremely slow for AlPcS2a. Furthermore, they observed by confocal microscopy that human fibroblasts HS68 showed a different localization of the two porphyrins; for DP, labelling was diffuse, whereas for AlPcS2a, it was punctuate. The authors concluded that DP molecules quickly entered the cells by passive diffusion and relocated into other intracellular membrane structures, in contrast to AlPcS2a molecules whose permanently charged sulfonate groups attached to the cell surface and restrained molecular diffusion across the membrane. Consequently, AlPcS2a was mostly internalized by bulk endocytosis. [212]

In another work, Laville *et al.* [13] have evaluated the phototoxicity of glucoconjugated tri- and tetra(meta-hydroxyphenyl)chlorins on HT29 human adenocarcinoma cells. They found that the tetra glucoconjugated chlorin, TPC(*m*-O-GluOH)$_4$ was poorly internalized and weakly photoactive. Conversely, the asymmetric and more amphiphilic compound TPC(*m*-O-GluOH)$_3$, exhibited high phototoxicity. Similar results have been obtained with glycoconjugated porphyrins by Desroches *et al.* [103] and Csik *et al.* [213] using phospholipids monolayers and DMPC liposomes as membrane models, respectively. Both groups have demonstrated the absence of interaction in the case of tetraglycoconjugated compounds, but a strong interaction between triglycosylated amphiphilic compounds and membrane models.

In contrast, Ben-Dror and coworkers [170] could not find any clear correlation between the binding constant (K_b) to L-α-phosphatidylcholine liposomes of porphyrins derivatives with various amphiphilicities, and their uptake by CT26 mouse colon adenocarcinoma cells. Such discrepancy in results between cell culture studies and biophysical measurements using membrane models could be related to the differences in lipid composition of liposomes and cells, which might influence drugs uptake differently. Thus, choosing membrane models having a lipid composition similar to that in plasma cell membranes seems crucial to obtain good correlations.

Advantages and drawbacks of biomimetic models of cell membranes

Biomimetic models of cell membranes have been developed in order to study the interaction of drugs, peptides and membrane proteins in a functional manner. These membranes present many advantages over the use of cells culture to study drugs interaction.

1. Advantages:

Biomimetic models are easy to form and their composition can be varied in a controlled manner. They allow performing experiments under conditions in which cells would not survive, such as the absence of an adequately supplemented culture medium, and the variation of pH, ionic strength, medium composition or drug concentration. The results obtained using these systems are independent of biological variability. Another advantage is that they use very small amounts of materials, which is noteworthy when studying newly synthesized drugs or isolated proteins.

All three models described in this review are complementary from one another, as they allow studying drug binding and diffusion, non-specific interactions and molecular recognition mechanisms at different levels: (i) the microscale (liposome), (ii) the nanoscale (planar bilayer, monolayer), and (iii) the molecular level (monolayer); Furthermore, monolayers and planar bilayers provide *in situ* monitoring of the changes produced in the membrane during its interaction with an exogenous compound. Kinetics of interactions can thus be determined.

2. Drawbacks:

Whatever the level of sophistication that can be reached with a model system (lipid composition, protein reconstitution), and despite all the above-mentioned advantages, it is important to keep in mind that such a system remains an artificial imperfect model, and can only be complementary to cell cultures experiments. It cannot replicate all the complexity of a cell membrane, and mimic a whole cellular uptake process. If the composition of a cell membrane at a very local level can be approached, still the whole cell machinery behind it is missing. If model systems are developing very fast, especially since tools allowing formation and analysis of supported and suspended planar bilayers have been improved, it is still difficult to reconstitute in these membranes heavy transmembrane proteins or receptors (all the more when they have not been isolated yet), to reproduce the active process of endocytosis [(28)] and evaluate the role of biological transporters implicated in drugs transport

such as albumin and LDL, which are efficient carriers for photosensitizers. [83-84] When the system becomes too complex, the reliability of results obtained by physical measurements may be compromised. This is an important limitation. However, the possibility of taking apart the various components of an interacting system, and investigate the molecular and dynamic changes produced in the membrane during the interaction remains promising. Moreover, when it is done while progressively making the system more complex (by adding one by one more and more components), it might allow, step by step, getting a better correlation between drugs-membrane model interaction and actual cellular interaction and therapeutic efficacy.

Conclusion

Biomimetic model systems (Langmuir monolayer, liposomes, planar bilayer) are useful tools for the investigation of drugs-membrane interaction because they offer the possibility to overcome the complexity of biological membranes, which restrict their direct investigation at the nanoscale. However at the same time, because of their imperfection, correlation remains sometimes difficult to establish between results obtained using these models and data provided by *in vitro* cell cultures experiments. The composition of a model membrane is usually much too simple to mimic the complexity of a membrane. The liposome bilayer for example, which is the most described system for assessing photosensitizer-membrane interactions, is formed, at best, of two phospholipids or of a phospholipid and cholesterol. Thus, despite the great interest of these models in biophysical studies, they are still considered as a retrospective approach to drug-membrane investigation, and very often, studies involving these systems are led only after *in vitro* and *in vivo* evaluation of drugs, when they should precede them. Without reaching a level of complexity compromising the achievement of accurate results, it is possible to envision more complex systems, in which lipids with different molecular structures and charges would coexist in a controlled manner. Furthermore, when the case applies, a protein involved in the recognition process could be incorporated into the system so that the whole interaction (non-specific and specific) is taken into account. This would considerably increase the credibility of such systems. Many attempts have been made to reach this level of complexity, but the methodology has to be carefully developed. Thus, efforts should continue to gain satisfying prediction of the behaviour of a drug in contact with a biological membrane. Lipid membrane models could then become a powerful and inexpensive tool for (i) understanding the critical role of biological membrane composition and dynamics in cellular uptake, (ii) analysing the mechanisms of drug transport,

(iii) predicting toxicity of drugs, and eventually (iv) optimizing efficient drug delivery systems in photodynamic therapy.

References

1. Ackroyd, R., Kelty, C., Brown, N., and Reed, M. (2001) The History of Photodetection and Photodynamic Therapy&para, *Photochemistry and Photobiology 74*, 656-669.
2. Dolmans, D. E., Fukumura, D., and Jain, R. K. (2003) Photodynamic therapy for cancer, *Nat Rev Cancer 3*, 380-387.
3. Stephan, H., Boeloeni, R., Eggert, A., Bornfeld, N., Schueler, A. (2008) Photodynamic Therapy in Retinoblastoma: Effects of Verteporfin on Retinoblastoma Cell Lines, *Invest. Ophthalmol. Vis. Sci. 49*, 3158-3163.
4. Ochsner, M. (1997) Photophysical and photobiological processes in the photodynamic therapy of tumours, *Journal of Photochemistry and Photobiology B: Biology 39*, 1-18.
5. van Hillegersberg, R., Kort, W. J., Wilson, J. H. (1994) Current status of photodynamic therapy in oncology, *Drugs 48*, 510-527.
6. Klyashchitsky, B. A., Nechaeva, I. S., and Ponomaryov, G. V. (1994) Approaches to targetted photodynamic tumor therapy, *Journal of Controlled Release 29*, 1-16.
7. Hatz, S., Lambert, J. D., and Ogilby, P. R. (2007) Measuring the lifetime of singlet oxygen in a single cell: addressing the issue of cell viability, *Photochem Photobiol Sci 6*, 1106-1116.
8. Dougherty, T. J., Gomer, C. J., Henderson, B. W., Jori, G., Kessel, D., Korbelik, M., Moan, J., and Peng, Q. (1998) Photodynamic therapy, *J Natl Cancer Inst 90*, 889-905.
9. Buytaert, E., Dewaele, M., and Agostinis, P. (2007) Molecular effectors of multiple cell death pathways initiated by photodynamic therapy, *Biochimica et Biophysica Acta (BBA) - Reviews on Cancer 1776*, 86-107.
10. Margaron, P., Gregoire, M. J., Scasnar, V., Ali, H., and van Lier, J. E. (1996) Structure-photodynamic activity relationships of a series of 4-substituted zinc phthalocyanines, *Photochem Photobiol 63*, 217-223.
11. Boyle, R. W., and Dolphin, D. (1996) Structure and biodistribution relationships of photodynamic sensitizers, *Photochem Photobiol 64*, 469-485.
12. Wiehe, A., Simonenko, E. J., Senge, M. O., and RÖder, B. (2001) Hydrophilicity vs hydrophobicity - varying the amphiphilic structure of porphyrins related to the photosensitizer m-THPC, *Journal of Porphyrins and Phthalocyanines 5*, 758-761.
13. Laville, I., Figueiredo, T., Loock, B., Pigaglio, S., Maillard, Ph., Grierson, D.S., Carrez, D., Croisy, A., Blais, J. (2003) Synthesis, cellular internalization and photodynamic activity of glucoconjugated derivatives of tri and tetra(meta-hydroxyphenyl)chlorins, *Bioorg. & Med. Chem. 11*, 1643-1652.
14. Laville, I., Pigaglio, S., Blais, J. C., Doz, F., Loock, B., Maillard, Ph., Grierson, D.S., Blais, J. (2006) Photodynamic Efficiency of Diethylene Glycol-Linked Glycoconjugated Porphyrins in Human Retinoblastoma Cells, *J. Med. Chem. 49*, 2558-2567.
15. Maillard, P., Loock, B., Grierson, D. S., Laville, I., Blais, J., Doz, F., Desjardins, L., Carrez, D., Guerquin-Kern, J. L., Croisy, A. (2007) In vitro phototoxicity of glycoconjugated porphyrins and chlorins in colorectal adenocarcinoma (HT29) and retinoblastoma (Y79) cell lines, *Photodiag. and Photody. Ther. 4*, 261-268.
16. Ballut, S., Makky, A., Loock, B., Michel, J. P., Maillard, P., Rosilio, V. (2009) New strategy for targeting of photosensitizers. Synthesis of glycodendrimeric phenylporphyrins, incorporation into a liposome membrane and interaction with a specific lectin, *Chem Commun* 224-226.
17. Croisy, A., Lucas, B., and Maillard, P. (2005) Les macrocycles tétrapyrroliques glycoconjugués., *Actualités de chimie thérapeutique 31*, 181-244.
18. Swamy, N., James, D. A., Mohr, S. C., Hanson, R. N., and Ray, R. (2002) An estradiol-Porphyrin conjugate selectively localizes into estrogen receptor-Positive breast cancer cells, *Bioorganic & Medicinal Chemistry 10*, 3237-3243.
19. Hoebeke, M. (1995) The importance of liposomes as models and tools in the understanding of photosensitization mechanisms, *J. Photochem. and Photobiol. B. Biol. 28*, 189-196.
20. Hendrich, A. B., and Michalak, K. (2003) Lipids as a target for drugs modulating multidrug resistance of cancer cells, *Curr Drug Targets 4*, 23-30.
21. Wojtyk, J. T. C., Goyan, R., Gudgin-Dickson, E., and Pottier, R. (2006) Exploiting tumour biology to develop novel drug delivery strategies for PDT, *Medical Laser Application 21*, 225-238.

22. Tannock, I. F., and Rotin, D. (1989) Acid pH in tumors and its potential for therapeutic exploitation, *Cancer Res 49*, 4373-4384.
23. McFall, R. C., Sery, T. W., and Makadon, M. (1977) Characterization of a new continuous cell line derived from a human retinoblastoma, *Cancer Res 37*, 1003-1010.
24. Sackmann, E. (1995) Biological membranes architecture and function, In *Handbook of Biological Physics* (Lipowsky, R., and Sackmann, E., Eds.), pp 1-63, North-Holland.
25. Maget-Dana, R. (1999) The monolayer technique: a potent tool for studying the interfacial properties of antimicrobial and membrane-lytic peptides and their interactions with lipid membranes, *Bioch. et Biophy. Acta (BBA) - Biomembranes 1462*, 109-140.
26. Brockman, H. (1999) Lipid monolayers: why use half a membrane to characterize protein-membrane interactions?, *Curr. Opin. in Struct. Biol. 9*, 438-443.
27. Brezesinski, G., and Möhwald, H. (2003) Langmuir monolayers to study interactions at model membrane surfaces, *Adv. in Colloid and Interface Sci. 100-102*, 563-584.
28. Peetla, C., Stine, A., and Labhasetwar, V. (2009) Biophysical interactions with model lipid membranes: applications in drug discovery and drug delivery, *Mol Pharm 6*, 1264-1276.
29. Eytan, G. D. (1982) Use of liposomes for reconstitution of biological functions, *Bioch. et Biophy. Acta (BBA) - Rev. on Biomembranes 694*, 185-202.
30. Tamm, L. K., and McConnell, H. M. (1985) Supported phospholipid bilayers, *Biophys. J. 47*, 105-113.
31. Phillips, D. (1995) The photochemistry of sensitisers for photodynamic therapy, *Pure & Appl. Chern 67*, 117-126.
32. Bonnett, R. (1995) Photosensitizers of the porphyrin and phthalocyanine series for photodynamic therapy, *Chem. Soc. Rev. 24*, 19-33.
33. Allison, R. R., Downie, G. H., Cuenca, R., Hu, X.-H., Childs, C. J. H., and Sibata, C. H. (2004) Photosensitizers in clinical PDT, *Photodiagnosis and Photodynamic Therapy 1*, 27-42.
34. Detty, M. R., Gibson, S. L., and Wagner, S. J. (2004) Current clinical and preclinical photosensitizers for use in photodynamic therapy, *J Med Chem 47*, 3897-3915.
35. Morgan, A. R., Garbo, G. M., Keck, R. W., and Selman, S. H. (1988) New photosensitizers for photodynamic therapy: combined effect of metallopurpurin derivatives and light on transplantable bladder tumors, *Cancer Res 48*, 194-198.
36. Moan, J., and Berg, K. (1992) Photochemotherapy of cancer: experimental research, *Photochem Photobiol 55*, 931-948.
37. Ferrand, Y., Bourré, L., Simonneaux, G., Thibaut, S., Odobel, F., Lajat, Y., and Patrice, T. (2003) Hydroporphyrins as tumour photosensitizers: synthesis and photophysical studies of 2,3-Dihydro-5,15-di(3,5-dihydroxyphenyl) porphyrin, *Bioorganic & Medicinal Chemistry Letters 13*, 833-835.
38. Maillard P, G. J., Momenteau M, Gaspard S. (1989) Glycoconjugated Tetrapyrrolic Macrocycles, *J. Am. Chem. Soc. 111*, 9125-9127.
39. Momenteau, M., Maillard, P., De Belinay, M. A., Carrez, D., Croisy, A. (1999) Tetrapyrrolic glycosylated macrocycles for an application in PDT, *J. Biomed. Opt. 4*, 298-318.
40. Chen, X., Hui, L., Foster, D. A., and Drain, C. M. (2004) Efficient Synthesis and Photodynamic Activity of Porphyrin-Saccharide Conjugates: Targeting and Incapacitating Cancer Cells†, *Biochemistry 43*, 10918-10929.
41. Vrouenraets, M. B., Visser, G. W., Stigter, M., Oppelaar, H., Snow, G. B., and van Dongen, G. A. (2002) Comparison of aluminium (III) phthalocyanine tetrasulfonate- and meta-tetrahydroxyphenylchlorin-monoclonal antibody conjugates for their efficacy in photodynamic therapy in vitro, *Int J Cancer 98*, 793-798.
42. Schneider, R., Schmitt, F., Frochot, C., Fort, Y., Lourette, N., Guillemin, F., Müller, J.-F., and Barberi-Heyob, M. (2005) Design, synthesis, and biological evaluation of folic acid targeted tetraphenylporphyrin as novel photosensitizers for selective photodynamic therapy, *Bioorganic & Medicinal Chemistry 13*, 2799-2808.
43. Nawalany, K., Rusin, A., Kepczynski, M., Mikhailov, A., Kramer-Marek, G., Snietura, M., Poltowicz, J., Krawczyk, Z., and Nowakowska, M. (2009) Comparison of photodynamic efficacy of tetraarylporphyrin pegylated or encapsulated in liposomes: In vitro studies, *Journal of Photochemistry and Photobiology B: Biology 97*, 8-17.
44. Hamblin, M. R., Miller, J. L., Rizvi, I., Loew, H. G., and Hasan, T. (2003) Pegylation of charged polymer-photosensitiser conjugates: effects on photodynamic efficacy, *Br J Cancer 89*, 937-943.
45. Monsigny, M., Roche, A. C., and Midoux, P. (1988) Endogenous lectins and drug targeting, *Ann N Y Acad Sci 551*, 399-413; discussion 413-394.
46. Lotan, R., and Raz, A. (1988) Lectins in cancer cells, *Ann N Y Acad Sci 551*, 385-398.

47. Mikata, Y., Onchi, Y., Tabata, K., Ogura, S.-i., Okura, I., Ono, H., and Yano, S. (1998) Sugar-dependent photocytotoxic property of tetra- and octa-glycoconjugated tetraphenylporphyrins, *Tetrahedron Letters 39*, 4505-4508.
48. Zheng, G., Graham, A., Shibata, M., Missert, J. R., Oseroff, A. R., Dougherty, T. J., and Pandey, R. K. (2001) Synthesis of β-Galactose-Conjugated Chlorins Derived by Enyne Metathesis as Galectin-Specific Photosensitizers for Photodynamic Therapy, *The Journal of Organic Chemistry 66*, 8709-8716.
49. Sylvain, I., Zerrouki, R., Granet, R., Huang, Y. M., Lagorce, J. F., Guilloton, M., Blais, J. C., and Krausz, P. (2002) Synthesis and biological evaluation of thioglycosylated porphyrins for an application in photodynamic therapy, *Bioorganic & Medicinal Chemistry 10*, 57-69.
50. Alberts B., J. A. L. J., Raff M., Roberts K., Walter P. (2008) Membrane structure, In *Molecular biology of the cell* (Alberts, B., Ed.) 5th reference ed ed., pp 617-629.
51. Spector, A. A., and Yorek, M. A. (1985) Membrane lipid composition and cellular function, *J Lipid Res 26*, 1015-1035.
52. Seydel, P. D. J. K. (2003) Drug-Membrane Interaction and Pharmacokinetics of Drugs, In *Drug-Membrane Interactions* (Prof. Dr. Joachim K. Seydel, P. D. M. W., Ed.), pp 141-215.
53. Redelmeier, T. E., Hope, M. J., and Cullis, P. R. (1990) On the mechanism of transbilayer transport of phosphatidylglycerol in response to transmembrane pH gradients, *Biochemistry 29*, 3046-3053.
54. Markin, V. S. (1981) Lateral organization of membranes and cell shapes, *Biophysical Journal 36*, 1-19.
55. Seydel, P. D. J. K. (2003) Drug-Membrane Interactions and Pharmacodynamics, In *Drug-Membrane Interactions* (Prof. Dr. Joachim K. Seydel, P. D. M. W., Ed.), pp 217-289.
56. Negendank, W. (1992) Studies of human tumors by MRS: a review, *NMR Biomed 5*, 303-324.
57. Merchant TE, d. G. P., Minsky BD, Obertop H, Glonek T. (1993) Esophageal cancer phospholipid characterization by 31P NMR., *NMR in Biomed. 6*, 187-193.
58. Leach, M. O. (1996) Introduction to in vivo MRS of cancer: new perspectives and open problems, *Anticancer Res 16*, 1503-1514.
59. Preetha, A., Huilgol, N., and Banerjee, R. (2006) Comparison of paclitaxel penetration in normal and cancerous cervical model monolayer membranes, *Colloids Surf. B: Biointerfaces 53*, 179-186.
60. van Blitterswijk, W. J., de Veer, G., Krol, J. H., and Emmelot, P. (1982) Comparative lipid analysis of purified plasma membranes and shed extracellular membrane vesicles from normal murine thymocytes and leukemic GRSL cells, *Bioch. et Biophys. Acta (BBA) - Biomembranes 688*, 495-504.
61. Calderon, R. O., Grogan, W. M., and Collins, J. M. (1991) Membrane Structural Dynamics of Plasma-Membranes of Living Human Prostatic-Carcinoma Cells Differing in Metastatic Potential, *Exp Cell Res 196*, 192-197.
62. Ho, Y. K., Smith, R. G., Brown, M. S., and Goldstein, J. L. (1978) Low-density lipoprotein (LDL) receptor activity in human acute myelogenous leukemia cells, *Blood 52*, 1099-1114.
63. Gal, D., MacDonald, P. C., Porter, J. C., and Simpson, E. R. (1981) Cholesterol metabolism in cancer cells in monolayer culture. III. Low-density lipoprotein metabolism, *Int J Cancer 28*, 315-319.
64. Garin-Chesa, P., Campbell, I., Saigo, P. E., Lewis, J. L., Jr., Old, L. J., and Rettig, W. J. (1993) Trophoblast and ovarian cancer antigen LK26. Sensitivity and specificity in immunopathology and molecular identification as a folate-binding protein, *Am J Pathol 142*, 557-567.
65. Griegel, S., Rajewsky, M. F., Ciesiolka, T., Gabius, H. J. (1989) Endogenous sugar receptor (lectin) profiles of human retinoblastoma and retinoblast cell lines analyzed by cytological markers, affinity chromatography and neoglycoprotein-targeted photolysis, *Anticancer Res 9*, 723-730.
66. Róg, T., Pasenkiewicz-Gierula, M., Vattulainen, I., and Karttunen, M. (2009) Ordering effects of cholesterol and its analogues, *Biochimica et Biophysica Acta (BBA) - Biomembranes 1788*, 97-121.
67. Yeagle, P. L. (1993) The biophysics and cell biology of cholesterol: an Hypothesis for the essential role of cholesterol in mammalian cells, In *Cholesterol in membrane models* (Finegold, L., Ed.), pp 1-12, CRC Press.
68. Falck, E., Patra, M., Karttunen, M., Hyvönen, M. T., and Vattulainen, I. (2004) Lessons of Slicing Membranes: Interplay of Packing, Free Area, and Lateral Diffusion in Phospholipid/Cholesterol Bilayers, *Biophysical Journal 87*, 1076-1091.
69. Li, L. K., So, L., and Spector, A. (1985) Membrane cholesterol and phospholipid in consecutive concentric sections of human lenses, *J Lipid Res 26*, 600-609.
70. Chabanel, A., Flamm, M., Sung, K. L., Lee, M. M., Schachter, D., and Chien, S. (1983) Influence of cholesterol content on red cell membrane viscoelasticity and fluidity, *Biophys J 44*, 171-176.
71. Raffy, S., and Teissié, J. (1999) Control of Lipid Membrane Stability by Cholesterol Content, *Biophysical Journal 76*, 2072-2080.
72. May, G. L., Wright, L. C., Dyne, M., Mackinnon, W. B., Fox, R. M., and Mountford, C. E. (1988) Plasma membrane lipid composition of vinblastine sensitive and resistant human leukaemic lymphoblasts, *Int J Cancer 42*, 728-733.

73. Zhao, L., and Feng, S.-S. (2006) Effects of cholesterol component on molecular interactions between paclitaxel and phospholipid within the lipid monolayer at the air-water interface, *Journal of Colloid and Interface Science 300*, 314-326.
74. Liebes, L. F., Pelle, E., Zucker-Franklin, D., and Silber, R. (1981) Comparison of lipid composition and 1,6-diphenyl-1,3,5-hexatriene fluorescence polarization measurements of hairy cells with monocytes and lymphocytes from normal subjects and patients with chronic lymphocytic leukemia, *Cancer Res 41*, 4050-4056.
75. Merchant, T. E., Meneses, P., Gierke, L. W., Den Otter, W., and Glonek, T. (1991) 31P magnetic resonance phospholipid profiles of neoplastic human breast tissues, *Br J Cancer 63*, 693-698.
76. Michael I. Gurr, J. L. H., Keith N. Frayn (2002) Lipid transport, In *Lipid Biochemistry: An Introduction* (Science, B., Ed.) 5th ed., pp 170-214.
77. Brown, M. S., and Goldstein, J. L. (1976) Receptor-mediated control of cholesterol metabolism, *Science 191*, 150-154.
78. Reyftmann, J. P., Morliere, P., Goldstein, S., Satus, R., Dubertret, L., and Lagrange, D. (1984) Interaction of human serum low density lipoproteins with porphyrins: a spectroscopic and photochemical study, *Photochem Photobiol 40*, 721-729.
79. Kessel, D. (1986) Porphyrin-Lipoprotein Association as a Factor in Porphyrine Localization, *Cancer Letters 33*, 183-188.
80. Maziere, J. C., Maziere, C., Mora, L., and Polonovski, J. (1981) [Metabolism of cholesterol in normal hamster fibroblasts and those transformed by the SV 40 virus. Effect of low density lipoproteins], *Biochimie 63*, 221-226.
81. Lombardi, P., Norata, G., Maggi, F. M., Canti, G., Franco, P., Nicolin, A., and Catapano, A. L. (1989) Assimilation of LDL by experimental tumours in mice, *Biochim Biophys Acta 1003*, 301-306.
82. Vitols, S., Peterson, C., Larsson, O., Holm, P., and Aberg, B. (1992) Elevated uptake of low density lipoproteins by human lung cancer tissue in vivo, *Cancer Res 52*, 6244-6247.
83. Maziere, J. C., Santus, R., Morliere, P., Reyftmann, J. P., Candide, C., Mora, L., Salmon, S., Maziere, C., Gatt, S., and Dubertret, L. (1990) Cellular uptake and photosensitizing properties of anticancer porphyrins in cell membranes and low and high density lipoproteins, *Journal of Photochemistry and Photobiology B: Biology 6*, 61-68.
84. Hamblin, M. R., and Luke Newman, E. (1994) New trends in photobiology: On the mechanism of the tumour-localising effect in photodynamic therapy, *Journal of Photochemistry and Photobiology B: Biology 23*, 3-8.
85. Candide, C., Morliere, P., Maziere, J. C., Goldstein, S., Santus, R., Dubertret, L., Reyftmann, J. P., and Polonovski, J. (1986) In vitro interaction of the photoactive anticancer porphyrin derivative photofrin II with low density lipoprotein, and its delivery to cultured human fibroblasts, *Febs Lett 207*, 133-138.
86. Schmidt-Erfurth, U., Diddens, H., Birngruber, R., and Hasan, T. (1997) Photodynamic targeting of human retinoblastoma cells using covalent low-density lipoprotein conjugates, *Br J Cancer 75*, 54-61.
87. Mody, R., Joshi, S. H. a., and Chaney, W. (1995) Use of lectins as diagnostic and therapeutic tools for cancer, *Journal of Pharmacological and Toxicological Methods 33*, 1-10.
88. Cerra, R. F., Haywood-Reid, P. L., and Barondes, S. H. (1984) Endogenous mammalian lectin localized extracellularly in lung elastic fibers, *J Cell Biol 98*, 1580-1589.
89. Ashwell, G., and Harford, J. (1982) Carbohydrate-Specific Receptors of the Liver, *Annual Review of Biochemistry 51*, 531-554.
90. Komath, S. S., Kavitha, M., and Swamy, M. J. (2006) Beyond carbohydrate binding: new directions in plant lectin research, *Org; & Biomolec. Chem. 4*, 973-988.
91. Lis, H., and Sharon, N. (1998) Lectins: Carbohydrate-Specific Proteins That Mediate Cellular Recognition†, *Chemical Reviews 98*, 637-674.
92. Monsigny, M., Roche, A.-C., Kieda, C., Midoux, P., and Obrénovitch, A. (1988) Characterization and biological implications of membrane lectins in tumor, lymphoid and myeloid cells, *Biochimie 70*, 1633-1649.
93. Joshi, S. S., Tilden, P. A., Jackson, J. D., Sharp, J. G., and Brunson, K. W. (1987) Cell surface properties associated with malignancy of metastatic large cell lymphoma cells, *Cancer Res 47*, 3551-3557.
94. Lotan, R., Matsushita, Y., Ohannesian, D., Carralero, D., Ota, D. M., Cleary, K. R., Nicolson, G. L., and Irimura, T. (1991) Lactose-binding lectin expression in human colorectal carcinomas. Relation to tumor progression, *Carbohydr Res 213*, 47-57.
95. Gabius, H.-J. (1991) Detection and functions of mammalian lectins -- with emphasis on membrane lectins, *Biochimica et Biophysica Acta (BBA) - Reviews on Biomembranes 1071*, 1-18.
96. Yamazaki, N., Kojima, S., Bovin, N. V., André, S., Gabius, S., and Gabius, H. J. (2000) Endogenous lectins as targets for drug delivery, *Advanced Drug Delivery Reviews 43*, 225-244.

97. Faivre, V., Rosilio, V. (2010) Interest of glycolipids in drug delivery: from physicochemical properties to drug targeting, *Expert Opin Drug Deliv 7*, 1031-1048.
98. Laville, I., Pigaglio, S., Blais, J. C., Loock, B., Maillard, Ph., Grierson, D.S., Blais, J. (2004) A study of the stability of tri(glucosyloxyphenyl)chlorin, a sensitizer for photodynamic therapy, in human colon tumoural cells: a liquid chromatography and MALDI-TOF mass spectrometry analysis, *Bioorg. & Med. Chem. 12*, 3673-3682.
99. Lupu, M., Thomas, C.D., Maillard, Ph., Loock, B., Chauvin, B., Aerts, I., Croisy, A., Belloir, E., Volk, A., Mispelter, J. (2009) 23Na MRI longitudinal follow-up of PDT in a xenograft model of human retinoblastoma, *Photodiag. and Photody. Ther. 6*, 214-220.
100. Seydel, P. D. J. K. (2003) Analytical Tools for the Analysis and Quantification of Drug-Membrane Interactions, In *Drug-Membrane Interactions* (Prof. Dr. Joachim K. Seydel, P. D. M. W., Ed.), pp 51-139.
101. Ménez, C., Legrand, P., Rosilio, V., Lesieur, S., Barratt, G. (2006) Physicochemical Characterization of Molecular Assemblies of Miltefosine and Amphotericin B, *Molecular Pharmaceutics 4*, 281-288.
102. Filho, J. M. N., de Melo, C. P., Santos-Magalhães, N. S., Rosilio, V., Maciel, M. A. M., and Andrade, C. A. S. (2010) Thermodynamic investigation of mixed monolayers of trans-dehydrocrotonin and phospholipids, *Colloids and Surfaces A: Physicochemical and Engineering Aspects 358*, 42-49.
103. Desroches, M. C., Kasselouri, A., Meyniel, M., Fontaine, P., Goldmann, M., Prognon, P., Maillard, P., Rosilio, V. (2004) Incorporation of Glycoconjugated Porphyrin Derivatives into Phospholipid Monolayers: A Screening Method for the Evaluation of Their Interaction with a Cell Membrane, *Langmuir 20*, 11698-11705.
104. Fernandez-Botello, A., Comelles, F., Alsina, M. A., Cea, P., and Reig, F. (2008) A monolayer study on interactions of docetaxel with model lipid membranes, *J Phys Chem B 112*, 13834-13841.
105. Reig, F., Mestres, C., Haro, I., Valencia, G., Anton, J. M. G., and Alsina, M. A. (1989) Colloid Science - Mixed Monolayers Composed OF PC/PS/CHOL Interaction with Opioid Molecules, *Colloid and Polymer Science 267*, 139-144.
106. García, M. L., Egea, M. A., Valero, J., Valls, O., and Alsina, M. A. (1997) Interaction of flurbiprofen sodium with cornea model monolayers at the air-water interface, *Thin Solid Films 301*, 169-174.
107. Teixeira, H., Rosilio, V., Laigle, A., Lepault, J., Erk, I., Scherman, D., Benita, S., Couvreur, P., and Dubernet, C. (2001) Characterization of oligonucleotide/lipid interactions in submicron cationic emulsions: influence of the cationic lipid structure and the presence of PEG-lipids, *Biophysical Chemistry 92*, 169-181.
108. Fradin, C., Daillant, J., Braslau, A., Luzet, D., Alba, M., and Goldmann, M. (1998) Microscopic measurement of the linear compressibilities of two-dimensional fatty acid mesophases, *The European Physical Journal B - Condensed Matter and Complex Systems 1*, 57-69.
109. Weis, R. M. (1991) Fluorescence microscopy of phospholipid monolayer phase transitions, *Chemistry and Physics of Lipids 57*, 227-239.
110. Stine, K. J. (1994) Investigations of monolayers by fluorescence microscopy, *Microscopy Research and Technique 27*, 439-450.
111. Weis, R. M., and McConnell, H. M. (1984) Two-dimensional chiral crystals of phospholipid, *Nature 310*, 47-49.
112. Hoenig, D., and Moebius, D. (1991) Direct visualization of monolayers at the air-water interface by Brewster angle microscopy, *The Journal of Physical Chemistry 95*, 4590-4592.
113. Hidalgo, A. A., Tabak, M., and Oliveira Jr, O. N. (2005) The interaction of meso-tetraphenylporphyrin with phospholipid monolayers, *Chem. and Phys. of Lipids 134*, 97-108.
114. Glomm, W. R., Volden, S., Halskau, Ø., and Ese, M.-H. G. (2009) Same System−Different Results: The Importance of Protein-Introduction Protocols in Langmuir-Monolayer Studies of Lipid-Protein Interactions, *Analytical Chemistry 81*, 3042-3050.
115. Prieto, I., Martín Romero, M. T., Camacho, L., and Möbius, D. (1998) Organization of a Water-Soluble Porphyrin in Mixed Monolayers with Phospholipids Studied by Brewster Angle Microscopy, *Langmuir 14*, 4175-4179.
116. Harke, M., Stelzle, M., and Motschmann, H. R. (1996) Microscopic ellipsometry: imaging monolayer on arbitrary reflecting supports, *Thin Solid Films 284-285*, 412-416.
117. Gregoriadis, G. (1995) Engineering liposomes for drug delivery: progress and problems, *Trends in Biotechnology 13*, 527-537.
118. Sharma, A., and Sharma, U. S. (1997) Liposomes in drug delivery: Progress and limitations, *International Journal of Pharmaceutics 154*, 123-140.
119. Bangham, A. D., Standish, M. M., and Watkins, J. C. (1965) Diffusion of univalent ions across the lamellae of swollen phospholipids, *J. Molec. Biol. 13*, 238-252, IN226-IN227.

120. Saunders, L., Perrin, J., and Gammack, D. (1962) Ultrasonic irradiation of some phospholipid sols, *J Pharm Pharmacol 14*, 567-572.
121. Deamer, D. W. (1978) Preparation and properties of ether-injection liposomes, *Ann N Y Acad Sci 308*, 250-258.
122. Machy, P., and LESERMAN, L. (1987) *Les liposomes en biologie cellulaire et pharmacologie; John Libbey EUROTEXT*, 2-18.
123. Pinto-Alphandary, H., Andremont, A., and Couvreur, P. (2000) Targeted delivery of antibiotics using liposomes and nanoparticles: research and applications, *International Journal of Antimicrobial Agents 13*, 155-168.
124. Larabi, M., Yardley, V., Loiseau, P. M., Appel, M., Legrand, P., Gulik, A., Bories, C., Croft, S. L., and Barratt, G. (2003) Toxicity and antileishmanial activity of a new stable lipid suspension of amphotericin B, *Antimicrob Agents Chemother 47*, 3774-3779.
125. de Oliveira, M. C., Rosilio, V., Lesieur, P., Bourgaux, C., Couvreur, P., Ollivon, M., and Dubernet, C. (2000) pH-Sensitive liposomes as a carrier for oligonucleotides: a physico-chemical study of the interaction between DOPE and a 15-mer oligonucleotide in excess water, *Biophysical Chemistry 87*, 127-137.
126. Fattal, E., Couvreur, P., and Dubernet, C. (2004) "Smart" delivery of antisense oligonucleotides by anionic pH-sensitive liposomes, *Advanced Drug Delivery Reviews 56*, 931-946.
127. Urbinati, G., Marsaud, V., Plassat, V., Fattal, E., Lesieur, S., and Renoir, J.-M. (2010) Liposomes loaded with histone deacetylase inhibitors for breast cancer therapy, *International Journal of Pharmaceutics 397*, 184-193.
128. Oku, N., Namba, Y., and Okada, S. (1992) Tumor accumulation of novel RES-avoiding liposomes, *Biochimica et Biophysica Acta (BBA) - Lipids and Lipid Metabolism 1126*, 255-260.
129. G. Niggemann, M. K. a. W. H. (1995) The Bending Rigidity of Phosphatidylcholine Bilayers: Dependences on Experimental Method, Sample Cell Sealing and Temperature, *J. Phys. II France 5*, 413-425.
130. Evans, E. (1995) Chapter 15 Physical actions in biological adhesion, In *Handbook of Biological Physics* (Lipowsky, R., and Sackmann, E., Eds.), pp 723-754, North-Holland.
131. Seifert, U. (1997) Configurations of fluid membranes and vesicles, *Advances in Physics 46*, 13-137.
132. Baumgart, T., Hess, S. T., and Webb, W. W. (2003) Imaging coexisting fluid domains in biomembrane models coupling curvature and line tension, *Nature 425*, 821-824.
133. Lipowsky, R., and Seifert, U. (1991) Adhesion of Vesicles and Membranes, *Molecular Crystals and Liquid Crystals 202*, 17-25.
134. Okumura, Y., Higashi, N., Rosilio, V., and Sunamoto, J. (1997) Poly(ethylene oxide)-bearing lipids and interaction of functionalized liposomes with intact cells, In *Poly(Ethylene Glycol) - Chemistry and Biological Applications* (Harris, J. M., and Zalipsky, S., Eds.), pp 82-98.
135. Morone, N., Ueda, T., Tsudo, Y., Okumura, Y., Rosilio, V., Baszkin, A., and Sunamoto, J. (2007) Surface pressure analysis of poly(ethylene oxide)-modified fusogenic liposomes incorporated into a phospholipid monolayer, *Journal of Bioactive and Compatible Polymers 22*, 5-18.
136. Toyran, N., and Severcan, F. (2003) Competitive effect of vitamin D2 and Ca2+ on phospholipid model membranes: an FTIR study, *Chemistry and Physics of Lipids 123*, 165-176.
137. Angelova, M. I., and Tsoneva, I. (1999) Interactions of DNA with giant liposomes, *Chemistry and Physics of Lipids 101*, 123-137.
138. Fischer, A., Oberholzer, T., and Luisi, P. L. (2000) Giant vesicles as models to study the interactions between membranes and proteins, *Biochimica et Biophysica Acta (BBA) - Biomembranes 1467*, 177-188.
139. Romanowski, M., Zhu, X., Ramaswami, V., Misicka, A., Lipkowski, A. W., Hruby, V. J., and O'Brien, D. F. (1997) Interaction of a highly potent dimeric enkephalin analog, biphalin, with model membranes, *Biochimica et Biophysica Acta (BBA) - Biomembranes 1329*, 245-258.
140. Kepczynski, M., Nawalany, K., Kumorek, M., Kobierska, A., Jachimska, B., and Nowakowska, M. (2008) Which physical and structural factors of liposome carriers control their drug-loading efficiency?, *Chemistry and Physics of Lipids 155*, 7-15.
141. Brian, A. A., and McConnell, H. M. (1984) Allogeneic Stimulation of Cyto-toxic T-cells by Supported Planar Membranes, *Proceedings of the National Academy of Sciences of the United States of America-Biological Sciences 81*, 6159-6163.
142. Sackmann, E. (1996) Supported membranes: scientific and practical applications, *Science 271*, 43-48.
143. Bieri, C., Ernst, O. P., Heyse, S., Hofmann, K. P., and Vogel, H. (1999) Micropatterned immobilization of a G protein-coupled receptor and direct detection of G protein activation, *Nature Biotechnology 17*, 1105-1108.

144. Svedhem, S., Pfeiffer, I., Larsson, C., Wingren, C., Borrebaeck, C., and Hook, F. (2003) Patterns of DNA-labeled and scFv-antibody-carrying lipid vesicles directed by material-specific immobilization of DNA and supported lipid bilayer formation on an Au/SiO2 template, *Chembiochem 4*, 339-343.
145. Leonenko, Z. V., Carnini, A., and Cramb, D. T. (2000) Supported planar bilayer formation by vesicle fusion: the interaction of phospholipid vesicles with surfaces and the effect of gramicidin on bilayer properties using atomic force microscopy, *Biochim. Biophys. Acta 1509*, 131-147.
146. Kalb, E., Engel, J., Tamm, L. K. (1990) Binding of proteins to specific target sites in membranes measured by total internal reflection fluorescence microscopy, *Biochemistry 29*, 1607-1613.
147. Brian, A. A., and McConnell, H. M. (1984) Allogeneic stimulation of cytotoxic T cells by supported planar membranes, *Proc Natl Acad Sci U S A 81*, 6159-6163.
148. Kloboucek, A., Behrisch, A., Faix, J., and Sackmann, E. (1999) Adhesion-induced receptor segregation and adhesion plaque formation: A model membrane study, *Biophys J 77*, 2311-2328.
149. Grandbois, M., Clausen-Schaumann, H., and Gaub, H. (1998) Atomic force microscope imaging of phospholipid bilayer degradation by phospholipase A2, *Biophys J 74*, 2398-2404.
150. Ross, M., Steinem, C., Galla, H.J., Janshoff, A. (2001) Visualization of Chemical and Physical Properties of Calcium-Induced Domains in DPPC/DPPS Langmuir−Blodgett Layers, *Langmuir 17*, 2437-2445.
151. Keller, C. A., and Kasemo, B. (1998) Surface Specific Kinetics of Lipid Vesicle Adsorption Measured with a Quartz Crystal Microbalance, *Biophys. J. 75*, 1397-1402.
152. Steinem, C., Janshoff, A., Ulrich, W. P., Sieber, M., Galla, H. J. (1996) Impedance analysis of supported lipid bilayer membranes: A scrutiny of different preparation techniques, *Biochim. Biophys. Acta-Biomembranes 1279*, 169-180.
153. Reimhult, E., Höök, F., and Kasemo, B. (2002) Intact Vesicle Adsorption and Supported Biomembrane Formation from Vesicles in Solution: Influence of Surface Chemistry, Vesicle Size, Temperature, and Osmotic Pressure†, *Langmuir 19*, 1681-1691.
154. Starr, T. E., and Thompson, N. L. (2000) Formation and Characterization of Planar Phospholipid Bilayers Supported on TiO2 and SrTiO3 Single Crystals, *Langmuir 16*, 10301-10308.
155. Kalb, E., Frey, S., and Tamm, L. K. (1992) Formation of supported planar bilayers by fusion of vesicles to supported phospholipid monolayers, *Biochimica et Biophysica Acta (BBA) - Biomembranes 1103*, 307-316.
156. Munro, J. C., and Frank, C. W. (2004) Adsorption of lipid-functionalized poly(ethylene glycol) to gold surfaces as a cushion for polymer-supported lipid bilayers, *Langmuir 20*, 3339-3349.
157. Wagner, M. L., and Tamm, L. K. (2001) Reconstituted Syntaxin1A/SNAP25 Interacts with Negatively Charged Lipids as Measured by Lateral Diffusion in Planar Supported Bilayers, *Biophysical Journal 81*, 266-275.
158. Rossi, C., and Chopineau, J. (2007) Biomimetic tethered lipid membranes designed for membrane-protein interaction studies, *Eur Biophys J 36*, 955-965.
159. Wong, J. Y., Majewski, J., Seitz, M., Park, C. K., Israelachvili, J. N., and Smith, G. S. (1999) Polymer-cushioned bilayers. I. A structural study of various preparation methods using neutron reflectometry, *Biophys J 77*, 1445-1457.
160. Jacobson, K., Sheets, E. D., and Simson, R. (1995) Revisiting the fluid mosaic model of membranes, *Science 268*, 1441-1442.
161. Richter, R. P., Bérat, R., Brisson, Alain R. (2006) Formation of Solid-Supported Lipid Bilayers: An Integrated View, *Langmuir 22*, 3497-3505.
162. Andreou, V. G., and Nikolelis, D. P. (1998) Flow injection monitoring of aflatoxin M-1 in milk and milk preparations using filter-supported bilayer lipid membranes, *Analytical Chemistry 70*, 2366-2371.
163. Favero, G., Campanella, L., D'Annibale, A., Santucci, R., and Ferri, T. (2003) Mixed hybrid bilayer lipid membrane incorporating valinomycin: improvements in preparation and functioning, *Microchemical Journal 74*, 141-148.
164. Suzuki, H., Tabata, K. V., Noji, H., and Takeuchi, S. (2006) Highly reproducible method of planar lipid bilayer reconstitution in polymethyl methacrylate microfluidic chip, *Langmuir 22*, 1937-1942.
165. Malmstadt, N., Nash, M. A., Purnell, R. F., and Schmidt, J. J. (2006) Automated formation of lipid-bilayer membranes in a microfluidic device, *Nano Lett 6*, 1961-1965.
166. Simon, A., Girard-Egrot, A., Sauter, F., Pudda, C., D'Hahan, N. P., Blum, L., Chatelain, F., and Fuchs, A. (2007) Formation and stability of a suspended biomimetic lipid bilayer on silicon submicrometer-sized pores, *Journal of Colloid and Interface Science 308*, 337-343.
167. Jeon, T. J., Poulos, J. L., and Schmidt, J. J. (2008) Long-term storable and shippable lipid bilayer membrane platform, *Lab on a Chip 8*, 1742-1744.
168. Romer, W., and Steinem, C. (2004) Impedance analysis and single-channel recordings on nano-black lipid membranes based on porous alumina, *Biophysical Journal 86*, 955-965.

169. Huang, Z., and Haugland, R. P. (1991) Partition coefficients of fluorescent probes with phospholipid membranes, *Biochem. and Biophys. Res. Comm. 181*, 166-171.
170. Ben-Dror, S., Bronshtein, I., Wiehe, A., Röder, B., Senge, M. O., and Ehrenberg, B. (2006) On the Correlation Between Hydrophobicity, Liposome Binding and Cellular Uptake of Porphyrin Sensitizers, *Photochem. and Photobiol. 82*, 695-701.
171. Maman, N., and Brault, D. (1998) Kinetics of the interactions of a dicarboxylic porphyrin with unilamellar lipidic vesicles: Interplay between bilayer thickness and pH in rate control, *Biochim. et Biophys. Acta (BBA) - Biomembranes 1414*, 31-42.
172. Ricchelli, F. (1995) Photophysical properties of porphyrins in biological membranes, *J. Photochem. and Photobiol. B: Biology 29*, 109-118.
173. Ricchelli, F., Stevanin, D., and Jori, G. (1988) Porphyrin-liposome interactions: influence of the physico-chemical properties of the phospholipid bilayer, *Photochem Photobiol 48*, 13-18.
174. Ricchelli, F., and Jori, G. (1986) Distribution of porphyrins in the various compartments of unilamellar liposomes of dipalmitoyl-phosphatidylcholine as probed by fluorescence spectroscopy, *Photochem Photobiol 44*, 151-157.
175. Ricchelli, F., Jori, G., Moreno, G., Vinzens, F., and Salet, C. (1990) Factors influencing the distribution pattern of porphyrins in cell membranes, *Journal of Photochemistry and Photobiology B: Biology 6*, 69-77.
176. Bronshtein, I., Afri, M., Weitman, H., Frimer, A. A., Smith, K. M., and Ehrenberg, B. (2004) Porphyrin Depth in Lipid Bilayers as Determined by Iodide and Parallax Fluorescence Quenching Methods and Its Effect on Photosensitizing Efficiency, *Biophysical Journal 87*, 1155-1164.
177. Lukomsky, I., Gottfried, V., and Kimel, S. (1994) Delayed fluorescence of porphyrins in different media, *Journal of Fluorescence 4*, 49-51.
178. Maiti, N. C., Mazumdar, S., and Periasamy, N. (1998) J- and H-Aggregates of Porphyrin−Surfactant Complexes: Time-Resolved Fluorescence and Other Spectroscopic Studies†, *J. Phys. Chem. B 102*, 1528-1538.
179. Emiliani, C., and Delmelle, M. (1983) THE LIPID SOLUBILITY OF PORPHYRINS MODULATES THEIR PHOTOTOXICITY IN MEMBRANE MODELS, *Photochemistry and Photobiology 37*, 487-490.
180. Engelmann, F. M., Mayer, I., Gabrielli, D. S., Toma, H. E., Kowaltowski, A. J., Araki, K., and Baptista, M. S. (2007) Interaction of cationic meso-porphyrins with liposomes, mitochondria and erythrocytes, *J Bioenerg Biomembr 39*, 175-185.
181. Lakowicz, J. R. (2006) Quenching of fluorescence, In *Principles of Fluorescence Spectroscopy* 3rd ed., pp 277-329, Springerlink.
182. Ford, W. E., and Tollin, G. (1984) CHLOROPHYLL PHOTOSENSITIZED ELECTRON TRANSFER IN PHOSPHOLIPID BILAYER VESICLE SYSTEMS: EFFECTS OF CHOLESTEROL ON RADICAL YIELDS AND KINETIC PARAMETERS*, *Photochemistry and Photobiology 40*, 249-259.
183. Ehrenberg, B., and Gross, E. (1988) THE EFFECT OF LIPOSOMES' MEMBRANE COMPOSITION ON THE BINDING OF THE PHOTOSENSITIZERS HPD AND PHOTOFRIN II, *Photochemistry and Photobiology 48*, 461-466.
184. Lavi, A., Weitman, H., Holmes, R. T., Smith, K. M., and Ehrenberg, B. (2002) The depth of porphyrin in a membrane and the membrane's physical properties affect the photosensitizing efficiency, *Biophys. J. 82*, 2101-2110.
185. Voszka, I., Galántai, R., Maillard, P., and CsIk, G. (1999) Interaction of glycosylated tetraphenyl porphyrins with model lipid membranes of different compositions, *Journal of Photochemistry and Photobiology B: Biology 52*, 92-98.
186. Minnes, R., Ytzhak, S., Weitman, H., and Ehrenberg, B. (2008) The effect of solution electrolytes on the uptake of photosensitizers by liposomal membranes: a salting-out effect, *Chem. and Phys. of Lipids 155*, 38-42.
187. Koynova, R., Brankov, J., and Tenchov, B. (1997) Modulation of lipid phase behavior by kosmotropic and chaotropic solutes, *European Biophysics Journal 25*, 261-274.
188. Aroti, A., Leontidis, E., Dubois, M., and Zemb, T. (2007) Effects of Monovalent Anions of the Hofmeister Series on DPPC Lipid Bilayers Part I: Swelling and In-Plane Equations of State, *Biophysical Journal 93*, 1580-1590.
189. Brault, D. (1990) Physical chemistry of porphyrins and their interactions with membranes: The importance of pH, *Journal of Photochemistry and Photobiology B: Biology 6*, 79-86.
190. Barrett, A. J., Kennedy, J. C., Jones, R. A., Nadeau, P., and Pottier, R. H. (1990) The effect of tissue and cellular pH on the selective biodistribution of porphyrin-type photochemotherapeutic agents: A volumetric titration study, *Journal of Photochemistry and Photobiology B: Biology 6*, 309-323.

191. Pottier, R., and Kennedy, J. C. (1990) New trends in photobiology : The possible role of ionic species in selective biodistribution of photochemotherapeutic agents toward neoplastic tissue, *Journal of Photochemistry and Photobiology B: Biology 8*, 1-16.
192. Brault, D., Vever-Bizet, C., and Kuzelova, K. (1993) Interactions of dicarboxylic porphyrins with membranes in relation to their ionization state, *Journal of Photochemistry and Photobiology B: Biology 20*, 191-195.
193. Bonneau, S., Maman, N., and Brault, D. (2004) Dynamics of pH-dependent self-association and membrane binding of a dicarboxylic porphyrin: a study with small unilamellar vesicles, *Biochimica et Biophysica Acta (BBA) - Biomembranes 1661*, 87-96.
194. Kuzelova, K., and Brault, D. (1995) Interactions of dicarboxylic porphyrins with unilamellar lipidic vesicles: drastic effects of pH and cholesterol on kinetics, *Biochemistry 34*, 11245-11255.
195. Galantai, R., Bardos-Nagy, I., Modos, K., Kardos, J., Zavodszky, P., and Fidy, J. (2000) Serum albumin-lipid membrane interaction influencing the uptake of porphyrins, *Arch Biochem Biophys 373*, 261-270.
196. Voszka, I., Budai, M., Szabó, Z., Maillard, P., Csík, G., and Gróf, P. (2007) Interaction of photosensitizers with liposomes containing unsaturated lipid, *Chemistry and Physics of Lipids 145*, 63-71.
197. Mojzisova, H., Bonneau, S., Maillard, P., Berg, K., and Brault, D. (2009) Photosensitizing properties of chlorins in solution and in membrane-mimicking systems, *Photochem Photobiol Sci 8*, 778-787.
198. Kelvin M.G. Taylor, D. Q. M. C. (2003) Physical methods of study: Differential scanning calorimetry, In *Liposomes: a practical approach* (V. P. Torchilin, V. W., Ed.) Second edition ed., pp 92-103.
199. Cristani, M., D'Arrigo, M., Mandalari, G., Castelli, F., Sarpietro, M. G., Micieli, D., Venuti, V., Bisignano, G., Saija, A., and Trombetta, D. (2007) Interaction of four monoterpenes contained in essential oils with model membranes: implications for their antibacterial activity, *J Agric Food Chem 55*, 6300-6308.
200. El Maghraby, G. M., Barry, B. W., and Williams, A. C. (2008) Liposomes and skin: From drug delivery to model membranes, *European Journal of Pharmaceutical Sciences 34*, 203-222.
201. Butler, S., Wang, R., Wunder, S. L., Cheng, H.-Y., and Randall, C. S. (2006) Perturbing effects of carvedilol on a model membrane system: Role of lipophilicity and chemical structure, *Biophysical Chemistry 119*, 307-315.
202. Wiltschi, B., Knoll, W., and Sinner, E.-K. (2006) Binding assays with artificial tethered membranes using surface plasmon resonance, *Methods 39*, 134-146.
203. Besenicar, M., Macek, P., Lakey, J. H., and Anderluh, G. (2006) Surface plasmon resonance in protein-membrane interactions, *Chemistry and Physics of Lipids 141*, 169-178.
204. Plant, A. L. (1993) Self-assembled phospholipid/alkanethiol biomimetic bilayers on gold, *Langmuir 9*, 2764-2767.
205. Lang, H., Duschl, C., and Vogel, H. (1994) A new class of thiolipids for the attachment of lipid bilayers on gold surfaces, *Langmuir 10*, 197-210.
206. Melikov, K. C., Frolov, V. A., Shcherbakov, A., Samsonov, A. V., Chizmadzhev, Y. A., and Chernomordik, L. V. (2001) Voltage-Induced Nonconductive Pre-Pores and Metastable Single Pores in Unmodified Planar Lipid Bilayer, *Biophysical Journal 80*, 1829-1836.
207. Stozhkova, I. N., and Mirskii, V. M. (1990) [Modeling of damage to cell membranes during photodynamic therapy: photosensitization of planar lipid bilayers by hematoporphyrin dimethyl ether], *Biull Eksp Biol Med 110*, 45-46.
208. Rokitskaya, T. I., Antonenko, Y. N., and Kotova, E. A. (1993) The interaction of phthalocyanine with planar lipid bilayers. Photodynamic inactivation of gramicidin channels, *Febs Lett 329*, 332-335.
209. Makky, A., Michel, J. P., Ballut, S., Kasselouri, A., Maillard, Ph., Rosilio, V. (2010) Effect of Cholesterol and Sugar on the Penetration of Glycodendrimeric Phenylporphyrins into Biomimetic Models of Retinoblastoma Cells Membranes, *Langmuir 26*, 11145-11156.
210. Gross, E., and Ehrenberg, B. (1989) The partition and distribution of porphyrins in liposomal membranes. A spectroscopic study, *Bioch. et Biophys. Acta (BBA) - Biomembranes 983*, 118-122.
211. Ehrenberg, B. (1992) Assessment of the partitioning of probes to membranes by spectroscopic titration, *Journal of Photochemistry and Photobiology B: Biology 14*, 383-386.
212. Bonneau, S., Morlière, P., and Brault, D. (2004) Dynamics of interactions of photosensitizers with lipoproteins and membrane-models: correlation with cellular incorporation and subcellular distribution, *Biochemical Pharmacology 68*, 1443-1452.
213. Csík, G., Balog, E., Voszka, I., Tölgyesi, F., Oulmi, D., Maillard, P., and Momenteau, M. (1998) Glycosylated derivatives of tetraphenyl porphyrin: photophysical characterization, self-aggregation and membrane binding, *Journal of Photochemistry and Photobiology B: Biology 44*, 216-224.

Travaux expérimentaux

Chapitre 1: Etude du comportement interfacial des porphyrines dendrimériques et de leur interaction non spécifique avec une matrice lipidique

Article 2: New strategy for targeting of photosensitizers. Synthesis of glycodendrimeric phenylporphyrins, incorporation into a liposome membrane and interaction with a specific lectin

Séverine Ballut, Ali Makky, Bernard Loock, Jean-Philippe Michel, Philippe Maillard and Véronique Rosilio

Article publié dans Chem Commun 2009;(2):224-6

Cet article présente la synthèse organique et l'étude du comportement interfacial de nouvelles porphyrines glycodendrimériques. Ces nouvelles molécules ont été synthétisées à l'institut Curie par Séverine Ballut et caractérisées aux interfaces par nous-mêmes. La Figure 1 présente plus particulièrement la structure des porphyrines dendrimériques étudiées dans le cadre de cette thèse. Comme ces nouvelles molécules ont une faible solubilité en milieu aqueux, l'objectif de ce chapitre est d'évaluer leur capacité à se solubiliser avec des phospholipides, comme la DMPC qui forme facilement des liposomes, par incorporation dans la bicouche liposomiale. Pour cela, nous avons d'abord étudié la compression de monocouches mixtes composées de porphyrines avec ou sans DMPC, étalées à l'interface air/tampon. Dans un deuxième temps, nous avons formé des liposomes mixtes DMPC-porphyrine, puis nous avons vérifié la bonne orientation des sucres portés par les porphyrines dans la bicouche liposomiale en évaluant par des mesures de DLS leur capacité à interagir spécifiquement avec une lectine spécifique de mannose (Con A).

New strategy for targeting of photosensitizers. Synthesis of glycodendrimeric phenylporphyrins, incorporation into a liposome membrane and interaction with a specific lectin

Séverine Ballut,[ab] Ali Makky,[cd] Bernard Loock,[ab] Jean-Philippe Michel,[cd] Philippe Maillard*[ab] and Véronique Rosilio*[cd]

* Corresponding authors: philippe.maillard@curie.u-psud.fr,

veronique.rosilio@u-psud.fr

[ab]UMR 176 CNRS, Institut Curie, Section de Recherches, Centre Universitaire, Univ. Paris-Sud, F-91405 Orsay, France; [c d] Univ. Paris-Sud, UMR CNRS 8612, Lab. Physico-Chimie des Surfaces, 5 rue J-B. Clément, F-92296 Châtenay-Malabry, France.

Introduction

The incorporation of carbohydrates on tetrapyrrolic macrocyclic cores usable in photodynamic therapy (PDT) continues to be pursued vigorously by a number of research teams.[(1)] In our laboratories, efforts have been focused on the preparation and *in vitro* evaluation of the phototoxicity of a series of neutral glycoconjugated tetrapyrrolic macrocycles as potential photosensitizing agents for photodynamic therapy.[(2-4)] However, these compounds are usually poorly water-soluble molecules, and tend to form aggregates in the aqueous solution. This affects unfavourably both their formulation and bioavailability, and limits pharmacologic studies. Glycoconjugation modifies the amphiphilicity of macrocycles, and can favour their interaction with the tumor cell surface membrane.[(5)] Concerning this latter property, indications are that glycosylation provides the possibility for specific interaction of the resulting conjugate with lectin type receptors overexpressed in certain malignant cells.[(6-7)] Glycoconjugation can thus be a potentially effective strategy for targeting photosensitizers toward tumor cells.[(8-9)] The identification of the transport mechanisms through the biological membranes was a crux. However, it would be advantageous to use these mechanisms for the optimization of photosensitizer targeting towards tumor cells. In this context, the use of glycodendrimers as recognition motifs was very exciting. It has been widely accepted that carbohydrate–protein interactions play a crucial role in a large number of biological processes.[(10-12)] Since most proteins possess multiple carbohydrate-recognition domains and typically exist as oligomeric structures, this limitation is often overcome through multivalency.[(13-16)] Lectin receptors are multisubunit and multivalent proteins with many important biological functions. Due to the weak nature, in the millimolar range, of interactions between a single specific carbohydrate and a receptor protein subunit, nature uses cluster carbohydrates in order to obtain biologically meaningful affinities for the receptors.

The cluster effect appears when the multivalent carbohydrates interact with more than one receptor binding site simultaneously and cooperatively, resulting in better cellular recognition. Several methods of carbohydrate clustering have been described, including the attachment of carbohydrates to natural scaffolds, synthetic polymers, synthetic glycopeptides or simple oligomerization through organic linkers. (*17*) Among these various ways, dendritic structures (glycodendrimers) are emerging as ligands for carbohydrate-binding proteins. (*18-19*) Due to rapid advances in this area, promising potential medicinal applications have appeared in the last ten years, including treatment of cancers. (*20-22*)

Results and discussion

In a continuation of our work to prepare and study neutral targeting glycoconjugated photosensitizers, we report the synthesis, characterization and behavior in liposomes of glycodendrimers linked to meso-tetraaryl-porphyrins shown in Figure 8. Recently, Ballardini et al. described the synthesis of two symmetric dendrimers, incorporating tetrasubstituted porphyrin units as the core and, in one case, four benzyloylated or deprotected and in the other case, twelve acetylated β-D-glucopyranosyl- or β -D-glucopyranosyl residues at the peripheries of the tetrapyrrolic macrocycle. (*23*) These unprotected tetrasubstituted molecules are very water-soluble. We have shown that an amphiphilic structure of the glycoconjugated photosensitizers induces a better photocytotoxicity in vitro. (*8-9*) With the aim of increasing this photoefficiency, we designed a new family of glycoconjugated photosensitizers bearing only one glycodendrimer moiety, with variable length for the spacer linking the carbohydrate to the porphyrin, on the para position of one meso-phenyl group.

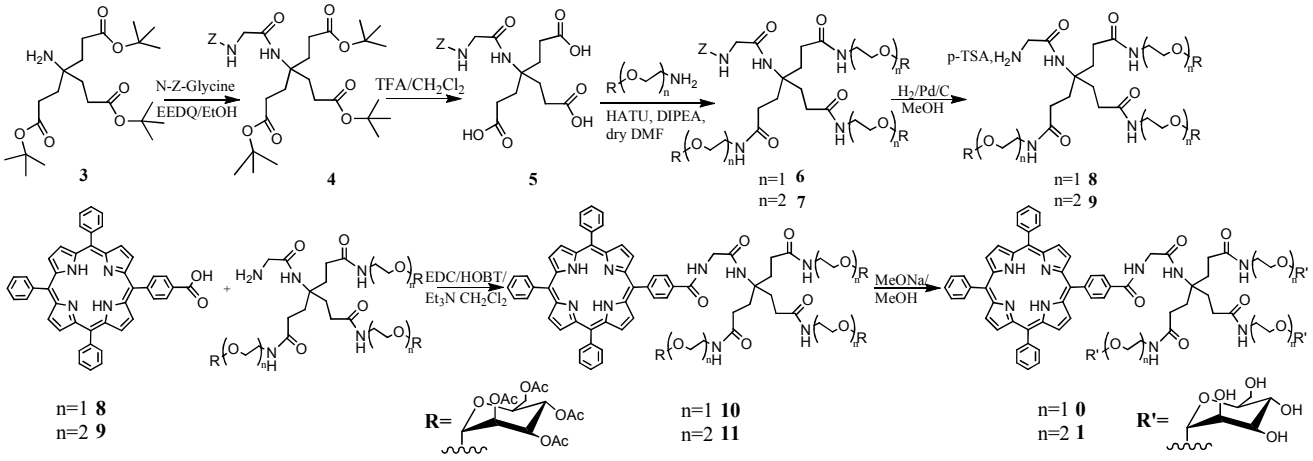

Figure 8: Synthesis of glycodendrimeric porphyrins.

Synthesis of the glycodendrimeric porphyrins is shown in Figure 8. N-Z-glycine was linked to 3 by EEDQ in ethanol (yield 86%) to give 4 then the tertio-butyl protection of carboxylic acid was removed by trifluoroacetic acid in methylene chloride to give compound 5 (92%). 2-Aminoethoxy-O-aperacetyl- D-mannose, and 2-aminoethoxy-ethoxy-O-a-peracetyl- D-mannose prepared by the protocol described by Dahmen et *al.* and Sasaki et *al*. [24-25] were selected for peptide coupling with triacid 5. HATU [26] promoted peptide coupling allowed the preparation of branched glycopeptides with good yields (6 70%, 7 72%).[27] Catalytic hydrogenation was used for selective cleavage of benzyloxycarbonyl group into amine, in the presence of p-toluensulfonic acid (H2–Pd/C 10%, MeOH) to afford the key building blocks with good yields (8 96%, 9 82%). Dendrimeric moieties 8 and 9 were linked to 5-para-benzoic acid-10,15,20- triphenyl porphyrin using a mixture of HOBT, EDC and Et3N with good or acceptable yields to give protected glycodendrimeric porphyrins 10, and 11 (yield 86% and 57%, respectively) then were quantitatively O-deacetylated under Zemplén's conditions to afford glycodendrimeric porphyrins **1** and **2**. To evaluate the conditions of incorporation of compounds **1** and **2** into a liposome membrane, the two derivatives were mixed with dimyristoylphosphatidylcholine (DMPC) in a (1 : 1) ratio and the mixtures were spread at the air–water interface.[28-30] Figure 9 shows that, whereas the isotherm of the DMPC-compound **1** mixed monolayer lies between those of the pure components, that of the mixed DMPC-compound 0 one is located at higher molecular areas and surface pressures. Obviously in both cases, the phospholipid and porphyrin derivatives interacted. However, if for compound **1**, this interaction was apparently attractive, for compound **0**, it was most probably repulsive. Thus, DMPC would mix better with compound **1** than with compound **0**. The incorporation of compound **1** in liposome membranes led to the formation of larger vesicles than DMPC ones (Table 2).

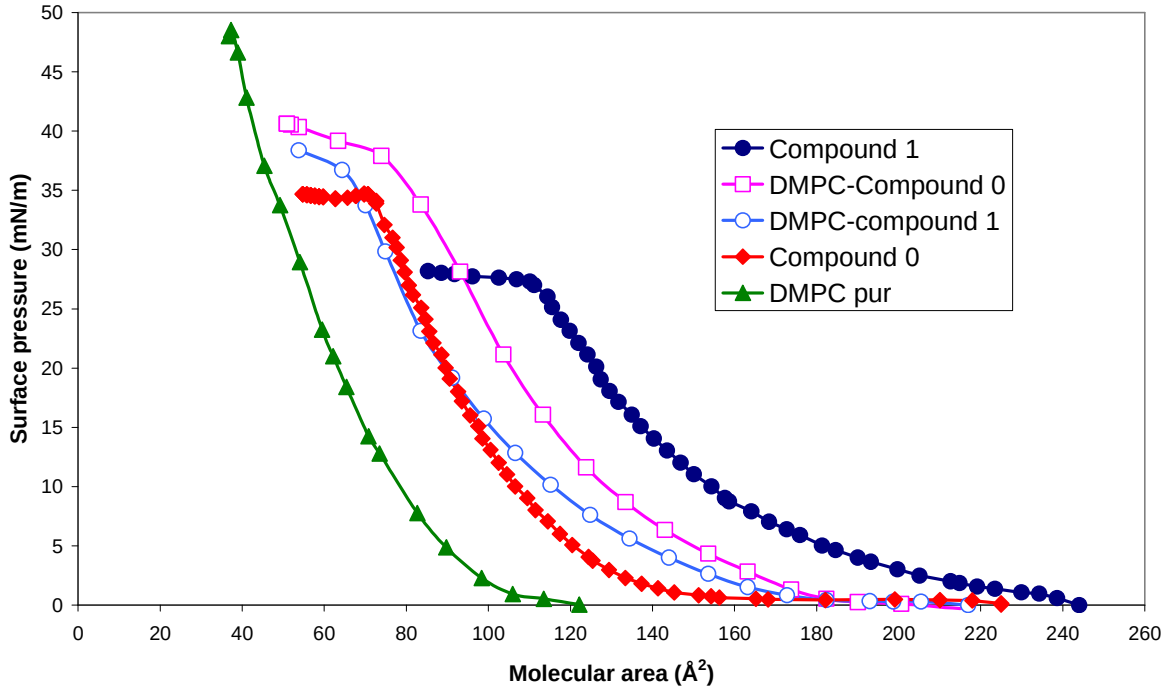

Figure 9: Interfacial behaviour of mixed monolayers (1 : 1) of dimyristoylphosphatidylcholine and compounds **0** and **1**.

This is consistent with the π–A isotherms in Figure 9, which show an expansion of the phospholipid monolayer in the presence of compound **1**. For DMPC liposomes bearing compound **0**, vesicles appeared smaller and less stable with time than those prepared from DMPC or mixtures of DMPC and compound **1**. This is also in agreement with the results in Figure 9 that show an unfavourable interaction between DMPC and compound **0**, probably due to the presence of the sugar moieties in the vicinity of phospholipid headgroups. This repulsive interaction between DMPC and compound **0** could hinder the formation and stabilisation of vesicles and lead to the separation of DMPC vesicles on one side and self-aggregated compound **0** molecules on another. Fresh vesicles batches of DMPC and its mixtures with the glycodendrimeric phenylporphyrin derivatives were left in contact for 1 hour with Concanavalin A (Con A), a mannose-specific lectin (0.5 mg/ml). Their diameters were measured before and after addition of Con A.

Liposome composition	Mean diameter before Con A addition±σ (nm)	Polydispersity index	Mean diameter after Con A addition ±σ (nm)	Polydispersity index
Pure DMPC	185±0.08	0.0103±0.029	187.0±1.3	0.142±0.036
DMPC-compound **0**	178±2.2	0.096±0.013	210±4.15	0.229±0.007
DMPC-compound **1**	218±1.2	0.179±0.034	2510±821	0.617±0.229

Table 2: Mean diameter of liposomes before and after incubation with Concanavalin A (Con A) at room temperature for 1 hour.

The results in Table 2 show that the size of vesicles of pure DMPC and DMPC–compound **0** was not affected (or only slightly) by addition of the lectin. Conversely, for liposomes of DMPC–compound **1**, a dramatic increase in the vesicle diameter and polydispersity index was observed. These striking results could originate from (i) the poor mixing properties of compound **0** with DMPC that would lead to the low incorporation rate of this porphyrin into phospholipid bilayers, and thus to a limited interaction of those liposomes with Con A, (ii) the longer spacer in compound **1** compared to that in compound **0**, which would increase the mobility of mannose moieties and facilitate their interaction with Con A, and (iii) the existence of Con A dimmers and tetramers at the studied pH, allowing lectin interaction with more than one porphyrin molecule possibly borne by different liposomes. Such a multiple interaction would lead to the formation of a network of vesicles bridged by Con A molecules, resulting in a dramatic increase in their apparent size.

Conclusion

In this work, two glycodendrimeric phenylporphyrines (compounds **0** and **1**) were synthesized and their interaction with phospholipids was studied at the air–water interface and in liposome bilayers. The expansion of the DMPC-compound **0** mixed monolayer compared to monolayers of the pure components accounts for an unfavourable interaction that affected the formation and stabilisation of liposomes. Conversely, compound **1** favourably interacted with phospholipid molecules and formed mixed liposomes, which aggregated in the presence of a-mannose specific concanavalin A. These results show that the tetrapyrrolic macrocycle **1** was indeed embedded into the phospholipid bilayer and that its sugar moieties protruded into the surrounding aqueous phase. Such liposomes bearing glycodendrimeric phenylporphyrin could constitute an efficient carrier for drug targeting in photodynamic therapy.

Acknowledgement

The authors acknowledge financial support from the ‘‘Programme Incitatif et Coopératif Rétinoblastome’’ of Institut Curie, and for A. Makky’s PhD grant, from ARC (Association pour la Recherche contre le Cancer).

References

1. Aksenova, A. A., Sebyakin, Y. L., and Mironov, A. F. (2003) Conjugates of Porphyrins with carbohydrates, *Russian Journal of Bioorganic Chemistry 29*, 201-219.
2. Maillard P, G. J., Momenteau M, Gaspard S. (1989) GLYCOCONJUGATED TETRAPYRROLIC MACROCYCLES, *JOURNAL OF THE AMERICAN CHEMICAL SOCIETY 111*, 9125-9127.
3. Momenteau, M., Maillard, P., De Belinay, M. A., Carrez, D., Croisy, A. (1999) Tetrapyrrolic glycosylated macrocycles for an application in PDT, *J. Biomed. Opt. 4*, 298-318.
4. Croisy A., L. **B.,** Maillard Ph. (2005) Les macrocycles tétrapyrroliques glycoconjugués., *Actualités de chimie thérapeutique 31*, 181-244.
5. Laville, I., Figueiredo, T., Loock, B., Pigaglio, S., Maillard, Ph., Grierson, D.S., Carrez, D., Croisy, A., Blais, J. (2003) Synthesis, cellular internalization and photodynamic activity of glucoconjugated derivatives of tri and tetra(meta-hydroxyphenyl)chlorins, *Bioorg. & Med. Chem. 11*, 1643-1652.
6. Monsigny, M., Roche, A.-C., Kieda, C., Midoux, P., and Obrénovitch, A. (1988) Characterization and biological implications of membrane lectins in tumor, lymphoid and myeloid cells, *Biochimie 70*, 1633-1649.
7. Lotan, R., and Raz, A. (1988) Lectins in cancer cells, *Ann N Y Acad Sci 551*, 385-398.
8. Laville, I., Pigaglio, S., Blais, J. C., Doz, F., Loock, B., Maillard, Ph., Grierson, D.S., Blais, J. (2006) Photodynamic Efficiency of Diethylene Glycol-Linked Glycoconjugated Porphyrins in Human Retinoblastoma Cells, *J. Med. Chem. 49*, 2558-2567.
9. Maillard, P., Loock, B., Grierson, D. S., Laville, I., Blais, J., Doz, F., Desjardins, L., Carrez, D., Guerquin-Kern, J. L., Croisy, A. (2007) In vitro phototoxicity of glycoconjugated porphyrins and chlorins in colorectal adenocarcinoma (HT29) and retinoblastoma (Y79) cell lines, *Photodiag. and Photody. Ther. 4*, 261-268.
10. Varki, A. (1993) Biological roles of oligosaccharides: all of the theories are correct, *Glycobiology 3*, 97-130.
11. Wells, L., Vosseller, K., and Hart, G. W. (2001) Glycosylation of nucleocytoplasmic proteins: signal transduction and O-GlcNAc, *Science 291*, 2376-2378.
12. Schueler, M. G., Higgins, A. W., Rudd, M. K., Gustashaw, K., and Willard, H. F. (2001) Genomic and genetic definition of a functional human centromere, *Science 294*, 109-115.
13. Kiessling, L. L., and Pohl, N. L. (1996) Strength in numbers: non-natural polyvalent carbohydrate derivatives, *Chem Biol 3*, 71-77.
14. Mammen, M., Choi, S. K., and Whitesides, G. M. (1998) Polyvalent interactions in biological systems: Implications for design and use of multivalent ligands and inhibitors, *Angewandte Chemie-International Edition 37*, 2755-2794.
15. Kiessling, L. L., Gestwicki, J. E., and Strong, L. E. (2000) Synthetic multivalent ligands in the exploration of cell-surface interactions, *Curr Opin Chem Biol 4*, 696-703.
16. Monsigny, M., Mayer, R., and Roche, A. C. (2000) Sugar-lectin interactions: sugar clusters, lectin multivalency and avidity, *Carbohydr Lett 4*, 35-52.
17. Wong, S. Y. C. (1995) NEOGLYCOCONJUGATES AND THEIR APPLICATIONS IN GLYCOBIOLOGY, *Current Opinion in Structural Biology 5*, 599-604.
18. Roy, R. (1996) Syntheses and some applications of chemically defined multivalent glycoconjugates, *Current Opinion in Structural Biology 6*, 692-702.
19. Lindhorst, T. K., and Kieburg, C. (1996) Glycocoating of oligovalent amines: Synthesis of thiourea-bridged cluster glycosides from glycosyl isothiocyanates, *Angewandte Chemie-International Edition in English 35*, 1953-1956.
20. Alper, J. (2001) Searching for medicine's sweet spot, *Science 291*, 2338-2343.
21. Bezouska, K. (2002) Design, functional evaluation and biomedical applications of carbohydrate dendrimers (glycodendrimers), *J Biotechnol 90*, 269-290.
22. Sampathkumar, S. G., and Yarema, K. J. (2005) Targeting cancer cells with dendrimers, *Chem Biol 12*, 5-6.
23. Ballardini, R., Colonna, B., Gandolfi, M. T., Kalovidouris, S. A., Orzel, L., Raymo, F. M., and Stoddart, J. F. (2003) Porphyrin-containing glycodendrimers, *European Journal of Organic Chemistry*, 288-294.
24. Sasaki, A., Murahashi, N., Yamada, H., and Morikawa, A. (1994) SYNTHESES OF NOVEL GALACTOSYL LIGANDS FOR LIPOSOMES AND THEIR ACCUMULATION IN THE RAT-LIVER, *Biological & Pharmaceutical Bulletin 17*, 680-685.
25. Sasaki, A., Murahashi, N., Yamada, H., and Morikawa, A. (1995) SYNTHESES OF NOVEL GALACTOSYL LIGANDS FOR LIPOSOMES AND THE INFLUENCE OF THE SPACER ON ACCUMULATION IN THE RAT-LIVER, *Biological & Pharmaceutical Bulletin 18*, 740-746.

26. Carpino, L. A., Imazumi, H., El-Faham, A., Ferrer, F. J., Zhang, C., Lee, Y., Foxman, B. M., Henklein, P., Hanay, C., Mugge, C., Wenschuh, H., Klose, J., Beyermann, M., and Bienert, M. (2002) The uronium/guanidinium Peptide coupling reagents: finally the true uronium salts, *Angew Chem Int Ed Engl 41*, 441-445.
27. Rockendorf, N., and Lindhorst, T. K. (2004) Glucuronic acid derivatives as branching units for the synthesis of glycopeptide mimetics, *J Org Chem 69*, 4441-4445.
28. Desroches, M. C., Kasselouri, A., Meyniel, M., Fontaine, P., Goldmann, M., Prognon, P., Maillard, P., Rosilio, V. (2004) Incorporation of Glycoconjugated Porphyrin Derivatives into Phospholipid Monolayers: A Screening Method for the Evaluation of Their Interaction with a Cell Membrane, *Langmuir 20*, 11698-11705.
29. Berthelot, L., Rosilio, V., Costa, M. L., Chierici, S., Albrecht, G., Boullanger, P., and Baszkin, A. (1998) Behavior of amphiphilic neoglycolipids at the air/solution interface: Interaction with a specific lectin, *Colloid Surf. B: Biointerfaces 11*, 239-248.
30. Dynarowicz-Latka, P., Rosilio, V., Boullanger, P., Fontaine, P., Goldmann, M., and Baszkin, A. (2005) Influence of a neoglycolipid and its PEO-lipid moiety on the organization of phospholipid monolayers, *Langmuir 21*, 11941-11948.

Article 3: Effect of Cholesterol and Sugar on the Penetration of Glycodendrimeric Phenylporphyrins into Biomimetic Models of Retinoblastoma Cells Membranes

Ali Makky, Jean-Philippe Michel, Séverine Ballut, Athena Kasselouri, Philippe Maillard , and Véronique Rosilio

Article publié dans Langmuir 2010, vol. 26, n°13, pp. 11145-11156.

Après la caractérisation des porphyrines glycodendrimériques et l'étude de leur incorporation dans des liposomes, nous avons étudié l'effet de la composition lipidique de la membrane cellulaire, et plus particulièrement l'augmentation du taux du cholestérol, sur l'interaction non spécifique des porphyrines dendrimériques avec des monocouches et des liposomes modélisant la matrice lipidique du rétinoblastome. La composition des membranes cellulaires rétinienne inclut une proportion en cholestérol proche de 10% chez le sujet adulte sain. Elle est altérée dans le cas du rétinoblastome avec notamment une augmentation du taux de cholestérol. Malheureusement, l'augmentation de cette proportion est encore inconnue. Nous avons formés nos monocouches et liposomes en utilisant trois phospholipides (SOPC, SOPE, SOPS) et le cholestérol que nous avons fait varier de 10 à 30 mol%. Ces modèles lipidiques à composition complexe mais dénués de récepteur lectinique modèle sont une première étape dans l'élaboration de modèles membranaires véritablement biomimétiques des membranes naturelles de rétinoblastome.

Nous avons analysé l'interaction entre nos porphyrines et les monocouches de phospholipides de deux façons, d'une part sous forme de monocouches mixtes et d'autre part, en injectant les porphyrines libres dans la sous-phase, sous les monocouches de lipide étalées. Ces études de tension superficielle, microscopie à l'angle de Brewster et de compression isotherme nous ont permis d'évaluer d'une part, la qualité des mélanges phospholipide-cholestérol et la capacité des porphyrines à se mélanger avec eux et d'autre part, leur capacité à pénétrer effectivement dans la monocouche à différents états de compression. Notre objectif était de répondre aux questions suivantes : une proportion croissante de cholestérol favorise-t-elle la

pénétration passive de porphyrines glycodendrimériques ? Quelle est l'influence respective du macrocycle et des sucres ?

Une analyse similaire a été réalisée sur le système sous forme de bicouches liposomales, en utilisant l'analyse calorimétrique différentielle pour évaluer l'homogénéité des mélanges ainsi que la température de transition de phase, la charge des vésicules par mesure du potentiel zêta et l'interaction avec les porphyrines par spectroscopie de fluorescence.

Effect of Cholesterol and Sugar on the Penetration of Glycodendrimeric Phenylporphyrins into Biomimetic Models of Retinoblastoma Cells Membranes

Ali Makky[a,b], Jean-philippe Michel[a,b], Séverine Ballut[c,d], Athena Kasselouri[f], Philippe Maillard[c,d], and Véronique Rosilio[a,b,*]

[a b] Univ Paris-Sud 11, UMR CNRS 8612, Laboratoire de Physico-chimie des Surfaces, 5 rue Jean-Baptiste Clément, F-92296 Châtenay-Malabry cedex, France; [c d] UMR CNRS 176, Institut Curie, Centre de Recherche, Bât 110-112, Orsay, F-91405, France; [f] Université Paris-Sud 11, EA 4041, Laboratoire de Chimie Analytique, IFR 141, F-92296 Châtenay-Malabry, France.

* Corresponding author: veronique.rosilio@u-psud.fr

Introduction

Retinoblastoma is the most common malignant childhood intraocular tumor with an incidence of 1/15 000 births. About 40% of cases are unilateral and result from a RB1 gene mutation. (1) Photodynamic therapy (PDT) is considered as one of retinoblastoma alternative treatments. (2-4) This technique is based on the administration of a photosensitizer, which preferentially concentrates in tumor cells, followed by laser illumination of pathological areas. Upon sensitizer photoactivation, generation of reactive oxygen species such as singlet oxygen leads to irreversible destruction of treated tissues. (5) PDT efficiency is correlated, at least within certain limits, with a photosensitizer hydrophobicity and cellular localization. (6) Therefore, comprehension of the passage of such photocytotoxic molecules through retinal membranes is essential to improve the bioavailability of active molecules, and has become a major focus of research. (7-8)

Natural lipid bilayers are the generic scaffold of all cell membranes. Their constituents are organized into a complex structure controlling their properties. Systems with the full biological complexity cannot be reproduced and studied in great detail, as it is difficult to control and vary single parameters. To overcome this difficulty, a simple approach consists in using membrane models, such as lipid monolayers, (9-12) liposomes (13) and planar lipid bilayers. (14) Retina cell membranes are constituted by the most representative lipids of vertebrate retina, i.e. phosphatidylcholine (PC), phosphatidylethanolamine (PE), and phosphatidylserine (PS) at the 4:4:1 molar ratio. (15-17) Less is known about the composition, length and unsaturation rate of hydrocarbon chains. However, some studies show that fatty acids in retinoblastoma Y79 cell membranes are mainly saturated palmitic and stearic acids (16 or 18:0) and mono- and bi-unsaturated oleic acids (18:1 and 18:2).(18) Moreover,

membranes of healthy adult retinal cells have an average cholesterol molar content of 10%. [15] However, many studies have shown changes in phospholipids pattern associated with malignancy. [19] These changes seem to affect the total cholesterol:phospholipid molar ratio [20] as well as the relative percentage and degree of saturation of phospholipid chains. [21] Such changes in cells lipid pattern have been found to alter a number of important functions in plasma cell membranes. [22-23] Although the cholesterol content in retinoblastoma cell membranes has not been precisely determined, it is thought to be higher than in healthy adult retinal cells, especially because retinoblastoma affects young physically growing children. We have therefore built and characterized three models of the retinoblastoma cell membrane with a cholesterol molar content varying from 10 to 30% at pH 6.5, a pH close to that reported for tumorous tissues. [24]

Most photosensitizers used in PDT are porphyrin-based compounds with a tetrapyrrolic macrocyclic core providing the required photophysical properties, and peripheral substituents aimed at controlling their biodistribution and pharmacokinetics. [25] However, these compounds are usually poorly water-soluble molecules, and tend to form aggregates in aqueous solution. Glycoconjugation is considered as a potential effective way to increase both their water solubility and amphiphilicity. Moreover, it provides the possibility for specific interaction of the resulting conjugate with lectin-like receptors over-expressed in some types of malignant cells among which retinoblastoma cells. [7-8, 26-28] Coupling multivalent carbohydrates to the porphyrin core allows their interaction with more than one receptor binding site at the same time, and increases their receptors affinity, which results in a better cellular recognition. [29] Thus, efforts have been focused on the preparation and *in vitro* evaluation of the phototoxicity of a broad series of neutral glycoconjugated tetrapyrrolic macrocycles. It has been shown that triglycoconjugated sensitizers are more phototoxic than the parent tetrapyrrolic and symmetrical tetraglycoconjugated derivatives. [8] This has been attributed not only to the interaction of sugar moieties with a still unidentified lectin-like membrane receptor to mannose, [7] but also to a strong interaction of the tetrapyrrolic compound and its triglyconconjugated derivative with phospholipids. [30] In this context, new glycodendrimeric porphyrins have been synthesized in order to improve tumor selectivity and porphyrin penetration into cells. [7, 26-29]

The aim of this work was to analyze the non-specific interaction of glycodendrimeric porphyrins with biomimetic models of retina cancerous cells membrane in the absence of the lectin-like receptor.

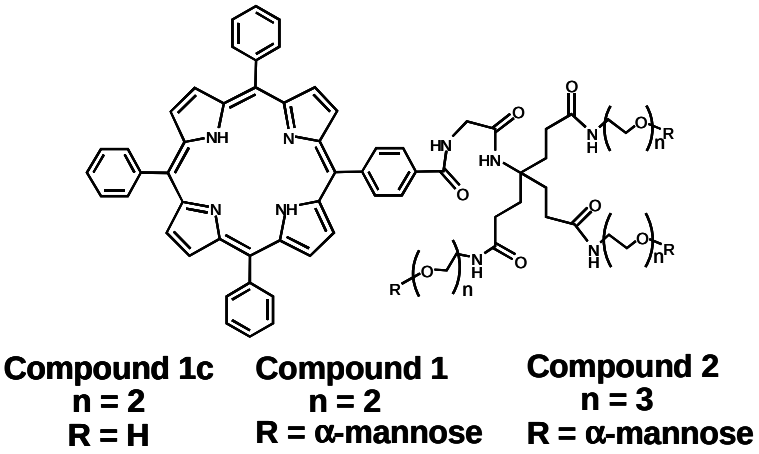

Figure 10: Chemical structure of porphyrins.

We focused on the effects of cholesterol rate on compression isotherms of model monolayers and on the thermal behavior of hydrated lamellar phases. The penetration of photosensitizers into biomimetic monolayers and liposome bilayers was then studied, by surface pressure measurements and fluorescence spectroscopy.

Materials and methods

A. Materials

The glycodendrimeric porphyrins, **compound 1** (Mw = 1692.81 g/mol) and **compound 2** (Mw = 1823.8 g/mol) were prepared as described previously by *Ballut et al.* [29] Both are tri-mannosylated but fitted with spacers of different length, a diethylene glycol and a triethylene glycol for **compounds 1** and **2**, respectively. We have also studied the non glyconconjugated **compound 1c** (Mw = 1236.09 g/mol) in which the mannose moieties of **compound 1** are replaced by OH groups. This compound was thus considered as the control for **compound 1**. All these porphyrin derivatives are poorly soluble in pure water but soluble in methanol and in the mixture of chloroform and methanol (9:1) used for spreading at air/liquid interface, and for liposome preparation. The chemical structures of the studied porphyrins are shown in Figure 10.

The phospholipids 1-stearoyl-2-oleoyl-*sn*-glycero-3-phospho-L-serine (sodium salt) (SOPS, Mw = 812.05 g/mol), 1-stearoyl-2-oleoyl-*sn*-glycero-3-phosphocholine (SOPC, Mw = 788.14 g/mol) and 1-stearoyl-2-oleoyl-*sn*-glycero-3-phosphoethanolamine (SOPE, Mw = 746.06 g/mol) were purchased from Instruchemie (Delfzijl, The Netherlands). They were 99% pure and were used without any further purification. Cholesterol (CHOL, 99% pure, Mw = 386.66 g/mol), HEPES (99.5% pure, Mw = 238.31 g/mol), sodium chloride (NaCl, 99% pure, Mw =

58.44 g/mol), calcium chloride ($CaCl_2$, 98% pure, Mw = 147.02 g/mol), nickel chloride ($NiCl_2.6H_2O$, 98% pure, Mw = 237.69 g/mol), sodium thiosulfate ($Na_2S_2O_3$, Mw = 157.12 g/mol) and potassium iodide (KI, Mw = 165.87 g/mol) were purchased from Sigma (St. Louis, USA). Chloroform, methanol and pyridine (99% pure) were analytical grade reagents and provided by Merck (Germany). The ultrapure water (γ = 72.2 mN/m at 22°C) was produced by a Millipore Synergy 185 apparatus coupled with a RiOs5^{TM}, with a resistivity of 18.2 MΩ.cm was used in all experiments. All glassware were soaked for an hour in a freshly prepared TFD4 (Franklab) detergent solution (15% v/v), and then rinsed thoroughly with milli-Q water and finally oven-dried.

B. Methods

Composition of the biomimetic models

The models of retinoblastoma cell membranes consisted of three phospholipids (SOPC, SOPE and SOPS) and cholesterol. We chose mixed-chain phospholipids containing one saturated stearic acid (18:0) in the *sn*-1 position and one monounsaturated oleic acid (18:1) in order to mimic the most representative headgroups, chain lengths and unsaturation of natural lipids present in retinoblastoma cells. Molar fractions of the various lipids are listed in Table 3.

Membrane Model	SOPC	SOPE	SOPS	Cholesterol
	Molar fraction (%)			
M0	**45**	**45**	**10**	**0**
M1	**40**	**40**	**10**	**10**
M2	**35**	**35**	**10**	**20**
M3	**30**	**30**	**10**	**30**

Table 3: Lipidic composition of retinoblastoma models.

Surface pressure-Area (π-A) measurements

Compression of lipid monolayers was performed at 22±1°C, using a homemade auto-recording Langmuir-type film trough (160 cm^3, 217.2 cm^2) equipped with a R&K Wilhelmy pressure transducer (Riegler and Kirstein, GmbH, Germany) enclosed into a Plexiglas box to limit surface contamination.

Mixed lipid monolayers, pure porphyrins and lipid-porphyrin mixtures (9:1 molar ratio) were spread from chloroform/methanol (9:1 v/v) solutions onto the buffer subphase (10 mM HEPES, 150 mM NaCl, 1 mM $CaCl_2.2H_2O$ and 1 mM $NiCl_2.6H_2O$, pH 6.5) with a Gilson micropipette (Gilson, France). Prior to monolayer spreading, the subphase surface was

cleaned by suction. Monolayers were left for 15 minutes to allow complete evaporation of the solvents. Compression was then performed at the speed of 9.57 cm^2 / min.

From the (π-A) isotherms, the surface compressional moduli K of monolayers at a given temperature were calculated from the equation:

$$K = A\left(\frac{d\pi}{dA}\right)_T \quad \text{(Eq. 1)}$$

To assess whether addition of cholesterol to the phospholipid species (M0 model) would lead to an expansion or condensation of the resulting phospholipid-cholesterol mixtures, experimentally observed areas A_{EXP} of these mixtures were compared to that of the M0 model at the same surface pressure π. Apparent cholesterol-induced relative area variations of the phospholipids species were thus calculated at the indicated surface pressure π as follows: [31]

$$\text{PL apparent area variation in \%} = \left[\frac{A_{EXP} - A_{chol} X_{chol}}{X_{PL}\ A_{PL}} - 1\right]_\pi \quad \text{(Eq. 2)}$$

where X_{PL} and X_{chol} are the molar fractions of phospholipids and cholesterol, in the mixed monolayer and A_{PL} and A_{chol} the molecular areas of the phospholipid M0 model and pure cholesterol monolayers, respectively. The net result is to express and normalize cholesterol-induced area variation as area change imparted to the PL molecules. [32]

To assess the relative average area variations induced by addition of porphyrin (X_P = 0.1) to the phospholipid-cholesterol mixtures, experimentally observed molecular areas of the lipid-porphyrin monolayers ($A_{L\text{-}P}$) at a given pressure π were compared to theoretical areas A_{TH} calculated for the lipid-porphyrin mixtures according to the additivity rule:

$$[A_{TH}]_\pi = [X_L\ A_L + (X_P)A_P]_\pi \quad \text{(Eq. 3)}$$

where X_L and A_L were the molar fraction and molecular area of the lipid mixtures and X_P and A_P the molar fraction and molecular area of the added porphyrin component. The excess molecular areas ΔA^{EXC} were calculated from the difference $A_{L\text{-}P}$-A_{TH}. Negative deviations from the additivity rule indicate area condensation and may imply intermolecular accommodation and/or dehydration interactions between lipids in the mixed films. [33] Positive deviations from the additivity rule are the result of area expansion and would account for unfavorable interactions between the different components leading to poor mixing.

The free energy of mixing ΔG^M was calculated according to the Eq. 3: [34]

$$\Delta G^M = \Delta G^{EXC} + \Delta G^{IDEAL} \quad \text{(Eq. 4)}$$

with ΔG^{EXC} the excess free energy and ΔG^{IDEAL} the free energy of mixing for an ideal mixture, where R is the universal gas constant and T the absolute temperature.

$$\Delta G^{EXC} = \int_0^{\pi} \Delta A^{EXC}\, d\pi \quad \text{(Eq. 5)} \quad \text{and} \quad \Delta G^{IDEAL} = RT\,(X_L \ln X_L + X_P \ln X_P) \quad \text{(Eq. 6)}$$

Brewster Angle Microscopy (BAM)

The morphology of the monolayers at the air-water interface was monitored with a Brewster angle microscope (MicroBAM 3, Nima Technology Ltd, Coventry, U.K) mounted on the Langmuir trough. The microscope was equipped with a frequency laser diode (λ = 659 nm, 30 mW optical power) generating a collimated beam of approximately 6 mm diameter, with a p-polarizer, analyzer and a USB camera. The spatial resolution of the BAM was about 6 µm per pixel, with a field of view of 3.6 x 4.1 mm^2, resolved over 640 x 480 pixels. Image size was 2.0 mm^2 after rescaling.

Surface tension measurements

Penetration of porphyrins into model monolayers was inferred from the change in surface pressure measured by the Wilhelmy plate method using a K10 tensiometer (Krüss, Germany). In this experiment, 10 µl of porphyrin solution in pure methanol (5.48 $x10^{-4}$ M) was injected in a glass cell (20 ml, 11.9 cm^2) through a side arm into the buffer subphase (10 mM HEPES, 150 mM NaCl, 1 mM $CaCl_2.2H_2O$ and 1 mM $NiCl_2.6H_2O$, pH 6.5), beneath a spread lipid monolayer at the initial surface pressure of about 30 mN/m. This surface pressure was considered as that in a cell membrane. [35] The final concentration of the porphyrins in the measurement cell was 2.74 x 10^{-7} M. The injection of 10 µl of pure methanol had no effect on the surface pressure of the lipid monolayer.

All experiments were run at 22±1°C, and the results reported are mean values of at least three measurements. The experimental uncertainty was estimated to be 0.2 mN/m.

Liposomes preparation

Liposomes were prepared according to Bangham's method followed by the extrusion of vesicles suspensions. [36-38] In brief, phospholipid solutions in chloroform/methanol (9:1 v/v) were evaporated for 3 hours under reduced pressure, and the resulting dry lipid film was hydrated by 10 ml of buffer (10 mM HEPES, 150 mM NaCl, pH 6.5). The 4 mM lipid suspension thus obtained was then extruded 15 times through a 200 nm polycarbonate membrane at 60°C (Avestin Lipofast extruder, Ottawa, California). The diameter and zeta

potential (ζ) of the vesicles were measured using a Zeta-sizer (Nano ZS90, Malvern) after dilution of the liposome suspension in deionised water. All measurements were carried out at 25°C. The average liposome size was 150 ±10 nm for all formulations.

DSC measurements

The thermal behavior of liposomes was analyzed by differential scanning calorimetry (DSC) by means of a DSC7 (Perkin-Elmer, Wellesley, Maine, USA) and the Pyris software. DSC measurements were performed in an atmosphere of flowing nitrogen gas using standard aluminium sample pans. The DSC was calibrated with indium and *n*-decane from Perkin-Elmer. The temperature was increased from -30°C to 70°C at a rate of 5°C/min with an empty pan as a reference. The lipid concentration was 2 mM in the HEPES buffer and 10 µl of liposome suspension was carefully placed and sealed in the aluminium hermetic pans. Enthalpy ΔH values were calculated by the Pyris software from the areas under the curves.

Spectroscopic measurements in liposome suspension

UV-visible absorption measurements were carried out on a CARY 100 Bio UV-visible spectrophotometer (Varian, USA). Fluorescence emission spectra were recorded at 37°C on a Perkin-Elmer LS-50B computer controlled luminescence spectrophotometer (Massachusetts, USA) equipped with a red sensitive R6872 photomultiplier. Excitation was performed at the maximum of the Soret band at a wavelength of $\lambda_{excitation}$ = 421 nm and emission was measured at $\lambda_{emission}$ = 653 nm. All tested samples had a low optical density (<0.05) at the wavelength of excitation in order to avoid the inner filter effects.

The partition of porphyrins between the aqueous phase and the liposome was studied by recording the fluorescence emission spectra of series of solutions with various phospholipid concentrations. [39-41] To do so, the fluorescence intensity of the peak corresponding to porphyrins, F_{obs}, was plotted as a function of increasing lipid molar concentrations L, and fitted using the following equation: [40]

$$F_{obs} = \frac{F_0 \times L}{\left[\left(W/K_p\right) + L\right]} \qquad \text{(Eq. 7)}$$

where F_0 is the maximum fluorescence intensity resulting from total porphyrin incorporation into liposome membrane, W is water molar concentration in liposome, considered as pure water (i.e. 55.6 M), and K_p the membrane partition coefficient of porphyrins. The fluorescence

resulting from liposome titration against a constant porphyrin concentration yielded a saturation curve from which K_p values were deduced.

Experimentally, 10^{-4} M porphyrin stock solutions in methanol/pyridine (98/2 v/v) were prepared and diluted to $2x10^{-7}$ M using buffer (10 mM HEPES, 150 mM NaCl, 1 mM $CaCl_2.2H_2O$ and 1 mM $NiCl_2.6H_2O$, pH 6.5) just before the experiments. 1 ml of porphyrin aqueous solutions was added to 1 ml of liposome suspensions with increasing lipid concentrations. The final porphyrin concentration was $1x10^{-7}$ M and [lipid]/[porphyrin] ratios were in the range [0-2000]. The samples were mixed and kept in darkness at 37°C for 2 hours, and the measurements were performed at the same temperature. Kinetic measurements were achieved in the same conditions and showed after 2 hours incubation that incorporation of porphyrins into liposomes has reached equilibrium (data not shown).

The relative depth of porphyrins penetration into liposome bilayer was assessed from fluorescence quenching with iodide ions (I^-). The deeper the tetrapyrrole ring was inserted into a lipid bilayer, the less accessible it was to the KI quencher, yielding a lower Stern-Volmer quenching constant K_{SV}, as compared to the pure porphyrin in aqueous solution. [42-43] K_{SV} is defined by:

$$F_0/F = 1 + K_{SV}[Q] \qquad \text{(Eq. 8)}$$

where F_0 and F were the fluorescence intensities in the absence and presence of I^- ions, respectively, and [Q] was the quencher concentration.

Practically, fluorescence quenching studies were performed after 2 hours of liposome-porphyrin incubation at 37°C, after adding KI with increasing concentrations in the liposome suspension. For this purpose, a solution containing 5 M KI and 10^{-3} M $Na_2S_2O_3$ in buffer was prepared, and eleven aliquots of 10 µl of it was successively added to 2 ml of a lipid/porphyrin (ratio 1000/1) suspension, then mixed and kept in darkness for 10 min at 37°C before measurement. This procedure was repeated until reaching the final KI concentration of 0.26 M.

Results

Interfacial behavior of the pure dendrimeric phenylporphyrines

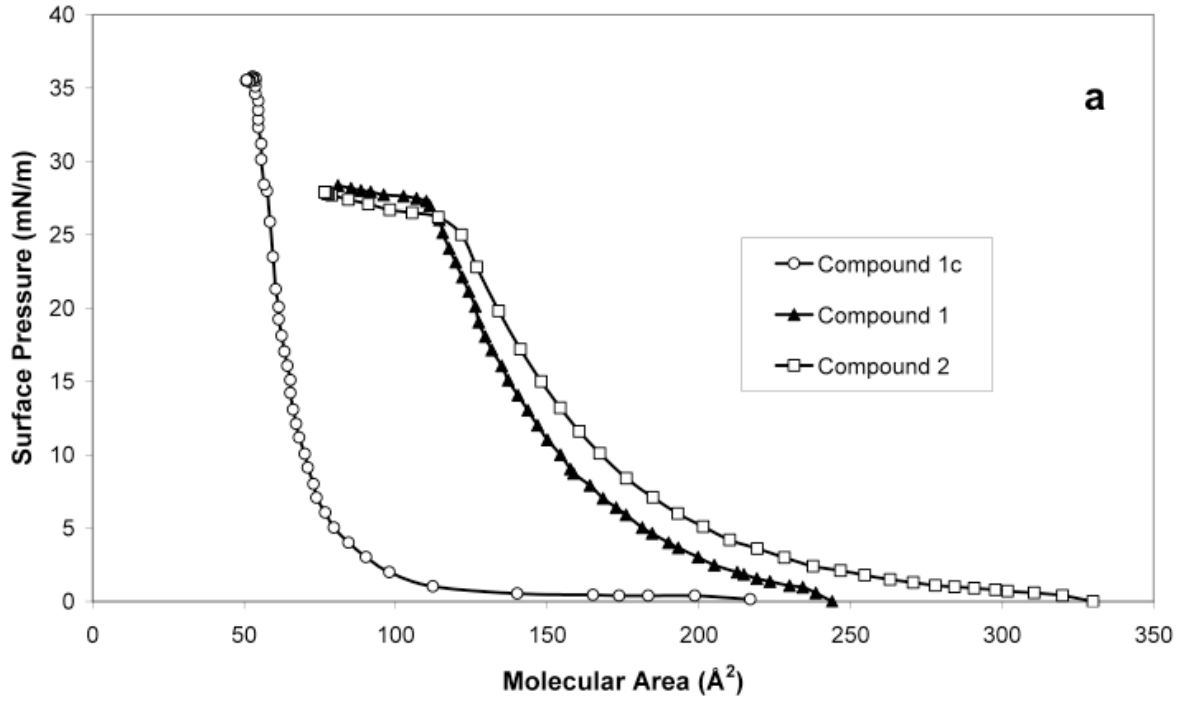

Figure 11: *π-A* isotherms for the pure porphyrin monolayers spread at the air/buffer interface.

Figure 11: shows the π-A relationships for the studied porphyrins spread at the air-buffer interface. The glycoconjugated porphyrins formed much more expanded monolayers than the non-glycoconjugated one. **Compound 1c** showed the highest surface pressure and smallest molecular area at collapse (A_c = 52.8 Å^2). The same A_c value was obtained in a previous work for the 5,10,15,20-*meso*-tetra-(*meta*-hydroxyphenyl) porphyrin (*m*-THPP), and it was suggested that it corresponded to the side-on orientation of the tetraphenyl-porphyrin macrocycle at the interface. [30] The molecular areas at collapse for **compounds 1** and **2** (110 Å^2 and 118 Å^2, respectively) were much larger due to the presence of the sugar moieties immersed into the subphase. The 8 % area increase observed for **compound 2** compared to **compound 1** could be related to the presence of the additional monomer of ethylene glycol in the spacer of **compound 2**, enlarging the volume of the hydrophilic group, which would hinder close packing of the molecules in the monolayer. As expected from the shape of the isotherms and the surface pressure and area values at collapse, the maximum compression modulus K_{max} was much higher for **compound 1c** (210.9 mN/m) than for **compounds 1** and **2** (79.3 and 68.0 mN/m, respectively). The **compound 1c** monolayer was much more rigid than those of the two other compounds.

Interfacial behavior of phospholipid-cholesterol mixtures mimicking the retinoblastoma cell membrane

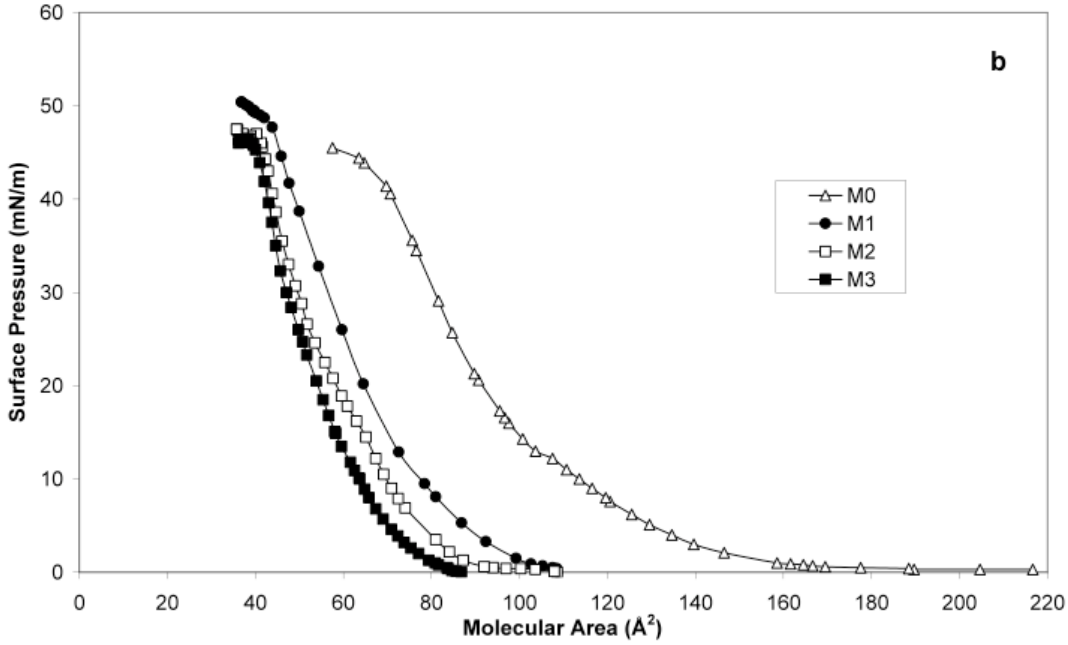

Figure 12 : π-*A* isotherms for the biomimetic monolayers M0 (0% cholesterol), M1 (10%), M2 (20%) and M3 (30%).

Figure 12 shows the surface pressure-area isotherms of mixed phospholipid monolayers mimicking the composition of retina cell membranes, with increasing molar fractions of cholesterol. Compared to the mixed phospholipids monolayer (M0), the isotherms for the phospholipid-cholesterol systems were all shifted toward smaller molecular areas. Apparent phospholipid area reduction clearly demonstrated the condensing effect of cholesterol on phospholipid species, the largest decrease in molecular area being observed between 0 and 10 mol% cholesterol (27.2% apparent condensation, see Table 4). The isotherm for M0 showed a slight inflexion at a surface pressure of 13 mN/m, which vanished when cholesterol was added to the mixtures. These results would account for the miscibility of the three lipids with cholesterol, even when the latter was incorporated at a high molar ratio.

Composition of the monolayer	A_c ($Å^2$)	π_c (mN/m)	A_{30} ($Å^2$) at 30 mN/m	PL apparent area variation at 30 mN/m (%)	Lipid/porphyrin area variation at 30mN/m (%)	K_{max} (mN/m)
Compound 1c	52.8	35.5	55.7	--	--	210.9
Compound 1	110.0	27.5	70.2*	--	--	79.3
Compound 2	118.0	26.0	76.6**	--	--	68.0
M 0	69.0	46.1	80.6	0	--	96.3
M 1	43.1	49.3	56.4	-27.2	--	85.7
M 2	41.0	47.5	49.6	-34.3	--	107.0
M 3	40.0	46.5	47.0	-35.9	--	130.0
M1-Compound 1c	62.0	44.7	76.3	--	35.4	98.0
M2-Compound 1c	61.8	42.6	74.4	--	48.2	66.5
M3-Compound 1c	55.0	41.9	67.8	--	41.6	75.3
M1-Compound 1	59.0	47.3	71.7	--	24.1	89.6
M2-Compound 1	63.0	41.4	74.7	--	44.6	76.5
M3-Compound 1	59.3	43.2	71.3	--	44.6	74.2
M1-Compound 2	61.0	44.0	75.2	--	28.7	102.0
M2-Compound 2	66.0	42.1	78.1	--	49.3	62.9
M3-Compound 2	60.0	41.6	72.2	--	44.5	62.6

Table 4: Molecular area (A_c), surface pressure (π_c) at collapse, and molecular area (A_{30}), PL apparent area variation and area variation of the lipid/porphyrin mixtures at the surface pressure of 30 mN/m; maximal compressional modulus K_{max} for pure porphyrin monolayers, lipid and lipid-porphyrin mixtures.
*A_0 is measured at a surface pressure of 27.5 mN/m for **compound 1**, **and at 26.0 mN/m for **compound 2**. The average relative area condensations were calculated from the quotient $(A_{L\text{-}P}\text{-}A_{TH})/A_{TH}$.

ΔA^{EXC} calculations confirmed monolayers condensation induced by cholesterol (Figure 13). All excess free energies (ΔG^{EXC}) values were negative indicating the existence of attractive interactions between the film forming components, and ΔG^{M} values calculated using Eq. 4 showed that the most thermodynamically stable system was M3 (Figure 14).

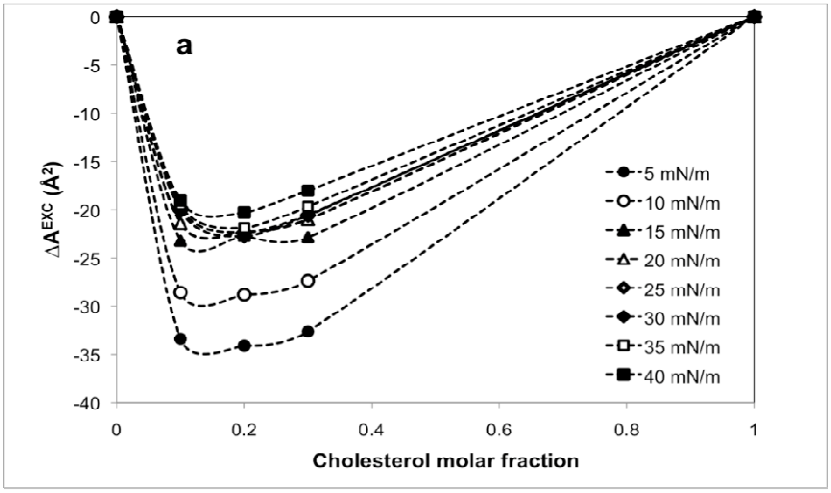

Figure 13 : ΔA^{EXC} values for model monolayers M1, M2 and M3.

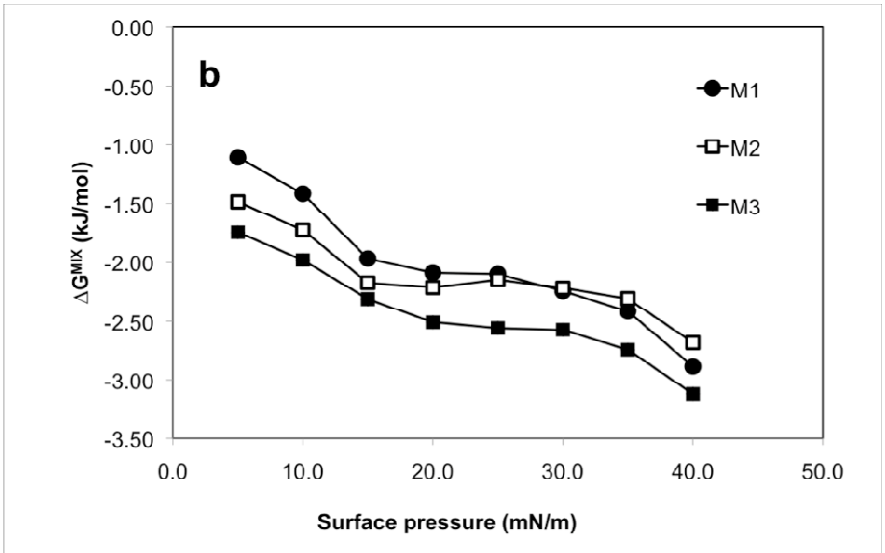

Figure 14 : ΔG^{MIX} values for model monolayers M1, M2 and M3.

The lateral compressibility moduli K were calculated and their maximum values are indicated in Table 4. According to Davies and Rideal,[(44)] K values below 12.5 mN/m, in the range of 13-50 mN/m, 100 to 250 mN/m, and above 250 mN/m would account for the gaseous state, the liquid-expanded state, the liquid condensed state and the solid state of a monolayer, respectively. The M1 mixture formed the less organized monolayer and M3 the most rigid one (Table 4). The latter was expected to play the role of an effective barrier against molecules akin to interact and penetrate into it.

The compression of the M1 mixture depicted in Figure 12 was also performed at pH 7.4 (“healthy system”). The pH reduction from 7.4 to 6.5 (tumor pH) only induced a 2% monolayer condensation, negligible with respect to that induced by addition of cholesterol to the monolayers. Therefore, all following experiments were performed at pH 6.5 only.

Thermal behavior of lipid mixtures:

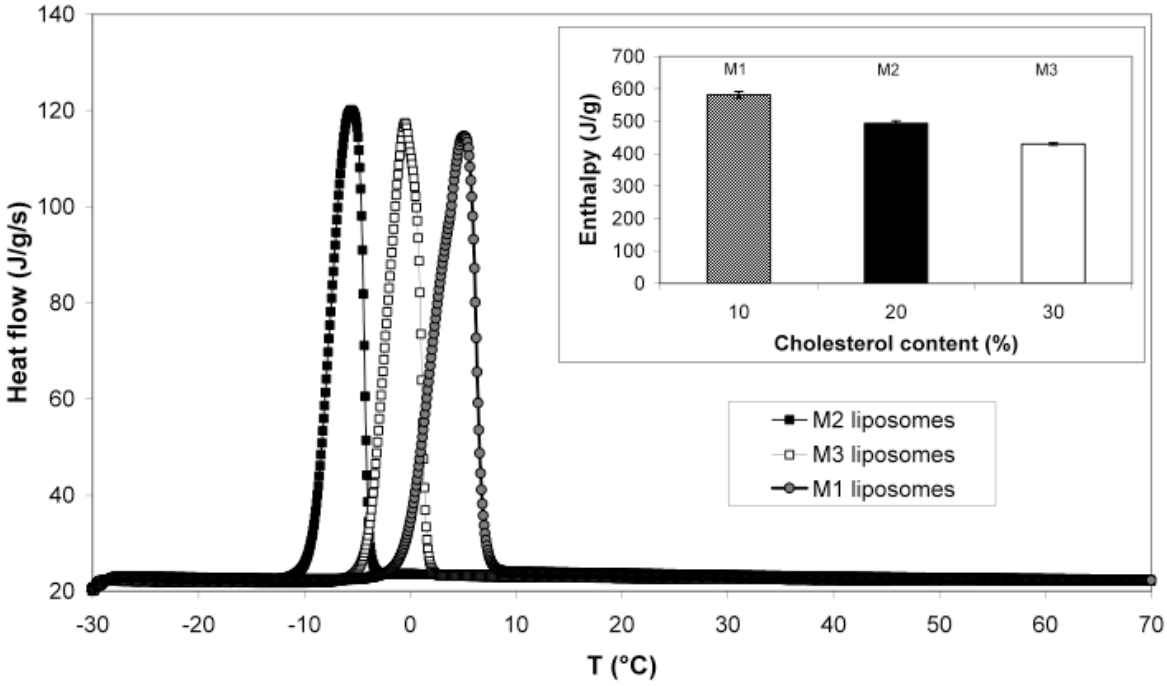

Figure 15: DSC thermograms for M1, M2 and M3 mixtures in HEPES buffer. The transition enthalpies (Δ*H* values) at the transition are compared in the inset.

Figure 15 shows DSC measurements performed on hydrated lipid mixtures. Each thermogram displays a unique fine peak corresponding to the main thermotropic transition from the gel phase to the fluid liquid crystal phase. This would account for homogeneous lipid mixtures. The phase transition temperatures for SOPC, SOPE and SOPS in solution are 6.0, [45] 30.0 [46] and 17.0°C, [47] respectively. DSC measurements showed that mixing the three components and adding cholesterol shifted the phase transition temperature of the mixtures toward lower values than those of the pure components. The thermal behavior of the mixtures was significantly affected by the presence of cholesterol, however not to the same extent, as shown by the comparison of the phase transition temperatures.

Indeed, the M2 hydrated lipid phases exhibited a lower temperature value (-5.62 ± 0.07°C), than both the M3 and M1 systems (-0.50 ± 0.02°C and 4.34 ± 0.54°C, respectively). The areas below peaks allowed determination of the ΔH values for the three mixtures and the results are presented in the inset to Figure 15. The transition enthalpy decreased when the cholesterol content increased in the order 581.6 ± 10.3 J/g, 493.8 ± 7.9 J/g, and 430.1 ± 3.8 J/g for M1, M2 and M3, respectively. Apparently, the system needed less energy to achieve the transition as the cholesterol content increased from 10 to 30 mol%.

Effect of lipid composition on the zeta potential (ζ) of liposome suspensions:

Liposomes were prepared from the M1, M2 and M3 lipid mixtures. The zeta potential (ζ) values measured for these liposomes were -62.0 ± 0.9 mV, -43.6 ± 2.7 mV, and -43.6 ± 2.7 mV, respectively. They were negative for all three models, as expected from the presence of negatively charged SOPS molecules in the composition of the vesicles. Although the SOPS molar fraction was kept constant in all studied mixtures, increasing cholesterol content from 10 to 20 mol% led to a less negative ζ potential value. There was no further change above 20 mol%. It is worth noting that the hydrodynamic diameter of the liposomes (150 nm) was not affected by lipid composition change.

Surface pressure changes induced in lipid monolayers upon porphyrin injection into the subphase

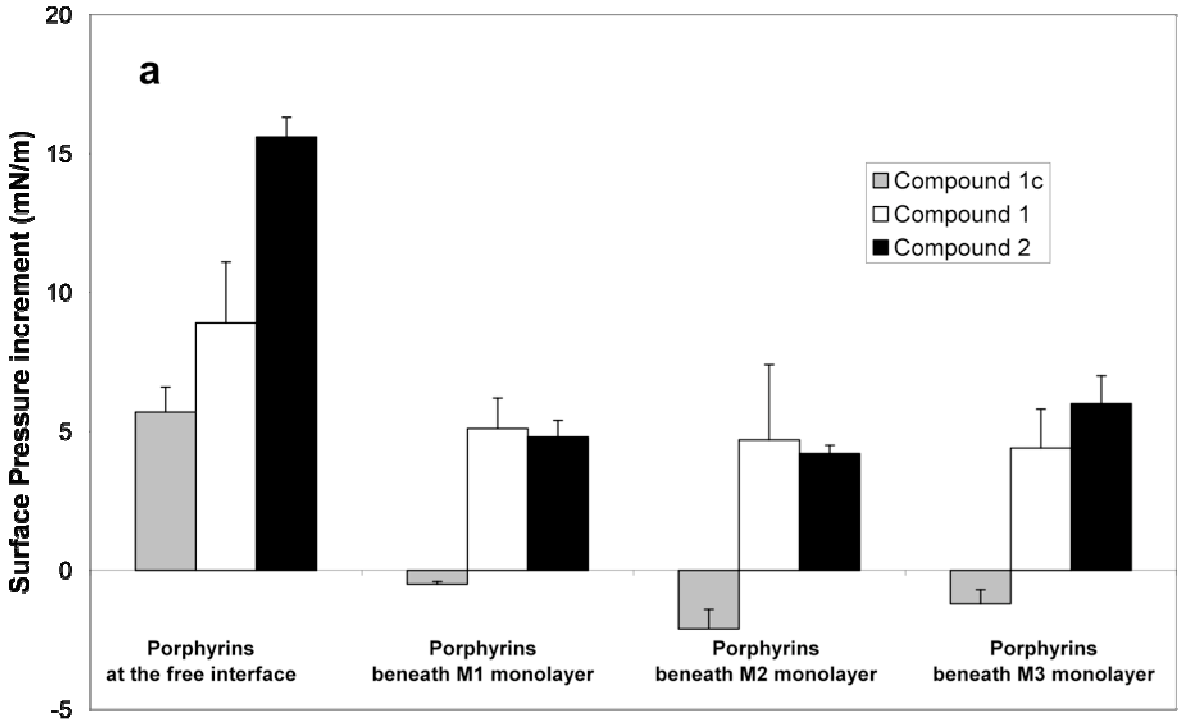

Figure 16 : Surface pressure change induced by porphyrin injection beneath the model monolayers at the initial pressure of 30 mN/m.

Figure 16 summarizes the surface pressure changes induced by the adsorption of porphyrin derivatives dissolved in the buffer, at the free interface and into the model monolayers compressed to the initial pressure (π_i) of 30 mN/m. This high initial surface pressure was aimed at mimicking the primary interaction of the photosensitizers with a biological membrane. The values were taken at equilibrium, following porphyrin derivatives injection.

Compounds 1 and **2** adsorbed better at the free air/buffer interface than the more hydrophobic **compound 1c**, which was less soluble than the others and therefore aggregated more in the subphase, even if its concentration (2.74 $x10^{-7}$ M) was low. The longer spacer in **compound 2** reinforced its amphiphily, as deduced from its more extensive adsorption at the interface, compared to **compound 1**.

When injected beneath a condensed lipid monolayer (π_i = 30 mN/m), the glycodendrimeric phenylporphyrins induced almost the same surface pressure change ($\Delta\pi \approx +5$ mN/m), independently of cholesterol content in the lipid monolayers. This pressure increment could account for the penetration of porphyrins into the monolayers, despite the high initial surface pressure. Conversely, for **compound 1c**, all $\Delta\pi$ values were negative, as if lipid monolayers acted as a barrier to its adsorption. This was surprising since it was expected that the adsorption of the most hydrophobic compound would be enhanced in the presence of a lipid layer compared to the hydrophilic glycodendrimeric porphyrins. On the contrary, **compound 1c** destabilized the lipid monolayers, but apparently did not penetrate into them.

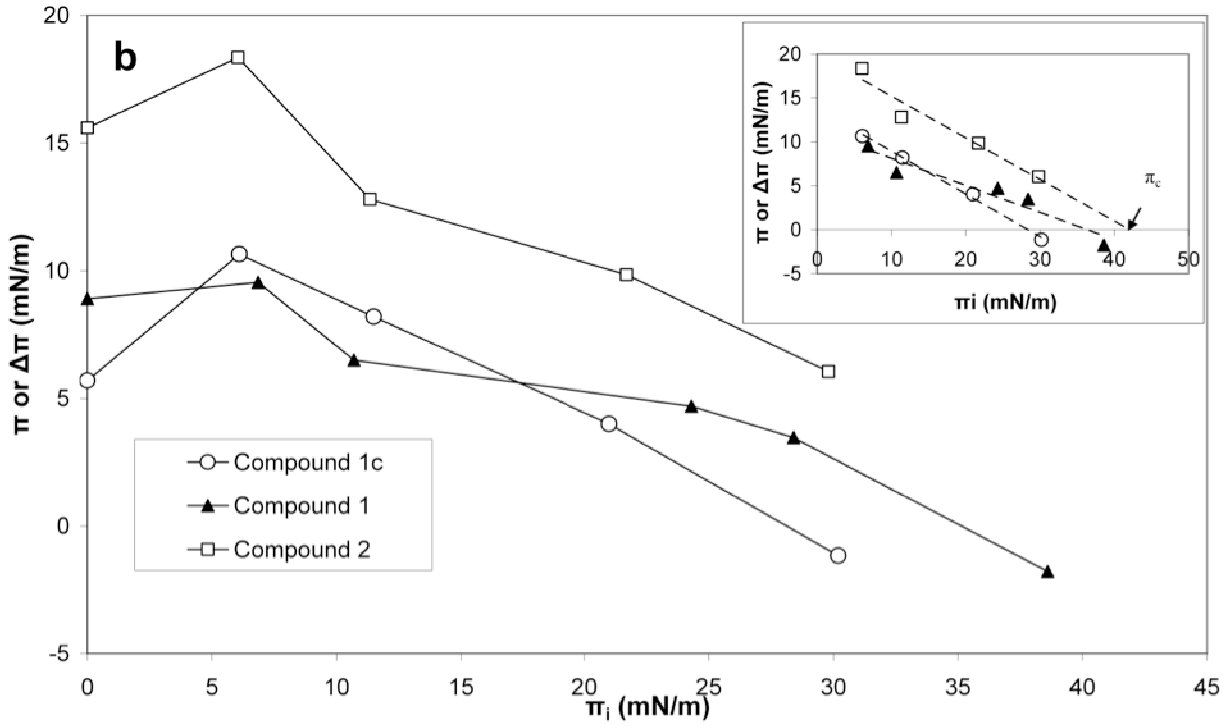

Figure 17 : Surface pressure change ($\Delta\pi$) induced by injection of the porphyrins beneath the M3 model membrane, spread at various initial surface pressures π_i. Inset shows the linear plot and extrapolation of the increment in surface pressure at high initial surface pressure.

In order to get a better insight into the mechanism of interaction of the porphyrins with the monolayers, we studied the surface pressure change following injection of the porphyrin derivatives beneath the M3 monolayer at increasing initial surface pressures (π_i). These initial

surface pressures were chosen in the 0-30 mN/m range, and the surface pressure increments were taken at equilibrium (Figure 17). A maximum in the curves was identified at π_i = 5 mN/m, especially high for **compound 2**, indicating that at low surface pressure, the lipids generally favored porphyrin penetration into the monolayer. A similar result has been reported for the interaction between Flurbiprofen and cornea model monolayers containing cholesterol [(48)]. Moreover, increments in surface pressure were in average twice larger for **compound 2** than for **compound 1** or **1c**, confirming the promoting effect of the longer spacer in the interfacial behavior of the porphyrins.

Above 5 mN/m, as the initial surface pressure increased in the monolayer, the surface pressure change diminished. Fewer molecules were able to penetrate into the densely packed lipid monolayer, which acted as a barrier. This effect became predominant at very high surface pressures, hindering the insertion of all porphyrin derivatives. Although there was apparently not much difference in the interfacial behavior of **compounds 1** and **1c** in the presence of the M3 monolayer up to π_i = 15 mN/m, above this pressure **compound 1** appeared more efficient.

The critical surface pressures π_{cr} were deduced from the extrapolation of the $\Delta\pi$-π_i relationships enlarged in the inset to Figure 17. They were determined by the intersection of the line coming from extrapolation of the fitting of the experimental curve ($\Delta\pi \rightarrow 0$) and the horizontal *x*-axis. The π_{cr} preventing any penetration of a porphyrin into the M3 monolayer were found to be 28, 35 and 42 mN/m for **compounds 1c**, **1** and **2** respectively. So up to 28 mN/m, all porphyrin compounds were able to penetrate into the phospholipid monolayers, even at high cholesterol content. At surface pressures exceeding that of a cell membrane (about 28 mN/m), however, the glycoconjugated porphyrins could still affect the surface pressure, whereas **compound 1c** could not. All these results demonstrate that sugar moieties played a role in the interaction of **compounds 1** and **2** with the lipids and that it was not solely due to their higher hydrophily and lower aggregation in aqueous medium, as compared to **compound 1c**.

Compression isotherms of mixed lipids-porphyrins monolayers

In order to assess whether a porphyrin, once inserted in the monolayers could interact favorably with the lipids, and which of the sugar moiety or the cholesterol content would have the predominant effect, mixtures of lipids and porphyrin (X_P = 0.1) were spread at the air/buffer interface. The incorporation of porphyrin molecules altered significantly the organization of phospholipid-cholesterol mixed monolayers (Figure 18-20 and Table 4).

All porphyrins apparently counterbalanced the condensing effect of cholesterol, especially when mixed to M2 and M3. They also affected the maximum compressibility modulus of the mixed monolayers, which significantly decreased when the porphyrins were mixed to M2 and M3, but increased when they were mixed to M1, accounting for a less fluid monolayer. Apparently, the insertion of the large hydrophobic macrocycles modified the already complex interactions between phospholipids and cholesterol within the monolayer, and altered their packing.

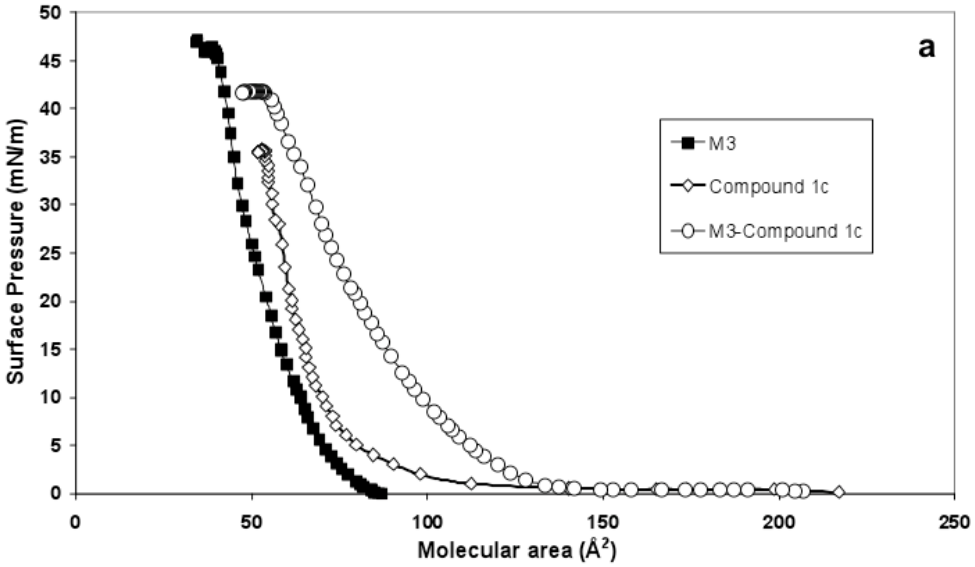

Figure 18 : π-*A* isotherms for the M3 model monolayer, the pure **compound 1c** and the mixed M3-**compound 1c** monolayers.

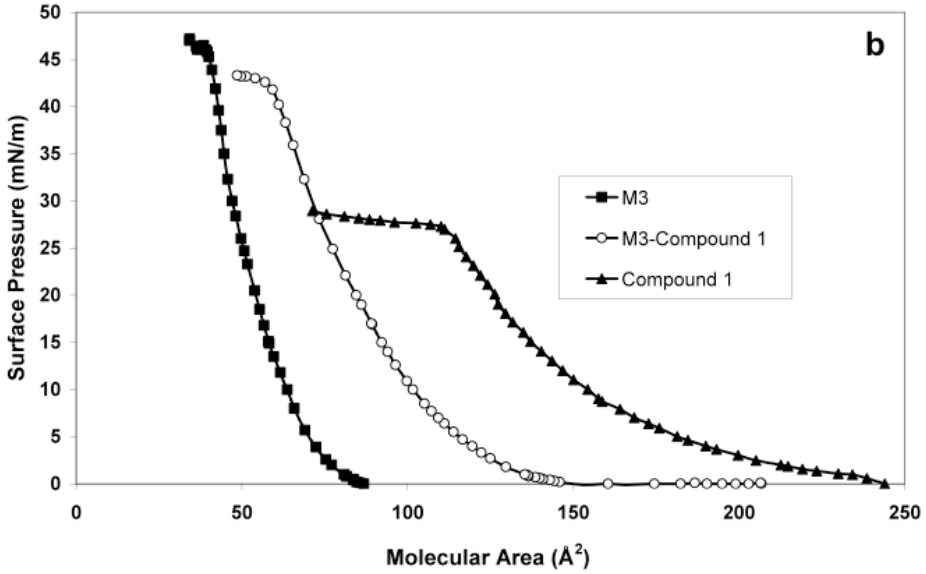

Figure 19 : *π-A* isotherms for the M3 model monolayer, the pure **compound 1** and the mixed M3-**compound 1** monolayers.

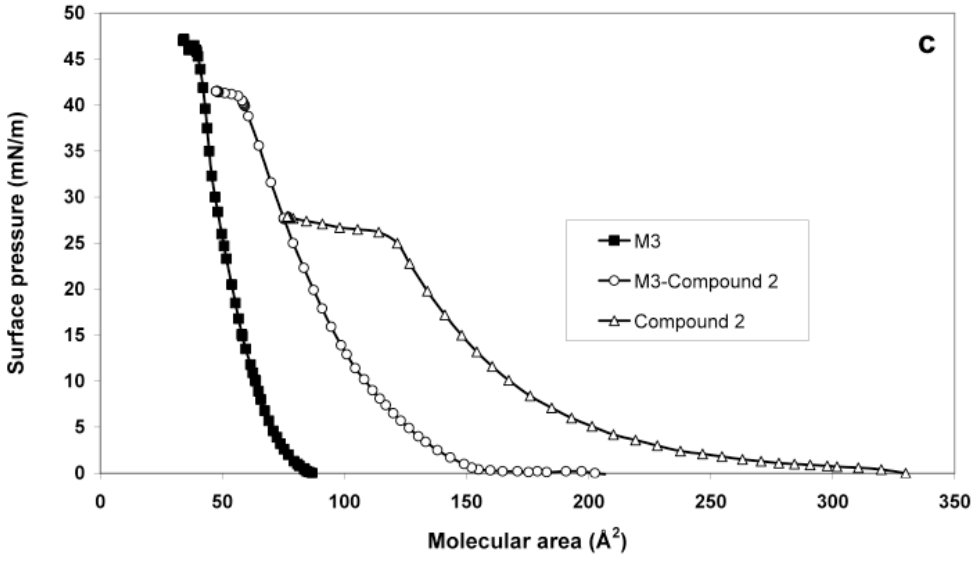

Figure 20 : *π-A* isotherms for the M3 model monolayer, the pure **compound 2** and the mixed M3-**compound 2** monolayers.

Analysis of the morphology of the mixed monolayers by Brewster angle microscopy

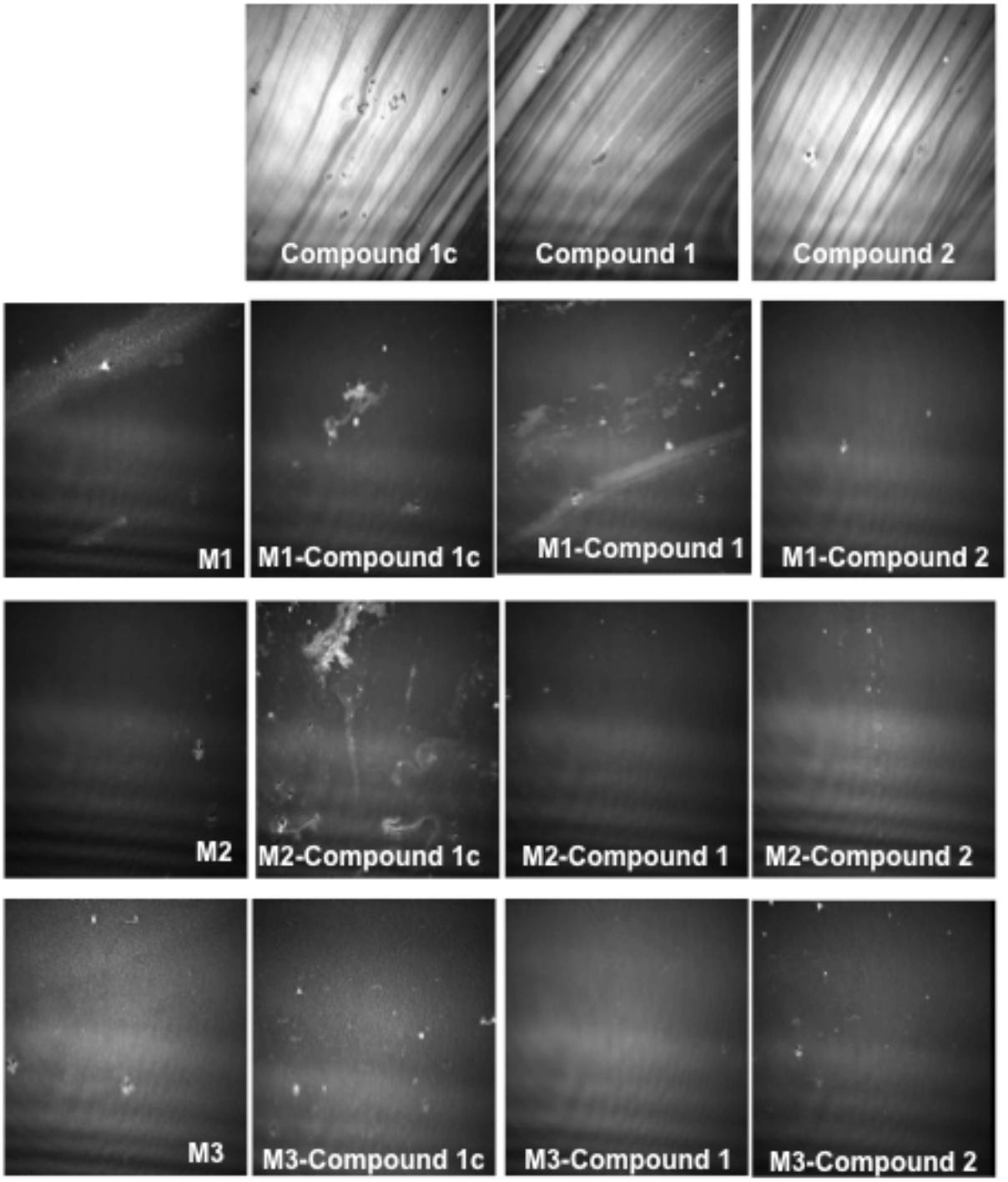

Figure 21: BAM images of spread lipid models, pure porphyrins and mixed lipid-porphyrin monolayers at 27-30 mN/m. Image size: 2 mm.

Figure 21 shows BAM images of the pure porphyrin monolayers (top images) compressed to 28 mN/m. The observed brightness of the monolayers was probably due to the proximity between the wavelength of the BAM laser (659 nm) and the last Q band of the porphyrins (650 nm). Films appeared organized in parallel stacked stripes. No difference in the width of these stripes was observed between **compound 1c** and **compounds 1** and **2**. These structures

probably resulted from intermolecular π-π stacking of the hydrophobic cores of tetraphenylporphyrins, [49-50] corresponding to a side-on orientation of the molecules with respect to the air/buffer interface. [51] Figure 21 also shows BAM images of the M1, M2 and M3 monolayers at 28 mN/m, in the absence (left column in Figure 21) and in the presence of 10 mol% of porphyrin. M1 exhibited 2D-crystallized domains contrasting with more fluid ones. M2 showed domains only when mixed with **compound 1c**. Compared to the other lipid monolayers, M3 looked grainy, with a grain size estimated below 1 µm. This grainy structure appeared attenuated in the presence of **compounds 1** and **2**. These observations are in agreement with the π-A isotherms, which showed the deorganizing effect of the glycoconjugated porphyrins on phospholipid monolayers with high cholesterol content (Figure 18-20 and Table 4).

Effect of liposomes-porphyrin interaction on fluorescence intensity and quenching

To complete the monolayer data on porphyrin-lipid interactions, we analyzed porphyrin penetration into vesicle bilayers by fluorescence spectroscopy.

Porphyrins fluoresce better in an apolar environment than in aqueous medium. Their interactions with membrane lipids can thus be quantified by measuring the change in fluorescence following their addition to a liposome suspension. This approach allows to work with a very low porphyrin concentration ($1x10^{-7}$ M) and thus, with a great excess of phospholipids (1000/1: lipid/porphyrin); these conditions are closer to *in vivo* ones.

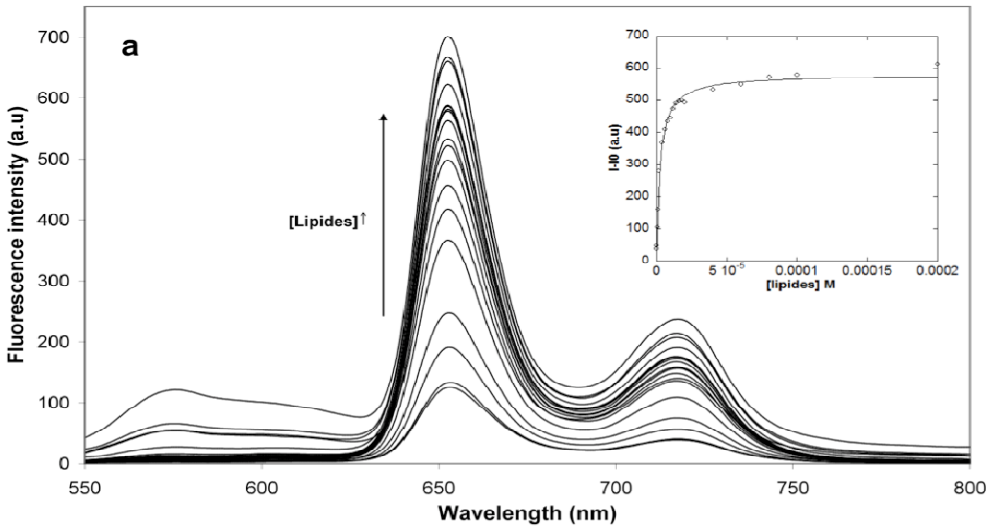

Figure 22 : Fluorescence emission spectra for **compound 1** ($1x10^{-7}$ M) upon addition of M2 liposomes with lipid concentrations ranging from 0 up to $2x10^{-3}$ M, so that [lipid]/[porphyrin] ratios were in the range [0-2000]. The inset shows the variation of fluorescence peak intensities ($\lambda_{emission}$ = 653 nm, $\lambda_{excitation}$ = 421 nm) versus increasing lipid concentration (open circles) and its fit line by using Eq. 7.

Figure 22 shows that the emission spectra for **compound 1** were markedly enhanced upon addition of M2 liposomes. No shift of the fluorescence emission bands was observed in the presence of liposomes in agreement with previous study of interaction between *meso*-substituted porphyrins and L-α-phosphatidylcholine liposomes. [52]

Moreover, the fluorescence intensity for the pure porphyrin solution (Figure 22, bottom spectrum) was always lower than that obtained in the presence of liposomes, due to the well-known self association of porphyrins in aqueous media. Addition of liposomes led to the dissociation of porphyrin aggregates and binding of free monomers, which had a stronger fluorescence. These results indicate that addition of liposomes improved porphyrin solubilization. The same results were obtained for the two other porphyrin derivatives (data not shown).

Spectroscopic measurements allowed calculating porphyrin membrane partition coefficient (K_p) using Eq. (7) (see inset to Figure 22 as an example for the M2-**compound 1** association). The results are collected in Table 5. The calculated K_p values were all above or close to $2x10^7$, demonstrating very high affinities of the three dendrimeric phenylporphyrins. K_p values for **compounds 1** and **2** were similar for the three models, although **compound 2** showed slightly lower values. However, all differences were within the experimental error, except for the interaction between **compound 1c** and M2, which yielded a K_p value ($3.6\ x10^7$) almost twice that obtained for the other complexes. Thus, the most hydrophobic porphyrin, **compound 1c,** seemed to exhibit the highest affinity for M2 liposomes, and a comparable affinity to that of the glyconjugated porphyrins with the two other models. This apparently contradicted the results obtained with monolayers, which showed that **compound 1c** penetrated to a lower extent than the other porphyrins in the lipid monolayers (Figure 16). However, it must be noted that **compound 1c** also adsorbed to a lesser extent at the free air/buffer interface, although it showed the highest collapse surface pressure and smaller molecular area when spread from organic solvents (Figure 11). This was due to its high hydrophobicity and tendency to aggregate in the subphase. The spread lipid monolayer was insufficient to induce its disaggregation. Conversely in liposome suspensions, the vesicles and porphyrins were both in the bulk and could easily interact, thus promoting **compound 1c** disaggregation and binding to the liposomes.

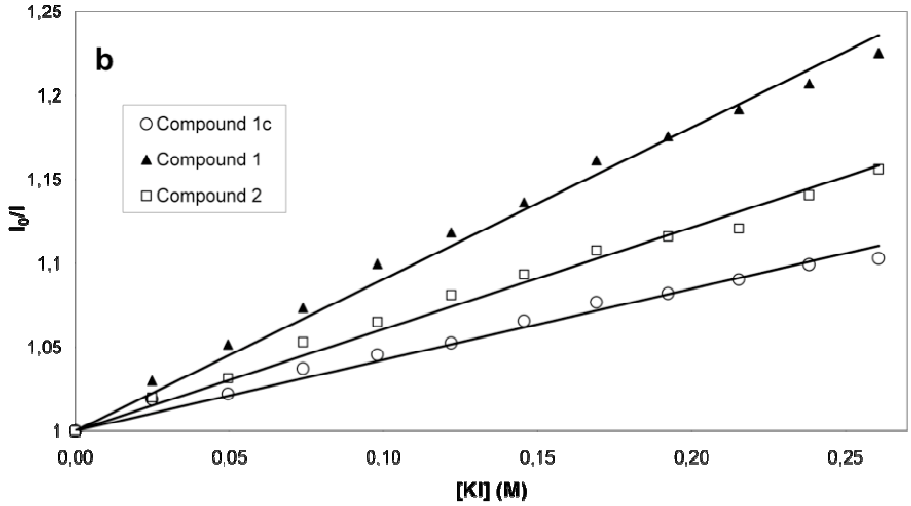

Figure 23 : Stern-Volmer plots for iodide quenching of porphyrins in 10 mM HEPES buffer in the presence of M2 vesicles (lipids/porphyrin ratio = 1000/1) at 37°C.

Porphyrin-liposome interactions were also studied by fluorescence quenching, using iodide as dynamic quencher. The Stern Volmer plots obtained in the presence of M2 liposomes are presented as an example in Figure 23. Accurate K_{SV} values could not be calculated in HEPES buffer (without liposomes) due to porphyrins self-aggregation. However in a methanol:water 50:50 (v/v) mixture (where no aggregation takes place), K_{SV} values were found to be 3.2 M^{-1} for **compound 1** and 3.3 M^{-1} for **compound 1c**; these values are much higher than those in Table 5, suggesting that in the presence of liposomes these compounds were inserted into the phospholipid bilayer and protected from the water-soluble iodide quencher. In another work (unpublished data), the compounds exhibited similar fluorescence lifetimes τ, in methanol (τ = 9.4 ns for **compound 1** and 9.5 ns for **compound 1c**), and when associated to DMPC liposomes (τ = 12.3 ns at 37°C). Based on these results, the K_{SV} values for the three porphyrins were compared. The results in Table 5 show that their quenching efficiencies were similar when they interacted with M1 and M3 liposomes, suggesting similar insertion for the three compounds. Conversely, when they were bound to M2 vesicles, significant differences in K_{SV} values were observed between them (Table 5). **Compound 1c** exhibited the lowest K_{SV} (0.43 ± 0.01 M^{-1}) whereas for **compounds 1** and **2,** K_{SV} values were equal to 0.90 ± 0.01 M^{-1} and 0.61 ± 0.01 M^{-1}, respectively. Apparently, **compound 1c** penetrated deeper into this bilayer than the two other compounds.

Liposome	Porphyrin derivatives					
	Compound 1		Compound 2		Compound 1c	
	K_p ($x10^7$)	K_{SV} (M^{-1})	K_p ($x10^7$)	K_{SV} (M^{-1})	K_p ($x10^7$)	K_{SV} (M^{-1})
M1	2.0±0.2	1.1±0.2	1.7±0.2	0.98±0.08	2.1±0.2	0.96±0.07
M2	2.2±0.2	0.90±0.01	1.9±0.1	0.61±0.01	3.6±0.5	0.43±0.01
M3	2.3±0.1	0.80±0.01	1.9±0.1	0.80±0.02	1.8±0.3	0.90±0.01

Table 5 : Partition coefficients (K_p) and Stern-Volmer quenching constants (K_{SV}) of liposome-porphyrin complexes.

Discussion

Effect of cholesterol on phospholipid monolayers and liposomes

Our results showed that the increase in cholesterol content from 10 to 30% had no significant effect on dendrimeric porphyrin penetration into the studied model monolayers and liposomes. It is well known that the presence of cholesterol has a non-negligible effect on the organization of phospholipid monolayers, and indeed we observed that cholesterol strongly condensed M1, M2 and M3 monolayers relative to M0, the model without cholesterol (Figure 12). Cholesterol is also known to mix differently with phospholipids depending on the saturation degree of their hydrocarbon chains, and the nature of their polar headgroups. In our system, PE, PC and PS molecules coexisted in the phospholipids mixture, and each of them could interact in a different way with cholesterol molecules. Indeed, Cheetham *et al*. [53] have shown that cholesterol solubility was low in the major amino-phospholipids compared to phosphatidylcholine (PC). This was confirmed by McMullen *et al*. [54] who attributed the limited lateral miscibility of cholesterol in PE relative to PC bilayers to the relatively strong inter-headgroup hydrogen bonding and electrostatic interactions of PE, favoring phospholipid–phospholipid contacts over cholesterol–phospholipid interactions.

Cholesterol also showed a limited solubility in phosphatidylserines (PS) inducing phase separation in monolayers and forming crystallites at X_{CHOL} above 0.3. [47, 55-57] With SOPS, crystallites were even observed from X_{CHOL}= 0.2. The presence of cations such as calcium contributed to diminish PS-cholesterol miscibility by rigidifying the head group region and acyl chains of PS. [47, 57] In our mixed monolayers, the increase in cholesterol led to more condensed and rigid monolayers with a grainy surface (Figure 12 and Figure 21). In liposomes, a less negative ζ potential was measured when cholesterol content increased from 10 to 20%. However, the reason for this phenomenon is still unclear.

Effect of metal ions on phospholipid monolayers in the presence of cholesterol

The effect of ions on monolayers and liposomes was not specifically studied in this work but should be taken into account since it certainly adds to the complexity of the biomimetic systems. Cations were necessary for the specific interaction with the mannose-receptor, which is not reported here. If in liposome experiments, calcium and nickel ions were added just before liposome interaction with porphyrins, in monolayer ones, they were present in the buffer subphase before lipid spreading, and could affect both monolayer formation and organization. As mentioned above, cations could bind to anionic PS and to a lesser extent to PC groups. They could also bind to PE groups. However, this binding would not be favored due to the strong interaction between neighboring phosphate and amine groups in PE monolayers. [(58)] Cholesterol could also interfere with cations adsorption.

Moreover, the effect of cations might not be limited to their interaction with lipids in monolayers and bilayers. Minnes et *al.* have recently reported that the presence of Mg^{2+} cations induced a clear salting-out process of photosensitizer molecules from the aqueous phase into neutral liposome bilayers. [(59)] The cations in the presence of our complex and charged systems could thus play a role in lipid organization, as well as in porphyrin penetration into the membranes.

Penetration of porphyrins into phospholipid-cholesterol monolayers

When a soluble amphiphilic compound is injected beneath a lipid monolayer, the extent of its adsorption into the monolayer depends on its surface properties, its affinity for the spread lipid molecules and the surface density of lipid molecules. In a typical adsorption-penetration mechanism, as the initial surface pressure is increased, the available surface area decreases. A lesser number of porphyrin molecules is expected to penetrate into the monolayer. This is usually supported by a decrease in the surface pressure change as π_i increases. For all three porphyrin derivatives, such a decrease in the surface pressure change was indeed observed (Figure 17). Up to 28 mN/m, all porphyrins penetrated into lipid monolayers. **Compound 1c** being the most hydrophobic compound of the series was expected to interact more strongly with the phospholipid monolayers than the glycodendrimeric porphyrins, especially at high cholesterol content. Instead, it produced lower surface pressure changes than the other compounds, due to its aggregation in the subphase. Moreover, at the initial surface pressure of 30 mN/m, a negative surface pressure change was observed, showing that the molecule was unable to penetrate into a monolayer anymore (Figure 16). Surprisingly, in the same conditions, both glycodendrimeric derivatives led to a significant increment in surface

pressure, accounting for the adsorption of these molecules into the lipid monolayers, even at the high initial surface pressure. It seems unlikely, however, that **compounds 1** and **2** could actually penetrate into these condensed monolayers. They more probably interacted with the hydrated polar headgroups of the phospholipids, forming hydrogen bonds with them and stabilizing the monolayers as disaccharides do. [60-61] Indeed, the glycodendrimeric porphyrins with their three sugar moieties in the same vicinity could exert the same effect. This would explain why at 30 mN/m and above, a positive surface pressure increment was observed for **compounds 1** and **2** whereas for **compound 1c** devoid of sugars, the surface pressure change was negative.

Interaction of porphyrin derivatives with liposomes

Fluorescence experiments have shown that the studied compounds generally exhibited similar membrane partition coefficients (K_p) when incubated with liposomes. (Table 5). This is consistent with the results obtained at the air/solution interface, which showed that all porphyrins interacted with the phospholipids and were able to penetrate into the monolayers (Figure 17). No significant difference was apparent between the model liposomes as if cholesterol had no particular effect on porphyrin penetration, although for **compound 1c**, the interaction with M2 was apparently stronger than with the others (Table 5).

K_p and K_{sv} values for **compound 1c** were higher and lower, respectively, than could be expected from interfacial measurements. This discrepancy could be related to the difference in the experimental conditions between interfacial and fluorescence measurements. In monolayer experiments, porphyrin molecules were injected in the aqueous subphase beneath a single lipid monolayer. In the fluorescence experiments, lipids were added to the porphyrin solutions in the form of liposomes with a much higher lipid/porphyrin ratio than in monolayer experiments. Moreover, these liposomes were colloidal dispersions, which could allow a better dissociation of porphyrins aggregates in the bulk compared to a monolayer spread at the interface only. This would be particularly favorable to the more hydrophobic **compound 1c**, which was strongly aggregated in buffer. This compound could thus interact more with the liposomes, than with the monolayers. Interestingly, the penetration efficiency appeared better for **compound 2** than that for **compound 1**. This is in agreement with monolayer experiments, which showed that when mixed to the lipids, **compound 2** affected much more M2 and M3 monolayers than **compound 1** (Table 4).

Conclusion

This work showed that the three studied dendrimeric porphyrins could penetrate into phospholipid monolayers and bilayers mimicking the retinoblastoma cell membrane. If the increase in cholesterol molar fraction affected the organization of phospholipid molecules in monolayers and liposomes membrane, it had almost no effect on the effective penetration of the drugs into the lipid layers. Conversely, the chemical structure of a porphyrin and the presence of sugars moieties especially, played a crucial role. Although the non glycoconjugated porphyrin penetrated to a higher extent than the glycodendrimeric derivatives into the liposome membrane, this could be achieved at high lipid/porphyrin ratio only. Glycodendrimeric porphyrins, due to their higher hydrophilicity exhibited better surface properties, and could penetrate into lipid layers even at low lipid/porphyrin ratios. They interacted with phospholipid-cholesterol monolayers even at surface pressures where the packing of lipid molecules was too tight to allow their effective penetration. However their interaction with the phospholipid mixtures appeared complex. Hydrogen bonding between porphyrin sugar moieties and phospholipid polar headgroups, as well as hydrophobic interactions of the macrocycle with phospholipid hydrocarbon chains and cholesterol could control their incorporation and limit their penetration depth into membranes. Glycodendrimeric porphyrins have been designed to interact with mannose-specific receptors at the surface of cancer cells. This work showed that independently of their potential penetration controlled by specific interaction, they could penetrate by passive diffusion as well.

References

1. Doz F (2006) Rétinoblastome : aspects récents. *Arch. de Pédiatrie* 13(10):1329-1337.
2. Maillard P, *et al.* (2007) In vitro phototoxicity of glycoconjugated porphyrins and chlorins in colorectal adenocarcinoma (HT29) and retinoblastoma (Y79) cell lines. *Photodiag. and Photody. Ther.* 4(4):261-268.
3. Stephan H, Boeloeni R, Eggert A, Bornfeld N, & Schueler A (2008) Photodynamic Therapy in Retinoblastoma: Effects of Verteporfin on Retinoblastoma Cell Lines. *Invest. Ophthalmol. Vis. Sci.* 49(7):3158-3163.
4. Lupu M, *et al.* (2009) 23Na MRI longitudinal follow-up of PDT in a xenograft model of human retinoblastoma. *Photodiag. and Photody. Ther.* 6(3-4):214-220.
5. van Hillegersberg R, Kort WJ, & Wilson JH (1994) Current status of photodynamic therapy in oncology. (Translated from eng) *Drugs* 48(4):510-527 (in eng).
6. Mojzisova H, Bonneau S, & Brault D (2007) Structural and physico-chemical determinants of the interactions of macrocyclic photosensitizers with cells. *Eur. Bioph. J. with Bioph. Let.* 36(8):943-953.
7. Laville I, *et al.* (2003) Synthesis, cellular internalization and photodynamic activity of glucoconjugated derivatives of tri and tetra(meta-hydroxyphenyl)chlorins. *Bioorg. & Med. Chem.* 11(8):1643-1652.
8. Laville I, *et al.* (2006) Photodynamic Efficiency of Diethylene Glycol-Linked Glycoconjugated Porphyrins in Human Retinoblastoma Cells. *J Med Chem* 49(8):2558-2567.

9. Maget-Dana R (1999) The monolayer technique: a potent tool for studying the interfacial properties of antimicrobial and membrane-lytic peptides and their interactions with lipid membranes. *Bioch. et Biophy. Acta (BBA) - Biomembranes* 1462(1-2):109-140.
10. Brockman H (1999) Lipid monolayers: why use half a membrane to characterize protein-membrane interactions? *Curr. Opin. in Struct. Biol.* 9(4):438-443.
11. Brezesinski G & Möhwald H (2003) Langmuir monolayers to study interactions at model membrane surfaces. *Adv. in Colloid and Interface Sci.* 100-102:563-584.
12. Peetla C, Stine A, & Labhasetwar V (2009) Biophysical interactions with model lipid membranes: applications in drug discovery and drug delivery. (Translated from eng) *Mol Pharm* 6(5):1264-1276 (in eng).
13. Eytan GD (1982) Use of liposomes for reconstitution of biological functions. *Bioch. et Biophy. Acta (BBA) - Rev. on Biomembranes* 694(2):185-202.
14. Tamm LK & McConnell HM (1985) Supported phospholipid bilayers. *Biophys. J.* 47(1):105-113.
15. Fliesler AJ & Anderson RE (1983) Chemistry and metabolism of lipids in the vertebrate retina. *Prog. in Lipid Res.* 22(2):79-131.
16. Huster D, Arnold K, & Gawrisch K (1998) Influence of Docosahexaenoic Acid and Cholesterol on Lateral Lipid Organization in Phospholipid Mixtures. *Biochemistry* 37(49):17299-17308.
17. Huster D, Arnold K, & Gawrisch K (2000) Strength of Ca2+ Binding to Retinal Lipid Membranes: Consequences for Lipid Organization. *Biophys. J.* 78(6):3011-3018.
18. Yorek MA, Figard PH, Kaduce TL, & Spector AA (1985) A comparison of lipid metabolism in two human retinoblastoma cell lines. (Translated from eng) *Invest Ophthalmol Vis Sci* 26(8):1148-1154 (in eng).
19. Merchant TE dGP, Minsky BD, Obertop H, Glonek T. (1993) Esophageal cancer phospholipid characterization by 31P NMR. *NMR in Biomed.* 6(3):187-193.
20. Preetha A, Huilgol N, & Banerjee R (2006) Comparison of paclitaxel penetration in normal and cancerous cervical model monolayer membranes. *Colloids Surf. B: Biointerfaces* 53(2):179-186.
21. van Blitterswijk WJ, de Veer G, Krol JH, & Emmelot P (1982) Comparative lipid analysis of purified plasma membranes and shed extracellular membrane vesicles from normal murine thymocytes and leukemic GRSL cells. *Bioch. et Biophys. Acta (BBA) - Biomembranes* 688(2):495-504.
22. Hendrich AB & Michalak K (2003) Lipids as a target for drugs modulating multidrug resistance of cancer cells. (Translated from eng) *Curr Drug Targets* 4(1):23-30 (in eng).
23. Calderon RO, Grogan WM, & Collins JM (1991) Membrane Structural Dynamics of Plasma-Membranes of Living Human Prostatic-Carcinoma Cells Differing in Metastatic Potential. (Translated from English) *Exp Cell Res* 196(2):192-197 (in English).
24. Mordon S, Devoisselle JM, & Soulié S (1995) Fluorescence spectroscopy of pH in vivo using a dual-emission fluorophore (C-SNAFL-1). *J. of Photochem. and Photobiol. B: Biology* 28(1):19-23.
25. Bonnett R (1995) Photosensitizers of the porphyrin and phthalocyanine series for photodynamic therapy. *Chem. Soc. Rev.* 24:19-33.
26. Griegel S, Rajewsky MF, Ciesiolka T, & Gabius HJ (1989) Endogenous sugar receptor (lectin) profiles of human retinoblastoma and retinoblast cell lines analyzed by cytological markers, affinity chromatography and neoglycoprotein-targeted photolysis. (Translated from eng) *Anticancer Res* 9(3):723-730 (in eng).
27. Monsigny M, Roche AC, & Midoux P (1988) Endogenous lectins and drug targeting. (Translated from eng) *Ann N Y Acad Sci* 551:399-413; discussion 413-394 (in eng).
28. Lotan R & Raz A (1988) Lectins in cancer cells. (Translated from eng) *Ann N Y Acad Sci* 551:385-396; discussion 396-388 (in eng).
29. Ballut S, *et al.* (2009) New strategy for targeting of photosensitizers. Synthesis of glycodendrimeric phenylporphyrins, incorporation into a liposome membrane and interaction with a specific lectin. *Chem Commun* (2):224-226.
30. Desroches M-C, *et al.* (2004) Incorporation of Glycoconjugated Porphyrin Derivatives into Phospholipid Monolayers: A Screening Method for the Evaluation of Their Interaction with a Cell Membrane. *Langmuir* 20(26):11698-11705.
31. Lund-Katz S, Laboda HM, McLean LR, & Phillips MC (1988) Influence of molecular packing and phospholipid type on rates of cholesterol exchange. *Biochemistry* 27(9):3416-3423.
32. Evans RW, Williams MA, & Tinoco J (1987) Surface areas of 1-palmitoyl phosphatidylcholines and their interactions with cholesterol. (Translated from eng) *Biochem J* 245(2):455-462 (in eng).
33. Cadenhead DA & Müller-Landau F (1980) Molecular accommodation and molecular interactions in mixed insoluble monomolecular films. *J. of Colloid and Interf. Sci.* 78(1):269-270.
34. Chou T-H, Chu IM, & Chang C-H (2002) Interaction of paclitaxel with DSPC in monolayers at the air/water interface at different temperatures. *Colloids Surf. B: Biointerfaces* 25(2):147-155.

35. Zwaal RFA, Demel RA, Roelofsen B, & van Deenen LLM (1976) The lipid bilayer concept of cell membranes. *Trends in Biochem. Sci.* 1(2):112-114.
36. Bangham AD, Standish MM, & Watkins JC (1965) Diffusion of univalent ions across the lamellae of swollen phospholipids. *J. of Molec. Biol.* 13(1):238-252, IN226-IN227.
37. Faivre V, Rosilio V, Boullanger P, Martins Almeida L, & Baszkin A (2001) Fucosyled neoglycolipids: synthesis and interaction with a phospholipid. *Chem. and Phys. of Lipids* 109(1):91-101.
38. Faivre V, Costa MdL, Boullanger P, Baszkin A, & Rosilio V (2003) Specific interaction of lectins with liposomes and monolayers bearing neoglycolipids. *Chem. and Phys. of Lipids* 125(2):147-159.
39. Gross E & Ehrenberg B (1989) The partition and distribution of porphyrins in liposomal membranes. A spectroscopic study. *Bioch. et Biophys. Acta (BBA) - Biomembranes* 983(1):118-122.
40. Huang Z & Haugland RP (1991) Partition coefficients of fluorescent probes with phospholipid membranes. *Biochem. and Biophys. Res. Comm.* 181(1):166-171.
41. Maman N & Brault D (1998) Kinetics of the interactions of a dicarboxylic porphyrin with unilamellar lipidic vesicles: Interplay between bilayer thickness and pH in rate control. *Biochim. et Biophys. Acta (BBA) - Biomembranes* 1414(1-2):31-42.
42. Barenholz Y, Cohen T, Korenstein R, & Ottolenghi M (1991) Organization and dynamics of pyrene and pyrene lipids in intact lipid bilayers. Photo-induced charge transfer processes. *Biophys. J.* 60(1):110-124.
43. Lavi A, Weitman H, Holmes RT, Smith KM, & Ehrenberg B (2002) The depth of porphyrin in a membrane and the membrane's physical properties affect the photosensitizing efficiency. *Biophys. J.* 82(4):2101-2110.
44. Davies J.T. REK (1962) Interfacial phenomena *2nd ed., Academic Press, New York,* :265.
45. Polozov IV & Gawrisch K (2004) Domains in Binary SOPC/POPE Lipid Mixtures Studied by Pulsed Field Gradient 1H MAS NMR. *Biophys. J.* 87(3):1741-1751.
46. Pitman MC, Suits F, Gawrisch K, & Feller SE (2005) Molecular dynamics investigation of dynamical properties of phosphatidylethanolamine lipid bilayers. (Translated from eng) *J Chem Phys* 122(24):244715 (in eng).
47. Bach D, Wachtel E, Borochov N, Senisterra G, & Epand RM (1992) Phase behaviour of heteroacid phosphatidylserines and cholesterol. *Chem. and Phys. of Lipids* 63(1-2):105-113.
48. García ML, Egea MA, Valero J, Valls O, & Alsina MA (1997) Interaction of flurbiprofen sodium with cornea model monolayers at the air-water interface. *Thin Solid Films* 301(1-2):169-174.
49. Drain CM, Nifiatis F, Vasenko A, & Batteas JD (1998) Porphyrin tessellation by design: Metal-mediated self-assembly of large arrays and tapes. *Angewandte Chemie-International Edition* 37(17):2344-2347.
50. Drain CM, *et al.* (2002) Designing supramolecular porphyrin arrays that self-organize into nanoscale optical and magnetic materials. *Proc. Natl. Acad. Sci. U.S.A* 99(Suppl 2):6498-6502.
51. Paolesse R, *et al.* (2002) Langmuir-Blodgett films of a modified tetraphenylporphyrin. *Material Sci. and Eng. C* 22(2):219-225.
52. Ben-Dror S, *et al.* (2006) On the Correlation Between Hydrophobicity, Liposome Binding and Cellular Uptake of Porphyrin Sensitizers. *Photochem. and Photobiol.* 82(3):695-701.
53. Cheetham JJ, Wachtel E, Bach D, & Epand RM (1989) Role of the stereochemistry of the hydroxyl group of cholesterol and the formation of nonbilayer structures in phosphatidylethanolamines. (Translated from eng) *Biochemistry* 28(22):8928-8934 (in eng).
54. McMullen TPW, Lewis RNAH, & McElhaney RN (1999) Calorimetric and spectroscopic studies of the effects of cholesterol on the thermotropic phase behavior and organization of a homologous series of linear saturated phosphatidylethanolamine bilayers. *Bioch. et Biophys. Acta (BBA) - Biomembranes* 1416(1-2):119-134.
55. Bach D, Borochov N, & Wachtel E (1998) Phase separation of cholesterol in dimyristoyl phosphatidylserine cholesterol mixtures. *Chem. and Phys. of Lip.* 92(1):71-77.
56. Epand RM, Bach D, Epand RF, Borochov N, & Wachtel E (2001) A New High-Temperature Transition of Crystalline Cholesterol in Mixtures with Phosphatidylserine. *Biophys. J.* 81(3):1511-1520.
57. Bach D & Wachtel E (2003) Phospholipid/cholesterol model membranes: formation of cholesterol crystallites. *Biochimica et Biophysica Acta (BBA) - Biomembranes* 1610(2):187-197.
58. Iraolagoitia XLR & Martini MF (2010) Ca2+ adsorption to lipid membranes and the effect of cholesterol in their composition. *Colloids and Surf. B: Biointerfaces* 76(1):215-220.
59. Minnes R, Ytzhak S, Weitman H, & Ehrenberg B (2008) The effect of solution electrolytes on the uptake of photosensitizers by liposomal membranes: a salting-out effect. *Chem. and Phys. of Lipids* 155(1):38-42.
60. van den Bogaart G, Hermans N, Krasnikov V, de Vries AH, & Poolman B (2007) On the Decrease in Lateral Mobility of Phospholipids by Sugars. *Biophys. J.* 92(5):1598-1605.

61. MacCallum JL & Tieleman DP (2008) Chapter 8 Interactions between Small Molecules and Lipid Bilayers. *Current Topics in Membranes*, ed Scott EF (Academic Press), Vol Volume 60, pp 227-256.

Chapitre 2: Etude de l'interaction spécifique entre les porphyrines, libres ou incorporées dans des liposomes, et une lectine spécifique du mannose mimant le récepteur porté par les cellules de rétinoblastome

Article 4: Evaluation of specific interactions between glycodendrimeric porphyrins, free or incorporated into liposomes, and Concanavaline A by fluorescence spectroscopy, surface pressure and QCM-D measurements

Ali Makky, Jean-Philippe Michel, Athena Kasselouri, Elisabeth Briand, Philippe Maillard and Véronique Rosilio

Article publié dans Langmuir 2010, vol. 26, n°15, pp. 12761-12768.

Après avoir démontré le potentiel des porphyrines glycoconjuguées à interagir d'une manière non spécifique avec les modèles membranaires du rétinoblastome, nous avons voulu dans ce nouveau chapitre évaluer la capacité de ces porphyrines à interagir de manière spécifique avec une lectine, la concanavaline A, elle-même spécifique du mannose et choisie comme modèle pour mimer le récepteur au mannose de type lectinique surexprimé à la surface des cellules cancéreuses. Pour cela nous avons, dans un premier temps, étudié l'interaction entre les porphyrines et la Con A tous deux sous forme libre en solution par spectroscopie de fluorescence, en déterminant leur constante d'association, et puis entre les porphyrines incorporées dans des membranes de liposomes de DMPC et la Con A libre par diffusion de lumière. Dans un deuxième temps, nous avons immobilisé la Con A sous forme d'une monocouche dense greffée de manière covalente sur une surface d'or, et nous avons étudié la capacité de nos porphyrines incorporées dans des liposomes de DMPC à interagir spécifiquement avec cette lectine par QCM-D.

Evaluation of specific interactions between glycodendrimeric porphyrins, free or incorporated into liposomes, and Concanavaline A by fluorescence spectroscopy, surface pressure and QCM-D measurements

Ali Makky[a,b], Jean-philippe Michel[a,b], Athena Kasselouri[c], Elisabeth Briand[a,b], Philippe Maillard [d,e], and Véronique Rosilio[a,b]*

[a b] Univ Paris-Sud 11, UMR CNRS 8612, Laboratoire de Physico-chimie des Surfaces, Châtenay-Malabry; [c] Laboratoire de Chimie Analytique, IFR 141Châtenay-Malabry. [d e] UMR CNRS 176, Institut Curie, Centre de Recherche, Orsay, Université Paris-Sud 11.

* Corresponding author: Veronique.rosilio@u-psud.fr

Introduction

Retinoblastoma is a highly malignant congenital tumor arising multicentrically in one or both retinas. (1) In the past, external beam radiotherapy and retina enucleation were the only available treatments against it. (2) The recent developments of an alternative treatment involving photodynamic therapy (PDT) is of particular interest. (3) This technique is based on the administration of a sensitizer devoid of mutagenic properties, followed by the exposure of the pathological area to visible light. Upon sensitizer photoactivation, active oxygen species are generated and oxidize the tumor cell components leading to irreversible damage and consecutive cell death. (4) Most photosensitizers used for both experimental and clinical studies in PDT are porphyrin-based compounds with a macrocyclic core providing the required photoactivity, and peripheral substituents controlling their biodistribution and pharmacokinetics. (5) However, these compounds are usually poorly water-soluble molecules, and are prone to form aggregates in aqueous solution. Glycoconjugation is considered as a potential effective way to increase their water solubility by modifying the amphiphily of macrocycles. (6) Moreover, it provides the possibility for specific interaction of the resulting conjugate with lectin type receptors over-expressed in some types of malignant cells. (7-10) It is expected that coupling multivalent carbohydrates to the porphyrin core allows their interaction with more than one receptor binding site at the same time and increases their affinity, resulting in a better cellular recognition.

New glycodendrimeric porphyrins have been synthesized in order to improve tumor selectivity by targeting sugar receptors specifically exposed at the cell surface of neoplasic retinal tissues. (11) Although the structure of these receptors has not been yet determined, Griegel *et al*. and Laville *et al*. have shown evidence that they are lectin-like receptors with specific affinity for mannose and galactose. (12-13) The glycodendrimeric porphyrins described in this work are aimed at targeting the receptor to α-mannose. In a previous work, we have

analyzed their non-specific interactions with phospholipids and cholesterol in monolayers and bilayers mimicking the lipid matrix of the retinoblastoma cell membrane. [14] In the present study, we have focused on the ability of these glycodendrimeric porphyrins to interact specifically with Concanavalin A (Con A), a well-known mannose-specific lectin. Although they are more hydrophilic than non-glycoconjugated derivatives, glycodendrimeric porphyrins are still poorly soluble in water. To overcome this problem, the molecules were solubilized in liposomes, usable as drug delivery systems. It was expected that they would orient in the bilayers and expose their sugar moieties outwards, thus remaining able to interact with their target, as previously shown. [11]

The specific interaction was first assessed from fluorescence experiments in which both Con A and porphyrin derivatives were free to move in aqueous solution, by evaluation of binding constant values, and fluorescence quenching by methyl *α-D*-mannopyranoside, a high Con A affinity substrate. In a second step, free Con A was injected beneath mixed DMPC-porphyrin monolayers spread at the air/buffer interface and surface pressure increments were measured. Many works have shown that porphyrins can form organized monolayers at the air/liquid interface with specific orientation depending on substituted groups on the macrocycle, [14-15] and can interact with surfactant or lipids forming mixed monolayers or complexes. [14, 16-20] It is then possible to inject the soluble lectin at various initial surface pressures and analyze the extent and kinetics of protein adsorption into the mixed lipid-porphyrin monolayer. The changes in the size of porphyrin-bearing DMPC liposomes upon addition of free Con A into the aqueous phase were measured by dynamic light scattering. Finally, Con A was immobilized as a monolayer covering a QCM-D gold sensor whose frequency and dissipation changes were measured in real time, following injection of porphyrin-bearing liposomes in the measurement cell.

Materials and methods

Chemicals

The glycodendrimeric porphyrins **compound 1** (Mw = 1692.81 g/mol) and **compound 2** (Mw = 1823.8 g/mol) were prepared as described previously by *Ballut et al.*[11, 21] Both were tri-mannosylated with a DEG (diethylene glycol) and a TEG (triethylene glycol) spacer for **compound 1** and **compound 2**, respectively. We also studied a non-glycococonjugated porphyrin (compound 1c, Mw = 1236.09 g/mol),[21] which had the same structure as **compound 1**, except for the mannose residues replaced by OH groups. It was thus considered

as an appropriate control for **compound 1** and to a lower extent for **compound 2**. These three porphyrin derivatives were insoluble in pure water, but soluble in the mixtures of chloroform/methanol (9/1, v/v) used for spreading at the air/buffer interface and liposomes preparation, and in the methanol/pyridine (98/2, v/v) mixture used for their dissolution in fluorescence experiments. Their structures are shown in Figure 24.

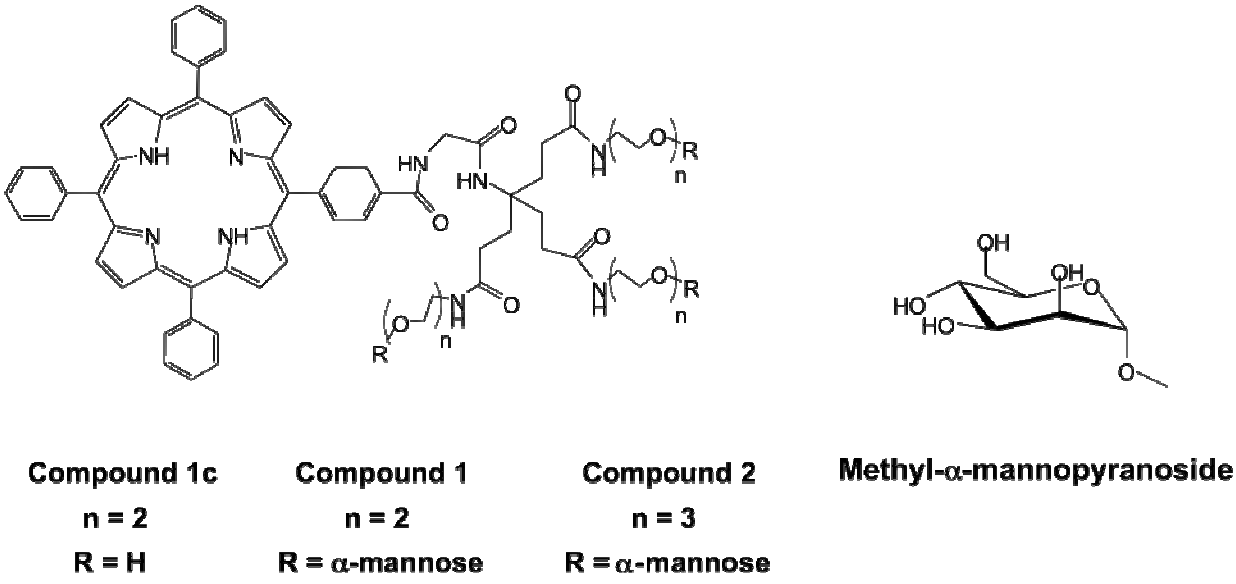

Figure 24: Chemical structures of the studied porphyrins and methyl *α-D*-mannopyranoside.

Concanavalin A (Type IV), methyl α-D-mannopyranoside (≥ 99% pure, Mw = 194.18 g/mol), HEPES (99.5% pure, Mw = 238.31 g/mol), sodium chloride (NaCl, 99% pure, Mw = 58.44 g/mol), calcium chloride ($CaCl_2.2H_2O$, 98% pure, Mw = 147.02g/mol), nickel chloride ($NiCl_2.6H_2O$, 98% pure Mw = 237.69 g/mol), 11-mercaptoundecanoic acid (MUA), 1-ethyl-3-[3-(dimethylamino)propyl]carbodiimide hydrochloride (EDC), N-hydroxysuccinimide (NHS) and ethanolamine were purchased from Sigma (Saint Louis, USA). Human serum albumin (HSA) was furnished by Behring (Marburg, Germany). Pyridine and methanol (99% pure) provided by Merck (Germany) were analytical grade reagents. The ultrapure water (γ = 72.2 mN/m at 22°C, resistivity: 18.2 MΩ.cm) produced by a Millipore Synergy 185 apparatus coupled with a RiOs 5^{TM} was used in all experiments. All glassware was soaked for an hour in a freshly prepared hot TFD4 (Franklab) detergent solution (15% v/v), then rinsed with milli-Q water and finally oven-dried.

The aqueous buffer contained 10 mM HEPES, 150 mM NaCl, 1 mM $CaCl_2.2H_2O$ and 1 mM $NiCl_2.6H_2O$, pH 6.5. The presence of divalent ions (Ca^{2+} and Ni^{2+}) was required for Con A activity. [22]

Spectroscopic measurements

Fluorescence emission spectra were recorded at 37°C on a Perkin-Elmer LS-50B computer controlled luminescence spectrophotometer (Massachusetts, USA) equipped with a red sensitive R6872 photomultiplier. Excitation was performed at the maximum of the Soret band at a wavelength of $\lambda_{excitation}$ = 421 nm, and emission was measured at $\lambda_{emission}$ = 653 nm.

Determination of porphyrin-Con A binding constants

Due to their poor-water solubility, most porphyrin molecules aggregate in solution. Porphyrin - protein association is a two-step process, with (i) the regeneration of porphyrin monomer and (ii) its association to the protein. The details of the process cannot be established, and only an apparent "macroscopic" binding constant can be calculated from the induced fluorescent enhancement. When Con A is in a great excess with respect to porphyrin molecules, the probability that two or more porphyrin molecules bind to the same Con A molecule is negligible. Therefore, we assumed a 1:1 stoichiometry: [23]

$$\text{Porphyrin + Con A} \xleftrightarrow{K_b} \text{Porphyrin-Con A}$$

$$K_b = \frac{[Porphyrin - ConA]}{[Porphyrin][ConA]} \quad \text{Eq. 1}$$

where [Porphyrin-Con A], [Porphyrin], and [Con A] were the concentrations of the porphyrin-Con A complex, and pure porphyrin derivative and lectin, respectively. The corresponding apparent binding constant K_b could be determined by fitting the experimental fluorescence intensity (F) versus Con A concentration according to equation 2:

$$F = F_0 + \frac{(F_{max} - F_0)\, K_b[ConA]}{1 + K_b[ConA]} \qquad \text{Eq. 2}$$

where F_0 and F_{max} were the fluorescence intensities of porphyrin in the absence and presence of the total Con A amount, respectively.

Experimentally, a 10^{-4} M porphyrin stock solution in methanol/pyridine (98/2, v/v) was prepared and diluted to $2x10^{-7}$ M with the aqueous buffer just before the experiments. Then, 1 ml of this diluted solution was added to 1 ml of Con A solutions with increasing concentrations. The final porphyrin concentration was $1x10^{-7}$ M and [Con A]/[porphyrin] ratios were in the range [0-1000]. The mixed solutions were kept in darkness at 37°C for 2 hours, and fluorescence measurements were then performed at the same temperature.

Kinetic measurements were achieved in the same conditions and showed that association of porphyrins to Con A had reached equilibrium after 2 hours incubation (data not shown). Protein concentrations were expressed on the basis of the monomeric subunit molecular weight (25 500 g/mol). [24]

Fluorescence quenching studies

When an excess of porphyrin is used, multiple porphyrin-Con A binding can occur, due to the presence of multiple binding sites on the lectin.[25] Indeed, it has been demonstrated that lectins have additional hydrophobic sites close to their primary carbohydrate binding site.[26] We assessed the specific interaction of porphyrins with Con A by fluorescence quenching using methyl α-D-mannopyranoside (α-MMP), a high affinity Con A substrate.[27] This substrate has been widely described as an effective competition inhibitor in carbohydrate-Con A interaction studies.[28-29] Our quenching strategy was first based on the formation of weakly fluorescent complexes of Con A and the glycodendrimeric porphyrins, followed by the addition of α-MMP, leading to the release of the weakly bound porphyrins, their re-aggregation in the aqueous phase, and consequent fluorescence quenching (Figure 25).

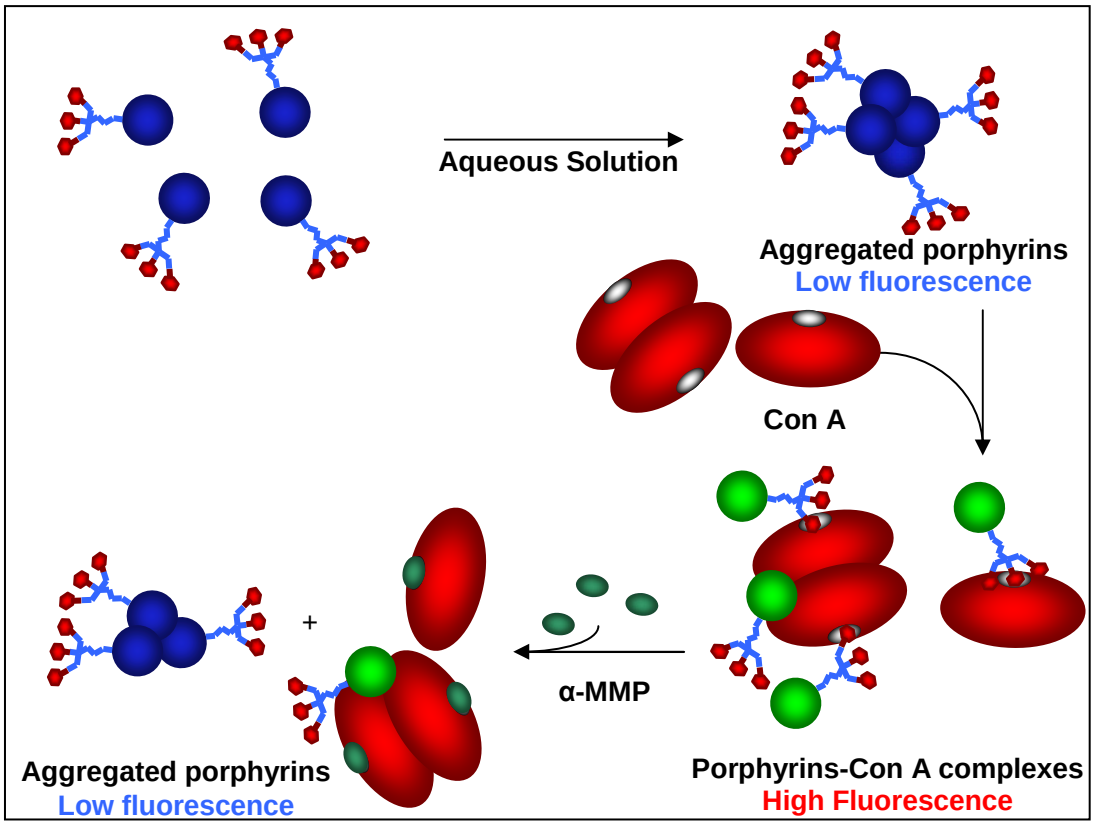

Figure 25 : Expected mechanism of porphyrin fluorescence intensity changes upon addition of methyl *α-D*-mannopyranoside to the complex lectin-porphyrin.

For this purpose, $5x10^{-4}$ M porphyrin stock solutions in methanol/pyridine (98/2, v/v) were prepared and diluted to $8x10^{-6}$ M in the aqueous buffer just before the experiments. 1ml of the porphyrin solution was added to 1ml of the Con A solution (1mg/ml). The final porphyrin concentration was $4x10^{-6}$ M, a much higher concentration than that used for K_b determination to ensure the saturation of all Con A specific binding sites prior to α-MMP addition. The mixed solutions were kept in darkness at 37°C for 2 hours. 100 µl of α-MMP solution with increasing concentrations were then added so that the [α-MMP]/[porphyrin] ratios varied in the range [0-1000]. Measurements were performed at 37°C after 2 hours incubation.

Monolayer experiments

The interfacial behavior of phospholipid-porphyrin monolayers was analyzed using a homemade auto-recording Langmuir-type film trough (160 cm^3, 217.2 cm^2) equipped with a R&K Wilhelmy pressure transducer (Riegler and Kirstein, GmbH, Germany) enclosed into a Plexiglas box to limit surface contamination. Prior to monolayer spreading, the subphase surface was cleaned by suction. Monolayers were left for 15 minutes to allow complete evaporation of the solvents. Compression was then performed at the speed of 9.57 cm^2 / min.
Interaction of Con A with mixed DMPC-porphyrin monolayers was inferred from the change in the surface pressure measured by the Wilhelmy plate method, using a K10 tensiometer (Krüss, Germany). Phospholipid-porphyrin mixtures (9:1 mol/mol) were spread from chloroform/methanol (9/1, v/v) solutions onto the buffer subphase (20 ml, 11.9 cm^2) and left for 3 hours to reach equilibrium at the chosen surface pressure. 100 µL of Con A solution (10 mg/ml in buffer) were then injected through a side arm beneath the mixed monolayer. The final Con A concentration in the subphase was 0.05 mg/ml. All experiments were performed at 22°C to limit water evaporation and temperature induced-lectin aggregation effects. The results reported are mean values of at least three measurements. The experimental uncertainty was estimated to be 0.2 mN/m.

Liposome preparation

Liposomes were prepared according to Bangham's method followed by the extrusion of vesicles suspensions.[30],[31],[32] In brief, DMPC-porphyrin mixed solutions (500:1 molar ratio) in chloroform/methanol (9/1, v/v) were evaporated for 3 hours under reduced pressure. The resulting dry lipid film was then hydrated with the aqueous buffer until reaching a final lipid concentration of 2 mM. The presence of divalent ions (Ca^{2+} and Ni^{2+}) was required for Con A

activity.[22] The pH was chosen to match that reported in cancer tissues. The lipid suspension was then extruded 15 times through a 200 nm-pore diameter polycarbonate membrane at 50°C (Avestin Lipofast extruder, Ottawa, California).

DLS measurements

The liposome diameter was measured using a Zeta-sizer (Nano ZS90, Malvern). The measurements were performed after dilution of the liposome suspension in deionized water. To evaluate Con A-induced aggregation of liposomes bearing porphyrins, 1 ml of fresh DMPC vesicles (2mM) bearing (or not) the glycodendrimeric porphyrins were left in contact with Con A solutions (1 mg/ml) for 1 hour at room temperature. Vesicles diameters were measured before and after addition of Con A. All measurements were carried out at 25°C.

Quartz crystal microbalance with dissipation measurements

Experiments using the quartz crystal microbalance with dissipation monitoring were performed at 25°C using a QCM-D E4 from Q-Sense (Gothenburg, Sweden). The QCM-D sensor allows the measurement of oscillation frequency shift (Δf) of the quartz crystal and simultaneous energy dissipation change (ΔD). Whereas changes in resonance frequency are related to the mass of the material deposited on or removed from the sensor, changes in energy dissipation provide information on the viscoelastic properties of the adsorbed material. Au-coated crystals were provided by Q-Sense AB. Prior to their use, they were cleaned in a mixture of H_2O/NH_3 (25%)/H_2O_2 (30%) in a 5/1/1 ratio at 70°C for 10 minutes. They were then thoroughly rinsed with ultrapure water and dried under a N_2 stream. After cleaning, the crystals were incubated for 12 hours in a 5 mM ethanolic MUA solution, rinsed and sonicated in ethanol for several seconds to remove all unattached thiol groups. Finally, they were thoroughly rinsed with ultrapure water and dried again under a stream of N_2. Lectin immobilization on the gold sensor was achieved by conversion of the carboxylic acid functions of MUA into N-hydroxysuccinimide esters by reaction with N-hydroxysuccinimide (NHS) in the presence of a water-soluble carbodiimide (EDC), followed by reaction with Con A (1mg/ml in HEPES buffer with 150 mM NaCl, pH 6.5). [33]

Results

Fluorescence Spectroscopy:

Porphyrins are fluorescent macrocycles. However, their tendency to aggregate in aqueous media generally results in a low fluorescence intensity.[23] Conversely, in the presence of

apolar molecules such as lipids or proteins (albumin, lectin), disaggregation may occur upon formation of a non covalent complex and a strong increase in fluorescence follows.[23, 34]

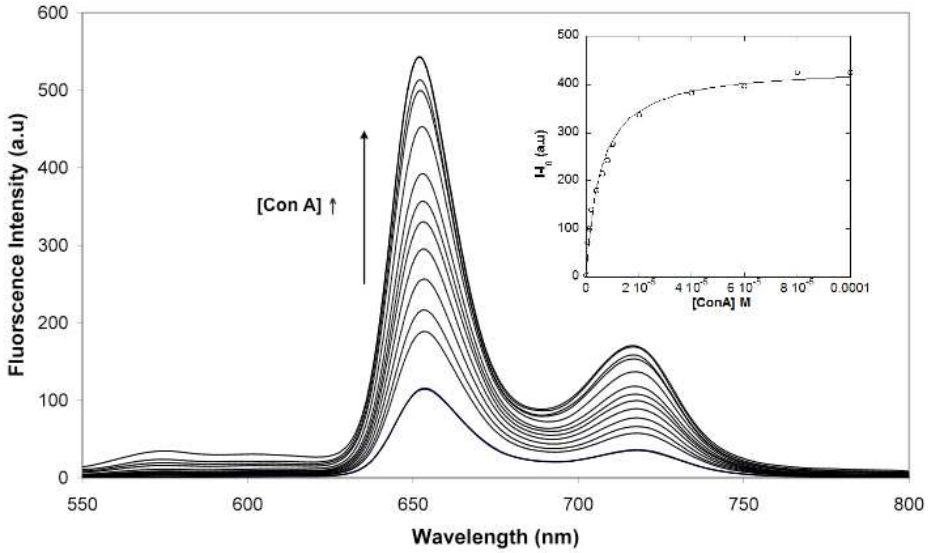

Figure 26: Fluorescence emission spectra of **compound 1** ($1x10^{-7}$ M) upon addition of increasing concentrations of Con A, with ConA/porphyrin ratios ranging from 0 up to 1000 ($\lambda_{excitation}$ = 421 nm). The inset shows the variation of fluorescence peak intensities ($\lambda_{emission}$ = 653 nm) versus increasing Con A concentration (open circles) and its fitted line using eq. 2.

Figure 26 shows that the emission spectra of **compound 1** were indeed markedly enhanced following addition of increasing concentrations of Con A. No shift of the fluorescence emission bands was observed. Fluorescence intensity for the pure porphyrin solutions (Figure 26, bottom spectrum) was always lower than that of mixed porphyrin-Con A ones. The same results were obtained for the two other porphyrins (data not shown).

From these spectra, porphyrin-Con A binding constants (K_b) have been calculated using equations 1 and 2 (see inset to Figure 26 as an example for Con A-**compound 1** binding). The results are presented in Table 6.

Porphyrin	**Con A** $K_b \times 10^5$ (M^{-1})	**HSA** $K_b \times 10^5$ (M^{-1})
Compound 1c	0.18±0.01	1.26±0.01
Compound 1	1.74±0.10	0.62±0.05
Compound 2	1.67±0.08	0.80±0.14

Table 6: Binding constants values for the porphyrin derivatives in mixtures with Con A or HSA.

Whereas the K_b values for both **compound 1** and **compound 2** were similar (1.74×10^5 and 1.67×10^5 M^{-1} respectively), that for the non-glycoconjugated **compound 1c** appeared 10-fold lower. This difference is consistent with a distinct binding mechanism between mannosylated

and non-mannosylated porphyrins. Although **compound 1c** is devoid of any mannose moieties, it could still bind to Con A through hydrophobic interactions. Non-specific interactions of porphyrins with lectins are well described in the literature. [35] The binding of the three compounds to human serum albumin (HSA) which is non-specific to mannose, but contains several hydrophobic binding sites, was also evaluated for comparison (Table 6). K_b values obtained with HSA showed a different trend than those obtained with Con A, and were more consistent with the relative hydrophobicity of the studied compounds.

Isothermal titration calorimetry studies have shown that Con A binds α-MMP with a K_b value of 0.82 $x10^4$ M^{-1},[36-37] a value 20-fold lower than those found with our approach for the two mannosylated porphyrins. The higher K_b for the glycodendrimeric porphyrins cannot be solely due the three mannosyl groups. As described in previous studies, hydrophobic interactions contribute to the overall interaction leading to sugar–lectin binding.[32, 38] Moreover, the highly specific saccharide recognition sites of many lectins bind to sugar derivatives containing large hydrophobic or aromatic rings such as a porphyrin macrocycle, much better than they do to simple mono- or disaccharides.[26] Hydrophobic sites play a significant role, which has to be taken into account in the interpretation of experiments aiming at the evaluation of the specific interaction.

Fluorescence quenching by α-MMP after Con A-porphyrin interaction:

The spectra in Figure 26 show that **compound 1** exhibited a weak fluorescence with an emission maximum at 653 nm due to its extensive aggregation in aqueous media. Addition of Con A caused porphyrin disaggregation and consequently a significant increase in fluorescence. The subsequent addition of α-MMP induced a decrease in the fluorescence intensity with a concentration dependent fluorescence quenching (Figure 27,28).

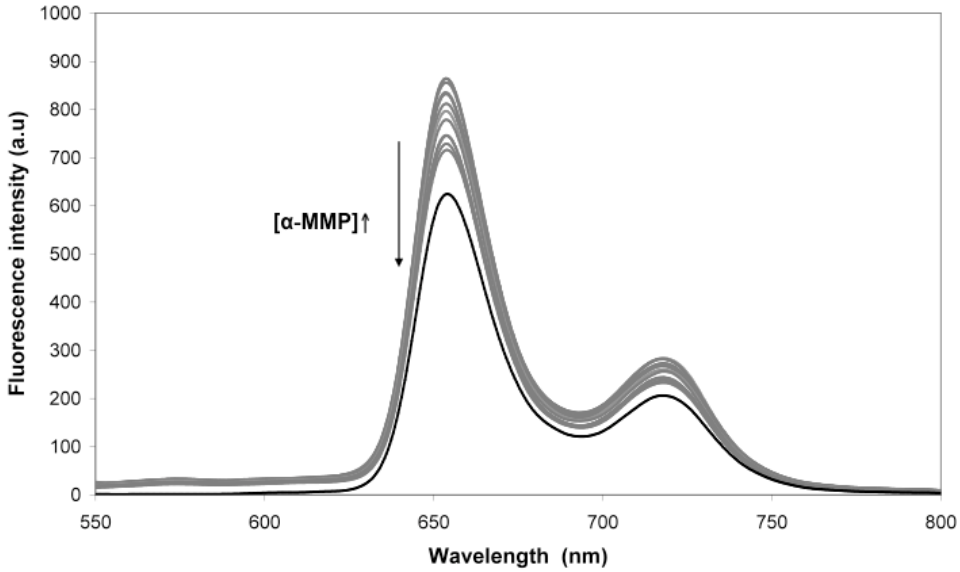

Figure 27: Con A-**compound 1** fluorescence spectra upon α-MMP addition (0-4mM) in HEPES buffer.

Compound 2 exhibited the exact same behavior. The fluorescence of both mannosylated porphyrins was quenched due to their displacement from Con A binding sites by α-MMP. However, no complete fluorescence quenching could be obtained even with large excess of α-MMP. Some porphyrin molecules remained bound to the lectin through non-specific interactions. A similar result has been reported for mannosylated sapphyrins and porphyrins used for non-covalent fluorescent labelling of proteins. [23]

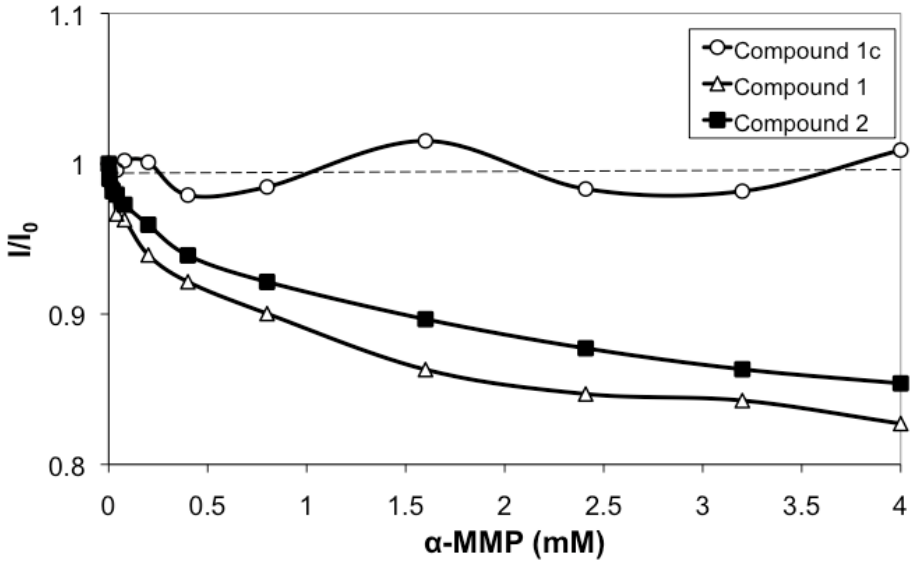

Figure 28 : Fluorescence quenching induced by addition of α-MMP (0-4mM) to Con A-porphyrin complexes.

For **compound 1c** as inferred from the upper curve in Figure 28, the increase in fluorescence intensity in the presence Con A was not altered by the subsequent addition of α-MMP.

These differences suggest that the binding modes of the glycoconjugated and non-glycoconjugated porphyrins to the lectin were different.

Interaction of Con A with porphyrin-bearing monolayers:

The surface tension measurements allowed analysis of the interaction of Con A with the porphyrins *in situ*. In these experiments, the porphyrins were dissolved with DMPC in a chloroform-methanol mixture and then spread at the air/buffer interface as a mixed (1:9) monolayer with an initial surface pressure of 20 mN/m. The surface tension of the mixed monolayers was stable for at least 8 hours.

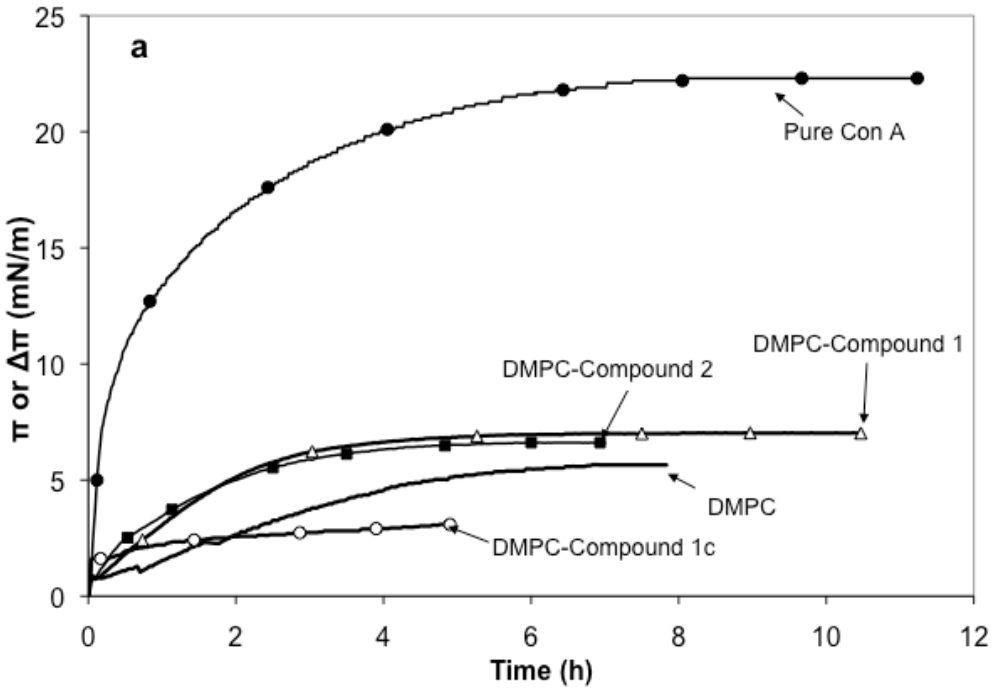

Figure 29 : Surface pressure (π) or surface pression change (Δπ) at 25°C induced by Con A adsorption at the air/solution interface and into DMPC-porphyrin (9:1) monolayers at the initial surface pressure of 20 mN/m;

Figure 29 shows the surface pressure change with time following Con A injection into the subphase. At the concentration of 0.05 mg/ml, Con A formed a stable monolayer with a surface pressure of 22 mN/m at equilibrium. When injected beneath pure DMPC and DMPC-**compound 1c** (9:1) monolayers, a maximum increase in surface pressure of 5.6 mN/m and 3 mN/m, respectively was recorded. It is interesting to note that the kinetics of the surface pressure increases were different for the two control monolayers. Whereas the maximum surface pressure change for the DMPC-**compound 1c** monolayer was reached in less than an hour, for the pure DMPC one, it took about 4.5 hours. This is due to the difference in

compressibility of the two monolayers as may be deduced from the shape of the isotherms in Figure 31.

Con A injection beneath mixed monolayers of DMPC and mannosylated porphyrins induced a higher surface pressure change of 7 and 6.7 mN/m for DMPC-**compound 1** and DMPC-**compound 2**, respectively. Equilibrium was reached after about 3 hours.

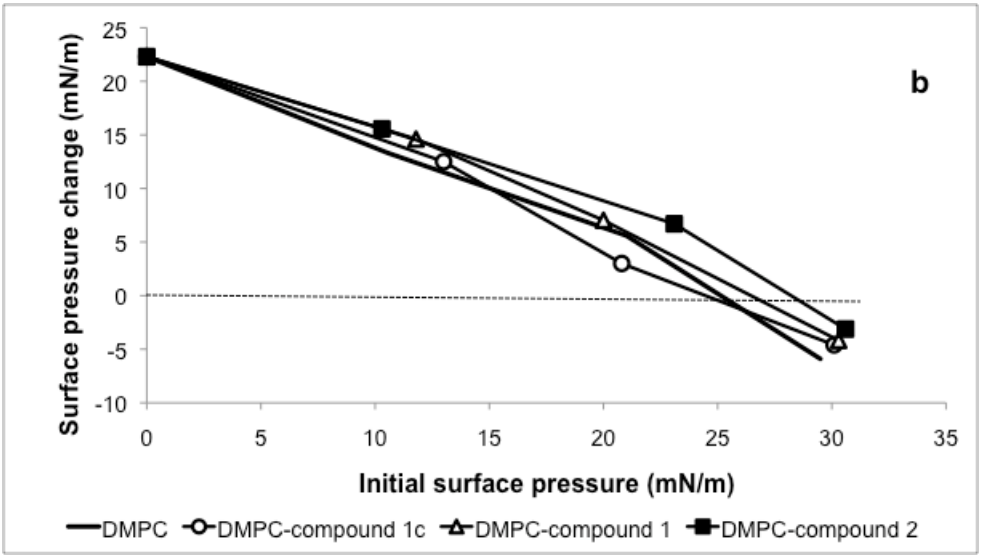

Figure 30 : Surface pressure changes induced by Con A adsorption at various initial surface pressures.

In Figure 30, the surface pressure changes induced by Con A adsorption into mixed monolayers with increasing initial surface pressures shows that above 25 mN/m, adsorption of Con A increased the surface pressure of mixed DMPC-glycodendrimeric porphyrins only. The effect was a little more pronounced for the monolayer containing **compound 2**.

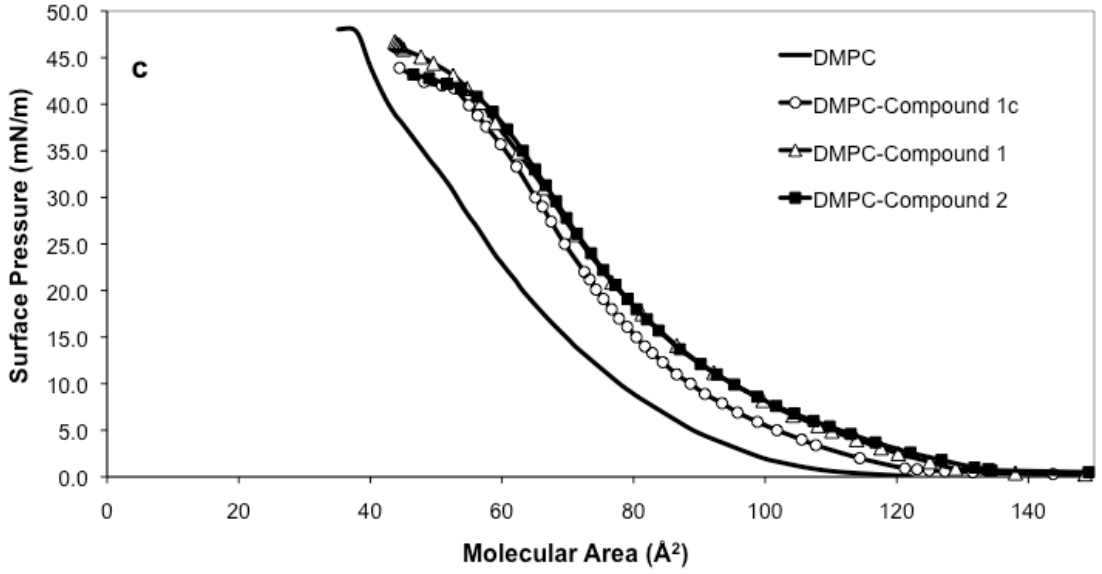

Figure 31 : π-A relationships for DMPC and DMPC-porphyrin (9:1) mixed monolayers.

Figure 31 shows the compression isotherms for DMPC and its mixtures with porphyrins spread at the air/buffer interface. The molecular areas at 20 mN/m were very similar for the mixed monolayers: 74.3, 77.8 and 78.1 $Å^2$, for DMPC-**compound 1c**, DMPC-**compounds 1** and **2,** respectively. It was smaller for pure DMPC (63.2 $Å^2$). Although the difference in molecular area was 3.5 to 4 $Å^2$ between **compound 1c** and **compounds 1** and **2**, the increment in surface pressure was two-fold higher. These results show that Con A interacted more with the glycoconjugated porphyrin-containing monolayers. However, no difference in the extent and kinetics of Con A adsorption could be observed between **compounds 1 and 2**, despite their different spacer lengths (Figure 29).

Interaction of Con A with porphyrin-bearing liposomes:

In a previous work,[(11)] we have shown that the porphyrins could be incorporated into the bilayers of DMPC liposomes. These liposomes could be used as efficient carriers for drug solubilization and possibly targeting.

We formed mixed DMPC-porphyrin liposomes at the 500:1 ratio, and measured their size by DLS before and after Con A addition. Results are presented in Table 7.

Liposomes	Before Con A addition		After Con A addition	
Composition	Diameter (nm)	Volume (%)	Diameter (nm)	Volume (%)
DMPC	 164	100	 175	100
DMPC-Compound 1c	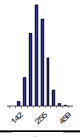 173	100	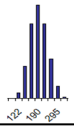 177	100
DMPC-Compound 1	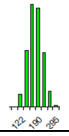 168	100	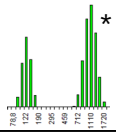 * 1090	66.2
DMPC-Compound 2	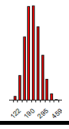 169	100	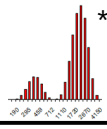 * 1690	81.9

Table 7 : Liposomes size before and following addition of Con A (1mg/ml) to liposome suspensions of varying compositions. Measurements were made after 1 h incubation at room temperature.

Apparently, the size of pure DMPC and DMPC–**compound 1c** liposomes was not affected by Con A addition. Conversely, for DMPC–**compound 1** and DMPC-**compound 2** liposomes, a dramatic increase in vesicles diameter was observed with values as high as 1090 nm and 1690 nm, respectively. This striking result demonstrates that mannosylated porphyrins were able to interact with Con A when incorporated into the liposomes membrane through the outward exposure of their mannoses moieties into the aqueous phase. The existence of Con A dimers and tetramers at the studied pH,[39] probably allowed lectin interaction with more than one porphyrin molecule, possibly borne by different liposomes, leading to the formation of liposome aggregates. This could explain the high DLS values measured, and the emergence of another vesicles family as shown by the two peaks in the size distribution for these liposomes (Table 7). Moreover, after addition of Con A, liposomes bearing **compound 2** were able to form populations of slightly larger size than those bearing **compound 1**. The percentage of larger aggregates was higher for the former. This result can be explained by the longer spacer in **compound 2,** which offered to the lectin a better accessibility to the sugar moieties.

Interactions of porphyrin-bearing liposomes with an immobilized Con A monolayer:

In the experiments described above, we studied the interaction of free Con A with the porphyrin derivatives immobilized in a phospholipid monolayer then in a phospholipid bilayer. As Con A was free in the aqueous phase, its binding sites were easily available, for both the hydrophobic and specific interactions. However, for a mannose receptor embedded in

a cell membrane, the binding sites might not be as easily accessible to a large molecule such as **compound 1** or **2** as to a small molecule like α-MMP.

In a previous work [14] we have shown that the two glycodendrimeric porphyrins interacted with phospholipids to a higher extent than the non-glycoconjugated dendrimeric one. In order to study specifically the Con A-porphyrin interactions, we focused on the interaction of DMPC-porphyrin liposomes with an immobilized pure Con A monolayer.

Following the immobilization of Con A onto the MUA surface, we have injected under flow conditions the various liposomes (DMPC, DMPC-**compound 1c**, DMPC-**compound 1** and DMPC-**compound 2**). Figure 32 shows the evolution of Δf and ΔD, respectively, as a function of time resulting from these injections.

A fast decrease in frequency change was observed and after 10 to 20 min depending on the composition of the liposomes, a quasi steady state was reached. The immediate decrease in resonant frequency can be explained by the increased effective mass onto the QCM-D electrode, due to liposomes adsorption. There was a concomitant increase in energy dissipation as more liposomes adsorbed, indicating a more viscous behaviour.

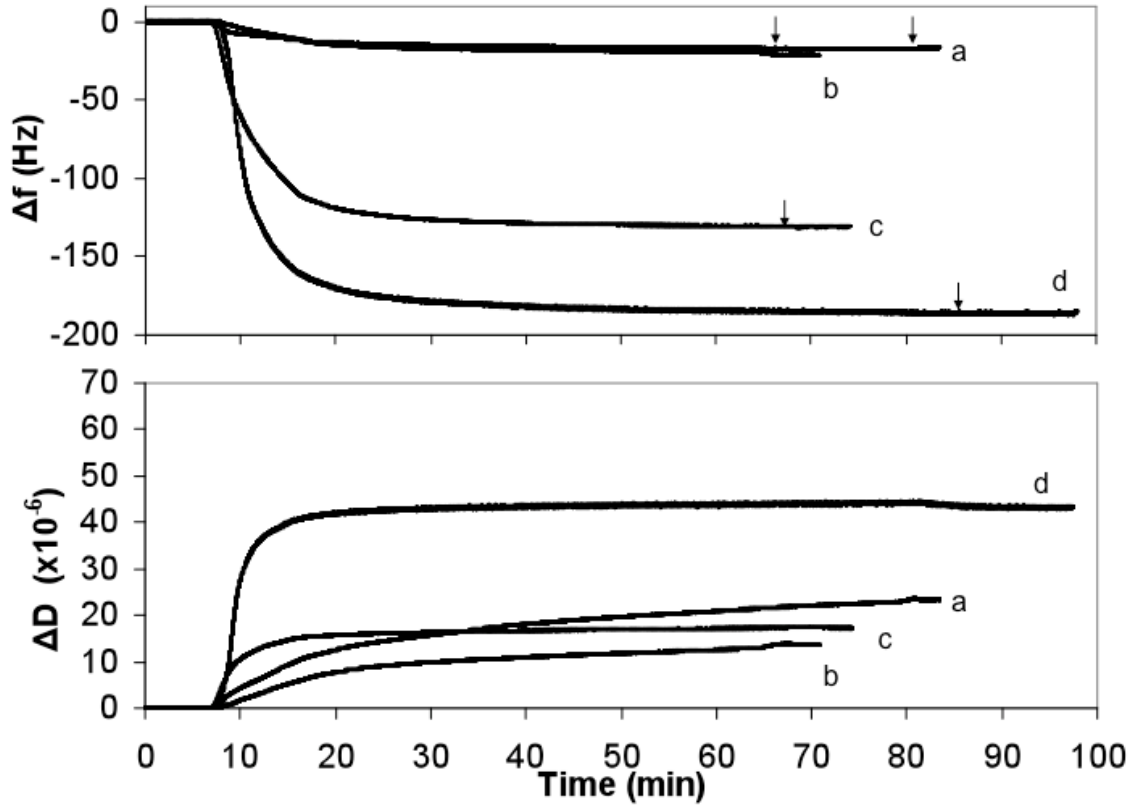

Figure 32: Δf (n=11) (a) and ΔD (n=11) (b) following liposomes injection into the QCM-D cell containing immobilized Con A onto the SAM functionalized gold surface. a: pure DMPC liposomes, b: DMPC-**compound 1c**, c: DMPC-**compound 1**, and d: DMPC-**compound 2**. Arrows indicate the times at which the electrodes were rinsed with HEPES buffer.

As shown in Figure 32, the amplitudes of the signals were highly dependent on the chemical structure of the porphyrin embedded in a liposome bilayer. Vesicles bearing mannosylated porphyrins induced the higher magnitudes of Δf and ΔD compared to DMPC or **compound 1c**-bearing liposomes. This would mean that the former adsorbed more to the Con A monolayer than the latter and altered its viscoelastic properties to a larger extent. For liposomes bearing mannosylated porphyrins Δf values were -130 and -186 Hz for DMPC-**compound 1** and DMPC-**compound 2**, respectively. These frequency shifts are in good agreement with those reported for liposome adsorption ranging from -90 to -400 Hz, depending on the liposome size and adhesion process. [40-43] Conversely, for pure DMPC and **compound 1c**-bearing liposomes, frequency shifts of -17 and -21 Hz only were observed, respectively. These frequency shifts were lower than those obtained for a supported planar bilayer (Δf ~ -26 Hz and ΔD ~ 0.3×10^{-6}) [44-45] or a complete layer of intact vesicles (Δf ~ -90 to -400 Hz). Furthermore, the normalized change in frequency (Δf/n) and dissipation (ΔD) for

the three overtones (n=3, 5, 7) did not overlap (data not shown). This indicates that the adsorbed liposomes formed a non-rigid incomplete layer of intact liposomes. [46-47]

The liposomes bearing **compound 2** induced the largest variations in Δf and ΔD. These results confirm those obtained by DLS when the liposomes were in contact with free Con A.

The following washing step with buffer resulted in only a slight increase in frequency (~5 Hz), which showed that adhesion of the liposomes to the lectin monolayer was stable.

In order to relate the observed changes in dissipation to changes in frequency, we have plotted in Figure 33 the variation of dissipation (ΔD) energy as a function of frequency shift (Δf), which eliminates time as an explicit parameter. [48]

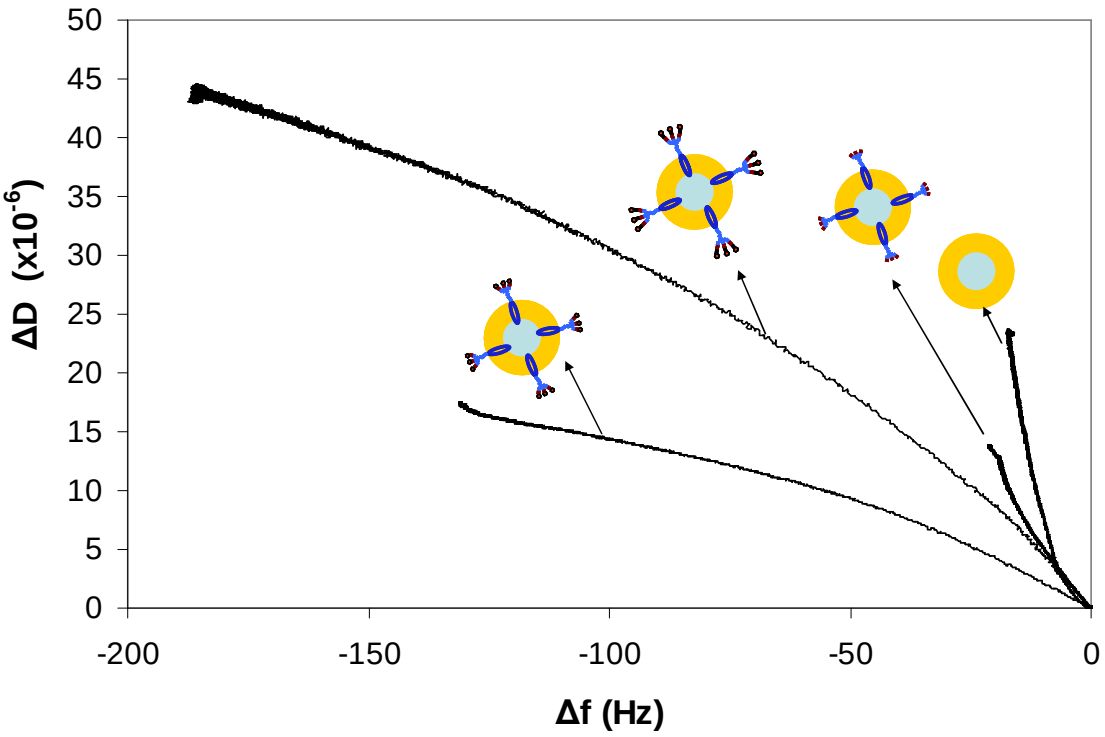

Figure 33 : Dissipation change versus frequency shift for the injected liposomes in the presence of immobilized Con A onto the SAM functionalized gold surface.

The different slopes in the ΔD-Δf plots reveal the different liposome behaviors during their adsorption. Pure DMPC and **compound 1c**-bearing liposomes exhibited the highest dissipation at a same given frequency. This result is not surprising since these liposomes were probably simply adsorbed onto the Con A surface and only weakly attached. Therefore, they could move freely during quartz crystal oscillations. Conversely, liposomes bearing the mannosylated porphyrins (**compounds 1** and **2**) induced lower energy dissipation. These liposomes were strongly bound to the Con A monolayer, probably by several attachments, and could not move as well as DMPC or **compound 1c**-bearing liposomes. Moreover, the

significant increase in dissipation caused by liposomes bearing **compound 2**, compared to those bearing **compound 1** would result from the higher mobility of mannose moieties provided by the longer spacer in **compound 2.** Indeed, this spacer would not only enhance porphyrin interaction with Con A, but also allow certain mobility to the liposomes subsequently bound to the lectin layer. Thus, the attached vesicles would not hinder the movements of the immobilized protein layer, and would even contribute to them during quartz crystal oscillations.

It is noteworthy that the measured signals were slightly affected after buffer rinsing, whatever the type of injected liposomes. To analyze the strength of the specific interaction in the mechanism of mannosylated porphyrins adhesion to the Con A monolayer, we injected α-MMP (0.004 M) after rinsing.

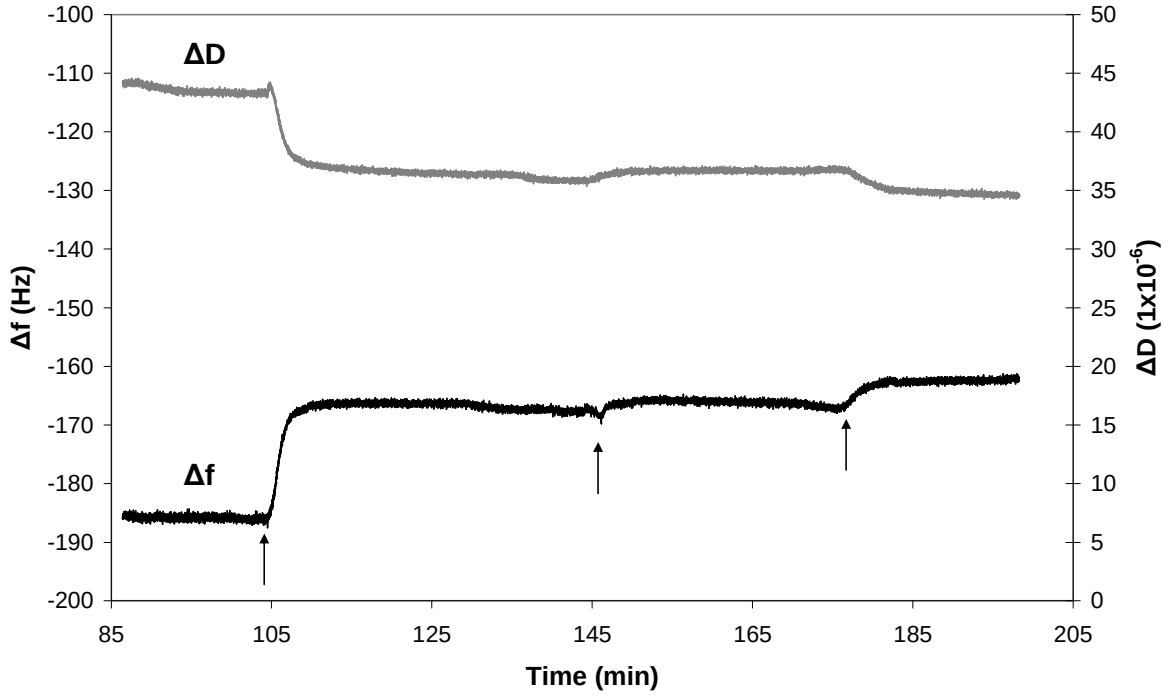

Figure 34 : Changes in frequency (Δf) and dissipation (ΔD) as a function of time upon injection of α-MMP following adsorption of DMPC-**compound 2** liposomes to the immobilized Con A. Arrows indicate the injections of α-MMP (0.004 M in HEPES buffer).

As shown in Figure 34, there was a rapid frequency increase (+24 Hz) upon the first injection of α-MMP, corresponding to a mass loss. This was followed by much less significant frequency increases after the second and third injections. Although the increase in frequency change would indicate the replacement of mannosylated porphyrin-bearing liposomes by α-MMP molecules, it is apparent that the excess inhibitor did not allow the release of all adsorbed mass. So, when porphyrin molecules were embedded into a liposome membrane, it

would be more difficult for α-MMP to displace them from Con A binding sites than when they were free in solution, as we observed in the fluorescence experiments (Figure 27 and Figure 28).

Discussion

We have previously studied the non-specific interactions and penetration ability of the glycodendrimeric porphyrins into phospholipid mixed monolayers or liposome bilayers with increasing cholesterol contents. These membranes lacked the lectin-like receptor at their surfaces. [(14)] We have clearly shown that the cancerous-dependent cholesterol changes in the retinoblastoma cell membranes did not modify the penetration ability of the studied porphyrins. Conversely, we have observed that the mannose moieties grafted to the porphyrins reinforced their amphiphily and promoted their interaction with the model membranes. This demonstrated that the glycodendrimeric porphyrins were able to interact more significantly with the lipids than the non-glycoconjugated dendrimeric one, even in the absence of a mannose receptor in these membranes. In the present work, we have focused on the specific interaction between glycoconjugated dendrimeric phenylporphyrins and the mannose receptors, using concanavalin A as a model. To avoid the non-specific interactions with the lipids observed in our previous work, Con A was studied alone, free in the aqueous medium or immobilized onto a SAM-functionalized QCM-D gold sensor. Although the conditions were not those of a receptor embedded in a membrane since Con A was not incorporated into a lipid monolayer or bilayer, the results obtained in this work allowed comparing the three porphyrin molecules with respect to their potential specific and non-specific interactions with a lectin-like protein.

When Con A was mixed to a dendrimeric porphyrin (glycoconjugated or not) solution, the fluorescence intensity of the porphyrin increased, indicating a more favorable environment for the porphyrin. The aggregated porphyrin molecules in aqueous solution disaggregated and associated to the protein. This association appeared independent of the presence or not of sugar moieties and was certainly driven by hydrophobic interactions between the phenylporphyrin macrocycle and the hydrophobic domains of the lectin. However, as shown in Table 6, the K_b values calculated for the glycodendrimeric porphyrins were higher than that for the dendrimeric porphyrin devoid of sugars (**compound 1c**). The glycoconjugated porphyrins are more amphiphilic than **compound 1c** and adsorb better at the air/buffer interface. [(14)] In order to verify that the higher K_b for the former were due to their interaction with both hydrophobic domains and sugar recognition sites of the lectin, the association of the

porphyrins to the lectin were compared to that with human serum albumin, which contains no binding site for mannose, but several hydrophobic sites. It was thus expected that the porphyrins would interact with it in a non-specific way. This was indeed confirmed by our measurements (Table 6), which showed that the K_b value was much higher for the non-mannosylated porphyrin than for the mannosylated ones. These results confirmed that **compound 1c** was more hydrophobic than **compounds 1** and **2**, and that in the presence of an ordinary circulating blood protein it would associate with it more than the other porphyrins. The similar binding constants obtained for the glycodendrimeric porphyrins accounted for their similar hydrophily.

The addition of excess α-MMP following interaction of the porphyrins with Con A, led to significant quenching of the fluorescence of the two glycoconjugated porphyrins, but barely affected the fluorescence intensity of **compound 1c**. This would demonstrate that the glycoconjugated porphyrins did not associate to the lectin merely due to their amphiphily, but also through specific interactions, and that the part of it would be significantly high to be noticed when a competitor for the sugar recognition sites was added to the mixture.

In the fluorescence experiments, no significant difference was observed between **compound 1** and **compound 2** in the presence of the lectin. All the molecules were free in the medium and could easily change their orientation to interact with the specific sites. The difference in only one ethylene oxide group in the spacer of the two porphyrins, although it improved the amphiphily of **compound 2** compared to **compound 1,**[(14)] did not affect the specific sugar-lectin interaction.

Results could be different if the lectin or a porphyrin, or both of them, were immobilized in a membrane, as expected if porphyrins were delivered after solubilization in liposomes. To analyze this aspect we studied the interaction of the porphyrins incorporated into a monolayer with free Con A injected into the subphase. The comparison of the interaction of the lectin with the three porphyrins confirmed that the lectin interacted more with the glycoconjugated porphyrins that with **compound 1c**. Again, no particular difference was observed between **compound 1** and **compound 2**. However, the porphyrins were diluted in the mixed monolayer (10 mol%) and the monolayer itself was not too much condensed (about 20 mN/m). Therefore, the lectin could reach porphyrin sugar moieties and the spacer length was not too critical. Additional experiments have indicated that above 25 mN/m, the lectin did no longer penetrate into DMPC and DMPC-**compound 1c** monolayers contrarily to DMPC-glycodendrimeric porphyrin ones (Figure 30). The π-A isotherms in Figure 31 showed that the three dendrimeric porphyrin molecules had similar packing between 20 and 30 mN/m.

To better model the delivery system, porphyrin-phospholipid mixtures were studied in another context, in which the porphyrins were embedded in the bilayer of DMPC liposomes and the changes in vesicle size upon Con A addition were measured. A clear difference was observed between DMPC and DMPC-**compound 1c** liposomes on one hand, and DMPC-glycodendrimeric porphyrins on the other hand, for which two size distributions were obtained. Although the difference in size of the aggregates was not very significant, the percentage of larger aggregates was higher for **compound 2**-bearing liposomes (Table 7).

The favorable effect of the spacer on the sugar-lectin interaction was even more apparent when both the lectin and the porphyrins were immobilized. In the QCM-D experiments where no change in orientation of the molecules was possible, especially for the porphyrins in the liposomes, **compound 2** appeared to be more effective than **compound 1**. There might be another reason than the length of the sugar groups exposed to the aqueous medium. In the preparation of liposomes, phospholipid and porphyrins molecules were mixed. They could be embedded in the inner or the outer phospholipid leaflet of the liposome bilayers. Due to the larger molecular area that they occupy at the interface, as shown in our previous work,[(14)] molecules of **compound 2** might be preferentially exposed to the outer surface compared to those of **compound 1**.

Conclusion

The glycodendrimeric porphyrins proved to interact specifically with Concanavalin A. **Compound 2** with a longer spacer appeared more efficient than **compound 1**. In all experiments and for all studied systems (monolayers, liposomes, free or immobilized molecules), the specific interaction appeared to contribute to a higher extent to the overall interaction with the lectin than the non-specific one. Added to our previous results, which showed that the sugar moieties of the glycoconjugated dendrimeric porphyrins favored their non-specific interaction with phospholipids-cholesterol model membranes compared to **compound 1c**, the glycodendrimeric porphyrins appear as very promising drugs. Their evaluation on mixed phospholipid-Con A model systems and on the retinoblastoma Y79 cell line is currently in progress.

Acknowledgments

The authors acknowledge the financial support of A. M.'s PhD by ARC (Association pour la Recherche contre le Cancer).

References

1. Ellsworth, R. M. (1969) The practical management of retinoblastoma, *Trans Am Ophthalmol Soc 67*, 462-534.
2. Phillips, C., Sexton, M., Wheeler, G., and McKenzie, J. (2003) Retinoblastoma: review of 30 years' experience with external beam radiotherapy, *Australas Radiol 47*, 226-230.
3. Stephan, H., Boeloeni, R., Eggert, A., Bornfeld, N., Schueler, A. (2008) Photodynamic Therapy in Retinoblastoma: Effects of Verteporfin on Retinoblastoma Cell Lines, *Invest. Ophthalmol. Vis. Sci. 49*, 3158-3163.
4. van Hillegersberg, R., Kort, W. J., Wilson, J. H. (1994) Current status of photodynamic therapy in oncology, *Drugs 48*, 510-527.
5. Bonnett, R. (1995) Photosensitizers of the porphyrin and phthalocyanine series for photodynamic therapy, *Chem. Soc. Rev. 24*, 19-33.
6. Momenteau, M., Maillard, P., De Belinay, M. A., Carrez, D., Croisy, A. (1999) Tetrapyrrolic glycosylated macrocycles for an application in PDT, *J. Biomed. Opt. 4*, 298-318.
7. Lotan, R., and Raz, A. (1988) Lectins in cancer cells, *Ann N Y Acad Sci 551*, 385-398.
8. Komath, S. S., Bhanu, K., Maiya, B. G., and Swamy, M. J. (2000) Binding of porphyrins by the tumor-specific lectin, jacalin [Jack fruit (Artocarpus integrifolia) agglutinin], *Biosci Rep 20*, 265-276.
9. Sylvain, I., Zerrouki, R., Granet, R., Huang, Y. M., Lagorce, J. F., Guilloton, M., Blais, J. C., and Krausz, P. (2002) Synthesis and biological evaluation of thioglycosylated porphyrins for an application in photodynamic therapy, *Bioorganic & Medicinal Chemistry 10*, 57-69.
10. Chen, X., Hui, L., Foster, D. A., and Drain, C. M. (2004) Efficient Synthesis and Photodynamic Activity of Porphyrin-Saccharide Conjugates: Targeting and Incapacitating Cancer Cells†, *Biochemistry 43*, 10918-10929.
11. Ballut, S., Makky, A., Loock, B., Michel, J. P., Maillard, P., Rosilio, V. (2009) New strategy for targeting of photosensitizers. Synthesis of glycodendrimeric phenylporphyrins, incorporation into a liposome membrane and interaction with a specific lectin, *Chem Commun* 224-226.
12. Griegel, S., Rajewsky, M. F., Ciesiolka, T., Gabius, H. J. (1989) Endogenous sugar receptor (lectin) profiles of human retinoblastoma and retinoblast cell lines analyzed by cytological markers, affinity chromatography and neoglycoprotein-targeted photolysis, *Anticancer Res 9*, 723-730.
13. Laville, I., Pigaglio, S., Blais, J. C., Doz, F., Loock, B., Maillard, Ph., Grierson, D.S., Blais, J. (2006) Photodynamic Efficiency of Diethylene Glycol-Linked Glycoconjugated Porphyrins in Human Retinoblastoma Cells, *J. Med. Chem. 49*, 2558-2567.
14. Makky, A., Michel, J. P., Ballut, S., Kasselouri, A., Maillard, Ph., Rosilio, V. (2010) Effect of Cholesterol and Sugar on the Penetration of Glycodendrimeric Phenylporphyrins into Biomimetic Models of Retinoblastoma Cells Membranes, *Langmuir 26*, 11145-11156.
15. Paolesse, R., Valli, L., Goletti, C., Di Natale, C., Froiio, A., Macagnano, A., Bussetti, G., Chiaradia, P., and D'Amico, A. (2002) Langmuir-Blodgett films of a modified tetraphenylporphyrin, *Material Sci. and Eng. C 22*, 219-225.
16. Yao, M., Iwamura, Y., Inoue, H., and Yoshioka, N. (2005) Amphiphilic meso-disubstituted porphyrins: synthesis and the effect of the hydrophilic group on absorption spectra at the air-water interface, *Langmuir 21*, 595-601.
17. Ruggles, J. L., Foran, G. J., Tanida, H., Nagatani, H., Jimura, Y., Watanabe, I., and Gentle, I. R. (2006) Interfacial behavior of tetrapyridylporphyrin monolayer arrays, *Langmuir 22*, 681-686.
18. Ruggles, J. L., Baldwin, K. M., Holt, S. A., Foran, G. J., and Gentle, I. R. (2007) Rigid Films of an Anionic Porphyrin and a Dialkyl Chain Surfactant, *The Journal of Physical Chemistry B 111*, 5651-5657.
19. Desroches, M. C., Kasselouri, A., Meyniel, M., Fontaine, P., Goldmann, M., Prognon, P., Maillard, P., Rosilio, V. (2004) Incorporation of Glycoconjugated Porphyrin Derivatives into Phospholipid Monolayers: A Screening Method for the Evaluation of Their Interaction with a Cell Membrane, *Langmuir 20*, 11698-11705.
20. Perez-Morales, M., Pedrosa, J. M., Martin-Romero, M. T., Mobius, D., and Camacho, L. (2004) Reversible Trilayer Formation at the Air−Water Interface from a Mixed Monolayer Containing a Cationic Lipid and an Anionic Porphyrin, *The Journal of Physical Chemistry B 108*, 4457-4465.
21. Ballut, S., Loock, B., and Maillard, P. (2010) *Submitted*.
22. Sanders, J. N., Chenoweth, S. A., and Schwarz, F. P. (1998) Effect of metal ion substitutions in concanavalin A on the binding of carbohydrates and on thermal stability, *J. Inorg. Bioch. 70*, 71-82.
23. Rusin, O., Kral, V., Escobedo, J.O., Strongin, R.M. (2004) A Supramolecular Approach to Protein Labeling. A Novel Fluorescent Bioassay for Concanavalin A Activity, *Org. Lett. 6*, 1373-1376.

24. Clegg, R. M., Loontiens, F. G., Van Landschoot, A., and Jovin, T. M. (1981) Binding kinetics of methyl .alpha.-D-mannopyranoside to concanavalin A: temperature-jump relaxation study with 4-methylumbelliferyl .alpha.-D-mannopyranoside as a fluorescence indicator ligand, *Biochemistry 20*, 4687-4692.
25. Davila, J., and Harriman, A. (2002) Photochemical and radiolytic oxidation of a zinc porphyrin bound to human serum albumin, *J. Am. Chem. Soc. 112*, 2686-2690.
26. Komath, S. S., Kavitha, M., and Swamy, M. J. (2006) Beyond carbohydrate binding: new directions in plant lectin research, *Org; & Biomolec. Chem. 4*, 973-988.
27. Becker, J. W., Reeke, G. N. Jr., Wang, J. L., Cunningham, B. A., Edelman, G. M. (1975) The covalent and three-dimensional structure of concanavalin A. III. Structure of the monomer and its interactions with metals and saccharides, *J. Biol. Chem. 250*, 1513-1524.
28. Bittiger, H., and Schnebli, H. P. (1974) Binding of concanavalin A and ricin to synaptic junctions of rat brain, *Nature 249*, 370-371.
29. Goldstein, I. J., and Hayes, C. E. (1978) The lectins: carbohydrate-binding proteins of plants and animals, *Adv Carbohydr Chem Biochem 35*, 127-340.
30. Bangham, A. D., Standish, M. M., and Watkins, J. C. (1965) Diffusion of univalent ions across the lamellae of swollen phospholipids, *J. Molec. Biol. 13*, 238-252, IN226-IN227.
31. Faivre, V., Rosilio, V., Boullanger, P., Martins Almeida, L., Baszkin, A. (2001) Fucosyled neoglycolipids: synthesis and interaction with a phospholipid, *Chem. Phys. Lipids 109*, 91-101.
32. Faivre, V., Costa, M.L., Boullanger, P., Baszkin, A., Rosilio, V. (2003) Specific interaction of lectins with liposomes and monolayers bearing neoglycolipids, *Chem. Phys. Lipids 125*, 147-159.
33. Briand, E., Salmain, M., Compère, C., and Pradier, C.-M. (2006) Immobilization of Protein A on SAMs for the elaboration of immunosensors, *Colloid Surf. B: Biointerfaces 53*, 215-224.
34. Komath, S. S., Kenoth, R., Giribabu, L., Maiya, B. G., and Swamy, M. J. (2000) Fluorescence and absorption spectroscopic studies on the interaction of porphyrins with snake gourd (Trichosanthes anguina) seed lectin, *Journal of Photochem. and Photobiol. B: Biology 55*, 49-55.
35. Komath, S. S., and Swamy, M. J. (1999) Fluorescence quenching, time-resolved fluorescence and chemical modification studies on the tryptophan residues of snake gourd (Trichosanthes anguina) seed lectin, *Journal of Photochem. and Photobiol. B: Biology 50*, 108-118.
36. Mandal, D. K., Kishore, N., and Brewer, C. F. (2002) Thermodynamics of Lectin-Carbohydrate Interactions. Titration Microcalorimetry Measurements of the Binding of N-Linked Carbohydrates and Ovalbumin to Concanavalin A, *Biochemistry 33*, 1149-1156.
37. Moothoo, D. N., Canan, B., Field, R. A., and Naismith, J. H. (1999) Man alpha1-2 Man alpha-OMe-concanavalin A complex reveals a balance of forces involved in carbohydrate recognition, *Glycobiology 9*, 539-545.
38. Berthelot, L., Rosilio, V., Costa, M. L., Chierici, S., Albrecht, G., Boullanger, P., and Baszkin, A. (1998) Behavior of amphiphilic neoglycolipids at the air/solution interface: Interaction with a specific lectin, *Colloid Surf. B: Biointerfaces 11*, 239-248.
39. Senear, D. F., and Teller, D. C. (1981) Thermodynamics of concanavalin A dimer-tetramer self-association: sedimentation equilibrium studies, *Biochemistry 20*, 3076-3083.
40. Reimhult, E., Höök, F., and Kasemo, B. (2002) Intact Vesicle Adsorption and Supported Biomembrane Formation from Vesicles in Solution: Influence of Surface Chemistry, Vesicle Size, Temperature, and Osmotic Pressure†, *Langmuir 19*, 1681-1691.
41. Reimhult, E., Zach, M., Hook, F., Kasemo, B. (2006) A multitechnique study of liposome adsorption on Au and lipid bilayer formation on SiO2, *Langmuir 22*, 3313-3319.
42. Patel, A. R., and Frank, C. W. (2006) Quantitative Analysis of Tethered Vesicle Assemblies by Quartz Crystal Microbalance with Dissipation Monitoring: Binding Dynamics and Bound Water Content, *Langmuir 22*, 7587-7599.
43. Brochu, H., and Vermette, P. (2007) Liposome Layers Characterized by Quartz Crystal Microbalance Measurements and Multirelease Delivery, *Langmuir 23*, 7679-7686.
44. Seantier, B., Breffa, C., Felix, O., Decher, G. (2005) Dissipation-Enhanced Quartz Crystal Microbalance Studies on the Experimental Parameters Controlling the Formation of Supported Lipid Bilayers, *J. Phys. Chem.B 109*, 21755-21765.
45. Reimhult E., H. F. a. K. B. (2002) Vesicle adsorption on SiO2 and TiO2: Dependence on vesicle size, *J. Chem. Phys. 117*, 7401 -7405.
46. Hook, F., Kasemo, B., Nylander, T., Fant, C., Sott, K., Elwing, H. (2001) Variations in Coupled Water, Viscoelastic Properties, and Film Thickness of a Mefp-1 Protein Film during Adsorption and Cross-Linking: A Quartz Crystal Microbalance with Dissipation Monitoring, Ellipsometry, and Surface Plasmon Resonance Study, *Anal. Chem. 73*, 5796-5804.

47. Dutta, A. K., Nayak, A., Belfort, G. (2008) Viscoelastic properties of adsorbed and cross-linked polypeptide and protein layers at a solid-liquid interface, *J. Colloid and Interf. Sci. 324*, 55-60.
48. Höök, F., Rodahl, M., Kasemo, B., and Brzezinski, P. (1998) Structural changes in hemoglobin during adsorption to solid surfaces: Effects of pH, ionic strength, and ligand binding, *PNAS 95*, 12271-12276.

Chapitre 3 : Construction et caractérisation physico-chimique d'un modèle membranaire du rétinoblastome exposant à sa surface une lectine spécifique de mannose et interaction avec les porphyrines incorporées dans des liposomes

Article 5: Biomimetic liposomes and planar supported bilayers for the assessment of glycodendrimeric porphyrins interaction with an immobilized lectin.

Ali Makky, Jean-philippe Michel, Philippe Maillard, and Véronique Rosilio

En attente pour publication dans BBA-Biomembranes

Jusqu'à maintenant, nous avons démontré que les porphyrines glycodendrimériques libres sont capables d'interagir d'une manière non spécifique avec les membranes et d'y pénétrer, au moins partiellement. Nous avons aussi montré qu'une élévation du cholestérol membranaire ne favorise pas une meilleure pénétration des molécules. Par la suite, nous avons évalué leur capacité à interagir de manière spécifique, sous forme libre ou véhiculées par de liposomes, avec la Con A, elle-même sous forme libre en solution ou immobilisée sur une surface. Mais ces configurations expérimentales ne sont pas suffisamment représentatives d'une interaction des porphyrines avec un modèle membranaire biomimétique du rétinoblastome. Dans ce troisième chapitre, nous avons franchi une étape supplémentaire importante en construisant et en caractérisant un modèle membranaire de rétinoblastome complètement original qui se rapproche d'un modèle membranaire véritablement biomimétique pour deux raisons: (i) sa structure en bicouche (plane ou liposomiale) et sa composition quaternaire miment mieux celles des membranes naturelles du rétinoblastome que tous les modèles présentés dans la littérature, (ii) il expose à sa surface une lectine modélisant le récepteur à mannose surexprimé à la surface des cellules de rétinoblastome.

Après avoir décrit l'élaboration de nos modèles sous forme de protéoliposomes et de bicouches planes supportées exposant à leur surface la Con A, nous avons étudié l'interaction globale (spécifique et non-spécifique) des porphyrines incorporées dans des liposomes de DMPC avec ces deux systèmes, par des mesures de diffusion de lumière et de QCM-D.

Biomimetic liposomes and planar supported bilayers for the assessment of glycodendrimeric porphyrins interaction with an immobilized lectin.

Ali Makky [a,b], Jean-Philippe Michel [a,b], Philippe Maillard [c,d], and Véronique Rosilio [a,b]

[a b] Univ Paris-Sud 11, UMR CNRS 8612, Laboratoire de Physico-chimie des Surfaces, 5 rue Jean-Baptiste Clément, F-92296 Châtenay-Malabry cedex, France; [c d] UMR CNRS 176, Institut Curie, Centre de Recherche, Bât 110-112, Orsay, F-91405, France; Université Paris-Sud 11.

* Corresponding author: veronique.rosilio@u-psud.fr

Introduction

Photodynamic therapy (PDT) is a relatively new treatment modality for various diseases including superficial tumours such as basal cell carcinomas of the skin, head and neck tumours as well as tumours accessible to endoscopy like oesophageal and lung cancers [(1)]. Moreover, due to its therapeutic efficacy and its fewer side effects compared to chemotherapy and radiotherapy, this technique would be considered as one of retinoblastoma alternative treatments [(2-5)]. PDT involves a nontoxic photosensitizing agent that is activated by light at an appropriate wavelength generally in the presence of oxygen. This results in the release of organic radicals or reactive oxygen species (ROS), especially singlet oxygen that oxidize the target tissue, lead to irreversible damage and consecutive cell death (necrosis, apoptosis or autophagy) [(6)]. However, because of its short half life (~ 4µs), singlet oxygen induces photodamage in its immediate vicinity only [(7)]. Therefore, the phototoxicity efficiency is highly dependent upon photosensitizers intracellular accumulation and subcellular localization [(7)].

Most photosensitizers used for both experimental and clinical studies in PDT are porphyrin-based compounds with a macrocyclic core providing the required photoactivity, and peripheral substituents controlling drug biodistribution and pharmacokinetics [(8)]. However, these compounds are usually poorly water-soluble molecules, and tend to form aggregates in aqueous solution [(9-11)]. Hence, to improve the efficacy of porphyrins photodynamic activity, many authors have used the glycoconjugation strategy as a potential effective way to (i) increase drug water solubility by modifying macrocycles amphipathy [(12-19)], and (ii) target lectin-like receptors over-expressed in some types of malignant cells [(20-21)] such as retinoblastoma cells [(20-23)]. With this aim, Ballut et *al.* [(22, 24)] have recently synthesized new glycodendrimeric porphyrins as drugs with higher specificity in the treatment of retinoblastoma by PDT. The specific receptors overexpressed at the surface of cells have not been identified yet, but it is known that they are receptors to mannose and galactose [(13, 22-23)].

Because membranes are considered as the primary targets of cell photodamage for most photosensitizers used in PDT [25], studying the mechanisms of phostosensitizer-cell membrane interaction is of great interest. The elaboration of biomimetic membrane models mimicking the *in vivo* situation would account for a real progress allowing better comprehension of such mechanisms. Many research groups have used different organized systems, such as monolayers [26-27] or liposomes [28-37] for modeling a cell membrane and studying porphyrin interaction with it. However, these model systems containing a single lipid or even a binary lipid mixture were not biomimetic enough of cancerous cell membranes, and they lacked the lectin-like receptors at their surface. In a previous work, we have focused on the non-specific interactions and penetration ability of glycodendrimeric porphyrins into mixed phospholipid monolayers and liposome bilayers having similar lipidic composition to that of the retinoblastoma cell membranes [38-41], with increasing cholesterol content from 10 to 30 mol% [42]. We have shown that cholesterol changes in retinoblastoma cell membranes did not modify the penetration ability of the studied porphyrins. Moreover, we have demonstrated that glycoconjugation of porphyrins reinforced their amphiphathy and promoted their interaction with those membranes [42]. In a more recent work, we have analyzed more specifically the ability of the porphyrin derivatives to be recognized by a mannose-specific protein, Concanavalin A, mimicking some of the receptors over-expressed at the surface of retinoblastoma cells [22, 43]. Our results showed that only mannosylated porphyrins could specifically interact with Concanavalin A (Con A), and that the spacer length between a porphyrin core and its mannose moieties played a crucial role in this interaction. To avoid non-specific interactions with the lipids, Con A has been studied alone, free in the aqueous medium or immobilized onto a SAM-functionalized QCM-D gold sensor. Herein, we have built and characterized liposomes and supported planar bilayers having a similar lipidic composition to that of retinoblastoma cell membranes as previously described [42], on which Con A has been grafted. This more complete model allowed us to better mimic the *in vivo* conditions and to get a better insight into the mechanisms of interaction between glycoconjugated porphyrins and retinoblastoma cells at a pH of 6.5, close to that reported for tumorous tissues [44].

Materials and Methods

Chemicals

The glycodendrimeric porphyrins **compound 1** (Mw = 1692.81 g/mol) and **compound 2** (Mw = 1823.8 g/mol) were prepared as described previously by Ballut *et al.* [22, 24] They

were tri-mannosylated with a DEG (diethylene glycol) and a TEG (triethylene glycol) spacer, respectively. We also studied a non-glycoconjugated porphyrin (compound **1c**, Mw = 1236.09 g/mol), [22, 24] which had the same structure as **compound 1**, except for the mannose residues replaced by OH groups. This non-glycoconjugated **compound 1c** was considered as a control for **compound 1** and to a lower extent for **compound 2**. The three porphyrin derivatives were poorly soluble in water but soluble in a (9:1 v/v) mixture of chloroform/methanol used for liposome preparation. Their chemical structures are presented in Figure 35.

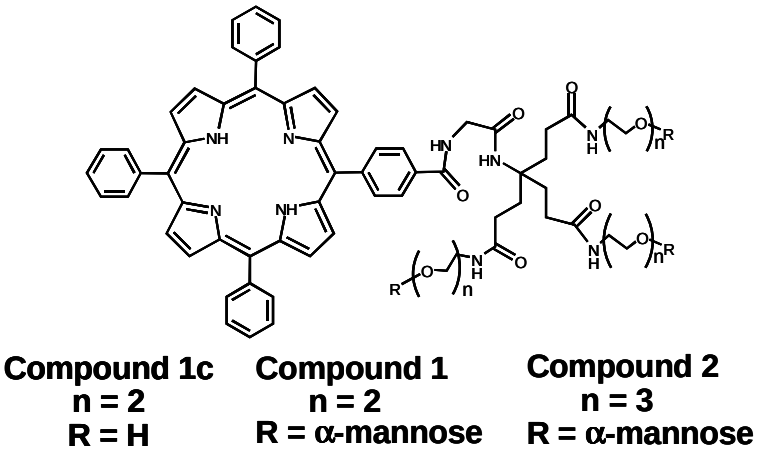

Figure 35 : Chemical structures of the studied porphyrins.

The phospholipids used for building the biomimetic membrane: 1-stearoyl-2-oleoyl-sn-glycero-3-phospho-L-serine (sodium salt) (SOPS, Mw = 812.05 g/mol), 1-stearoyl-2-oleoyl-sn-glycero-3-phosphocholine (SOPC, Mw = 788.14 g/mol), 1-stearoyl-2-oleoyl-sn-glycero-3-phosphoethanolamine (SOPE, Mw = 746.06 g/mol) and 1,2-dioleoyl-sn-glycero-3-phosphoethanolamine-N-(glutaryl) (sodium salt) (DOPE-glutaryl, Mw = 880.12 g/mol) were purchased from Instruchemie (Delfzijl, The Netherlands). They were 99% pure and were used without any further purification. Concanavalin A (Type IV, Mw: 25500 g/mol per monomer), Sepharose 4B gel, methyl α-D-mannopyranoside (≥ 99% pure, Mw = 194.18 g/mol), mannan from *Saccharomyces cerevisiae* (≥ 95% pure), 1,2-dimyristoyl-sn-glycero-3-phosphocholine (DMPC, 99% pure, Mw = 677.93 g/mol), cholesterol (CHOL, 99% pure, Mw = 386.66 g/mol), HEPES (99.5% pure, Mw = 238.31 g/mol), sodium chloride (NaCl, 99% pure, Mw = 58.44 g/mol), calcium chloride ($CaCl_2.2H_2O$, 98% pure, Mw = 147.02 g/mol), nickel chloride ($NiCl_2.6H_2O$, 98% pure Mw = 237.69 g/mol), 1-ethyl-3-[3-(dimethylamino)propyl] carbodiimide hydrochloride (EDC), N-hydroxysuccinimide (NHS), ethanolamine (99.5% pure, Mw = 61.08 g/mol) and glutaraldehyde (25% in H_2O, Mw = 100.12 g/mol) were purchased from Sigma (Saint-Louis, USA). Sodium acetate NORMAPUR™ AR (CH_3COONa, Mw = 82.03 g/mol) was purchased from VWR Prolabo (Briare, France).

Chloroform and methanol (99% pure) provided by Merck (Germany) were analytical grade reagents. Ultrapure water (γ = 72.2 mN/m at 22°C) produced by a Millipore Synergy 185 apparatus coupled with a RiOs5^{TM} with a resistivity of 18.2 MΩ.cm, was used in all experiments. All glassware were soaked for an hour in a freshly prepared TFD4 (Franklab) detergent solution (15% v/v), then abundantly rinsed with milli-Q water and finally oven-dried.

Methods

Preparation of liposomes for porphyrin solubilization, Con-A coupling, and supported bilayer formation

Liposomes were prepared according to Bangham's method followed by the extrusion of vesicles suspensions [45-47]. In brief, phospholipid solutions in chloroform/methanol (9:1 v/v) were evaporated for 3 hours under reduced pressure, and the resulting dry lipid film was hydrated by the corresponding buffer to achieve the desired concentration. The lipid suspension thus obtained was then extruded 15 times through a 200 nm polycarbonate membrane at 50°C for DMPC liposomes and 60°C for the others (Avestin Lipofast extruder, Ottawa, California).

In this work, 3 types of liposomes having different lipid compositions were prepared:

(i) Liposomes of DMPC bearing porphyrins (500:1 molar ratio) at 2mM were prepared as previously described [22]. In brief, DMPC and the porphyrin were solubilized in a (9:1) chloroform-methanol mixture. After complete evaporation of the organic solvents in a rotatory evaporator under reduced pressure, the resulting dry film was hydrated by HEPES buffer (HEPES 10 mM, 150 mM NaCl, pH 6.5) with divalent ions (1mM Ca^{2+} and 1mM Ni^{2+}). The divalent ions were required for Con A activity [48] and the pH was chosen to match that reported in cancer tissues. These liposomes were meant to "solubilise" and carry the porphyrins toward their target.

(ii) 10 mM liposomes formed of SOPC, SOPE, SOPS and cholesterol (4.5:3.5:1:1 molar fractions) in HEPES buffer (10 mM HEPES, 150 mM NaCl, pH 7.4). Concanavalin A was then grafted onto the surface of these liposomes for studying their interaction as models of the retinoblastoma cell membrane, with porphyrin-bearing DMPC vesicles.

(iii) 2 mM carboxylated liposomes (SOPC/DOPE-glutaryl/SOPS/CHOL: 4.5:3.5:1:1 molar fractions) for the formation of planar bilayers onto the SiO_2 surface of the QCM-D sensor, and subsequent coupling of Con A. These liposomes were prepared in sodium acetate buffer (10 mM sodium acetate, 150 mM NaCl, pH = 4) to facilitate their

adsorption onto the SiO_2 surface, by avoiding electrostatic repulsion with the negative charge of COOH moieties at higher pH.

Conjugation of Concanavalin A to SOPC/SOPE/SOPS/CHOL liposomes

Con A immobilization onto the surface of liposomes was achieved according to the method described by Nakano *et al.* [49] and Liu *et al.* [50] with some modifications. Briefly, 1 ml of SOPC/SOPE/SOPS/CHOL liposomes was added slowly (10 µl/min) to 0.6 ml of 5% aqueous glutaraldehyde solution with gentle stirring for 1 hour at 4°C. Glutaraldehyde in excess was removed by dialysis (MWCO 15 kD) overnight at 4°C. Then 0.2 ml of a Con A solution (10 mg/ml in HEPES, pH 7.4) was added under gentle stirring at 4°C. After 1 hour of incubation, 0.5 M ethanolamine-HCl (0.2 ml, pH 7.4) was added to liposomes to block excess aldehyde groups on the liposomes surface. The system was left for 1 hour at 4°C.

The Con A-conjugated liposomes thus obtained were separated from uncoupled Con A by gel permeation chromatography on Sepharose 4B columns with HEPES buffer (HEPES 10 mM, NaCl 150 mM, pH 7.4) as eluent The elution profiles of Con A and the liposomes were monitored using the BCA™ Protein Assay (Sigma St. Louis, USA**)** and phospholipid assay kit (Diagnostics Partners, France). Samples of the eluted fractions (2ml) were collected and analyzed using a CARY 100 Bio UV-visible spectrophotometer (Varian, USA) at 562 and 500 nm for protein and lipid assays, respectively.

Vesicle size and zeta potential measurements:

The analysis of the size and zeta potential (ζ) of the liposomes was carried out at 25°C using a Zeta-sizer (Nano ZS90, Malvern). The ζ measurements were performed after redispersion of 50 µl of 4 mM liposomes in HEPES buffer at pH 6.5 in 1 ml of deionised water. Dilution had no effect on liposome size.

Liposomes aggregation assay with immobilized Con A

To verify that the specific activity of Con A was maintained when it was coupled to liposomes, we have performed a similar aggregation assay to that of Chen *et al.* [51] using mannan, a Con A polyvalent substrate. In this assay, 200 µl of a mannan solution (1mg/ml in HEPES buffer (10 mM HEPES, 150 mM NaCl, 1 mM $CaCl_2.2H_2O$ and 1 mM $NiCl_2.6H_2O$, pH 6.5) was added to 500 µl of fresh Con A-liposomes (2 mM) saturated (or not) beforehand with methyl α-D-mannopyranoside (α-MMP), a substrate with a high affinity to Con A [52]. Con A activity was considered as preserved if no liposome aggregation occurred when Con A

specific sites were saturated with α-MMP. The mixture was vortexed for 10 min and incubated for 1 h at room temperature. Vesicles diameters were measured before and after addition of mannan using the Zetasizer. All measurements were carried out at 25°C.

Formation of a Con A conjugated-planar lipid bilayer

Experiments using the quartz crystal microbalance with dissipation monitoring were performed with a QCM-D E4 (Q-Sense, Gothenburg, Sweden). The QCM-D sensor allows the measurement of the oscillation frequency shift (Δf) of a quartz crystal and simultaneous energy dissipation change (ΔD). Whereas changes in resonance frequency are related to the mass of the material adsorbed on or removed from the sensor, changes in energy dissipation provide information on the viscoelastic properties of the adsorbed material. AT-cut SiO_2-coated quartz crystals with a fundamental frequency of 5 MHz were provided by Q-Sense AB. These crystals were stored in 10 mM sodium dodecyl sulfate (SDS) solution between measurements. Prior to their use, they were thoroughly rinsed with ultrapure water, dried under a N_2 stream and treated in an UV-ozone chamber for 20 minutes.

A supported planar bilayer (SPB) was easily obtained by spreading and then spontaneous breaking of phospholipid-cholesterol vesicles onto the SiO_2 quartz. However, it was not possible to subsequently graft the lectin onto this SPB by *in situ* activation of the phosphatidylethanolamine (PE) headgroups by glutaraldehyde, as described for the Con A-conjugated liposomes. Indeed, the addition of glutaraldehyde probably created a network between free PE headgroups, hindering Con A grafting to the surface. The alternative method consisted in replacing SOPE in the liposomes formulation by DOPE-glutaryl, a commercially available phospholipid derivative. As such, PE groups were already activated and presented a free COOH group for Con A coupling. Lectin immobilization on the preformed supported bilayer was further achieved by conversion of the carboxylic acid functions of DOPE-glutaryl into N-hydroxysuccinimide esters by reaction with N-hydroxysuccinimide (NHS) in the presence of a water-soluble carbodiimide (EDC), followed by reaction with Con A.

Results

Elution profiles of Con A-conjugated liposomes

After conjugation, Con A-bearing liposomes were separated from the unbound lectin by gel permeation chromatography, and the various fractions were analyzed. As shown in Figure 36, the free Con A was collected in one peak. This result is consistent with the elution profile

described by Santos *et al*. for this lectin [53]. When Con A was incubated with pre-activated liposomes, its elution profile drastically changed and two peaks of Con A were observed (Figure 36). The first one appeared in the fourth fraction, in which liposomes were totally eluted, and the second one in the eighth fraction, corresponding to the unbound Con A.

Using the immobilization procedure, lectin-liposome conjugates were obtained with a lectin/lipid molar ratio of 6.7 ± 1.0 $x10^{-4}$, in good agreement with those (up to $5x10^{-4}$) obtained by Bogdanov *et al.* [54] for Ricinus communis agglutinin (RCA) and wheat germ agglutinin (WGA) immobilizations onto a liposome surface, using carbodiimide chemistry [54].

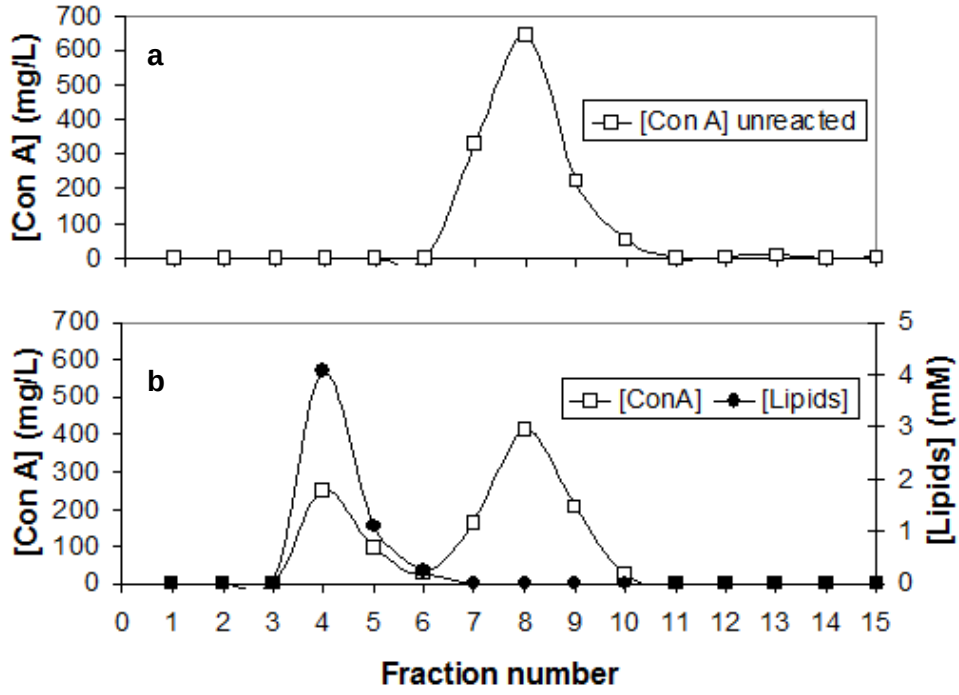

Figure 36 : Elution profiles for (a) the free Con A, and (b) Con A after reaction with pre-activated liposomes.

Aggregation assay of Con A-conjugated liposomes with mannan

No liposome aggregation was observed upon addition of a mannan solution to non-conjugated liposomes. Their size measured by DLS remained unchanged (Table 8). Conversely, addition of the polysaccharide to Con A-conjugated liposomes induced a dramatic increase in vesicles diameter accounting for their aggregation. This result proved that mannan was able to interact with the lectin immobilized onto a vesicle surface. The multiplicity of binding sites on the polysaccharide probably promoted the interaction of mannan with more than one conjugated lectin molecule, leading to liposomes bridging and formation of large aggregates. This would explain the high diameter values measured, and the bimodal size distribution observed for

these liposomes. In the presence of α-MMP, which saturated the specific sites of Con A, the addition of mannan did not induce any liposomes aggregation: their size remained unchanged. These data demonstrated the effective conjugation of Con A to the liposomes outer surface and the preservation of Con A functional binding activity to mannose moieties.

Liposomes	Before mannan addition		After mannan addition	
Composition	Diameter (nm)	Volume (%)	Diameter (nm)	Volume (%)
SOPC/SOPE/SOPS/CHOL	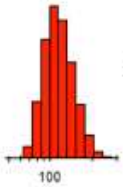 139	100	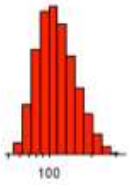 140	100
Liposomes-Con A	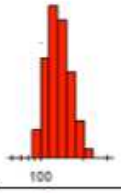 148	100	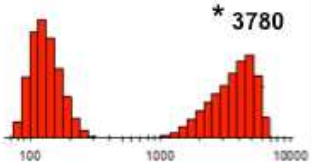 * 3780	* 48.3
Liposomes-Con A saturated with α-MMP	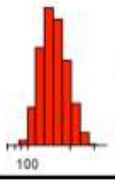 164	100	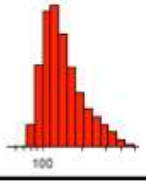 166	100

Table 8: Liposome diameters before and following addition of 200 µl of a 1 mg/ml mannan solution to 2mM of unmodified liposomes, Con A-conjugated liposomes and Con A-conjugated liposomes saturated with α-MMP.

Zeta Potential measurements

We have also evaluated the effect of Con A on the zeta potential of vesicles suspension.

Liposomes	Zeta (mV)
Non conjugated liposomes	-66.8±2.9
Free Con A	-14.2±0.3
Con A-conjugated liposomes	-79.4±2.5
Con A mixed with liposomes	-62.2±2.5

Table 9 : Zeta potential (ζ) values for liposomes and Con A samples.

Non-conjugated liposomes and free Con A exhibited zeta potential values of -64.5 ± 2.3 mV and -14.2 ± 0.3 mV, respectively (table 9). When free Con A was mixed with unmodified liposomes in the buffer solution, no significant change in zeta potential was observed (-62.2 ±2.5 mV). Conversely, when the lectin was grafted to liposomes surface, the zeta potential was significantly lowered to -79.4 ± 2.5 mV. This result is consistent with the effective

grafting of Con A to the surface of liposomes, making it more negatively charged than the unmodified liposomes. A similar result has been reported by Santos *et al.* with doxorubicin-loaded Con A-Liposomes [(53)].

Interaction of porphyrin-bearing DMPC vesicles with Con A-conjugated SOPC/SOPE/SOPS/CHOL liposomes

In a previous work [(22)], we have shown that compounds **1c, 1** and **2** could be solubilised into the bilayer of DMPC liposomes. The liposomes bearing mannosylated porphyrins were able to interact significantly with free Con A through the outward exposure of their mannoses moieties into the aqueous phase. Herein we have studied the ability of these porphyrin-loaded liposomes to interact with Con A immobilized onto SOPC-SOPE-SOPS-CHOL liposomes surfaces, mimicking more efficiently the *in vivo* conditions than did the free Con A in solution.

Liposomes	**Before interaction with Con A-conjugated liposomes 148 nm (100%)**		**After interaction with Con A-conjugated liposomes 148 nm (100%)**	
Composition	**Diameter (nm)**	**Volume (%)**	**Diameter (nm)**	**Volume (%)**
DMPC-Compound 1c	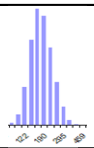 **146**	**100**	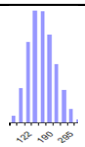 **157**	**100**
DMPC-Compound 1	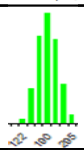 **160**	**100**	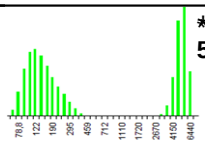 *** 5180**	*** 35.6**
DMPC-Compound 2	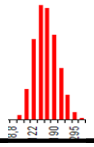 **161**	**100**	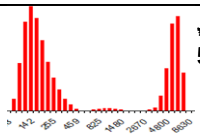 *** 5090**	*** 33.6**

Table 10 : DLS measurements of Con A-conjugated liposomes size before and after addition of porphyrin-bearing liposomes.

The size of Con A-conjugated liposomes was not significantly affected by the addition of DMPC-compound **1c** vesicles (148 nm versus 157 nm). Conversely, after adding DMPC-compound **1** and DMPC-compound **2** liposomes, a dramatic increase in vesicles diameter was observed with emergence of new vesicle families having a diameter of about 5000 nm (Table 10). This striking result demonstrates that mannosylated porphyrins borne by DMPC liposomes were able to interact specifically with multiple Con A-conjugated liposomes, leading to the formation of liposome aggregates (Figure 37), even if Con A was immobilized

onto the vesicles surface at a low density (Con A was grafted to superficial PE head groups only). However, no significant difference in the aggregates size between DMPC-compound **1** and DMPC-compound **2** liposomes could be drawn, because the obtained values were beyond the detection limits of the DLS apparatus. The influence of the spacer length was thus not apparent from these measurements.

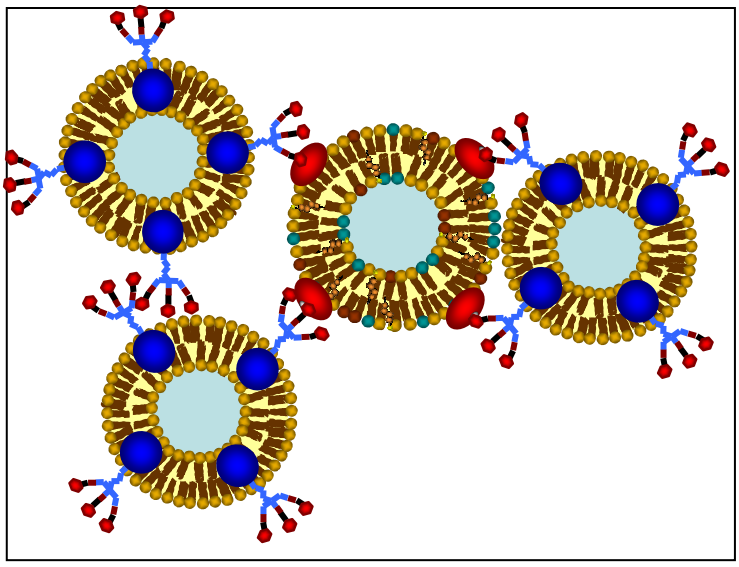

Figure 37 : schematic representation of aggregates formation following mixing mannosylated porphyrin-bearing vesicle and Con A-conjugated liposome suspensions.

Formation of a biomimetic supported planar bilayer (SOPC/SOPS/CHOL/DOPE-glutaryl)

Solid-supported membranes are widely used as well-defined model systems for fundamental biophysical research and have been proposed as biomimetic surfaces to elucidate the physical behaviour of cell membranes [(55)] and membrane-bound macromolecules [(56)]. To create supported planar bilayers, a multitude of methods has been proposed, including Langmuir-Blodgett techniques [(57-58)] and spreading of vesicles on various preconditioned supports [(55, 59-63)]. In this work, we have used the latter approach by spreading small lipid vesicles onto hydrophilic solid SiO_2 substrates (Figure 38).

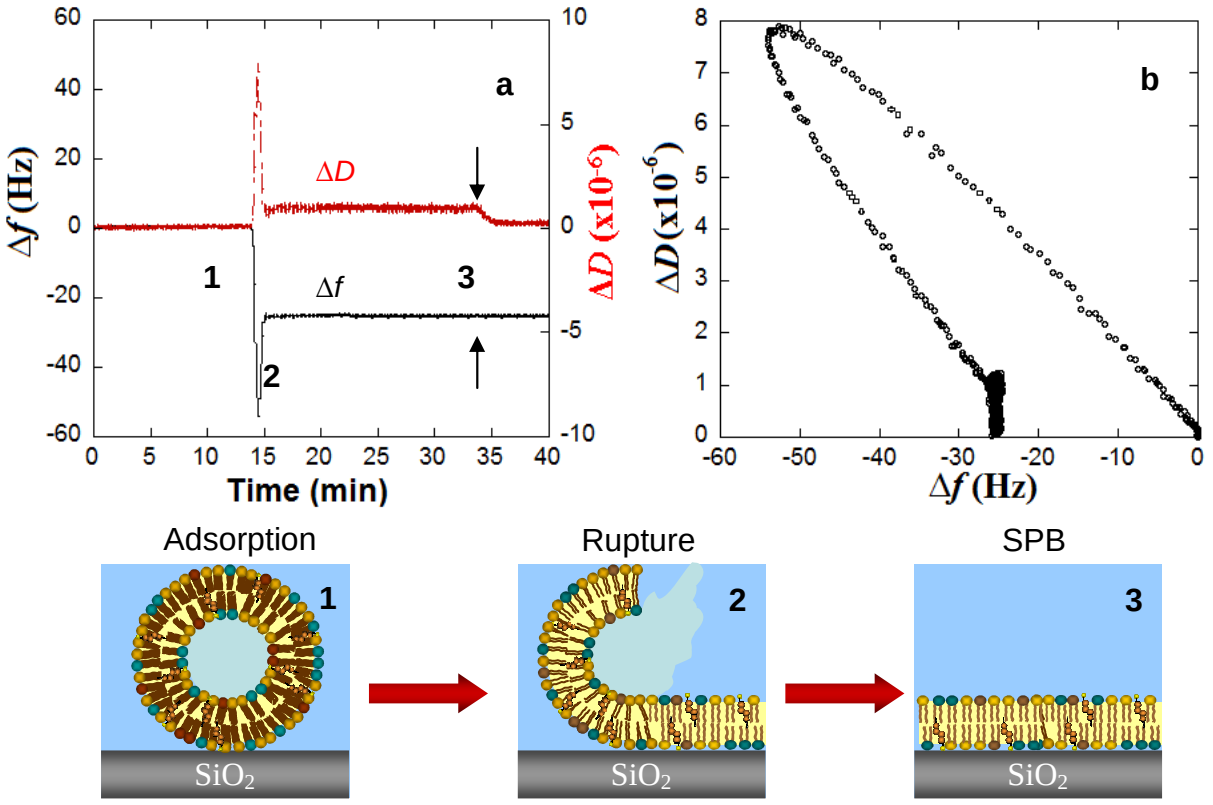

Figure 38 : Deposition and rupture of COOH-liposomes onto the SiO_2 surface ([lipids] = 2 mM in acetate buffer, at pH = 4, vesicles size ~ 146 nm): (a) Δf and ΔD change with time at 15 MHz; Arrows indicate buffer rinsing. (b) Dissipation vs. frequency shift.

Figure 38a shows the process of planar bilayer formation on the SiO_2 quartz followed by QCM-D measurement at the third overtone (15 MHz). After injection of the 2 mM COOH-liposome suspension, the frequency decreased (**1**, mass uptake) and simultaneously the dissipation increased (indicating that the film became more viscous) until a critical density of adsorbed intact vesicles was reached. This critical density of vesicles relates to the minimum in frequency (~ -53Hz) and the maximum in dissipation (7.5 $x10^{-6}$). At this point, and as described by many authors [59, 64], the vesicle rupture usually starts. Following this rupture onto the quartz surface, Δf increased (**2**), indicating a mass loss, and ΔD decreased accounting for the presence of a more rigid adsorbed film. Finally (**3**), Δf and ΔD curves stabilized at Δf ~ - 25.3 Hz and ΔD ~ $0.2x10^{-6}$, and no significant change in the baseline was observed upon rinsing with HEPES buffer (arrows in Figure 38a). This result demonstrated the formation of a stable supported planar bilayer (SPB). Indeed, the Δf and ΔD values corresponding to the breaking of COOH-liposomes fully matched those reported for a complete homogeneous supported planar bilayer (Δf ~ -26 Hz and ΔD ~ $0.3x10^{-6}$) [61, 64-66]. Moreover the final low dissipation shift (ΔD ~ $0.2x10^{-6}$) attested the good quality of the supported bilayer formed [62].

The Δf-ΔD plot in Figure 38b allows discarding time as an explicit parameter and highlights the mechanistic details of bilayer formation following liposomes deposition. After a simultaneous Δf decrease and ΔD increase from the zero coordinate, the plot shows a cusp at Δf = -52.3 Hz and $\Delta D \sim 7.8 \times 10^{-6}$. This cusp corresponds to maximal liposome adsorption. The following phase of vesicles rupture is indicated by the simultaneous Δf increase and ΔD decrease, until they both reach stable values. Similar plots have been obtained by many authors describing supported bilayer formation [61, 65].

Con A immobilization onto the phospholipid-cholesterol planar bilayers

The time-dependent frequency and dissipation shifts were recorded during Con A immobilization on the supported planar bilayer (Figure 39). At t = 20 min after SPB formation, the Con A solution was injected into the QCM-D cell. This induced a decrease of the crystal resonance frequency below -40 Hz and a simultaneous ΔD increase up to 12×10^{-6}, corresponding to the adsorption of a viscous layer of Con A onto the bilayer surface. Three rinsing steps were applied as shown by the arrows in Figure 39, first with HEPES buffer to eliminate weakly bound Con A then one with the ethanolamine solution to inactivate the free glutaryl groups. Finally the cell was rinsed with HEPES buffer and the measured Δf and ΔD signals were only slightly affected, indicating that the covalently bound Con A molecules remained firmly attached to the bilayer surface. The obtained final values were $\Delta f \sim$ -36.7 Hz and $\Delta D \sim 10.6 \times 10^{-6}$.

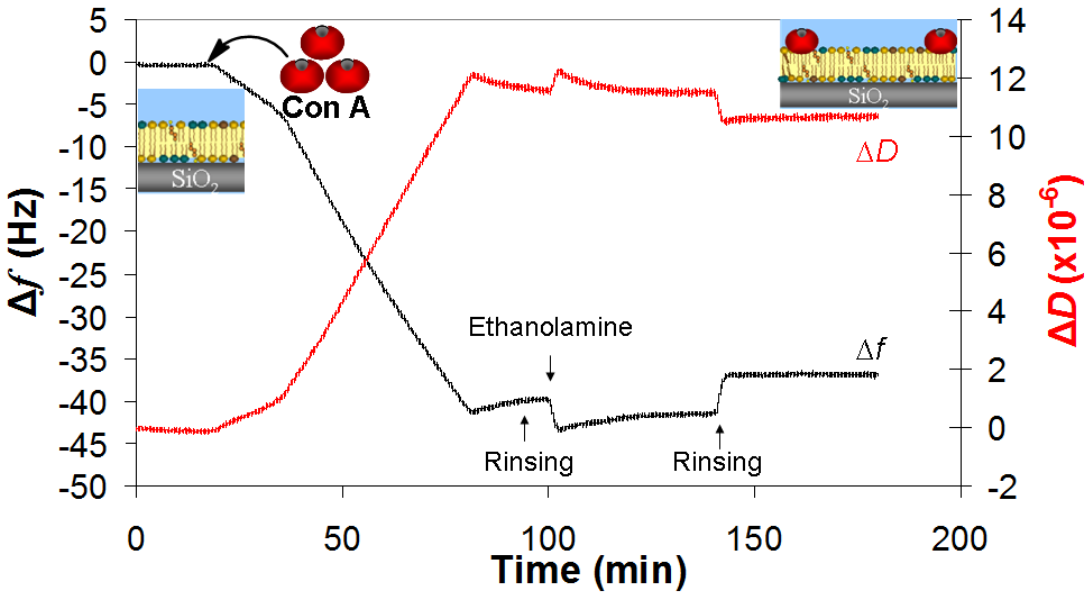

Figure 39 : Δf and ΔD (n=11) following Con A immobilization onto activated COOH-supported planar bilayer by EDC/NHS.

Interactions of porphyrin-bearing DMPC liposomes with the biomimetic Con A-conjugated supported bilayer

After formation onto the quartz surface of a planar biomimetic bilayer with similar lipidic composition to that of the retinoblastoma cell membrane [(42)], with Con A - mimicking the sugar receptor- covalently bound to the upper leaflet, we have injected under flow conditions DMPC, DMPC-compound **1c**, DMPC-compound **1** and DMPC-compound **2** liposomes into the measurement cell. Figure 40 shows the following evolution of Δf and ΔD as a function of time.

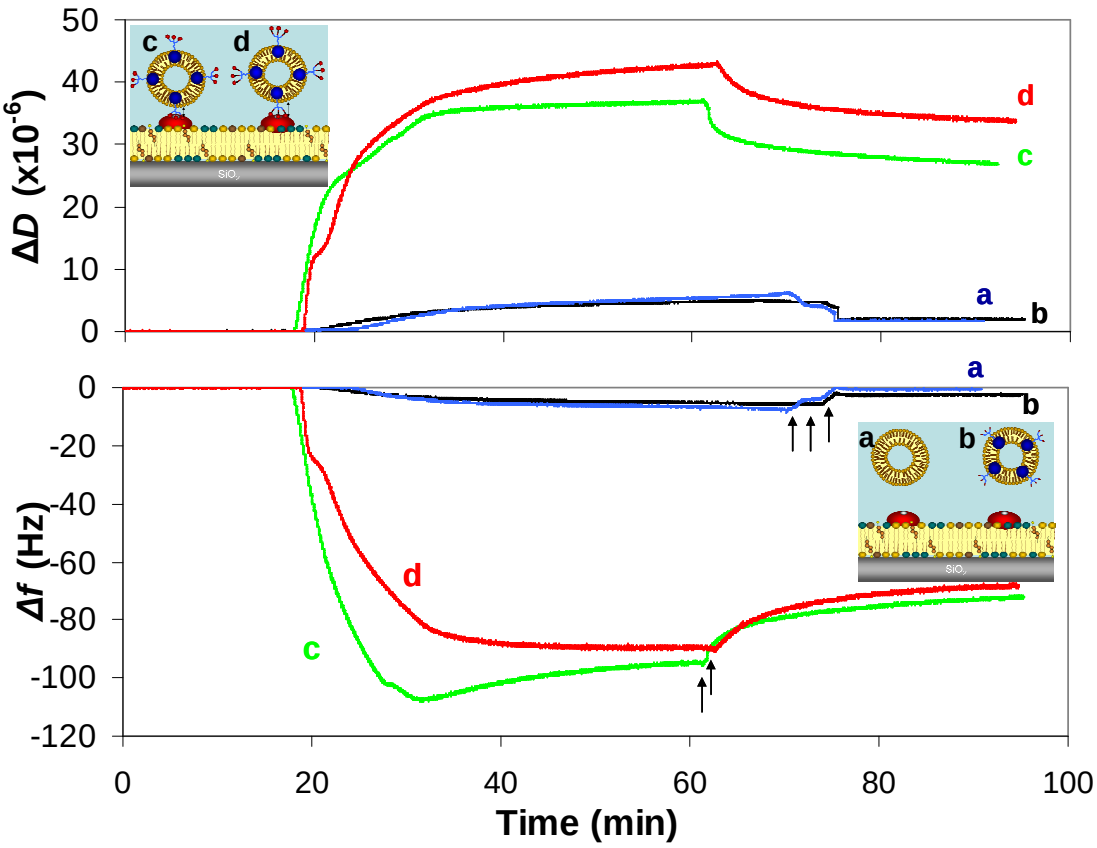

Figure 40 : Δf and ΔD (n=11) evolution following liposomes injection into the QCM-D cell containing immobilized Con A onto the supported planar bilayer. *a*: pure DMPC liposomes, *b*: DMPC-**compound 1c**, *c*: DMPC-**compound 1**, and *d*: DMPC-**compound 2**. Arrows indicate the times at which the electrodes were rinsed with HEPES buffer.

As shown in Figure 40, whatever the composition of the liposomes injected into the QCM-D measurement cell, variations in Δf and ΔD signals were always observed. In all cases, a quasi steady state was reached after 20 to 30 min. The immediate decrease in resonant frequency can be explained by the increased effective mass onto the QCM-D sensor, due to vesicles adsorption. A simultaneous increase in energy dissipation would indicate a more viscous

behaviour as more liposomes were adsorbed onto the bilayer. However, the amplitudes of the signals appeared highly dependent on the porphyrin derivative embedded into the DMPC liposomes bilayer. Upon injection, vesicles bearing mannosylated porphyrins induced the highest magnitudes of Δf and ΔD compared to pure DMPC and compound **1c**-liposomes. A difference in frequency shift between the mannosylated porphyrin-bearing vesicles was observed only in the first part of the curve, and could be related to a different distribution of grafted Con A onto the supported planar bilayer. At equilibrium, after buffer rinsing, the glycodendrimeric porphyrin-bearing vesicles led to the same Δf value (~ -72 Hz), but different ΔD ones, 27.8 and 33.7 $x10^{-6}$ for compound **1** and compound **2**, respectively. The maximal frequency shift value (-72 ± 3 Hz) was lower than that reported for the adsorption of a layer of intact liposomes, which usually ranges from -90 to -400 Hz, depending on liposome size and adhesion process [61, 67-69]. Conversely, it was much higher than that obtained for a supported planar bilayer (Δf ~ -26 Hz). Also, the ΔD values were very high, 27.8 and 33.7 $x10^{-6}$ for liposomes bearing compounds **1** and **2** respectively, compared to that for a planar bilayer (ΔD ~ $0.3x10^{-6}$). Moreover, the normalized change in frequency (Δf/n) and dissipation (ΔD) for the six overtones (n=3, 5, 7, 9, 11, 13) did not overlap (data not shown). This would indicate that the adsorbed liposomes formed a non-rigid incomplete layer of intact liposomes [70-71].
Conversely, for pure DMPC and compound **1c**-bearing liposomes, very small frequency and dissipation shifts were observed after their injection into the measurement cells (Δf = -5 Hz only, and ΔD = 5 to 6 $x10^{-6}$). Moreover, the following washing step with buffer induced complete removal of the liposomes from the bilayer surface, as inferred from the evolution of the Δf value towards zero. The non-null Δf and ΔD values measured after a single buffer rinsing could indicate the presence of residual liposomes or remains of them weakly bound to the bilayer.

To get a better insight into the mechanisms of interaction of the various populations of liposomes with the Con A-conjugated planar bilayer, we have plotted the variation of dissipation energy as a function of the frequency shift, which allowed us analyzing the relationship between changes in rigidity and added/lost mass for the various porphyrin-bearing liposome systems (Figure 41).

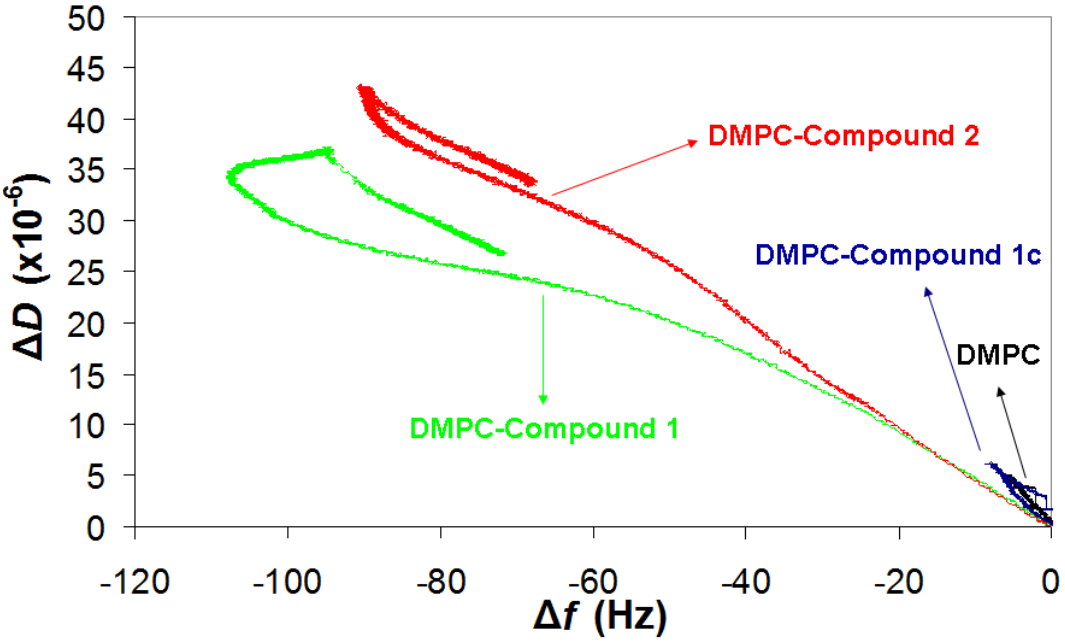

Figure 41 : Dissipation change versus frequency shift for DMPC and DMPC-porphyrin liposomes injected in the cell containing the immobilized Con A onto the planar phospholipid-cholesterol bilayer.

The comparison between the liposomes bearing the different porphyrins clearly showed that they did not interact in the same manner with the biomimetic planar bilayer. Indeed, DMPC and **compound 1c**-bearing liposomes, exhibited the highest dissipation at a same given frequency shift (-5 Hz) compared to liposomes bearing mannosylated porphyrins. Moreover, after buffer rinsing, Δf and ΔD values became null. These data indicate that the liposomes were simply adsorbed onto the Con A-bilayer surface. Therefore, they could move freely during quartz crystal oscillations. Conversely, **compounds 1** and **2**-bearing vesicles induced lower energy dissipation at the same frequency shift (-5 Hz). These liposomes were apparently strongly bound to the bilayer, and could not move as well as DMPC or **compound 1c**-bearing liposomes. Moreover, at a higher frequency shift (~ -72 Hz), liposomes bearing **compound 2** showed a much higher increase in dissipation compared to those bearing **compound 1.** Final parts of the curves show that most of the liposomes remained firmly bound to the bilayer despite the successive rinsing steps with buffer. This difference in behavior between liposomes bearing mannosylated porphyrins and non-mannosylated ones, indicates that vesicles bearing mannosylated porphyrins were able to interact significantly with Con A covalently bound to the phospholipid-cholesterol bilayer although Con A was grafted at a low density.

Considering the small difference in spacer length between compounds **1** and **2** (only one ethylene oxide) and the similar size of all studied liposomes (~ 146 nm), superimposition of

the curves in Figure 41 for the two compounds could be expected. However, this was not the case. The discrepancy in dissipation could originate from the greater mobility of mannose moieties provided by the longer spacers in compound **2**. DMPC-**2** liposomes would be less tightly bound to the bilayer surface and would form a more viscous layer than DMPC-**1** ones. The spacer length would therefore play a significant role in the binding process of compound **1**- and compound **2**-bearing liposomes with the biomimetic bilayer.

Interactions of porphyrin-bearing DMPC liposomes with the supported bilayer devoid of Con A

To analyze the predominance of the specific interaction over the non-specific one in the adsorption process of mannosylated porphyrin-bearing liposomes to the biomimetic bilayer, we have repeated the same experiment with a planar phospholipid-cholesterol bilayer lacking the Con A. As shown in Figure 42, only a small decrease in frequency (Δf ~ -5 ±1 Hz) and short increase in dissipation (ΔD ~ 5 x10^{-6}) occurred upon injection of liposomes bearing mannosylated porphyrins. Moreover, both Δf and ΔD returned to their initial values (Δf = 0 and ΔD ~ 0) after buffer rinsing. This clearly indicates that this time, liposomes were only weakly bound to the bilayer surface.

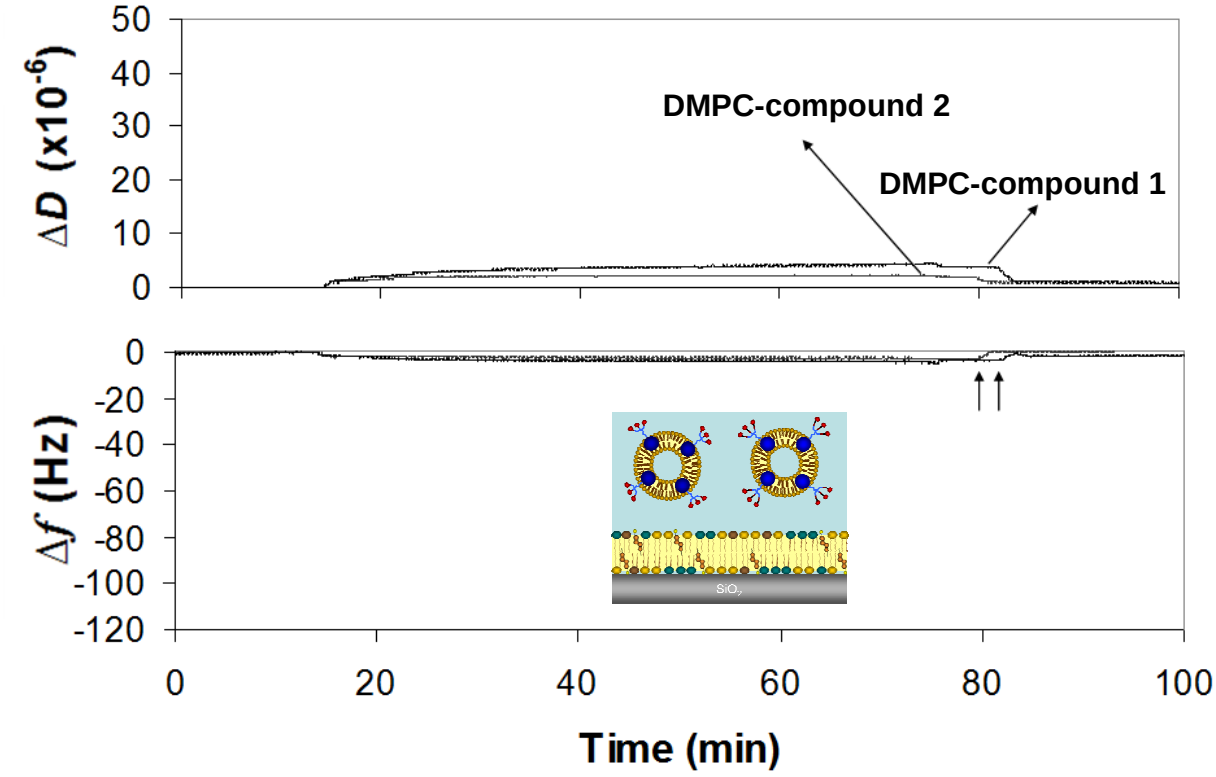

Figure 42 : Δ*f* (a) and Δ*D* (b) (n=11) following DMPC-**compound 1** and DMPC-**compound 2** liposomes injection into the QCM-D cell containing the phospholipid-cholesterol supported planar bilayer without Con A. Arrows indicate the times at which the sensors were rinsed with HEPES buffer.

Discussion

In this study, we have built and characterized, for the first time, a complex membrane model including three phospholipids, cholesterol, and a recognition protein, for assessing drug-membrane interactions. This membrane has been specifically built for studying the ability of glycodendrimeric porphyrins carried by DMPC liposomes to be recognized by a mannose specific receptor overexpressed at the surface of the retinoblastoma cells [(43)]. Prior to the analysis of the full system, we have studied the non-specific interactions of the porphyrins with the lipid bilayer without the lectin, but with increasing cholesterol content [(42)]. This first model showed that if the presence of cholesterol (10-30 mol%) strongly affected the viscoelastic properties of the lipid matrix, it did not particularly attract the porphyrin derivatives or hinder their penetration into the membrane. Since no difference in porphyrin penetration behaviour could be observed between lipid models with the different cholesterol contents, we chose to build our model with 10 mol% only. The reason for this choice was that the liposomes containing 30 mol% cholesterol had a very rigid membrane, and did not easily break and form a complete and homogeneous supported planar bilayer.

The study of the interaction of the glycodendrimeric porphyrins with the mono- and bilayer lipid models have shown another interesting trend: despite the absence of the recognition protein, the sugar moieties of glycoconjugated porphyrins were able to strongly interact with the mixed lipid monolayer, at the level of phospholipid headgroups. Thus, beside the expected hydrophobic interaction between the tetrapyrrolic macrocycle and phospholipid acyl chains, there was another non-specific interaction between the glycodendrimeric porphyrins and the lipids that had to be taken into account. In order to assess the purely specific interaction with the mannose-receptor, we have then used Concanavalin A, free in the aqueous medium or immobilized onto a SAM-functionalized QCM-D gold sensor [(43)]. We have demonstrated that the glycodendrimeric porphyrins incorporated into the bilayer of DMPC liposomes exposed their mannose moieties outwards and were able to interact specifically with the free or immobilized Concanavalin A. By comparing the behaviour of the three porphyrin derivatives in the presence of Con A and human serum albumin, we have observed that the binding of the glycodendrimeric porphyrins to Con A was mostly specific and did not merely result from hydrophobic interactions. Furthermore, we have shown that the spacer length played a crucial role in this interaction since compound **2** interacted more significantly with the lectin than compound **1**. However in this latter study, Con A was studied alone without the lipid matrix and was in large excess compared to *in vivo* conditions. This could lead to an overestimation of the strength of the specific interaction compared to the non-specific one. To achieve a more biomimetic model, we have in the present work grafted the lectin to the phospholipid-cholesterol matrix and studied the interaction of the whole model system with the various compounds. Compared to the *in vivo* system, it could have been more appropriate to incorporate the lectin into the lipid bilayer rather than graft it at the surface. Partial penetration of the protein in the membrane might be needed for optimal functionality [(72)]. However even after grafting, such a penetration could occur depending on the hydrophobic character of the lectin and the fluidity of the bilayer. Ramsden has shown that the fluidity of a lipid bilayer can allow protein post-binding rearrangement within the plane of the membrane [(72)]. We have studied the penetration of Con A into monolayers of SOPC/SOPE/SOPS/CHOL. The $\Delta\pi$-π_i relationship (with π_i, the initial pressure of the mixed monolayer) showed that the maximum insertion pressure was 27.0 mN/m (data not shown), lower than the pressure expected in membranes (30-35 mN/m) [(73)]. Penetration of Con A into the bilayer after grafting seems thus unlikely. The actual receptor is still unknown, and it is unclear if it is solely a recognition protein or a real transporter [(13)]. It appeared, therefore, both time-consuming and useless to try to incorporate Concanavalin A into the matrix, with a risk to lose its recognition

activity. Several trials have been made, however, to form mixed lipid-Con A monolayers with controlled surface density at the air-water interface that could be transferred on the SiO_2 quartz surface. They were unsuccessful, because Con A was partially solubilised into the subphase. Thus, we have developed one protocol to graft the lectin to liposomes and another to conjugate it to the supported bilayer. The purpose of using the two models was to study the interaction first in conditions where the system had a certain degree of freedom (both liposome systems being mobile in the medium), and then in conditions where the probability of interaction would be more limited (liposome-planar bilayer interaction). The liposome-liposome interaction producing multiple vesicle aggregation, the signal measured by DLS could be high, but was insufficient to get an insight into the kinetics of the interaction process or to monitor the changes in the organization of the system when the conditions were changed, as was allowed by QCM-D. The two systems were thus complementary.

In the liposome-liposome interaction experiment, liposomes bearing Con A as well as those bearing glycoconjugated porphyrins were in suspension in the bulk. The experiment allowed discrimination of the porphyrin derivatives depending on the presence or absence of sugar moieties. It confirmed that liposomes could be used as carriers for the studied compounds as previously suggested [(43)], because the glycodendrimeric porphyrins were embedded in the liposome bilayer with their glycodendrimeric arm exposed outward at the liposome surface, allowing recognition by the receptor.

These results could appear much less significant *in vivo*, where cells are not free in suspension. Using the QCM-D, we have shown that only mannosylated porphyrins borne by DMPC liposomes were strongly bound to the Con A-conjugated supported bilayer, although the Con A density on the bilayer surface was much lower than that in our previous study, where there was full coverage of the sensor surface [(43)]. In the present study, the Con A surface density could not exceed 35%. If the recognition process worked well for both mannosylated dendrimeric porphyrins, discrimination between compound **1** and compound **2** was more delicate, as also inferred from the DLS experiments. This could be due to the fact that the difference in the spacer length in the two porphyrins was only one ethylene oxide group, insignificant when the lectins were exposed at low density at the biomimetic membrane surface. There was enough space for mannose moieties to reach the lectin-binding site, without a long spacer. The situation was different when lectin molecules were grafted at high density and covered the entire sensor surface [(43)]. Con A molecules were closer to each other, and the longer spacer in compound **2** could allow cross-linking of lectin molecules at the surface, strengthening porphyrin attachment to them.

The specificity of the lectin-porphyrin interaction had a predominant effect in the overall interaction. The comparison of the results in Figures 40 and 42 shows that this specific interaction not only would drive the porphyrins toward their target, but also that it would allow porphyrin persistence at the cell surface, and could eventually favour its penetration into the membrane. A recent analysis by fluorescence measurements [(74)] has shown that compared to other series of tetraphenylporphyrin derivatives, dendrimeric compounds were able to penetrate deeper into a liposome bilayer. However within the dendrimeric porphyrin series, despite the stronger non-specific interaction with a monolayer of the glycoconjugated porphyrins compared to the non-glycoconjugated one, fluorescence quenching did not show any significant difference in penetration depth between the three compounds **1c**, **1** and **2** when Con A was absent [(42)]. Conversely, with respect to the specific interaction, both compounds **1** and **2** proved to be interesting molecules.

Conclusion

The glycodendrimeric porphyrins borne by DMPC liposomes proved to interact specifically with Con A grafted on a retinoblastoma biomimetic membrane model. No effect of the spacer length on the interaction has been observed between compound **1** and compound **2** for the two studied systems (liposomes and supported planar bilayer). The specific interaction appeared to be crucial to the overall interaction with the biomimetic membrane since only liposomes bearing mannosylated porphyrins were able to bind to the membrane model surface. Their evaluation on the retinoblastoma Y79 cell line is currently in progress to confirm their activity as well as the relevance of our biomimetic membrane model. Added to our previous results, which showed that the sugar moieties of the glycoconjugated dendrimeric porphyrins favoured their non-specific interaction with phospholipids-cholesterol model membranes compared to compound **1c** as well as their specific interaction with Con A (free or immobilized on SAM surface), the glycocodendrimeric porphyrins appear as very promising drugs.

Acknowledgments

The authors acknowledge the financial support of A. Makky's PhD by ARC (Association pour la Recherche contre le Cancer). The authors also wish to thank Professor Udo Bakowsky (Department of Pharmaceutical Technology and Biopharmacy, Philipps-Universität, Marburg, Germany) for helpful discussions and advices on the Con A coupling methods.

References

1. Dolmans, D. E., Fukumura, D., and Jain, R. K. (2003) Photodynamic therapy for cancer, *Nat Rev Cancer 3*, 380-387.
2. Stephan, H., R. Boeloeni, A. Eggert, N. Bornfeld , A. Schueler. (2008) Photodynamic Therapy in Retinoblastoma: Effects of Verteporfin on Retinoblastoma Cell Lines, *Invest. Ophthalmol. Vis. Sci. 49*, 3158-3163.
3. Lupu, M., C.D. Thomas , Ph. Maillard, B. Loock , B. Chauvin , I. Aerts, A. Croisy , E. Belloir , A.Volk , J. Mispelter. (2009) 23Na MRI longitudinal follow-up of PDT in a xenograft model of human retinoblastoma, *Photodiag. Photody. Ther. 6*, 214-220.
4. Maillard, P., M. Lupu, C. D. Thomas, J. Mispelter (2010) Vers un nouveau traitement du rétinoblastome ?, *Ann. Pharm. Fr. 68*, 195-202.
5. Aerts, I., P. Leuraud, J. Blais, A.-L. Pouliquen , Ph. Maillard, C. Houdayer, J. Couturier, X. Sastre-Garau, F. Doz, M.-F. Poupon (2010) In vivo efficacy of photodynamic therapy in three new xenograft models of human retinoblastoma., *Photodiag. Photody. Ther. in press*.
6. van Hillegersberg, R., W. J. Kort, J. H. Wilson. (1994) Current status of photodynamic therapy in oncology, *Drugs 48*, 510-527.
7. Dougherty, T. J., Gomer, C. J., Henderson, B. W., Jori, G., Kessel, D., Korbelik, M., Moan, J., and Peng, Q. (1998) Photodynamic therapy, *J Natl Cancer Inst 90*, 889-905.
8. Bonnett, R. (1995) Photosensitizers of the porphyrin and phthalocyanine series for photodynamic therapy, *Chem. Soc. Rev. 24*, 19-33.
9. Pasternack, R. F., Huber, P. R., Boyd, P., Engasser, G., Francesconi, L., Gibbs, E., Fasella, P., Cerio Venturo, G., and Hinds, L. d. (1972) Aggregation of meso-substituted water-soluble porphyrins, *JACS 94*, 4511-4517.
10. Csík, G., Balog, E., Voszka, I., Tölgyesi, F., Oulmi, D., Maillard, P., and Momenteau, M. (1998) Glycosylated derivatives of tetraphenyl porphyrin: photophysical characterization, self-aggregation and membrane binding, *J. Photochem. Photobiol. B: Biology 44*, 216-224.
11. Oulmi, D., Maillard, P., Vever-Bizet, C., Momenteau, M., and Brault, D. (1998) Glycosylated Porphyrins: Characterization of Association in Aqueous Solutions by Absorption and Fluorescence Spectroscopies and Determination of Singlet Oxygen Yield in Organic Media, *Photochem. Photobiol. 67*, 511-518.
12. Momenteau, M., P. Maillard, M. A. De Belinay, D. Carrez, A. Croisy. (1999) Tetrapyrrolic glycosylated macrocycles for an application in PDT, *J. Biomed. Opt. 4*, 298-318.
13. Laville, I., T. Figueiredo, B. Loock, S. Pigaglio, Ph. Maillard, D.S. Grierson, D. Carrez, A. Croisy, J. Blais. (2003) Synthesis, cellular internalization and photodynamic activity of glucoconjugated derivatives of tri and tetra(meta-hydroxyphenyl)chlorins, *Bioorg. & Med. Chem. 11*, 1643-1652.
14. Laville, I., S.Pigaglio, J. C. Blais, B. Loock, Ph. Maillard, D.S. Grierson, J. Blais (2004) A study of the stability of tri(glucosyloxyphenyl)chlorin, a sensitizer for photodynamic therapy, in human colon tumoural cells: a liquid chromatography and MALDI-TOF mass spectrometry analysis, *Bioorg. & Med. Chem. 12*, 3673-3682.
15. Laville, I., S. Pigaglio, J. C. Blais, F. Doz, B. Loock, Ph. Maillard, D.S. Grierson, J. Blais. (2006) Photodynamic Efficiency of Diethylene Glycol-Linked Glycoconjugated Porphyrins in Human Retinoblastoma Cells, *J. Med. Chem. 49*, 2558-2567.
16. Maillard, P., B.Loock, D. S. Grierson, I. Laville, J. Blais, F. Doz, L. Desjardins, D. Carrez , J. L. Guerquin-Kern, A. Croisy. (2007) In vitro phototoxicity of glycoconjugated porphyrins and chlorins in colorectal adenocarcinoma (HT29) and retinoblastoma (Y79) cell lines, *Photodiag. Photody. Ther. 4*, 261-268.
17. Chen, X., and Drain, C. M. (2004) Photodynamic Therapy using Carbohydrate Conjugated Porphyrins, *Drug Des. Rev. - Online 1*, 215-234.
18. Cavaleiro, J., Tomé, J., and Faustino, M. (2007) Synthesis of Glycoporphyrins, In *Heterocycles from Carbohydrate Precursors* (El Ashry, E., Ed.), pp 179-248, Springer Berlin / Heidelberg.
19. Zheng, X., and Pandey, R. K. (2008) Porphyrin-carbohydrate conjugates: impact of carbohydrate moieties in photodynamic therapy (PDT), *Anti canc Agents Med Chem 8*, 241-268.
20. Monsigny, M., Roche, A. C., and Midoux, P. (1988) Endogenous lectins and drug targeting, *Ann N Y Acad Sci 551*, 399-413; discussion 413-394.
21. Lotan, R., and Raz, A. (1988) Lectins in cancer cells, *Ann N Y Acad Sci 551*, 385-398.
22. Ballut, S., A. Makky, B. Loock, J. P. Michel, P. Maillard, V. Rosilio. (2009) New strategy for targeting of photosensitizers. Synthesis of glycodendrimeric phenylporphyrins, incorporation into a liposome membrane and interaction with a specific lectin, *Chem Commun* 224-226.

23. Griegel, S., M. F. Rajewsky, T. Ciesiolka, H. J. Gabius. (1989) Endogenous sugar receptor (lectin) profiles of human retinoblastoma and retinoblast cell lines analyzed by cytological markers, affinity chromatography and neoglycoprotein-targeted photolysis, *Anticancer Res 9*, 723-730.
24. Ballut, S., Loock, B., and Maillard, P. (2010) *Submitted*.
25. Spikes, J., and Jori, G. (1987) Photodynamic therapy of tumours and other diseases using porphyrins, *LASER MED. SCI. 2*, 3-15.
26. Desroches, M. C., A. Kasselouri, M. Meyniel, P. Fontaine, M. Goldmann, P. Prognon, P. Maillard , V. Rosilio. (2004) Incorporation of Glycoconjugated Porphyrin Derivatives into Phospholipid Monolayers: A Screening Method for the Evaluation of Their Interaction with a Cell Membrane, *Langmuir 20*, 11698-11705.
27. Hidalgo, A. A., Tabak, M., and Oliveira Jr, O. N. (2005) The interaction of meso-tetraphenylporphyrin with phospholipid monolayers, *Chem. and Phys. of Lipids 134*, 97-108.
28. Ricchelli, F., and Jori, G. (1986) Distribution of porphyrins in the various compartments of unilamellar liposomes of dipalmitoyl-phosphatidylcholine as probed by fluorescence spectroscopy, *Photochem Photobiol 44*, 151-157.
29. Hoebeke, M. (1995) The importance of liposomes as models and tools in the understanding of photosensitization mechanisms, *J. Photochem. Photobiol. B. Biol. 28*, 189-196.
30. Ricchelli, F. (1995) Photophysical properties of porphyrins in biological membranes, *J. Photochem. Photobiol. B: Biology 29*, 109-118.
31. Ricchelli, F., S. Gobbo, G. Moreno, C. Salet, L. Brancaleon, A. Mazzini. (1998) Photophysical properties of porphyrin planar aggregates in liposomes, *Eur. J. Biochem. 253*, 760-765.
32. Brault, D. (1990) Physical chemistry of porphyrins and their interactions with membranes: The importance of pH, *J. Photochem. Photobiol. B: Biology 6*, 79-86.
33. Kuzelova, K., and Brault, D. (1995) Interactions of dicarboxylic porphyrins with unilamellar lipidic vesicles: drastic effects of pH and cholesterol on kinetics, *Biochemistry 34*, 11245-11255.
34. Maman, N., and Brault, D. (1998) Kinetics of the interactions of a dicarboxylic porphyrin with unilamellar lipidic vesicles: Interplay between bilayer thickness and pH in rate control, *Biochim. Biophys. Acta (BBA) - Biomembranes 1414*, 31-42.
35. Ehrenberg, B., and Gross, E. (1988) The effect of liposomes membrane composition on the binding of the photosensitizers HPD and PHOTOFRIN II, *Photochem. Photobiol. 48*, 461-466.
36. Gross, E., and Ehrenberg, B. (1989) The partition and distribution of porphyrins in liposomal membranes. A spectroscopic study, *Bioch. Biophys. Acta (BBA) - Biomembranes 983*, 118-122.
37. Lavi, A., Weitman, H., Holmes, R. T., Smith, K. M., and Ehrenberg, B. (2002) The depth of porphyrin in a membrane and the membrane's physical properties affect the photosensitizing efficiency, *Biophys. J. 82*, 2101-2110.
38. Fliesler, A. J., and Anderson, R. E. (1983) Chemistry and metabolism of lipids in the vertebrate retina, *Prog. Lipid Res. 22*, 79-131.
39. Huster, D., Arnold, K., and Gawrisch, K. (1998) Influence of Docosahexaenoic Acid and Cholesterol on Lateral Lipid Organization in Phospholipid Mixtures, *Biochemistry 37*, 17299-17308.
40. Huster, D., Arnold, K., and Gawrisch, K. (2000) Strength of Ca2+ Binding to Retinal Lipid Membranes: Consequences for Lipid Organization, *Biophys. J. 78*, 3011-3018.
41. Yorek, M. A., P. H. Figard, T. L. Kaduce, A. A. Spector. (1985) A comparison of lipid metabolism in two human retinoblastoma cell lines, *Invest. Ophthalmol. Vis. Sci. 26*, 1148-1154.
42. Makky, A., J. P. Michel, S. Ballut, A. Kasselouri, Ph. Maillard, V. Rosilio. (2010) Effect of Cholesterol and Sugar on the Penetration of Glycodendrimeric Phenylporphyrins into Biomimetic Models of Retinoblastoma Cells Membranes, *Langmuir 26*, 11145-11156.
43. Makky, A., J. P. Michel, A. Kasselouri, E. Briand, Ph. Maillard, V. Rosilio. (2010) Evaluation of the Specific Interactions between Glycodendrimeric Porphyrins, Free or Incorporated into Liposomes, and Concanavaline A by Fluorescence Spectroscopy, Surface Pressure, and QCM-D Measurements, *Langmuir 26*, 12761-12768.
44. Mordon, S., Devoisselle, J. M., and Soulié, S. (1995) Fluorescence spectroscopy of pH in vivo using a dual-emission fluorophore (C-SNAFL-1), *J. Photochem. Photobiol. B: Biology 28*, 19-23.
45. Bangham, A. D., Standish, M. M., and Watkins, J. C. (1965) Diffusion of univalent ions across the lamellae of swollen phospholipids, *J. Molec. Biol. 13*, 238-252, IN226-IN227.
46. Faivre, V., V. Rosilio, P. Boullanger, L. Martins Almeida, A. Baszkin. (2001) Fucosyled neoglycolipids: synthesis and interaction with a phospholipid, *Chem. Phys. Lipids 109*, 91-101.
47. Faivre, V., M.L. Costa, P. Boullanger, A. Baszkin, V. Rosilio. (2003) Specific interaction of lectins with liposomes and monolayers bearing neoglycolipids, *Chem. Phys. Lipids 125*, 147-159.
48. Sanders, J. N., Chenoweth, S. A., and Schwarz, F. P. (1998) Effect of metal ion substitutions in concanavalin A on the binding of carbohydrates and on thermal stability, *J. Inorg. Bioch. 70*, 71-82.

49. Nakano, Y., M. Mori, S. Nishinohara, Y. Takita, S. Naito, H. Kato, M. Taneichi, K. Komuro, T. Uchida (2001) Surface-Linked Liposomal Antigen Induces IgE-Selective Unresponsiveness Regardless of the Lipid Components of Liposomes, *Bioconj. Chem. 12*, 391-395.
50. Liu, G., and Lin, Y. (2007) Nanomaterial labels in electrochemical immunosensors and immunoassays, *Talanta 74*, 308-317.
51. Chen, H., Torchilin, V., and Langer, R. (1996) Lectin-bearing polymerized liposomes as potential oral vaccine carriers, *Pharm. Res. 13*, 1378-1383.
52. Becker, J. W., G. N. Jr. Reeke, J. L. Wang, B. A. Cunningham, G. M. Edelman. (1975) The covalent and three-dimensional structure of concanavalin A. III. Structure of the monomer and its interactions with metals and saccharides, *J. Biol. Chem. 250*, 1513-1524.
53. H. M. L. R. Santos, F. B. de Queiroz, R. M. S. Maior, S. C. do Nascimento, and Magalhães, N. S. S. (2006) Cytotoxicity of doxorubicin-loaded Con A-liposomes, *Drug Dev. Res. 67*, 430-437.
54. Bogdanov jr, A. A., Klibanov, A. L., and Torchilin, V. P. (1988) Protein immobilization on the surface of liposomes via carbodiimide activation in the presence of N-hydroxysulfosuccinimide, *Febs Lett. 231*, 381-384.
55. Leonenko, Z. V., Carnini, A., and Cramb, D. T. (2000) Supported planar bilayer formation by vesicle fusion: the interaction of phospholipid vesicles with surfaces and the effect of gramicidin on bilayer properties using atomic force microscopy, *Biochim. Biophys. Acta 1509*, 131-147.
56. Kalb, E., J. Engel, L. K. Tamm. (1990) Binding of proteins to specific target sites in membranes measured by total internal reflection fluorescence microscopy, *Biochemistry 29*, 1607-1613.
57. Grandbois, M., Clausen-Schaumann, H., and Gaub, H. (1998) Atomic force microscope imaging of phospholipid bilayer degradation by phospholipase A2, *Biophys J 74*, 2398-2404.
58. Ross, M., C. Steinem, H.J. Galla, A. Janshoff. (2001) Visualization of Chemical and Physical Properties of Calcium-Induced Domains in DPPC/DPPS Langmuir−Blodgett Layers, *Langmuir 17*, 2437-2445.
59. Keller, C. A., and Kasemo, B. (1998) Surface Specific Kinetics of Lipid Vesicle Adsorption Measured with a Quartz Crystal Microbalance, *Biophys. J. 75*, 1397-1402.
60. Steinem, C., A. Janshoff, W. P. Ulrich, M. Sieber, H. J. Galla. (1996) Impedance analysis of supported lipid bilayer membranes: A scrutiny of different preparation techniques, *Biochim. Biophys. Acta-Biomembranes 1279*, 169-180.
61. Reimhult, E., Höök, F., and Kasemo, B. (2002) Intact Vesicle Adsorption and Supported Biomembrane Formation from Vesicles in Solution: Influence of Surface Chemistry, Vesicle Size, Temperature, and Osmotic Pressure†, *Langmuir 19*, 1681-1691.
62. Reimhult, E., Höök, F., and Kasemo, B. (2002) Vesicle adsorption on SiO2 and TiO2: Dependence on vesicle size, *J. Chem. Phys. 117*, 7401 -7405.
63. Starr, T. E., and Thompson, N. L. (2000) Formation and Characterization of Planar Phospholipid Bilayers Supported on TiO2 and SrTiO3 Single Crystals, *Langmuir 16*, 10301-10308.
64. Richter, R., A. Mukhopadhyay, A. Brisson. (2003) Pathways of Lipid Vesicle Deposition on Solid Surfaces: A Combined QCM-D and AFM Study, *Biophys. J. 85*, 3035-3047.
65. Seantier, B., C. Breffa, O. Felix, G. Decher. (2005) Dissipation-Enhanced Quartz Crystal Microbalance Studies on the Experimental Parameters Controlling the Formation of Supported Lipid Bilayers, *J. Phys. Chem.B 109*, 21755-21765.
66. Richter, R. P., R. Bérat, Alain R. Brisson. (2006) Formation of Solid-Supported Lipid Bilayers: An Integrated View, *Langmuir 22*, 3497-3505.
67. Reimhult, E., M. Zach, F. Hook, B. Kasemo. (2006) A multitechnique study of liposome adsorption on Au and lipid bilayer formation on SiO2, *Langmuir 22*, 3313-3319.
68. Patel, A. R., and Frank, C. W. (2006) Quantitative Analysis of Tethered Vesicle Assemblies by Quartz Crystal Microbalance with Dissipation Monitoring: Binding Dynamics and Bound Water Content, *Langmuir 22*, 7587-7599.
69. Brochu, H., and Vermette, P. (2007) Liposome Layers Characterized by Quartz Crystal Microbalance Measurements and Multirelease Delivery, *Langmuir 23*, 7679-7686.
70. Hook, F., B. Kasemo, T. Nylander, C. Fant, K. Sott, H. Elwing. (2001) Variations in Coupled Water, Viscoelastic Properties, and Film Thickness of a Mefp-1 Protein Film during Adsorption and Cross-Linking: A Quartz Crystal Microbalance with Dissipation Monitoring, Ellipsometry, and Surface Plasmon Resonance Study, *Anal. Chem. 73*, 5796-5804.
71. Dutta, A. K., A. Nayak, G. Belfort. (2008) Viscoelastic properties of adsorbed and cross-linked polypeptide and protein layers at a solid-liquid interface, *J. Colloid and Interf. Sci. 324*, 55-60.
72. Ramsden, J. J. (1998) Biomimetic protein immobilization using lipid bilayers, *Biosens. Bioelectron. 13*, 593-598.
73. Calvez, P., S. Bussieres, E. Demers, C. Salesse. (2009) Parameters modulating the maximum insertion pressure of proteins and peptides in lipid monolayers, *Biochimie 91*, 718-733.

74. Ibrahim, H., A. Kasselouri, C. You, Ph. Maillard, V. Rosilio, R. Pansu, P. Prognon. (2010) Glycoconjugated porphyrins usable in photodynamic therapy: self-aggregation, association with albumin, and localisation in DMPC liposomes as a simplified cell membrane model, *J. Photochem. Photobiol. A: Chemistry, in press*.

Discussion générale

Discussion générale

Une photothérapie dynamique efficace repose sur l'accumulation préférentielle d'un photosensibilisateur au niveau des tissus tumoraux. Cette accumulation préférentielle est souvent observée, mais demeure insuffisante pour limiter la photosensibilisation souvent déplorée lors de l'application de cette thérapie, et qui reste un effet secondaire redouté des médecins et patients. Certains chercheurs ont suggéré que l'altération de la composition lipidique des membranes cellulaires tumorales, en particulier le changement du taux de cholestérol, pourrait favoriser la diffusion passive des photosensibilisateurs (PS). D'autres ont relié l'accumulation sélective de ceux-ci à l'affinité élevée des PS hydrophobes pour les particules de LDL qui sont, par la suite, reconnues par les récepteurs Apo B/E surexprimés à la surface des cellules tumorales. [1-2] D'autres observations *in vitro* ont montré que les PS glycoconjugués pouvaient interagir de manière spécifique avec des récepteurs de type lectinique surexprimés à la surface de certains types de tumeurs, comme le rétinoblastome. L'équipe du Dr Philippe Maillard, qui synthétise des dérivés actifs pour le traitement de cette tumeur oculaire, a proposé une stratégie de recherche apparemment simple, destinée à augmenter la solubilité et l'amphiphilie des porphyrines afin d'améliorer leur diffusion passive, d'une part, et leur sélectivité, d'autre part. Il suffit d'ajouter des sucres à la structure des porphyrines pour leur permettre de satisfaire aux trois critères : les sucres rendent la molécule plus hydrophile donc plus soluble, contrebalancent l'hydrophobie du macrocycle tetrapyrrolique (en augmentant l'amphiphilie globale) et permettent de cibler des lectines endogènes portées par les cellules cancéreuses (spécificité). En théorie, cette approche est très prometteuse. Les premiers essais de greffage des sucres directement au niveau des phenyle ont permis de vérifier que ces molécules peuvent effectivement être intéressantes pour le ciblage. [1-2] Mais elles restent trop faiblement solubles et insuffisamment amphiphiles ce qui pourrait limiter leur pénétration passive. Les résultats ont cependant permis de mettre en évidence l'intérêt de molécules asymétriques portant trois sucres. [1-3] En outre, l'ajout d'un espaceur diethylène glycol entre les sucres et le phenyle a permis d'augmenter notablement l'efficacité *in vitro* de ces dérivés sur culture cellulaire. Lorsque nous avons commencé notre étude, la **TPP-(*p*-*O*-Deg-*O*-α-Man)$_3$** était le composé le plus intéressant de la série. Afin de renforcer l'amphiphilie et de créer un *cluster* de sucres souvent nécessaire à la reconnaissance moléculaire, les porphyrines glycodendrimériques ont été synthétisées (Figure 43).

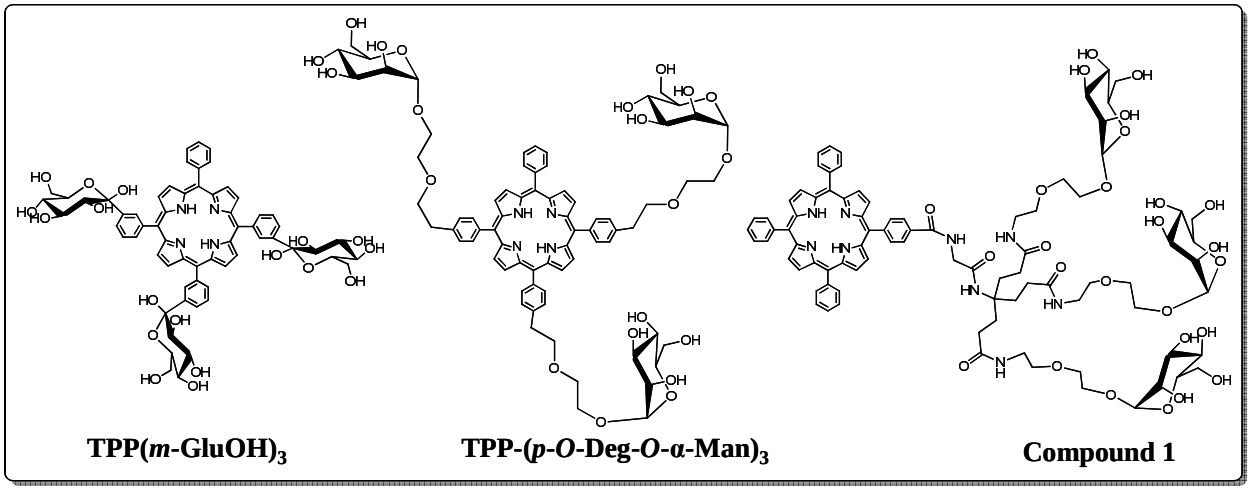

Figure 43: Structures chimiques de TPPGlu3, TPP-(*p*-*O*-Deg-*O*-α-Man)$_3$ et le dérivé glycodendrimérique 1

Avec une structure dendrimérique, séparant nettement les sucres du noyau porphyrine, l'amphiphilie de la molécule doit permettre une bonne orientation vis-à-vis de la membrane, le macrocycle hydrophobe favoriserait le mélange avec les lipides membranaires et le *cluster* de sucres permettrait une meilleure reconnaissance par la lectine de surface.

Comme le montrent les études du comportement interfacial des dérivés dendrimériques **1c**, **0, 1** et **2** présentés dans le premier chapitre de la partie expérimentale (articles 2 et 3) et dans la Figure 44, l'ajout des sucres et l'augmentation de la longueur de l'espaceur contribuent bien au renforcement de l'amphiphilie des molécules. La porphyrine non mannosylée forme la monocouche la plus condensée avec la pression de collapse la plus élevée. La structure dendrimérique rend la molécule plus hydrophobe. Ce sont les sucres qui font diminuer la pression de surface et qui contribuent à l'augmentation de l'aire occupée par les molécules à l'interface, même s'ils sont immergés dans la sous-phase. L'espaceur amplifie cet effet.

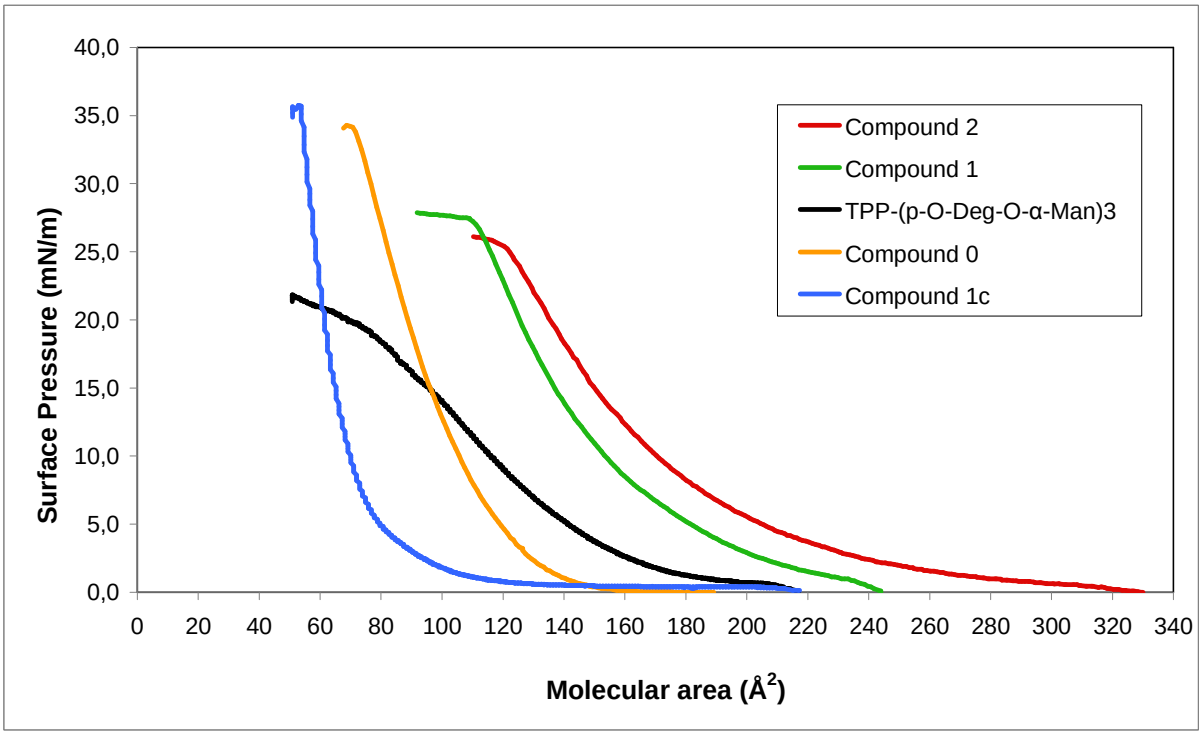

Figure 44 : Isothermes des porphyrines déposées à la surface du tampon HEPES pH 6,5 (10mM HEPES, 150 mM NaCl, 1 mM $CaCl_2$,$2H_2O$, et 1mM $NiCl_2$,$6H_2O$).

Lorsqu'on compare le comportement interfacial des porphyrines dendrimériques à celui de **TPP-(*p*-*O*-Deg-*O*-α-Man)$_3$** (Figure 44) et de **TPP-(*m*-GluOH)$_3$** [3], on constate que la structure dendrimérique a bien une influence très significative sur l'organisation des molécules à l'interface. Elle conduit, dans tous les cas, à des pressions de surface beaucoup plus élevées, quelle que soit la longueur de l'espaceur. Le comportement de **TPP-(*p*-*O*-Deg-*O*-α-Man)$_3$**, en revanche, ressemble davantage à celui de **TPP-(*m*-GluOH)$_3$** (au moins jusqu'à 80Å^2). L'aire d'onset de pression et la pression de surface à 80Å^2, sont cependant plus élevées que pour **TPP-(*m*-GluOH)$_3$**, ce qui pourrait résulter de la présence des espaceurs DEG portant chaque sucre. Les isothermes de la Figure 44 montrent également que les porphyrines glycodendrimériques **1** et **2** occupent des aires plus grandes que **TPP-(*p*-*O*-Deg-*O*-α-Man)$_3$**.

Si l'amphiphilie augmentée des porphyrines dendrimériques est bien attestée par leur meilleure organisation à l'interface par rapport aux autres molécules étudiées, leur solubilité n'est guère améliorée. Cela pose un réel problème pour l'évaluation de ces molécules, notamment en ce qui concerne leur capacité à interagir avec les membranes. Nous avons donc envisagé d'incorporer ces porphyrines dans la membrane de liposomes : elles seraient ainsi « solubilisées » et leurs sucres seraient exposés à la surface des vésicules, permettant l'interaction avec la lectine. Nous avons évalué la capacité des porphyrines à se mélanger à

concentration élevée (fraction molaire de porphyrine, X_P = 0.5) à de la dimyristoylphosphatidylcholine, un phospholipide qui forme facilement des liposomes. Nous avons observé que le dérivé dont l'espaceur est le plus court (**dérivé 0**) se mélange moins bien avec le phospholipide. Une forte expansion de la monocouche mixte a été observée par rapport aux composants purs (Figure 45).

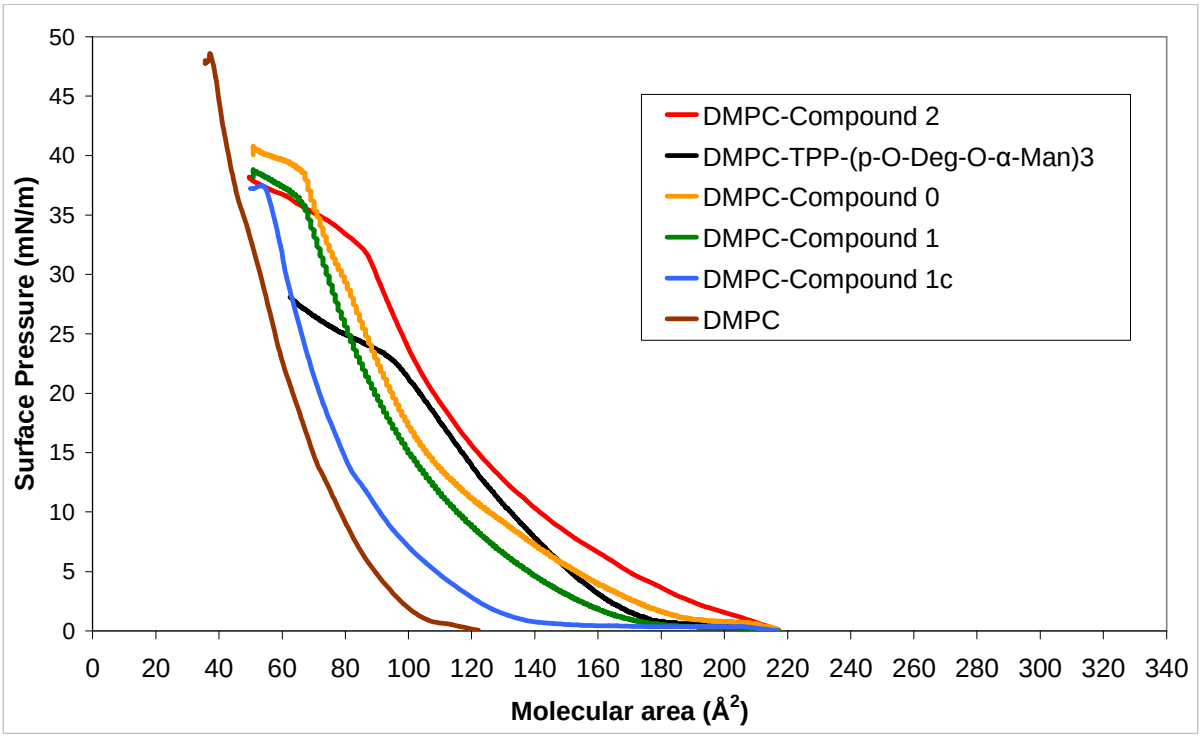

Figure 45 : Isothermes des mélanges de DMPC-porphyrines (ratio molaire 1-1) déposés à la surface du tampon HEPES pH 6,5 (10mM HEPES, 150 mM NaCl, 1 mM $CaCl_2$,$2H_2O$, et 1mM $NiCl_2$,$6H_2O$).

Lors de l'étude d'interaction des liposomes de DMPC-**dérivé 0** avec la Con A (article 2), nous n'avons pas observé d'agrégation significative et reproductible des vésicules. Il n'est pas clair si ce phénomène est dû à la longueur trop faible de l'espaceur (qui ne permet pas une bonne accessibilité de la lectine aux sucres) ou si elle résulte d'un défaut d'incorporation du **dérivé 0** dans la membrane du liposome, en raison de sa mauvaise miscibilité avec la DMPC. Cette mauvaise miscibilité a été montrée par les isothermes de compression des monocouches des composants purs et du mélange. Dans des essais complémentaires non présentés précédemment, nous avons également observé une expansion de la monocouche mixte DMPC-**TPP-(*p*-*O*-Deg-*O*-α-Man)$_3$** par rapport aux composants purs. Or, il n'a pas été non plus possible d'incorporer ce dérivé dans nos liposomes, probablement en raison de la forte interaction des sucres avec les têtes polaires de la DMPC. Cette interaction pourrait rigidifier la structure de la membrane par formation de liaisons hydrogènes et empêcherait la formation de vésicules mixtes. En effet, les sucres, mêmes portés par des espaceurs DEG sont très

mobiles et localisés très proches de la région polaire des domaines phospholipidiques. De plus, comme ils sont portés par les phényles, ils pourraient affecter plusieurs domaines phospholipidiques simultanément. De manière intéressante, nous avons également observé une expansion de la monocouche mixte DMPC-**dérivé 1c** par rapport aux composants purs. Pourtant, nous n'avons rencontré aucune difficulté à former des liposomes avec cette porphyrine. Si les deux phénomènes sont liés, cela mettrait en exergue le rôle des sucres dans la déstabilisation des liposomes. Là où avec le **dérivé 1c** la gêne serait essentiellement stérique, avec les porphyrines glycoconjuguées, la formation de liaisons hydrogènes serait un élément très déstabilisateur.

En raison de la difficulté à incorporer **TPP-(*p*-*O*-Deg-*O*-α-Man)$_3$** dans nos liposomes de DMPC et à obtenir des résultats d'interaction reproductibles avec le **dérivé 0**, nous les avons laissés de côté pour la suite de l'étude d'interaction avec les modèles membranaires. L'incorporation des porphyrines dans les liposomes n'avait pas seulement un objectif de solubilisation (bien que celui-ci soit majeur) ; Nous nous sommes rendus compte très vite que la microbalance à cristal de quartz que nous voulions utiliser pour former nos bicouches planes et étudier l'interaction avec les porphyrines n'était pas suffisamment sensible pour « voir » les porphyrines libres. Leur incorporation dans des liposomes permettait l'amplification du signal.

Après cette étude préliminaire de caractérisation des porphyrines et d'incorporation dans des liposomes, nous nous sommes intéressés, d'une part, à l'étude de l'effet de la composition lipidique de la membrane cellulaire (essentiellement l'augmentation du taux du cholestérol) sur la diffusion passive des porphyrines glycoconjuguées et, d'autre part, à la capacité des porphyrines glycoconjuguées à interagir spécifiquement avec des modèles membranaires exprimant une lectine spécifique du mannose à leur surface.

La proportion de cholestérol dans les membranes rétiniennes humaines adultes saines serait de 10% (en mole). [4-5] Chez des enfants, mêmes sains, cette proportion devrait être augmentée, en raison de leur croissance (communication personnelle d'Isabelle Aertz, pédiatre à l'institut Curie, impliquée dans le traitement du rétinoblastome par PDT). En l'absence d'information publiée à ce sujet dans la littérature, nous avons étudié l'effet du cholestérol sur l'organisation des monocouches et nous ne sommes pas allés au-delà de 30%.

Si nous avons observé un net effet condensant du cholestérol à 10 mol% (modèle M1) par rapport aux monocouches de SOPC/SOPE/SOPS sans cholestérol (modèle M0), nous n'avons pas observé de différence significative à 20 et 30%. C'est la présence de cholestérol, plus que

sa proportion qui semblait affecter l'état de nos monocouches de phospholipides. Mais, ce n'était pas vrai pour tout. En effet, la proportion de 20 mol% (modèle M2) a montré des résultats différents de ceux de M3, en spectroscopie de fluorescence lors de l'étude de l'association des porphyrines aux liposomes (Table 5), en analyse calorimétrique différentielle (Figure 15), dans la morphologie des monocouches observées au microscope à l'angle de Brewster. Nous n'avons pas pu expliquer ces observations. Il serait intéressant d'y consacrer une étude plus approfondie dans la suite de ce travail.

Nous n'avons pas observé de différence significative entre les trois modèles en ce qui concerne l'interaction avec les porphyrines en monocouche, hormis un effet sur la fluidité de membrane (augmentée pour M2 et M3, diminuée pour M1). Quant à celle observée par spectroscopie de fluorescence, elle n'a concerné que la porphyrine non glycoconjuguée qui apparemment s'associait davantage au modèle M2 qu'aux deux autres. Devant ces informations parfois contradictoires et en raison de difficultés expérimentales pour le QCM-D, nous avons préféré étudier l'interaction des porphyrines avec le modèle M1 et c'est à ce modèle que nous avons greffé la lectine.

L'étude des caractéristiques physico-chimiques des mélanges M1, M2 et M3 a mené à une autre observation. Pour augmenter la proportion de cholestérol dans les monocouches et les liposomes, nous avons diminué celles de phosphatidylcholine et de phosphatidyléthanolamine. Mais nous n'avons pas touché à la phosphatidylsérine pour éviter de modifier les charges de surface. Or, comme nous l'avons montré dans l'article 3, les potentiels zêta des liposomes n'étaient pas les mêmes, surtout entre 10 et 20% de cholestérol. Nous n'avons pas trouvé à ce jour d'explication plausible à ce phénomène. En nous fondant sur les travaux de Bach *et al.* [(6-8)] ainsi que sur ceux qui ont suivis,[(9-10)] nous avons envisagé un mauvais mélange entre le cholestérol et la phosphatidylsérine, conduisant à une redistribution des molécules de phosphatidylsérine vers le feuillet interne des liposomes. [(11)] Ceci expliquerait les valeurs moins négatives du potentiel zêta observées. Cependant des études en monocouches sur les mélanges binaires équimolaires de phospholipide et de cholestérol n'ont pas permis de mettre en évidence un comportement particulier de la phosphatidylsérine en présence de cholestérol. Dans tous les cas, une condensation des monocouches mixtes a été observée. (Figure 46)

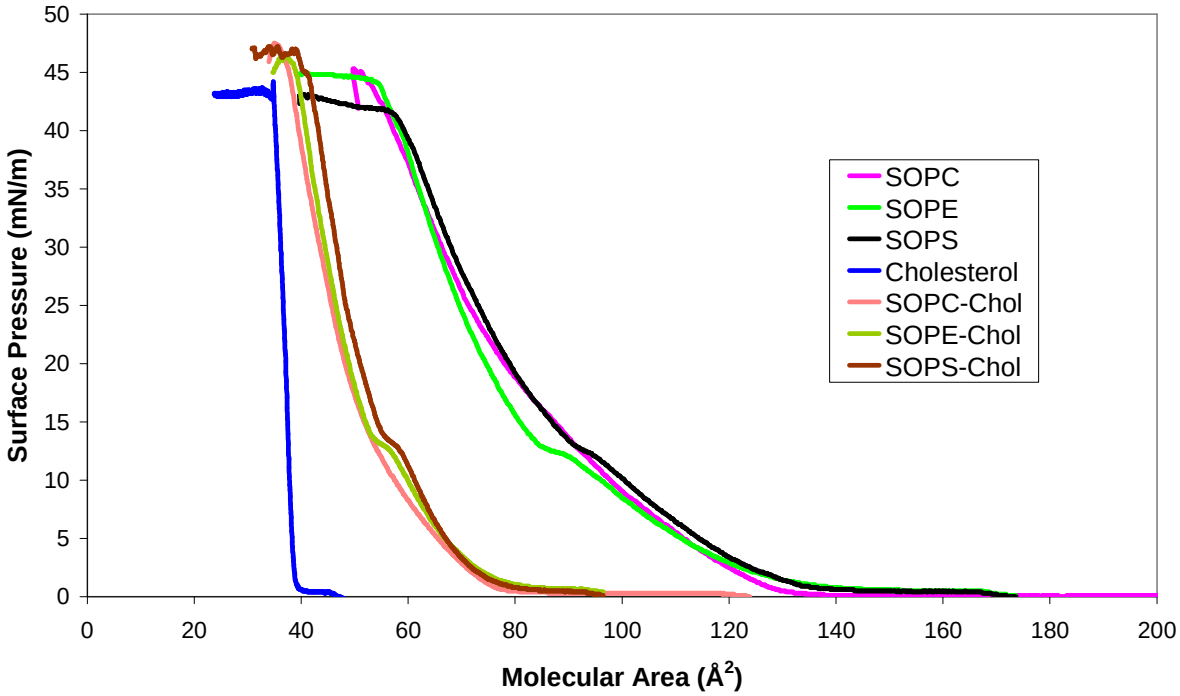

Figure 46: Isothermes des phospholipides purs, du cholestérol et de leurs mélanges (1:1) à l'interface air/tampon (10mM HEPES, 150 mM NaCl, 1 mM $CaCl_2$,$2H_2O$, et 1mM $NiCl_2$,$6H_2O$.

Des études plus approfondies réalisées par une étudiante de master, Katia Daghildjian, à différentes fractions molaires des composants, n'ont pas permis non plus de mettre en évidence une mauvaise miscibilité des trois phospholipides avec le cholestérol. Par ailleurs, les résultats d'analyse calorimétrique différentielle ont montré que les mélanges lipidiques étaient homogènes. Il est donc encore difficile de comprendre pourquoi la charge des liposomes varie entre 10 et 20% de cholestérol.

L'absence d'effet significatif du cholestérol membranaire sur l'interaction des porphyrines avec nos modèles nous a surpris, car dans la littérature, un effet du cholestérol soit en faveur, soit en défaveur de l'interaction de porphyrines avec des liposomes est généralement décrit, comme nous l'avons mentionné dans la partie bibliographique de ce mémoire. Or, nous n'avons observé aucune différence entre les modèles M1, M2, M3 dans leur interaction avec les porphyrines. Ce que nous n'avons pas étudié toutefois, c'est l'interaction avec les phospholipides seuls, sans cholestérol. Une différence aurait certainement pu être observée dans ce cas puisque c'est entre M0 et M1 que nous avons noté l'effet de condensation des monocouches le plus prononcé (Figure 12). Il faudra le vérifier.

Nous avons observé un autre effet inattendu dans les études d'adsorption des porphyrines aux monocouches mixtes de phospholipides : l'augmentation de la pression d'exclusion (ou

pression maximale d'insertion) en présence des porphyrines glycodendrimériques, par rapport à la porphyrine non glycoconjuguée. Apparemment, les sucres interagissent avec la membrane et lorsque les monocouches sont fortement condensées, ce phénomène est d'autant plus important, en raison du rapprochement des têtes polaires. Il affecte la tension superficielle.

Après avoir évalué l'interaction non spécifique des porphyrines avec les modèles membranaires, nous nous sommes intéressés à analyser leur capacité à interagir de manière spécifique avec la Concanavaline A (Con A), une lectine spécifique du mannose. L'objet des expériences menées avec cette lectine (décrites dans l'article 4) était de s'affranchir des interactions non spécifiques avec les lipides avant d'aborder l'étude du système tout entier (bicouche + Con A greffée).

La détermination, par spectroscopie de fluorescence, de la constante d'association des porphyrines (libres en solution) avec la Con A en solution, a montré que les porphyrines mannosylées s'associent davantage avec cette lectine, avec une constante d'association 10 fois plus importante que celle du dérivé non glycoconjugué. La spécificité de cette interaction a ensuite été démontrée par une étude de quenching de fluorescence en utilisant un substrat de la Con A : l'alpha-Methyl-*D*-mannopyranoside. Puis, nous avons préparé des liposomes de DMPC incorporant les porphyrines et nous les avons mis en contact avec la lectine en solution. Nous avons remarqué que seuls les liposomes incorporant les porphyrines glycoconjuguées interagissent avec la Con A d'une manière spécifique. En revanche, dans ces expériences, la Con A était libre en solution ce qui ne reflétait pas correctement la réalité physiologique de l'interaction, dans laquelle le récepteur est immobilisé à la surface des cellules.

Pour mimer cet aspect, nous avons étudié l'interaction des porphyrines incorporées dans des liposomes, avec la Con A immobilisée à la surface du capteur de QCM-D. Cette étude nous a confirmé que seuls les liposomes portant les porphyrines mannosylées se fixent à la Con A par une liaison spécifique. De plus, la porphyrine ayant le bras espaceur le plus long (**dérivé 2**, TEG) interagit mieux avec la Con A que le **dérivé 1** (DEG). Ce résultat nous a montré l'intérêt de l'espaceur, dont la longueur en passant de DEG à TEG améliore sa flexibilité et permet une meilleure exposition des sucres vis-à-vis de la lectine.

Ces expériences sont les seules qui nous ont permis d'observer un effet de l'espaceur. Les molécules de Con A étant très rapprochées (car nous avons essayé de recouvrir toute la surface du capteur), et les porphyrines étant incorporées dans des liposomes, ces liposomes pouvaient se gêner les uns les autres à proximité de la surface et empêcher une bonne accessibilité des sucres aux sites de fixation de la lectine. C'est sans doute pour cette raison

que nous avons observé un effet net de la longueur de l'espaceur. Dans les expériences qui ont suivi (article 5), dans lesquelles la Con A n'étaient fixée, au mieux, qu'à 35% des molécules de phospholipides exposées à la surface de la bicouche, on peut penser qu'il y avait un espace suffisant à l'interface entre les molécules de Con A pour que les liposomes ne se gênent pas. Il aurait pu y avoir « gêne » si les liposomes portant les porphyrines interagissaient aussi avec la bicouche lipidique dans les interstices. Or, en l'absence de Con A, nous n'avons pas observé d'adsorption des liposomes portant les porphyrines glycodendrimériques, en grande quantité, ni durablement aux bicouches lipidiques. Dans ces conditions, la longueur de l'espaceur a un effet moins critique.

Après avoir étudié les interactions non spécifique et spécifique des porphyrines dendrimériques avec les modèles membranaires, nous avons réalisé une étude préliminaire d'analyse de leur phototoxicité *in vitro* sur une lignée cellulaire de rétinoblastome (Y79) et sur une lignée d'adénocarcinome colorectal (HT29) qui nous a servi de contrôle. Dans cette étude, les porphyrines ont été mises en contact avec les cellules qui, après un certain délai, ont été illuminées par un laser. (Voir l'Annexe pour des détails sur le protocole).

Porphyrines	**IC_{50} cytotoxicité à l'obscurité (µM)±10%**		**IC_{50} Phototoxicité (µM)±10%**	
	Y79	**HT29**	**Y79**	**HT29**
Compound 1c	----*	----*	2 (5,8)**	2,1 (4,9)**
Compound 1	----*	----*	2,9 (5,6)**	2,3 (5,0)**
Compound 2	----*	----*	5,2 (5,2)**	3,7 (5,0)**

Table 11: Résultats de phototoxicité et de cytotoxicité à l'obscurité des porphyrines dendrimériques obtenus sur des lignées cellulaires d'Y79 et HT29. *les produits testés ne se sont pas avérés cytotoxiques dans la gamme de concentration utilisée [0,15-7,5µM].**Valeurs d'IC50 obtenues par Séverine Ballut dans le cadre de sa thèse.

D'après le tableau Table 11 et la Figure 47, on remarque que les porphyrines glycodendrimériques ne sont pas cytotoxiques à l'obscurité dans la gamme de concentration utilisée (0-7,5 µM) sur les deux lignées cellulaires. De plus, elles présentent une phototoxicité acceptable (<6 µM) sur les lignées cellulaires Y79 et HT29 en présence de lumière. Cependant, les valeurs d'IC_{50} des **dérivés 1** et **2** montrent qu'en dépit de la présence des 3 molécules de mannose, ces dérivés ne montrent pas de phototoxicité améliorée par rapport au **dérivé 1c**. Séverine Ballut a obtenu des résultats similaires (Table 11).

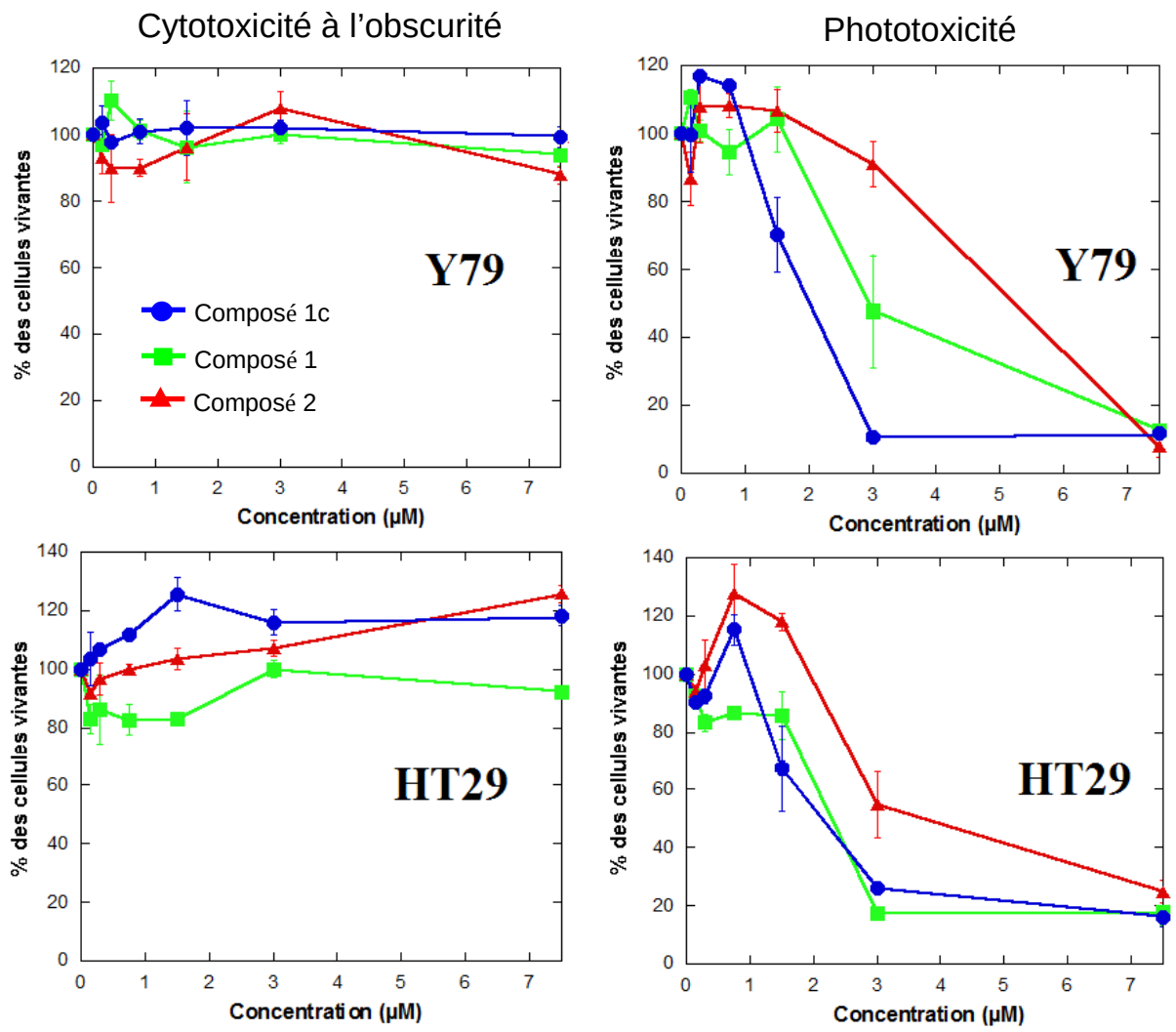

Figure 47: Cytotoxicité et phototoxicité comparatives des porphyrines dendrimériques (dérivé 1c, dérivé 1 et dérivé 2) vis-à-vis de cellules Y79 et HT29 à l'obscurité et après irradiation ($\lambda > 540$ nm, fluence 2 mW/cm^2).

Nous avons essayé de comparer les valeurs d'IC_{50} de nos porphyrines avec celle du composé **TPP-(*p*-*O*-Deg-*O*-α-Man)$_3$** . Selon Laville *et al.*, ce dernier présente une IC_{50} de 0,4 µM pour les cellules HT29 et de 0,35 µM pour les cellules Y79.[2, 12] Nous avons essayé d'étudier nous mêmes la **TPP-(*p*-*O*-Deg-*O*-α-Man)$_3$** avec nos conditions expérimentales, mais nous avons obtenu des résultats non concluants. De nouvelles expériences seront nécessaires.

Même si nous n'avons pas étudié la phototoxicité dans les mêmes conditions que Laville, [2, 12] nos résultats et ceux de Séverine Ballut montrent que les porphyrines glycodendrimériques sont à peu près 10 fois moins phototoxiques sur les cellules Y79 et 6 fois moins phototoxiques sur les cellules HT29 que la **TPP-(*p*-*O*-Deg-*O*-α-Man)$_3$**.

Pour expliquer ces résultats décevants pour les porphyrines dendrimériques, nous pouvons proposer quatre hypothèses :

i. Les porphyrines glycodendrimériques, après leur reconnaissance par le récepteur lectinique des cellules tumorales pourraient rester accrochées à la protéine et ne pas traverser la membrane. Cette hypothèse pourrait être vérifiée par détermination de la localisation cellulaire par microscopie confocale pour voir si ces porphyrines sont internalisées ou non d'une part, et par cytométrie en flux pour quantifier le taux de porphyrines internalisées dans la cellule d'autre part.

ii. Les porphyrines glycodendrimériques ne seraient pas reconnues par le récepteur. Ceci semble improbable : en effet, les résultats de Laville ont mis en évidence l'existence d'un récepteur à mannose et nos résultats avec les modèles membranaires ont montré que les porphyrines glycodendrimériques étaient capables d'interagir avec une lectine spécifique du mannose. Mais il est vrai également que nous ne connaissons pas la nature du véritable récepteur à mannose. Des travaux précédents ont montré que des lectines différentes n'interagissent pas forcément de la même façon avec un même sucre [(13)] : la Con A n'était peut-être pas le bon modèle et/ou le *cluster* de sucres peut-être pas adapté au récepteur membranaire. Il est aussi possible que la non-reconnaissance soit liée à la faible solubilité des porphyrines étudiées. L'agrégation dans le milieu de culture pourrait limiter leur interaction spécifique avec les cellules. Pour s'affranchir de l'effet d'agrégation, nous avons testé les porphyrines solubilisées dans des liposomes de DMPC. Les résultats ont été non concluants, car pour étudier les mêmes concentrations de porphyrines que lorsqu'elles sont libres, il a été nécessaire d'utiliser des concentrations molaires de lipides cytotoxiques.

iii. L'affinité des porphyrines pour les constituants du sérum bovin fœtal (LDL et albumine) : les porphyrines se fixeraient aux protéines et celles-ci contrôleraient leur transport intracellulaire.

En effet, à cause de la différence structurale entre les porphyrines étudiées, celles-ci pourraient se lier différemment aux constituants du sérum. Elles pourraient rester sous forme libre dans le milieu de culture, se lier aux protéines du sérum (principalement l'albumine) ou se lier préférentiellement aux particules de LDL comme dans le cas des porphyrines glycodendrimériques (**composés 1c, 1** et **2**) (résultat obtenu par Benoit

CHAUVIN, dans le cadre de sa thèse à l'EA 4041). On peut émettre l'hypothèse que les particules de LDL ayant une masse moléculaire importante de ~550 KDa, [14] elles auraient du mal à s'infiltrer au cœur des amas de cellules Y79 en suspension dans le milieu de culture. [15] (Figure 48) En revanche, les porphyrines qui se lient aux protéines sériques ou restent sous forme libres, seraient véhiculées vers toutes les cellules. Ceci aussi reste à vérifier.

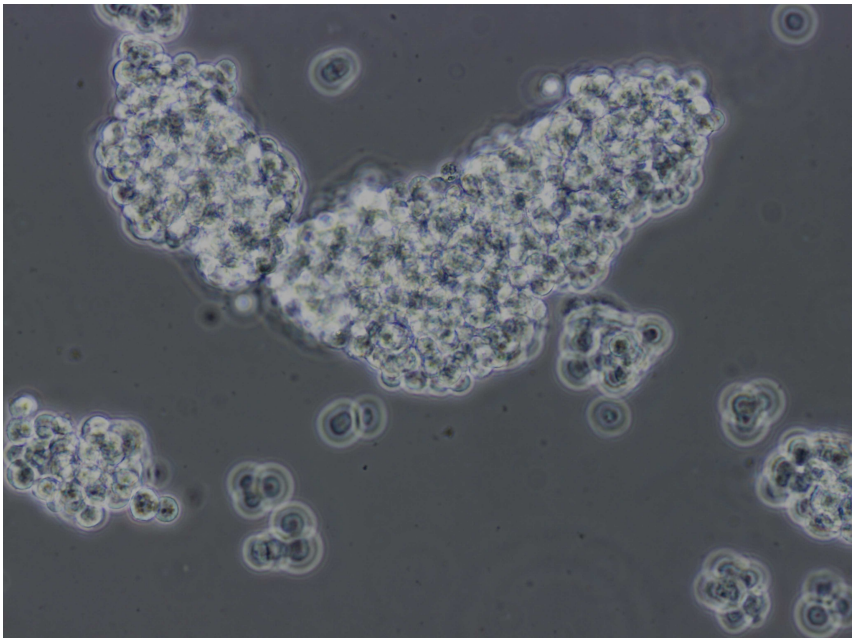

Figure 48 : Photo d'un amas cellulaire de Y79 en suspension dans le milieu de culture par microscopie optique.

iv. Les porphyrines glycodendrimériques seraient internalisées dans la cellule tumorale mais leur localisation intracellulaire pourrait être différente de celle de la **TPP-(*p*-*O*-Deg-*O*-α-Man)$_3$**. En effet, celle-ci se localise dans les mitochondries.[2] Les porphyrines glycodendrimériques seraient, par conséquent, moins efficaces. Cette hypothèse semble être la plus réaliste. En effet, une étude de localisation cellulaire sur des cellules HT29 a été effectuée par Séverine Ballut, dans le cadre de sa thèse à l'institut Curie, sur un dérivé glucosylé qui a la même composition que le **dérivé 0** (mais avec des molécules de glucose qui sont reconnues par les récepteurs membranaires de HT29). Cette étude, réalisée par microscopie confocale, a montré que la porphyrine glucoconjuguée pénètre dans la cellule, mais ne se localise pas au niveau du noyau, des lysosomes, ni à celui des mitochondries. Sa localisation exacte n'a pas encore pu être déterminée.

L'analyse de nos résultats de culture cellulaire sur les lignées Y79 et HT29 ne met pas en évidence un lien entre la nature du sucre de la porphyrine et le type du récepteur membranaire surexprimé par la lignée cellulaire, bien que la reconnaissance sucre-lectine ait été démontrée avec nos modèles membranaires. De nouveaux essais seront réalisés pour confirmer ces résultats et des études de localisation intracellulaire dans d'autres organites tels que l'appareil de Golgi, le réticulum endoplasmique et les endosomes seront effectuées. Ces études sont en cours d'étude à l'institut Curie (Orsay).

Références :

1. Laville, I., Figueiredo, T., Loock, B., Pigaglio, S., Maillard, Ph., Grierson, D.S., Carrez, D., Croisy, A., Blais, J. (2003) Synthesis, cellular internalization and photodynamic activity of glucoconjugated derivatives of tri and tetra(meta-hydroxyphenyl)chlorins, *Bioorg. & Med. Chem. 11*, 1643-1652.
2. Laville, I., Pigaglio, S., Blais, J. C., Doz, F., Loock, B., Maillard, Ph., Grierson, D.S., Blais, J. (2006) Photodynamic Efficiency of Diethylene Glycol-Linked Glycoconjugated Porphyrins in Human Retinoblastoma Cells, *J. Med. Chem. 49*, 2558-2567.
3. Desroches, M. C., Kasselouri, A., Meyniel, M., Fontaine, P., Goldmann, M., Prognon, P., Maillard, P., Rosilio, V. (2004) Incorporation of Glycoconjugated Porphyrin Derivatives into Phospholipid Monolayers: A Screening Method for the Evaluation of Their Interaction with a Cell Membrane, *Langmuir 20*, 11698-11705.
4. Huster, D., Arnold, K., and Gawrisch, K. (1998) Influence of Docosahexaenoic Acid and Cholesterol on Lateral Lipid Organization in Phospholipid Mixtures, *Biochemistry 37*, 17299-17308.
5. Huster, D., Arnold, K., and Gawrisch, K. (2000) Strength of Ca2+ Binding to Retinal Lipid Membranes: Consequences for Lipid Organization, *Biophys. J. 78*, 3011-3018.
6. Bach, D., Wachtel, E., Borochov, N., Senisterra, G., and Epand, R. M. (1992) Phase behaviour of heteroacid phosphatidylserines and cholesterol, *Chem. and Phys. of Lipids 63*, 105-113.
7. Bach, D., Borochov, N., and Wachtel, E. (1998) Phase separation of cholesterol in dimyristoyl phosphatidylserine cholesterol mixtures, *Chem. and Phys. of Lip. 92*, 71-77.
8. Bach, D., and Wachtel, E. (2003) Phospholipid/cholesterol model membranes: formation of cholesterol crystallites, *Biochimica et Biophysica Acta (BBA) - Biomembranes 1610*, 187-197.
9. Epand, R. M., Bach, D., Borochov, N., and Wachtel, E. (2000) Cholesterol Crystalline Polymorphism and the Solubility of Cholesterol in Phosphatidylserine, *Biophys. J. 78*, 866-873.
10. Epand, R. M., Bach, D., Epand, R. F., Borochov, N., and Wachtel, E. (2001) A New High-Temperature Transition of Crystalline Cholesterol in Mixtures with Phosphatidylserine, *Biophys. J. 81*, 1511-1520.
11. Roy, M. T., Gallardo, M., and Estelrich, J. (1997) Bilayer Distribution of Phosphatidylserine and Phosphatidylethanolamine in Lipid Vesicles, *Bioconjugate Chemistry 8*, 941-945.
12. Maillard, P., Loock, B., Grierson, D. S., Laville, I., Blais, J., Doz, F., Desjardins, L., Carrez, D., Guerquin-Kern, J. L., Croisy, A. (2007) In vitro phototoxicity of glycoconjugated porphyrins and chlorins in colorectal adenocarcinoma (HT29) and retinoblastoma (Y79) cell lines, *Photodiag. and Photody. Ther. 4*, 261-268.
13. Faivre, V., Costa, M.L., Boullanger, P., Baszkin, A., Rosilio, V. (2003) Specific interaction of lectins with liposomes and monolayers bearing neoglycolipids, *Chem. Phys. Lipids 125*, 147-159.
14. Kahlon, T., Shore, V., and Lindgren, F. (1992) Heterogeneity of molecular weight and apolipoproteins in low density lipoproteins of healthy human males, *Lipids 27*, 1055-1057.
15. McFall, R. C., Sery, T. W., and Makadon, M. (1977) Characterization of a new continuous cell line derived from a human retinoblastoma, *Cancer Res 37*, 1003-1010; et de Witte, P. (2010) Mechanisms underlying the accumulation of hypericin in non-muscle invasive bladder cancer., *Communication orale, congrès du GDR Photomed 2010.*

Conclusion générale et perspectives

Conclusion générale et perspectives

Les modèles membranaires artificiels constituent aujourd'hui des outils potentiellement intéressants pour l'analyse des interactions biophysiques entre les médicaments et la membrane cytoplasmique. Toutefois, l'utilisation de ces membranes biomimétiques (le plus souvent des liposomes) reste limitée à des études rétrospectives, effectuées une fois que les propriétés des molécules thérapeutiques *in vitro* et/ou *in vivo* ont été déterminées. Dans ce travail, nous avons pu réaliser une étude fondamentale en collaboration avec l'équipe de Philippe Maillard qui synthétise des porphyrines glycoconjuguées utilisables en thérapie photodynamique. Nous avons pu analyser, de manière systématique, une série de dérivés dendrimériques dont les seules différences résidaient dans la présence ou l'absence de sucre, et dans la longueur de l'espaceur séparant le sucre du répartiteur dendrimérique.

L'objectif de notre travail était plus particulièrement de construire des modèles biomimétiques de la membrane cellulaire du rétinoblastome, afin d'évaluer la capacité de ces nouvelles porphyrines glycodendrimériques à interagir avec elle, par des interactions spécifiques et/ou non spécifiques.

A cette fin, nous avons mis au point et caractérisé pour la première fois, un modèle complexe à quatre composants (SOPC, SOPE, SOPS, cholestérol) sous forme de monocouches, liposomes et bicouches planes supportées, respectant la composition lipidique physiologique de la membrane cytoplasmique et le pH cancéreux environnant. Ce modèle a été fonctionnalisé par une lectine modèle reconnaissant le mannose (Con A) afin d'étudier les interactions spécifiques avec les porphyrines mannosylées.

Les trois formes du modèle ont permis de recueillir des informations complémentaires sur l'interaction porphyrine-membrane. Les monocouches ont permis de révéler la complexité des interactions moléculaires entre lipides et photosensibilisateurs ; les liposomes, de démontrer la pénétration effective de ces molécules dans la membrane ; et les bicouches planes ont mis en évidence la prédominance de l'interaction spécifique sur l'interaction non spécifique.

Nos résultats ont montré l'absence d'effet d'une augmentation de la proportion de cholestérol sur la pénétration intra-membranaire des porphyrines étudiées et ont mis en évidence le rôle des sucres à la fois dans l'interaction spécifique et non spécifique. Dans certaines conditions (lectine libre en solution ou fixée à densité élevée sur une surface), l'intérêt de la longueur de l'espaceur a pu être vérifié.

L'évaluation des propriétés phototoxiques des porphyrines dendrimériques a été réalisée sur des lignées cellulaires Y79 du rétinoblastome humain. Elle n'a pas montré de différence significative entre les différents dérivés. Elle a également fait apparaître que leur efficacité était moins élevée que celles des dérivés de 2ème génération. Il est encore difficile de savoir si cette faible efficacité est liée à une pénétration limitée de ces molécules dans les cellules ou si elles sont internalisées, mais localisées au niveau d'organites moins critiques pour la vie cellulaire. Les porphyrines sont faiblement solubles et interagissent fortement avec les protéines du milieu aqueux. De nouvelles expériences doivent être réalisées en incorporant les photosensibilisateurs dans des liposomes qui permettront d'améliorer leur solubilité dans le milieu de culture et d'augmenter peut-être leur efficacité vis-à-vis des cellules du rétinoblastome.

Notre modèle est-il pertinent pour prédire l'interaction entre les porphyrines et la membrane cellulaire ? L'étude en culture cellulaire pourrait en laisser douter. Elle est encore préliminaire car seul un essai a pu être réalisé dans cette thèse. Mais des résultats concordants ont été obtenus en même temps par Séverine Ballut, à l'Institut Curie, sur une série plus complète de molécules dendrimériques. Les études en monocouches ont montré que si les porphyrines pénétraient dans une monocouche peu condensée, elles pénétraient beaucoup moins à des pressions comparables à celles de la membrane cellulaire. Bien que les valeurs de pression d'exclusion élevées puissent laisser penser que les porphyrines pénètrent davantage lorsqu'elles portent des sucres, il est plus vraisemblable que ces pressions ne soient que le reflet d'une interaction des mannoses avec les groupements polaires des phospholipides. Par ailleurs, les résultats obtenus avec les liposomes ont montré que les porphyrines s'associaient de la même façon aux vésicules et les études de quenching n'ont pas mis en évidence de pénétration plus profonde des porphyrines glycodendrimériques comparées à la porphyrine non glycoconjuguée (excepté pour le modèle M2, ce qui devrait être vérifié à nouveau). Enfin, les liposomes et bicouches planes ont permis de démontrer la possibilité d'une interaction spécifique et la prédominance de cette interaction sur l'interaction non spécifique. L'interaction spécifique aurait dû favoriser le passage des porphyrines glycodendrimériques, par rapport à la porphyrine non glycoconjuguée, lors des expériences en culture cellulaire. Cela n'a pas été le cas. Nous avons envisagé plusieurs hypothèses dans notre discussion, pour expliquer ce phénomène.

Plusieurs études peuvent être proposées pour poursuivre ce travail de thèse :

- Affiner la composition lipidique de notre modèle biomimétique en analysant le taux du cholestérol dans les cellules d'Y79 et/ou à partir des xénogreffes du rétinoblastome humain. Ceci permettrait d'étudier l'interaction non spécifique des photosensibilisateurs en se rapprochant le plus possible de la composition exacte de la membrane cellulaire du rétinoblastome.
- Isoler et identifier le récepteur naturel au mannose du rétinoblastome que nous pourrions incorporer par la suite dans les modèles membranaires, ce qui permettrait la construction de membranes artificielles véritablement biomimétiques. Nous pourrions tout d'abord étudier l'interaction spécifique de ces porphyrines avec le récepteur par des techniques de spectrométrie de fluorescence, SPR et surtout l'ITC, qui permettrait une meilleure compréhension de l'interaction des porphyrines avec le récepteur d'un point de vue thermodynamique. Une modélisation moléculaire de l'interaction pourrait aussi être envisagée.
- Coupler les expériences de QCM-D à l'EIS afin de caractériser les modifications des propriétés viscoélastiques et de la perméabilité des membranes planes supportées après leur interaction avec les porphyrines. Des expériences ont été récemment entreprises dans ce sens, en étudiant des porphyrines solubles et de masse molaire plus élevée que nos porphyrines. Elles ont donné des résultats encourageants.
- Evaluer la phototoxicité des porphyrines une fois solubilisées dans la matrice lipidique des liposomes sur des lignées Y79, pour voir si cette solubilisation améliore leur efficacité. Une étude de localisation intracellulaire de ces porphyrines pourrait être réalisée, à la suite, par microscopie confocale. Cette étude déjà entamée pourrait être achevée rapidement.
- Evaluer la capacité des porphyrines glycodendrimériques solubilisées dans des liposomes à cibler les cellules d'Y79 du rétinoblastome en essayant de fixer les cellules sur des surfaces d'or (QCM-D) et/ou SiO_2. Ceci permettrait de mieux valider l'adéquation de notre modèle membranaire par rapport aux cellules de rétinoblastome.
- Enfin, il serait intéressant d'incuber les liposomes avec les porphyrines en solution, puis de les irradier et de déterminer la phototoxicité par DSC et/ou spectroscopie de fluorescence afin de mieux comprendre le niveau de toxicité une fois dans la membrane tout en essayant de trouver une corrélation avec les résultats *in vitro*.

Si la recherche dans ce domaine est poursuivie et des corrélations sont trouvées entre les modèles membranaires et les études de culture cellulaire, ces modèles pourront constituer des

outils puissants, innovants et non coûteux pour prédire l'interaction de principes actifs (d'une manière générale) avec la membrane cellulaire.

Annexe

Annexe

Evaluation de la photocytotoxicité des porphyrines glycodendrimériques sur cultures cellulaires

Afin d'analyser la photocytotoxicité de nos porphyrines glycodendrimériques, nous avons effectué une étude d'interaction en culture cellulaire. Dans cette étude, les porphyrines sont mises en contact avec les cellules qui sont, après un certain délai, illuminées par un laser. Pour réaliser ce test, nous avons utilisé la méthodologie mise au point par le Dr Alain Croisy et sa collaboratrice Danièle Carrez à l'institut Curie d'Orsay. Les expériences ont été réalisées dans la salle de culture cellulaire de l'UMR CNRS 8612, avec le concours de Véronique Marsaud. Les porphyrines glycoconjuguées synthétisées par l'équipe du Dr Philippe Maillard à l'institut Curie sont systématiquement testées sur lignée de rétinoblastome immortalisée, mais aussi sur une lignée d'adénocarcinome du colon. Ainsi, les lignées cellulaires utilisées pour cette étude sont les lignées (a) Y79 (ATCC HTB 18) du rétinoblastome humain obtenue par Reid *et al.*[(1)] après culture d'explant d'une tumeur primaire extraite de l'œil d'un enfant de 2 ans et demi immédiatement après énucléation et (b) la lignée HT29 d'adénocarcinome colorectal qui nous a servi de contrôle. En effet, les cellules HT29 portent des récepteurs spécifiques du glucose et ne reconnaissent pas le mannose. [(2-3)]

1. Matériel et Méthodes

a. Conditions de culture cellulaire

- Lignée Y79 du rétinoblastome

Les cellules suspensives Y79 sont cultivées dans un flacon de culture de 75 cm^2 en suspension dans du milieu DMEM (Dulbecco's Modified Eagle's medium) 1X contenant 20% de sérum de veau fœtal (SVF, VWR), en présence d'1% de pénicilline/streptomycine (50 UI/ml et 50µg/ml) et d'1% de L-glutamine. Les cellules sont placées dans un incubateur, à 37°C, sous une atmosphère humide, saturée en vapeur d'eau et à 5% en CO_2. Les cellules sont divisées au 1/3 deux fois par semaine afin de multiplier leur nombre. Le contenu de chaque flacon (60 ml) est centrifugé pendant 5 minutes à une vitesse de 1000 tours/min, le surnageant est éliminé et le culot est alors repris par un nouveau milieu de culture. Cette suspension est alors divisée en 3 flacons contenant chacun un volume final de 60 ml.

Après 24 h d'incubation, un aliquot de cette suspension est prélevé pour effectuer un comptage cellulaire sur une lame de Malassez. La solution est alors diluée (ou concentrée)

dans le même milieu de culture afin d'obtenir une concentration de 500 000 cellules/ml. 1 ml de cette suspension est alors déposé dans des plaques de 24 puits.
Les porphyrines dissoutes dans du diméthylsulfoxyde (DMSO) sont alors ajoutées dans les puits pour atteindre des concentrations finales variant de 0,15 à 7,5 µM. Pour les plaques de contrôle, un même volume de DMSO pur est ajouté. La dissolution des porphyrines dans le DMSO est indispensable car leur faible solubilité dans le milieu de culture ne permet pas d'atteindre les concentrations à étudier.

Lignée HT29 d'adénocarcinome colorectal

Les mêmes conditions de culture décrites pour Y79 sont utilisées pour les cellules adhérentes HT29, mais avec 10% de sérum de veau fœtal seulement. Pour diviser les cellules en plusieurs flacons, le milieu de culture est éliminé et les cellules sont détachées par addition de 1 ml de trypsine dans le flacon de culture, puis placées quelques minutes à 37°C jusqu'à leur détachement complet. La réaction est alors inhibée par addition de milieu DMEM à 10% de SVF (v/v) et la suspension cellulaire est centrifugée pendant 5 minutes à une vitesse de 1000 tours/min. Après élimination du surnageant, le culot cellulaire est remis en suspension dans le même milieu avec tous les composants déjà cités. Ensuite, la suspension est répartie dans 4 flacons de 75 cm² dont chacun est complété avec 25 ml de milieu de culture.

La veille du jour du test d'efficacité des porphyrines, après détachement des cellules par la trypsine comme précédemment décrit, la suspension cellulaire est reprise par du DMEM frais contenant 10% de SVF. Un aliquot de cette suspension est prélevé pour effectuer un comptage cellulaire sur lame de Malassez. La solution est alors diluée dans le même milieu de culture afin d'obtenir une concentration de 50 000 cellules/ml. 1ml de cette suspension est déposé dans des plaques de 24 puits de 2,5 cm² et les cellules sont incubées une nuit à 37°C afin de permettre leur adhésion et leur étalement avant ajout des porphyrines.

b. Conditions de photoirradiation

Après 24 h d'incubation des cellules avec les molécules à tester, les plaques sont irradiées à 2 J/cm^2 pendant 14 min dans une chambre noire. Après irradiation, 100 µL de SVF est ajouté dans chaque puits pour les cellules Y79 pour obtenir une concentration finale de sérum de 20% (la même concentration utilisée pendant la multiplication des cellules), ensuite les plaques sont mises à l'étuve pendant 3 jours avant le test MTT. Dans le cas des cellules adhérentes HT29, le surnageant est aspiré (et remplacé par un nouveau milieu de culture) et

les plaques sont mises à l'étuve pendant 3 jours avant le test de MTT. La même procédure est réalisée sur des plaques contenant les porphyrines ou le DMSO seul, mais ces plaques ne sont pas irradiées, pour tester la cytotoxicité propre des molécules et du DMSO, respectivement.

c. Etude de la prolifération par le test au MTT

Principe

Ce test reflète la prolifération et la viabilité cellulaires. Il est basé sur la transformation du MTT (3-(4,5-diméthylthiazol-2-yl)-2,5-diphényl tétrazolium bromide) en cristaux violets de formazan par une enzyme mitochondriale, la succinate déshydrogénase. (Figure 49) Les cristaux de formazan formés sont solubilisés dans du DMSO et la solution colorée résultante est quantifiée au spectrophotomètre par mesure de l'absorbance à 570 nm. (Figure 49) Ce test est utilisé pour comparer la croissance des cellules témoins à celle des cellules traitées par les photosensibilisateurs.

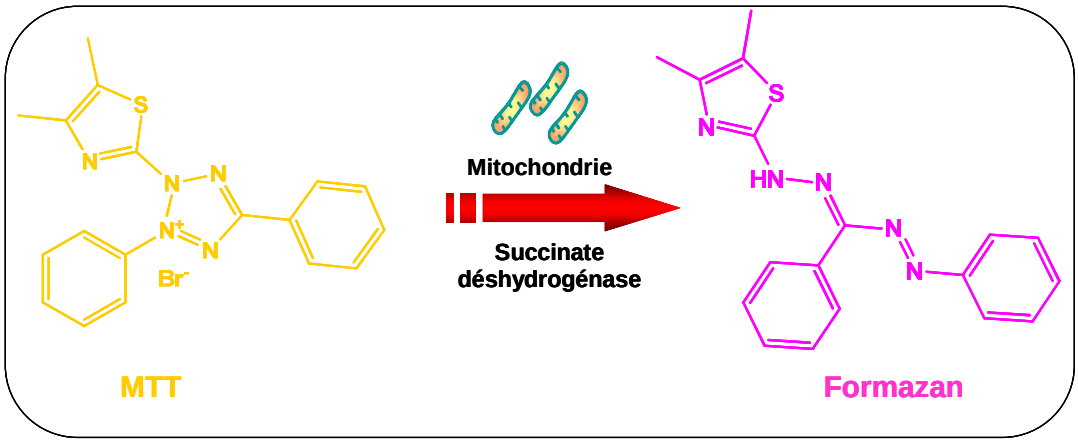

Figure 49 : Transformation du MTT en formazan par action de la succinate déshydrogénase mitochondriale.

La quantité de formazan formée est proportionnelle au nombre de cellules vivantes, ainsi on peut déterminer l'IC_{50} des produits en mesurant la diminution de l'absorbance en fonction de la concentration des porphyrines.

Mode opératoire

Expérimentalement, 50 µL d'une solution de MTT (5 mg/ml dans du tampon PBS) sont ajoutés dans chaque puit. Après 30 min d'incubation à 37°C en atmosphère humide, le surnageant des puits contenant les cellules HT29 est éliminé et les cellules sont lysées avec 750 µL de DMSO. Pour les cellules Y79 en suspension, le contenu des puits est centrifugé dans des eppendorfs à une vitesse de 5000 tours/min pendant 5 min, puis le surnageant est

aspiré et le culot cellulaire, lysé avec 750 µL de DMSO. Ensuite, le contenu des puits des plaques de 24 est transféré dans des plaques de 96 puits et la lecture de l'absorbance est effectuée par un lecteur de plaques à une longueur d'onde de 570 nm. Les blancs de lecture correspondent aux cellules non traitées, mais lysées avec du DMSO.

RESUME

La complexité des membranes biologiques est à l'origine du développement des modèles membranaires artificiels comme outils indispensables à la compréhension des mécanismes d'interaction entre médicaments et membrane cellulaire. Cette thèse porte sur l'étude des interactions non spécifiques et spécifiques entre de nouvelles porphyrines glycoconjuguées utilisables en thérapie photodynamique (PDT) et des modèles membranaires biomimétiques (monocouches, bicouches planes supportées et liposomes) du rétinoblastome portant à leur surface une lectine spécifique du mannose.

Les principales techniques utilisées pour cette étude sont la tensiométrie de surface, la spectrométrie de fluorescence, la microbalance à cristal de quartz avec mesure de dissipation (QCM-D) et diffusion quasi-élastique de lumière (DLS).

Les porphyrines glycoconjuguées se sont avérées comme des molécules prometteuses, capables à interagir d'une manière non spécifique (pénétration passive) et spécifique (ciblage des récepteurs de type lectinique) avec les modèles membranaires du rétinoblastome.

MOTS-CLES

Porphyrines glycodendrimériques; Thérapie photodynamique; Rétinoblastome; Modèles membranaires; Monocouches; Liposomes; Bicouches planes supportées; Lectine; Concanavaline A; Cholestérol; Spectrométrie de Fluorescence; Tensiométrie de surface; DLS; QCMD.

LABORATOIRE DE RATTACHEMENT

Laboratoire de Physico-Chimie des surfaces (UMR-CNRS 8612)

PÔLE : PHARMACOTECHNIE ET PHYSICO-CHIMIE PHARMACEUTIQUE

UNIVERSITÉ PARIS-SUD 11
UFR «FACULTÉ DE PHARMACIE DE CHATENAY-MALABRY »
5, rue Jean Baptiste Clément
92296 CHÂTENAY-MALABRY Cedex